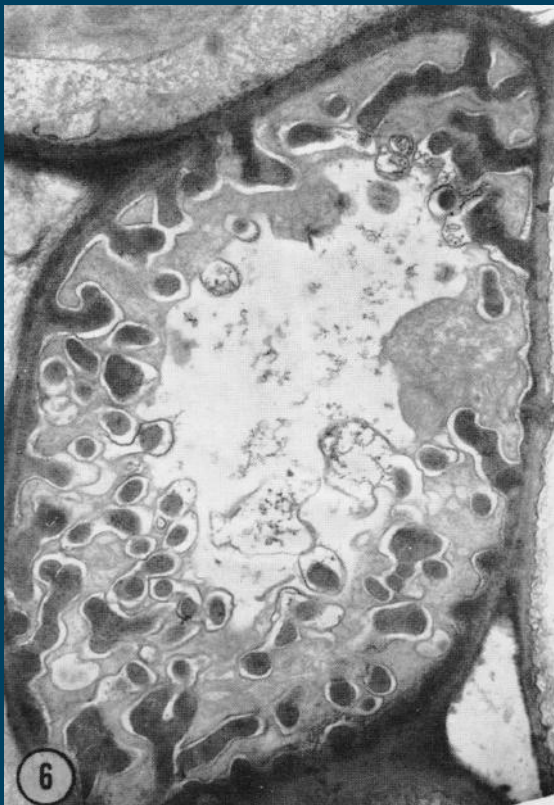


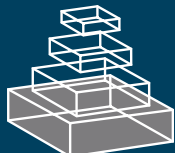
# frontiers RESEARCH TOPICS



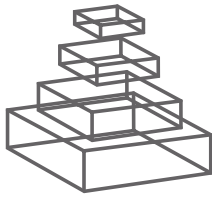
## TRANSFER CELLS

Topic Editors

David McCurdy and Gregorio Hueros



**frontiers in**  
**PLANT SCIENCE**



## FRONTIERS COPYRIGHT STATEMENT

© Copyright 2007-2015  
Frontiers Media SA.  
All rights reserved.

All content included on this site, such as text, graphics, logos, button icons, images, video/audio clips, downloads, data compilations and software, is the property of or is licensed to Frontiers Media SA ("Frontiers") or its licensees and/or subcontractors. The copyright in the text of individual articles is the property of their respective authors, subject to a license granted to Frontiers.

The compilation of articles constituting this e-book, wherever published, as well as the compilation of all other content on this site, is the exclusive property of Frontiers. For the conditions for downloading and copying of e-books from Frontiers' website, please see the Terms for Website Use. If purchasing Frontiers e-books from other websites or sources, the conditions of the website concerned apply.

Images and graphics not forming part of user-contributed materials may not be downloaded or copied without permission.

Individual articles may be downloaded and reproduced in accordance with the principles of the CC-BY licence subject to any copyright or other notices. They may not be re-sold as an e-book.

As author or other contributor you grant a CC-BY licence to others to reproduce your articles, including any graphics and third-party materials supplied by you, in accordance with the Conditions for Website Use and subject to any copyright notices which you include in connection with your articles and materials.

All copyright, and all rights therein, are protected by national and international copyright laws.

The above represents a summary only. For the full conditions see the Conditions for Authors and the Conditions for Website Use.

**ISSN** 1664-8714  
**ISBN** 978-2-88919-474-2  
**DOI** 10.3389/978-2-88919-474-2

## ABOUT FRONTIERS

Frontiers is more than just an open-access publisher of scholarly articles: it is a pioneering approach to the world of academia, radically improving the way scholarly research is managed. The grand vision of Frontiers is a world where all people have an equal opportunity to seek, share and generate knowledge. Frontiers provides immediate and permanent online open access to all its publications, but this alone is not enough to realize our grand goals.

## FRONTIERS JOURNAL SERIES

The Frontiers Journal Series is a multi-tier and interdisciplinary set of open-access, online journals, promising a paradigm shift from the current review, selection and dissemination processes in academic publishing.

All Frontiers journals are driven by researchers for researchers; therefore, they constitute a service to the scholarly community. At the same time, the Frontiers Journal Series operates on a revolutionary invention, the tiered publishing system, initially addressing specific communities of scholars, and gradually climbing up to broader public understanding, thus serving the interests of the lay society, too.

## DEDICATION TO QUALITY

Each Frontiers article is a landmark of the highest quality, thanks to genuinely collaborative interactions between authors and review editors, who include some of the world's best academicians. Research must be certified by peers before entering a stream of knowledge that may eventually reach the public - and shape society; therefore, Frontiers only applies the most rigorous and unbiased reviews.

Frontiers revolutionizes research publishing by freely delivering the most outstanding research, evaluated with no bias from both the academic and social point of view.

By applying the most advanced information technologies, Frontiers is catapulting scholarly publishing into a new generation.

## WHAT ARE FRONTIERS RESEARCH TOPICS?

Frontiers Research Topics are very popular trademarks of the Frontiers Journals Series: they are collections of at least ten articles, all centered on a particular subject. With their unique mix of varied contributions from Original Research to Review Articles, Frontiers Research Topics unify the most influential researchers, the latest key findings and historical advances in a hot research area!

Find out more on how to host your own Frontiers Research Topic or contribute to one as an author by contacting the Frontiers Editorial Office: [researchtopics@frontiersin.org](mailto:researchtopics@frontiersin.org)

# TRANSFER CELLS

Topic Editors:

**David McCurdy**, The University of Newcastle, Australia  
**Gregorio Hueros**, Universidad de Alcalá, Spain



Transmission electron micrograph showing extensive wall ingrowth deposition characteristic of a minor vein phloem transfer cell in leaves of *Pisum arvense*. This iconic image of a transfer cell was published in the first contemporary account of these cell types by Gunning, Pate and Briarty in 1963. The image shows reticulate wall ingrowths protruding into the cytoplasm from all wall faces of this cell. The increase in plasma membrane surface area as a consequence of wall ingrowth deposition, a hallmark of transfer cell identity, is clearly appreciated in this image. Image reproduced with permission - ©1968 Rockefeller University Press. *Journal of Cell Biology*. 37:C7-C12. doi:10.1083/jcb.37.3.C7

Transfer cells are anatomically specialized cells optimized to support high levels of nutrient transport in plants. These cells trans-differentiate from existing cell types by developing extensive and localized wall ingrowth labyrinths to amplify plasma membrane surface area which in turn supports high densities of membrane transporters. Unsurprisingly, therefore, transfer cells are found at key anatomical sites for nutrient acquisition, distribution and exchange. Transfer cells are involved in delivery of nutrients between generations and in the development of reproductive organs and also facilitate the exchange of nutrients that characterize symbiotic associations. Transfer cells occur across all taxonomic groups in higher plants and also in algae and fungi. Deposition of wall ingrowth-like structures are also seen in “syncytia” and “giant cells” which function as feeding sites for cyst and root-knot nematodes, respectively, following their infection of roots. Consequently, the formation of highly localized

wall ingrowth structures in diverse cell types appears to be an ancient anatomical adaption to facilitate enhanced rates of apoplastic transport of nutrients in plants. In some systems a role for transfer cells in the formation of an anti-pathogen protective barrier at these symplastic discontinuities has been inferred. Remarkably, the extent of cell wall ingrowth development at a particular site can show high plasticity, suggesting that transfer cell differentiation might be a dynamic process adapted to the transport requirements of each physiological condition. Recent studies exploiting different experimental systems to investigate transfer cell biology have identified signaling pathways inducing transfer cell development and genes/gene networks that define transfer cell identity and/or are involved in building the wall ingrowth labyrinths themselves. Further studies have defined the structure and composition of wall ingrowths in different systems, leading in many instances to the conclusion that this process may involve previously uncharacterized mechanisms for localized wall deposition in plants. Since transfer cells play important roles in plant development and productivity, the latter being relevant to crop yield, especially so in major agricultural species such as wheat, barley, soybean and maize, understanding the molecular and cellular events leading to wall ingrowth deposition holds exciting promise to develop new strategies to improve plant performance, a key imperative in addressing global food security. This Research Topic presents a timely and comprehensive treatise on transfer cell biology to help define critical questions for future research and thereby generating a deeper understanding of these fascinating and important cells in plant biology.

# Table of Contents

- 05 Transfer Cells**  
David W. McCurdy and Gregorio Hueros
- 07 Development of Endosperm Transfer Cells in Barley**  
Johannes Thiel
- 19 Endosperm Transfer Cell-Specific Genes and Proteins: Structure, Function and Applications in Biotechnology**  
Sergiy Lopato, Nikolai Borisjuk, Peter Langridge and Maria Hrmova
- 33 Two Maize END-1 Orthologs, BETL9 and BETL9like, Are Transcribed in a Non-Overlapping Spatial Pattern on the Outer Surface of the Developing Endosperm**  
Joaquín Royo, Elisa Gómez, Olivier Sellam, Denise Gerentes, Wyatt Paul and Gregorio Hueros
- 44 A Comparative Glycoproteome Study of Developing Endosperm in the Hexose-Deficient Miniature1 (*mn1*) Seed Mutant and Its Wild Type *Mn1* in Maize**  
Cecilia Silva-Sánchez, Sixue Chen, Jinxi Li and Prem S. Chourey
- 58 A PCR-Based Forward Genetics Screening, Using Expression Domain-Specific Markers, Identifies Mutants in Endosperm Transfer Cell Development**  
Luis M. Muñiz, Elisa Gómez, Virginie Guyon, Maribel López, Bouchaib Khbaya, Olivier Sellam, Pascual Peréz and Gregorio Hueros
- 71 Lignification of Developing Maize (*Zea mays L.*) Endosperm Transfer Cells and Starchy Endosperm Cells**  
Sara Rocha, Paulo Monjardino, Duarte Mendonça, Artur da Câmara Machado, Rui Fernandes, Paula Sampaio and Roberto Salema
- 81 On the Track of Transfer Cell Formation by Specialized Plant-Parasitic Nematodes**  
Natalia Rodiuc, Paulo Vieira, Mohamed Youssef Banora and Janice de Almeida Engler
- 95 Transcriptomic Signatures of Transfer Cells in Early Developing Nematode Feeding Cells of *Arabidopsis* Focused on Auxin and Ethylene Signaling**  
Javier Cabrera, Marta Barcala, Carmen Fenoll and Carolina Escobar
- 104 Role of Callose Synthases in Transfer Cell Wall Development in Tocopherol Deficient *Arabidopsis* Mutants**  
Hiroshi Maeda, Wan Song, Tammy Sage and Dean DellaPenna
- 119 Associations between the Acclimation of Phloem-Cell Wall Ingrowths in Minor Veins and Maximal Photosynthesis Rate**  
William W. Adams Iii, Christopher M. Cohu, Véronique Amiard and Barbara Demmig-Adams



# Transfer cells

David W. McCurdy<sup>1\*</sup> and Gregorio Hueros<sup>2</sup>

<sup>1</sup> Centre for Plant Science, School of Environmental and Life Sciences, The University of Newcastle, Newcastle, NSW, Australia

<sup>2</sup> Departamento Biomedicina y Biotecnología (Genética), Universidad de Alcalá, Madrid, Spain

\*Correspondence: david.mccurdy@newcastle.edu.au

**Edited and reviewed by:**

Steven Carl Huber, United States Department of Agriculture-Agricultural Research Service, USA

**Keywords:** transfer cells, cell wall ingrowths, basal endosperm transfer layer, syncytia, phloem parenchyma transfer cells, giant cells

Advances in plant science research will lie at the center of efforts to address global food security as demand for agricultural production is predicted to more than double by 2050. A key determinant of plant productivity and thus crop yield is efficient nutrient transport between sites of net nutrient synthesis and acquisition to sites of net utilization. Transfer cells (TCs) play key roles in optimizing such nutrient transport processes in plants, and thus research on these anatomically specialized cell types has the potential to contribute new approaches for improving plant performance. The collection of reviews and research articles in this Research Topic on Transfer Cells provides a valuable contribution to advancing our understanding of these important cell types in plant biology.

TCs *trans*-differentiate from existing cell types by developing extensive wall ingrowths. The resulting increase in plasma membrane surface area enables increased densities of membrane transporters to optimize nutrient transport across apoplastic/symplasmic boundaries at sites where TCs form. Key challenges in TC biology include understanding the signals and genetic pathways required for initiating and building the unique wall ingrowths that define TC identity. This knowledge in turn will provide a basis to investigate physiological and genetic factors explaining the variability observed in TC differentiation, even among equivalent anatomical situations in highly related species.

Amongst many other scenarios, TCs are involved in delivery of nutrients between generations and, as evidenced by the number of contributions in this Research Topic, considerable focus is being directed toward investigating endosperm TCs in seeds of cereals such as maize and barley. Thiel (2014) provides a comprehensive review of the development of these cells in barley, including transcript profiling studies which have revealed a likely role for two-component signaling pathways in endosperm TC differentiation, in addition to identifying a developmental switch across grain filling from active to passive modes of nutrient uptake as revealed by expression profiles of membrane transporter genes. Lopato et al. (2014) review the field of endosperm TC-specific genes and their encoded proteins, emphasizing the potential for using promoters of such genes for biotechnological applications. Identifying the repertoire of genes showing TC-specific expression provides important molecular insight into these cell types, and two research articles contribute to this goal. Royo et al. (2014) describe the non-overlapping expression of *BETL9* and *BETL9like*, two lipid transfer genes similar to *END-1* expressed specifically in barley endosperm TCs. While the functions of

these genes remain unknown, *BETL9* is expressed exclusively in the basal endosperm transfer layer (BETL), but protein product accumulates in maternal tissue adjacent to this layer. In contrast, *BETL9like* is expressed specifically in the endosperm aleurone layer. The expression domains of these genes completely surround the filial tissues, suggesting a protective role at the maternal-filial interface. The *miniature1* (*mn1*) mutant in maize is defective in a BETL-specific cell wall invertase (INCW2), resulting in reduced hexose levels and wall ingrowth development in this tissue. Silva-Sánchez et al. (2014) report a comparative glycoproteome analysis of developing endosperm in *mn1* seed compared to the wild type *Mn1*. Most of the identified proteins showing decreased glycosylation in *mn1* were involved in post-translational modification, protein turnover, chaperone function, carbohydrate metabolism and cell wall biosynthesis, suggesting links to endoplasmic reticulum stress and the unfolded protein response in the mutant due to compromised glycosylation levels. Muñiz et al. (2014) describe establishment of a PCR-based forward genetic screen using expression domain-specific markers to identify new mutant lines showing altered TC development. Application of this forward genetics approach using genes known to be tissue or developmental-stage specific offers new tools to extend the use of maize as a model for TC research. Finally, Rocha et al. (2014) report the unexpected finding that both reticulate-like and flange wall ingrowths in maize BETL contain significant amounts of lignin, a result counter-intuitive with the presumed need for high rates of nutrient diffusion through the wall ingrowths themselves (see Gunning and Pate, 1974) and the general role of lignification in providing cell wall rigidity and strength. A reassessment of wall ingrowth structure and ontogeny is needed in light of this finding.

Upon infection of root tissue, cyst and root-knot nematodes induce vascular cells to form enlarged feeding cells, termed syncytia and giant cells, respectively. These cell types both form wall ingrowth structures reminiscent of those seen in TCs, and are thought to function similarly to facilitate enhanced rates of apoplastic/symplasmic solute exchange required for feeding the invading nematode. Rodiuc et al. (2014) review the cellular modifications and transport functions of these nematode feeding sites in *Arabidopsis* roots, while Cabrera et al. (2014) review transcriptomic signatures of these cells in *Arabidopsis* with emphasis on auxin and ethylene signaling pathways. In contrast to endosperm TCs in cereals, genes involved in two-component signaling appear not to contribute significantly to the development of nematode

feeding cells, nor are genes associated with early signaling involving reactive oxygen species.

Arabidopsis provides a powerful genetic system to study TC biology (Arun Chinnappa et al., 2013). Phloem parenchyma TCs of leaf minor veins form wall ingrowths which are involved in phloem loading (Haritatos et al., 2000) by facilitating apoplastic unloading of sucrose via the recently discovered sucrose effluxers AtSWEET11 and 12 (Chen et al., 2012). The research paper by Maeda et al. (2014) analyzes the role of callose synthases in TC wall development in the tocopherol deficient mutant *vte2*. When grown at low temperature, *vte2* shows reduced photoassimilate export from leaves due to massive callose deposition specifically in phloem parenchyma TCs. Transcript profiling and knockout studies revealed the confounding result that while *GLUCAN SYNTHASE LIKE 4 (GSL4)* and *GSL11* were induced specifically at low temperature in *vte2*, only disruption of *GSL5* substantially reduced this phloem parenchyma TC-specific production of callose, but had no effect on the low temperature photoassimilate export phenotype of *vte2*. Adams et al. (2014) report a significant correlation between photosynthetic capacity and wall ingrowth development in minor-vein phloem parenchyma (Arabidopsis and *Senecio*) and companion TCs (pea and *Senecio*), consistent with the role of these TCs in supporting photoassimilate export from leaves. In contrast, responses to stress such as application of methyl jasmonate caused increased wall ingrowth deposition in phloem parenchyma TCs alone, indicating cell specific responses of TCs to different signals and possibly different roles for these TCs (sugar export vs physical defense against pathogen infection).

Collectively, the insights into TCs provided in the reviews and research articles assembled for this Research Topic establish a valuable platform for continued investigation of these fascinating cell types in plants. Further research on TCs may unlock key possibilities for improving crop yield and thus contribute to the rapidly approaching challenge of addressing global food security.

## ACKNOWLEDGMENTS

This work was supported by an Australian Research Council Discovery Project grant to David W. McCurdy (DP110100770) and by grants from the Spanish Ministerio de Ciencia e Innovacion to Gregorio Hueros (Gen2006-27783-E and BIO2012-39822).

## REFERENCES

- Adams, W. W. I. I. I., Cohu, C. M., Amiard, V., and Demmig-Adams, B. (2014). Associations between the acclimation of phloem-cell wall ingrowths in minor veins and maximal photosynthesis rate. *Front. Plant Sci.* 5:24. doi: 10.3389/fpls.2014.00024
- Arun Chinnappa, K. S., Nguyen, T. T. S., Hou, J., Wu, Y., and McCurdy, D. W. (2013). Phloem parenchyma transfer cells in Arabidopsis – an experimental system to identify transcriptional regulators of wall ingrowth formation. *Front. Plant Sci.* 4:102. doi: 10.3389/fpls.2013.00102

- Cabrera, J., Barcala, M., Fenoll, C., and Escobar, C. (2014). Transcriptomic signatures of transfer cells in early developing nematode feeding cells of Arabidopsis focused on auxin and ethylene signaling. *Front. Plant Sci.* 5:107. doi: 10.3389/fpls.2014.00107
- Chen, L. Q., Qu, X. Q., Hou, B. H., Sosso, D., Osorio, S., Fernie, A. R., et al. (2012). Sucrose efflux mediated by SWEET proteins as a key step for phloem transport. *Science* 335, 207–210.
- Gunning, B. E. S., and Pate, J. S. (1974). “Transfer cells,” in *Dynamic Aspects of Plant Ultrastructure*, ed A. W. Robards (London: McGraw-Hill), 441–479.
- Haritatos, E., Medville, R., and Turgeon, R. (2000). Minor vein structure and sugar transport in *Arabidopsis thaliana*. *Planta* 211, 105–111.
- Lopato, S., Borisjuk, N., Langridge, P., and Hrmova, M. (2014). Endosperm transfer cell-specific genes and proteins: structure, function and applications in biotechnology. *Front. Plant Sci.* 5:64. doi: 10.3389/fpls.2014.00064
- Maeda, H., Song, W., Sage, T., and DellaPenna, D. (2014). Role of callose synthases in transfer cell wall development in tocopherol deficient mutants. *Front. Plant Sci.* 5:46. doi: 10.3389/fpls.2014.00046
- Muñiz, L. M., Gómez, E., Guyon, V., López, M., Khbaya, B., Sellam, O., et al. (2014). A PCR-based forward genetics screening, using expression domain-specific markers, identifies mutants in endosperm transfer cell development. *Front. Plant Sci.* 5:158. doi: 10.3389/fpls.2014.00158
- Rocha, S., Monjardino, P., Mendonça, D., da Câmara Machado, A., Fernandes, R., Sampaio, P., et al. (2014). Lignification of developing maize (*Zea mays* L.) endosperm transfer cells and starchy endosperm cells. *Front. Plant Sci.* 5:102. doi: 10.3389/fpls.2014.00102
- Rodiuc, N., Vieira, P., Banora, M. Y., and de Almeida Engler, J. (2014). On the track of transfer cell formation by specialized plant-parasitic nematodes. *Front. Plant Sci.* 5:160. doi: 10.3389/fpls.2014.00160
- Royo, J., Gómez, E., Sellam, O., Gerentes, D., Paul, W., and Hueros, G. (2014). Two maize *END-1* orthologs, *BETL9* and *BETL9like*, are transcribed in a non-overlapping spatial pattern on the outer surface of the developing endosperm. *Front. Plant Sci.* 5:180. doi: 10.3389/fpls.2014.00180
- Silva-Sánchez, C., Chen, S., Li, J., and Chourey, P. S. (2014). A comparative glycoproteome study of developing endosperm in the hexose-deficient *miniature1 (mn1)* seed mutant and its wild type *Mn1* in maize. *Front. Plant Sci.* 5:63. doi: 10.3389/fpls.2014.00063
- Thiel, J. (2014). Development of endosperm transfer cells in barley. *Front. Plant Sci.* 5:108. doi: 10.3389/fpls.2014.00108

**Conflict of Interest Statement:** The authors declare that the research was conducted in the absence of any commercial or financial relationships that could be construed as a potential conflict of interest.

*Received: 21 October 2014; accepted: 11 November 2014; published online: 26 November 2014.*

*Citation: McCurdy DW and Hueros G (2014) Transfer cells. *Front. Plant Sci.* 5:672. doi: 10.3389/fpls.2014.00672*

*This article was submitted to Plant Physiology, a section of the journal Frontiers in Plant Science.*

*Copyright © 2014 McCurdy and Hueros. This is an open-access article distributed under the terms of the Creative Commons Attribution License (CC BY). The use, distribution or reproduction in other forums is permitted, provided the original author(s) or licensor are credited and that the original publication in this journal is cited, in accordance with accepted academic practice. No use, distribution or reproduction is permitted which does not comply with these terms.*



# Development of endosperm transfer cells in barley

Johannes Thiel\*

Department of Molecular Genetics, Leibniz Institute of Plant Genetics and Crop Plant Research (IPK), Gatersleben, Germany

**Edited by:**

Gregorio Hueros, Universidad de Alcalá, Spain

**Reviewed by:**

David McCurdy, The University of Newcastle, Australia  
Joaquín Royo, Universidad de Alcalá, Spain

**\*Correspondence:**

Johannes Thiel, Department of Molecular Genetics, Leibniz Institute of Plant Genetics and Crop Plant Research (IPK), Corrensstrasse 3, D-06466 Gatersleben, Germany  
e-mail: thiel@ipk-gatersleben.de

Endosperm transfer cells (ETCs) are positioned at the intersection of maternal and filial tissues in seeds of cereals and represent a bottleneck for apoplastic transport of assimilates into the endosperm. Endosperm cellularization starts at the maternal-filial boundary and generates the highly specialized ETCs. During differentiation barley ETCs develop characteristic flange-like wall ingrowths to facilitate effective nutrient transfer. A comprehensive morphological analysis depicted distinct developmental time points in establishment of transfer cell (TC) morphology and revealed intracellular changes possibly associated with cell wall metabolism. Embedded inside the grain, ETCs are barely accessible by manual preparation. To get tissue-specific information about ETC specification and differentiation, laser microdissection (LM)-based methods were used for transcript and metabolite profiling. Transcriptome analysis of ETCs at different developmental stages by microarrays indicated activated gene expression programs related to control of cell proliferation and cell shape, cell wall and carbohydrate metabolism reflecting the morphological changes during early ETC development. Transporter genes reveal distinct expression patterns suggesting a switch from active to passive modes of nutrient uptake with the onset of grain filling. Tissue-specific RNA-seq of the differentiating ETC region from the syncytial stage until functionality in nutrient transfer identified a high number of novel transcripts putatively involved in ETC differentiation. An essential role for two-component signaling (TCS) pathways in ETC development of barley emerged from this analysis. Correlative data provide evidence for abscisic acid and ethylene influences on ETC differentiation and hint at a crosstalk between hormone signal transduction and TCS phosphorelays. Collectively, the data expose a comprehensive view on ETC development, associated pathways and identified candidate genes for ETC specification.

**Keywords:** barley seed, endosperm transfer cells, cell wall ingrowths, tissue-specific analysis, nutrient transport, TCS, ABA, ethylene

## INTRODUCTION

Transfer cells (TCs) occur ubiquitously in all taxonomic groups of the plant kingdom as well as in algae and fungi. TCs represent highly specialized cells modified to facilitate enhanced transport capacities of nutrients. Unique characteristics of these cells are thickened cell walls and massive, localized wall ingrowths to enrich the membrane surface for transport processes. In general, TCs are located at strategically important positions for nutrient acquisition and exchange, such as symplasmic/apoplastic interfaces in vascular tissues and seeds, reproductive and secretory organs and at contact points of plant/symbiotic and plant/parasitic interactions. In the last decade, TCs in seeds have been the object of intensive investigation due to their pivotal role in feeding the new generation and the impact on seed filling. Developing seeds are sink tissues depending on nutrient supply from vegetative tissues, accordingly efficient assimilate transfer into seeds is yield-determining and of high agronomical interest. In the developing barley grain, incoming assimilates are released from the maternal grain part by the nucellar projection (NP), which is responsible for transfer but also for interconversion of assimilates, especially amino acids (Thiel et al., 2009). Released assimilates are taken up by endosperm transfer cells (ETCs) and supplied to the endosperm. ETCs are positioned

at the maternal-filial boundary of grains and might also play an essential role in communication of maternal and filial tissues by transmitting signals into the endosperm (Thiel et al., 2008).

Anatomy of TCs in seeds can be distinguished by two principle types of cell wall ingrowth architecture, the “flange” or “reticulate” type. A prominent example for the reticulate wall ingrowth-type is represented in epidermal TCs of *Vicia faba* cotyledons. Reticulate wall ingrowths are initiated as discrete papillar projections that appear as randomly located depositions on the primary cell wall. Further repetitions of branching and fusion with neighboring ingrowths result in the formation of a multi-layered, fenestrated wall ingrowth labyrinth (Talbot et al., 2001; McCurdy et al., 2008). Flange wall ingrowths are deposited as parallel ribs or bands of cell wall material emerging from the primary cell wall. By affiliation of adjacent ribs -predominantly toward the basal part of the cell- a dense network of flanges is created. This morphology is found in basal endosperm transfer cells (BETCs) of maize kernels (Talbot et al., 2002; Zheng and Wang, 2010) and ETCs in wheat and barley (Zheng and Wang, 2011; Thiel et al., 2012a). In addition to these peculiar anatomical differences between TCs observed in legume and cereal seeds, the genetic origin of the cells is fundamentally different. Legume

TCs originate from the diploid embryo by a trans-differentiation process converting abaxial epidermal cells of the cotyledons into TCs (Offler et al., 1997). This process of “re-differentiation” of cells is deemed to be part of the developmental program of several types of TCs or is induced by abiotic and/or biotic stresses. ETCs of cereal grains are part of the triploid endosperm which is composed of four different cell types: starchy endosperm, embryo-surrounding region, aleurone and TCs. After fertilization of the central cell of the megagametophyte by the second male gamete, endosperm development of barley starts with divisions of nuclei without building of cell walls resulting in the formation of the endosperm coenocyte. Cell fate specification occurs already in the endosperm coenocyte (Olsen, 2001) and is proposed to be determined by positional signaling (Gruis et al., 2006). Endosperm cellularization is accompanied by the differentiation of the NP, the part of the nucellus facing the main vascular bundle. Cellularization of the endosperm starts around 3–4 days after flowering (DAF) in the outermost cell row adjacent to NP generating the highly specialized ETCs whereas the other cells in peripheral positions assume aleurone cell fate later on (6/7 DAF). This raises the question which genetic regulators give rise for the early specification of this distinct region of the syncytium which later on differentiates to ETCs while other endosperm cells differentiate to aleurone, subaleurone and starchy endosperm. The *END1* gene of barley and its wheat ortholog has been associated to the specification of the ETC region due to the specific expression in the coenocytic nuclei which is a prerequisite for development of ETCs (Doan et al., 1996). Another molecular marker inducing TC identity has been found in maize BETCs by Gomez et al. (2002). ZmMRP-1 is a MYB-related R1-type transcription factor and has been shown to transactivate the promoters of *BETL1* (Gomez et al., 2002), *Meg1* (Gutierrez-Marcos et al., 2004) as well as *ZmTCRR1* (Muñiz et al., 2006) genes, which are also specifically expressed in BETCs. The imprinted *Maternally expressed gene 1* (*ZmMeg1*) is located at the plasma membrane and extracellular matrix of ETCs and has been shown to play a key role in specification and differentiation of BETCs. *Meg1*-knockdown resulted in impaired BETC development with diminished cell wall ingrowths and clearly affected nutrient uptake, sucrose partitioning and seed biomass (Gutierrez-Marcos et al., 2004; Costa et al., 2012). As mentioned, other genes specifically expressed in maize BETCs encode for members of the small, cysteine-rich BETL family (BETL1-4), two type-A response regulators (ZmTCRR1,-2; Muñiz et al., 2006, 2010) and for the *Mn1*-encoded cell wall invertase 2 (INCW2; Cheng et al., 1996). However, these genes are predominantly expressed during the mid-term endosperm development (8–16 DAP) and might therefore play a role in structural specification of TCs (i.e., establishment of wall ingrowths) rather than in acquisition of cell identity. Remarkably, the expression of *ZmMRP-1* is induced by sugars, most effectively by glucose (Barrero et al., 2009), which might be attributed to INCW2 activity. The phytohormones auxin and ethylene have been shown to function as important compounds determining TC differentiation. Dibley et al. (2009) uncovered a role for auxin and ethylene signaling in TC induction and development by using an *in vitro* culture system to selectively induce trans-differentiation to a TC morphology in

*V. faba* cotyledons. The expression of ethylene biosynthesis genes and ethylene signaling elements in tight correlation with ROS signaling might play an inductive role in formation of polarized cell wall ingrowths in *Vicia* cotyledons (Zhou et al., 2010; Adriunas et al., 2011). A role for ethylene in ETC differentiation in barley seeds was elucidated by LM-based transcript profiling of ETCs and cells of the NP (Thiel et al., 2008), which revealed a preferential expression of enzymes associated with ethylene biosynthesis and catabolism as well as several AP2/EREBP transcription factors in ETCs. This is in agreement with the finding that direct application of the ethylene precursor 1-aminocyclopropane-1-carboxylic acid (ACC) increased the number of cells forming wall ingrowths during TC formation in tomato roots (Schikora and Schmidt, 2002).

However, the underlying molecular mechanisms determining acquisition of TC fate and further development are poorly understood. Subsequently, the elucidation of signals activating key regulators directing ETC specification in the syncytial endosperm and further differentiation to achieve characteristic TC anatomy would be a challenging task toward a deeper understanding of these specialized plant cells.

This article reviews results from tissue-specific transcriptome and metabolome analyses which have been performed by using LM-based techniques for the isolation of this specific cell type. Transcriptionally activated pathways, regulatory networks as well as new modes of signal transduction potentially implicated in barley ETC differentiation are highlighted in the article.

## HISTOLOGICAL ANALYSIS OF BARLEY ENDOSPERM TRANSFER CELLS DEPICTS DISTINCT TIME POINTS IN ESTABLISHING TRANSFER CELL MORPHOLOGY

Morphogenesis of barley ETCs from initial steps (just before/at cellularization) until establishment of TC structure (3/4 to 12 DAF) was analyzed by light, scanning electron and transmission electron microscopy. An overview about barley grain tissues and a magnification of the crease region is given in **Figures 1A,B**. At 3/4 DAF, the filial grain part is composed of the endosperm coenocyte, a seam of cytoplasm containing free nuclei, surrounding the large endosperm vacuole (**Figure 1E**). Cellularization starts in the region of the syncytium facing the NP whereas in the dorsal part of the syncytium cellularization has not yet been initiated. First smooth and thin cell walls are visible in the emerging cell row, dividing nuclei indicate high mitotic activity in the ETC region (**Figures 1F,G**). The cells contain a dense cytoplasm rich in organelles of the endomembrane secretory system, like the endoplasmatic reticulum (ER), dictyosomes and secretory vesicles. Cellularization has just started and segments of cell walls are apparent but seem not to border complete cells (**Figure 1H**). At 5 DAF, cellularization of the ETC region is completed. Up to three rows of cells facing the NP are apparently different from the other cells of the endosperm (**Figure 1I**). They are characterized by a rounded shape, smaller size, and dense cytoplasm with small vacuoles. Cell walls appear subtle and thin; branching and deposition of cell wall ingrowths are not visible at 5 DAF (**Figure 1K**). The slender nature of wall anatomy is supported by DIC fluorescence microscopy (**Figure 1J**) which was used as

a method to visualize cell wall morphology by detecting the autofluorescence of cellulose-containing cell contents. As illustrated in further pictures (**Figures 1N,R,V**), the red autofluorescence reflects the changing cell wall architecture as observed by electron microscopy. Cells show a strong compartmentation with organelles of the secretory system (ER and dictyosomes) and multiple mitochondria predominantly adjacent to the cell wall (**Figure 1L**).

At 7 DAF, differences in the cell wall architecture between ETCs and endosperm cells became pronounced. Cell walls are clearly thickened preferentially in the direction toward the endosperm (**Figure 1M**). First branches of ribbed cell wall depositions covering the inner surface of walls can be detected (**Figure 1O**). Fusion of branched flange-like strands is predominantly visible in the basal part of the cell at the corners contacting adjacent cells and thereby indicating a differentiation gradient in the formation of wall ingrowths (**Figure 1P**). More generally, the structure of the intracellular compartments seems to change at 7 DAF: central vacuoles and deposition of small starch granules can be monitored as well as a strong orientation of mitochondria and banded ER to wall ingrowths. Presumably, this re-arrangement of cellular organization is related to the initiation of wall ingrowth formation. Areas of cell walls further increase during ongoing development of ETCs (10 DAF) and cells are completely lined by massive walls (**Figure 1R**). Cell walls show parallel rib-shaped projections fused at parallel protrusions (**Figure 1S**) which lead to the characteristic Y-shaped structure of flanges as visible in the TEM picture (**Figure 1T**). In contrast, cells of the starchy endosperm -located only some rows below- show a glossy surface without any wall depositions (**Figure 1D**). ETCs obtain a more rectangular shape and starch grains are visible in the second and third layer of ETCs (**Figure 1Q**). ER appeared to be constantly striped and nestled to the thickened walls. At 12 DAF, cell wall and its ingrowths emerge asymmetrically and thereby, covering the main part of the cell (**Figures 1U–X**). The cytoplasm of ETCs is less dense and seems to be reduced compared to earlier stages (**Figure 1X**); fewer mitochondria and dictyosomes can be observed and the cell surface is dominated by a large vacuole and storage bodies (starch, lipids).

#### ESTABLISHMENT OF TRANSFER CELL MORPHOLOGY PROCEEDS ENDOSPERM GROWTH

Growth behavior of ETCs and changes in size was determined using 3D histological images during barley grain development (5–14 DAF) by calculating the geometric expansions in transverse and longitudinal directions (Bollenbeck and Seiffert, 2008). The volume of ETCs increases 9-fold from 5 to 10 DAF but decreases thereafter around 30% at 14 DAF (**Figure 1C**). Interestingly, the volume increment of ETCs proceeds that of the endosperm which shows a strong augmentation between 10 and 14 DAF (Thiel et al., 2012a). Thus, it can be concluded that ETCs have to be fully developed before the endosperm growth rises exponentially. This clearly supports the concept that ETCs represent a kind of bottleneck for assimilate transfer into the filial grain parts and suggests that grain filling is tightly related to the developmental status of ETCs.

#### TISSUE-SPECIFIC STUDIES UNRAVELED DEVELOPMENTAL PROGRAMS AND ASSOCIATED PATHWAYS DURING ENDOSPERM TRANSFER CELL DIFFERENTIATION

##### EARLY ETC DIFFERENTIATION IS CHARACTERIZED BY TRANSCRIPTIONAL ACTIVITIES REGULATING CELL SHAPE AND RELATES INTENSIVE CELL WALL TO RESPIRATORY METABOLISM

Hidden inside the grain, ETCs are barely accessible by manual preparation. To get information about molecular processes occurring in ETCs, LM-assisted methods for transcript and metabolite analyses of barley grain tissues have been developed. Microarray analysis of ETCs at different stages of grain development (5–12 DAF) provided comprehensive information about transcriptionally activated pathways and underlying transcriptional networks determining ETC differentiation (Thiel et al., 2012a). Intriguingly, at the early stages of differentiation concurrent with the cellularization process a multitude of transcripts related to cell division, cell shape control, intracellular vesicle trafficking as well as cell wall biosynthesis and primary metabolism are preferentially expressed. Transcripts encoding cyclins, proteins controlling cell cycle and cell cycle-associated kinases as well as microtubule associated proteins,  $\beta$ -tubulins and expansins indicate distinct cell proliferation and cell shape control at 5 DAF. Simultaneously more than 40 transcripts related to vesicle formation and vesicle transport are predominantly expressed at 5 and 7 DAF, among them, genes encoding kinesins, motor-related proteins, actins and tubulins. Two transcripts encoding Rab-GTPases are upregulated at 7 DAF which potentially bind intracellular vesicles to recruit motor proteins (Deneka et al., 2003).

V-type ATPases, autophagy-related proteins and vacuolar sorting proteins might be involved in endocytic and secretory trafficking. This reflects the dense accumulation of organelles of the endomembrane secretory system in the cytoplasm of early ETCs. Cell wall biosynthesis is predominantly stimulated at 5 DAF and to a less degree at 7 DAF. Transcription of several cellulose synthase-like and cellulose synthase genes accompanied by glucan synthases and transferases, enzymes involved in biosynthesis of mannose sugars, arabinoxylans and pectins indicate complex patterns in cell wall biosynthesis. Remarkably is the expression profile of genes involved in callose metabolism like 1,3- $\beta$ -glucan synthases/transferases and 1,3- $\beta$ -glucanases with a preferential expression at 5 DAF indicating a high turnover just after cellularization. In endosperm cells, callose has been shown to be involved in cell plate formation and early cell wall development (Brown et al., 1997) but the exact role in ETC differentiation remains unclear. Distinct transcripts related to primary metabolism are preferentially expressed at 5 and 7 DAF: high transcript amounts of enzymes related to mitochondrial activity (TCA cycle, respiration) and glycolysis particularly at 7 DAF suggest the demand for energy which is probably needed for ATP-consuming processes, such as cell wall biosynthesis and its further differentiation. The abundance of transcripts involved in carbohydrate/starch metabolism supports this assumption. Furthermore, multiple genes transcriptionally activated at 5 and 7 DAF are associated to amino acid catabolism and the adjustment of C:N balances (Thiel et al., 2012a). Taken together, the data set provides insights into transcriptional pathways that relate energy-generating metabolic activities and stimulated cell wall biosynthesis. The developmental

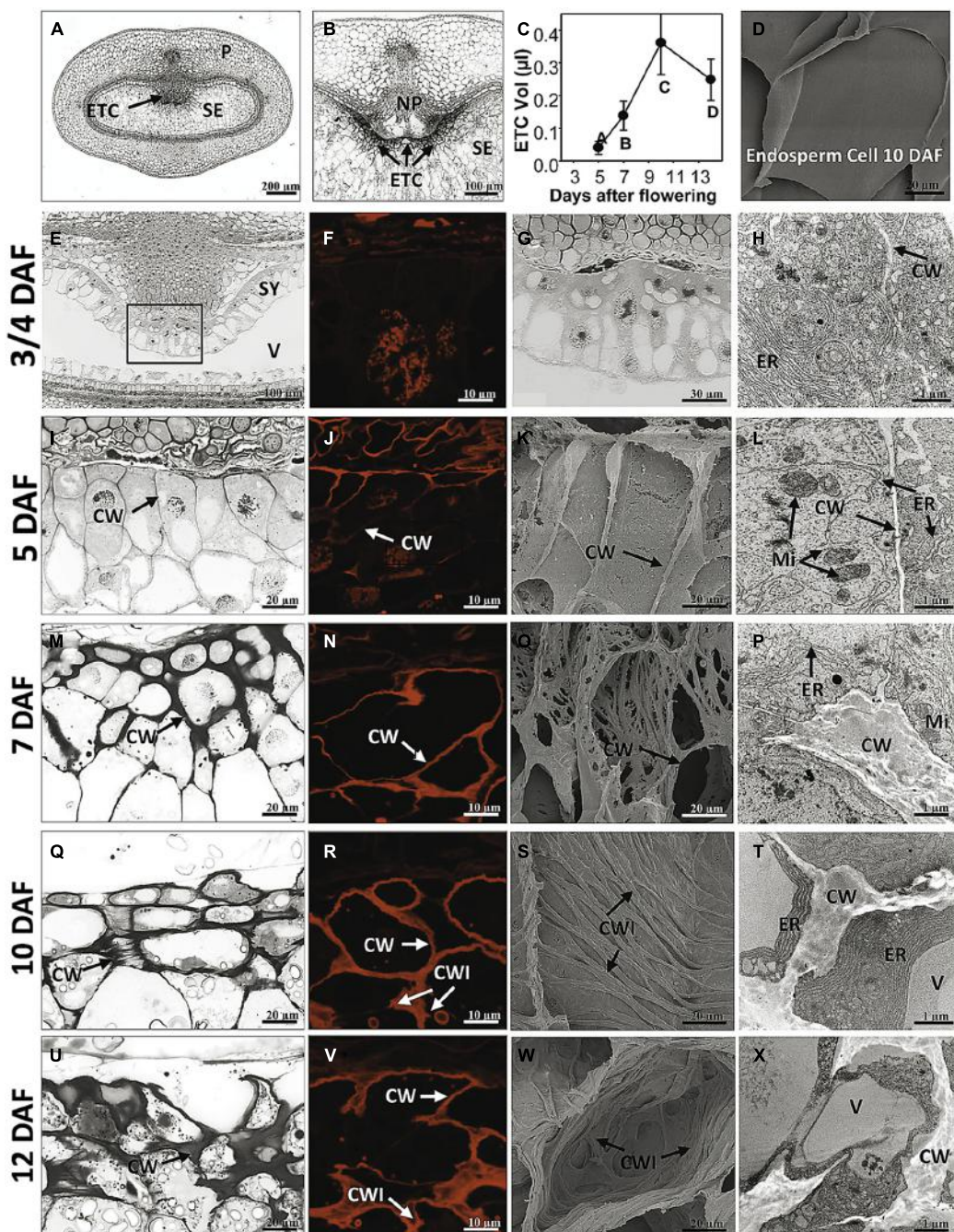


**FIGURE 1 | Morphological and ultrastructural analysis of barley ETC development.** Light microscopy (E,G,I,M,Q,U), DIC fluorescence microscopy (F,J,N,R,V), scanning electron (K,O,S,W) and transmission electron microscopy (H,L,P,T,X) images show ETC differentiation from cellularization (3/4 DAF) until the establishment of transfer cell structure (12 DAF). (A) Median cross section of a barley grain at 7 DAF depicts grain tissues and (B) magnification shows the transfer region of barley grains. (C) Volume of ETCs from 5 to 14 DAF, (D) scanning electron picture of an endosperm cell at 10 DAF. At 3/4 DAF, cellularization in the region of the syncytium facing the nucellar projection has just started (E,G). Cells contain a dense cytoplasm, rich in organelles of the endomembrane secretory system, and segments of cell walls are apparent but do not border complete cells (arrow, H). At 5 DAF, cellularization of the ETC region is completed; up to three rows of cells facing the NP are apparently different from the other cells of the

endosperm (I). Cell walls appear subtle and thin; branching and deposition of cell wall ingrowths are not visible (K). Cells show a strong compartmentation and multiple mitochondria predominantly adjacent to the cell wall (arrows, L). At 7 DAF, cell walls are clearly thickened (M) and first branches of ribbed cell wall depositions covering the inner surface of walls can be detected (O). At 10 DAF, area of cell walls further increase and cells are completely lined by massive walls (Q,R). Cell walls show parallel rib-shaped depositions characteristic for the flange-type ingrowths (S). ER appeared to be constantly striped and nested to the thickened walls (T). At 12 DAF, cell wall and ingrowths emerge asymmetrically and cover the main part of the cell (U–X). The cytoplasm is reduced compared to earlier stages (X). CW, cell wall; CWI, CW ingrowths; ER, endoplasmic reticulum; Mi, mitochondria; ETC, endosperm transfer cells; NP, nucellar projection; SE, starchy endosperm; SY, syncytium; V, vacuole (images modified after Thiel et al., 2012a).

stages just after cellularization when ETCs have adopted cell fate and first cell wall depositions can be detected (5–7 DAF) is consistent with the idea that the demand for respiratory energy and carbohydrates is high for cell wall development.

#### THE PATTERN OF TRANSCRIPTIONALLY ACTIVATED TRANSPORTER GENES CHANGES WITH THE ONSET OF GRAIN FILLING

As ETCs control assimilate and nutrient uptake from maternal tissues into the endosperm via an apoplastic barrier, the transcriptional activities of transporter genes address the main function of these cells. Developing seeds are sink tissues importing photoassimilates in solution by bulk flow through the phloem. Major transported solutes are sucrose, amino acids and monosaccharides. Expression of invertases and monosaccharide transporter in early legume and cereal seed development governs the distribution of free sugars which play a pivotal role in regulating TC function and simultaneously, determining final endosperm and embryo cell number (Thompson et al., 2001). ETC-specific transcriptome analysis at distinct stages of barley grain development showed a wide array of expressed transporter genes possibly related to endosperm development (Figure 2). Several genes show a peak of expression directly after cellularization (5 DAF); eight amino acid, nine sugar, and two potassium transporter are highly expressed. Transcriptional activity of several hexose transporters, including *HvSTP1* and transporter for Glc-6-phosphate, UDP-Glc and UDP-galactose, indicate a high influx of hexose sugars probably feeding glycolysis or providing precursors of cell wall synthesis. The high expression of transcripts related to cell wall biosynthesis, particularly to UDP-Glc metabolism corresponds to transporter gene activities. *HvSTP1* has been shown to be expressed in very early endosperm development (from the syncytial stage on) and to be spatially and temporally associated with the cell wall invertase1 (*HvCWIN1*) suggesting an interplay between liberation of hexoses by invertase activity and active uptake by *HvSTP1* (Weschke et al., 2003). An interesting gene is the barley ortholog to the wheat *TaSWEET2*, assigned as *HvSWEET2*, which depicts the same profile with highest transcript levels at 5 DAF. Most of the recently discovered membrane-associated SWEET proteins have been shown to function as monosaccharide, particular glucose transporter in *Arabidopsis* (Slewinsky, 2011). A genetic analysis of *AtSWEET11* and -12 revealed that these two transporters are capable of transporting sucrose and control sucrose release from phloem parenchyma TCs for uptake into sieve element/companion cell complexes (Chen et al., 2012). A set of amino acid transporter with different substrate specificities (neutral/aromatic, lysine/histidine, peptides; assignment according to Kohl et al., 2012) is predominantly expressed at 5 DAF corresponding to a stimulated amino acid metabolism at this time point. All of these transporters have in common that they catalyze proton-coupled/energy-dependent active transfer of nutrients. In addition to the transcriptome analysis, metabolite profiling of developing ETCs has been performed by a GC-MS approach (Thiel et al., 2012a). Metabolite abundances display distinct profiles during development from cellularization until further differentiation/maturation of ETCs. Several amino acids, among them the transport form glutamine and lysine, are most abundant at 5 DAF. Enhanced glutamine levels potentially result from high activity

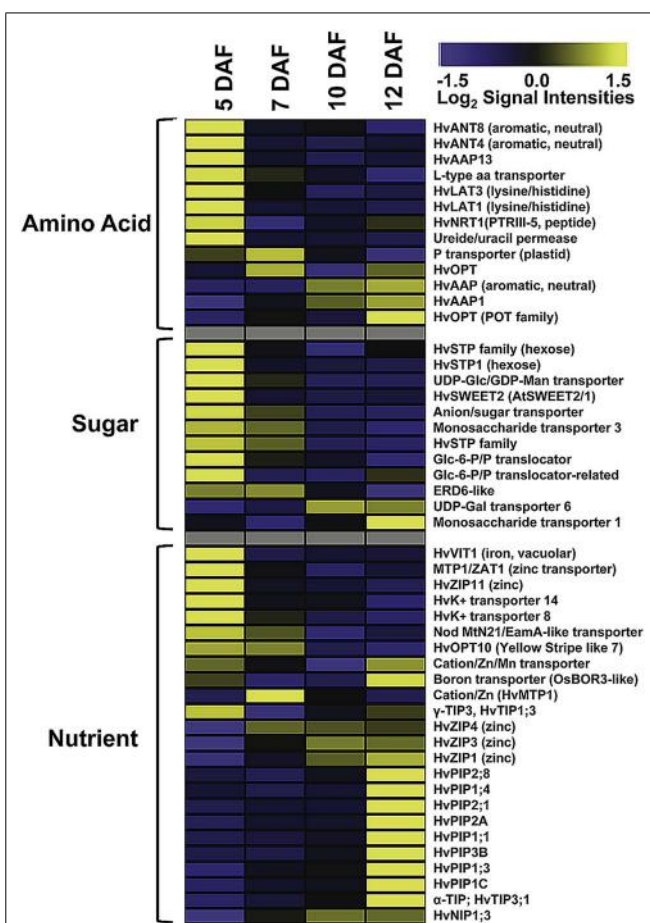


**FIGURE 2 | Expression profiles of transporter genes in developing ETCs as determined by microarray analysis.** Transcript levels are median-centered and  $\log_2$ -transformed. Transcript levels are indicated by color code: yellow, high; blue, low [data were selected from transcriptome analysis presented by Thiel et al. (2012a)].

of Gln synthase in the NP which has been observed by a tissue-specific metabolite analysis (Thiel et al., 2009). Cells of NP may convert amino acids in transport forms for active uptake from the apoplastic endosperm cavern by the ETCs. This example nicely demonstrates a coordinated action of these transfer-related tissues at the maternal/filial boundary in allocation of nitrogen to the endosperm. Hexose sugars, like fructose, glucose and glucose-6-phosphate show the highest concentrations at 5 and 7 DAF, respectively, and thereby correspond to the pronounced activities of monosaccharide transporter genes. Sucrose levels clearly peak at 7 DAF and may be an indicator for the switch from high to low hexose:sucrose ratios which might serve as an intracellular signal for the transition of the endosperm into a storage accumulating organ. A recent comparative transcriptome analysis of cells of NP and ETCs in barley grains was in line with these presumptions and revealed a pronounced expression of *HVSUT1* and two amino acid permeases (AAPs) in ETCs before the beginning of grain filling (Thiel et al., 2008).

As visible in Figure 2, the spectrum of transcriptionally activated transporter genes clearly changes with the onset of the

storage phase (10 DAF). Nutrient transporter with less defined substrate specificities, such as different members of the aquaporin family, and micronutrient transporter displayed a strong increase of transcript amounts at 12 DAF, whereas the expression of sugar and amino acid transporter significantly decreased. Aquaporins are channel proteins positioned in the plasma and intracellular membranes of plant cells and function as facilitators of water, neutral solute or gas transport. Aquaporins in plants can be classified into plasma membrane intrinsic proteins (PIPs), tonoplast intrinsic proteins (TIPs), NOD26-like proteins (NIPs), and small basic intrinsic proteins (SIPs). Several HvPIP isoforms specifically peak at 12 DAF and might regulate water and solute flow from the endosperm cavity into the endosperm. Different members of the PIP and TIP family have been shown to be transcriptionally activated in the seed coat and cotyledons of pea seeds and a role in nutrient release for the embryo is anticipated (Schuurmans et al., 2003). A general role in sensing the osmotic potential and regulation of turgor homeostasis necessary for water equilibrium between phloem and xylem is assumed for PIP aquaporins (Zhang et al., 2007). TIP isoforms are probably localized to different vacuolar compartments from which the subgroup of α-TIPs is postulated to be predominantly associated to protein storage vacuoles (Jauh et al., 1999) and has been found exclusively in developing embryos (Hunter et al., 2007) pinpointing to a role in lytic/remobilization processes. Noticeable is the emerging expression of three genes encoding zinc-/iron-regulated transporter-like proteins (ZIPs), cation/Zn transporter/metal tolerance protein (HTP1) and a boron transporter from 10 DAF on. ZIPs are capable of transporting divalent metal ions (i.e., zinc, iron) and are suggested to play critical roles in balancing metal uptake and homeostasis. Homeostasis of micronutrients is essential for plant growth and development as their deficiency or excess severely impaired physiological and biochemical reactions of plants. The storage of micronutrients in seeds is of high relevance for seedling growth after germination and represents also an important trait for the nutritional value of crop seeds. In maize kernels, novel identified ZmZIP genes revealed distinct temporal expression patterns in embryo and endosperm indicating a complex regulation of ion translocation and/or storage in embryo and endosperm development (Li et al., 2013). A transcriptome analysis of different tissues from barley grains observed specific patterns of metal transporter activities in embryo, endosperm, aleurone, and maternal tissues of the transfer zone (i.e., NP cells; Tauris et al., 2009). Comparable to ETCs (see **Figure 2**), members of the ZIP, VIT, and yellow stripe like (YSL) families have been shown to be highly expressed in the transfer zone and probably contribute to zinc/metal supply to the endosperm and/or embryo, but due to different developmental time points of the investigated grains (onset of storage phase – late storage phase) a direct relation is difficult to draw. A study visualizing nutrient distribution in the wheat grain at the end of the storage phase (25 DAF) by laser ablation inductively coupled plasma mass spectrometry (LA-ICP-MS) imaging showed an accumulation of micronutrients preferentially in the scutellum of the embryo (Wu et al., 2013). Besides, iron and zinc seem to be enriched in the ETC region but with lower amounts compared to the scutellum. Accordingly, a transfer route of these micronutrients for provision

of the embryo could start with an uptake from the maternal sites of efflux (NP) in the filial grain part by ETCs, from where it is directed toward the embryo-near region and actively absorbed by the scutellum. Assuming the high expression of ZIPs at the onset of the storage phase (10 DAF) this developmental stage could represent the starting point for Zn/Fe-accumulation in the embryo, although micronutrient distribution patterns have been analyzed later in grain development and need to be verified for earlier stages.

In conclusion, transcript profiles of transporter genes in ETCs revealed development-specific patterns of expression. Although transcript abundances do not necessarily reflect protein amounts or temporal protein activities, the data suggest a general transition from active to passive modes of transport. After cellularization and during early ETC development (5–7 DAF) active nutrient uptake seems to be dominating as concluded from high transcript amounts of amino acid, monosaccharide and potassium transporter, which are energy coupled and driven by the proton-motive force. High hexose and amino acid concentrations, which have been shown to peak between 5 and 7 DAF, are probably needed for differentiation processes in the ETCs itself but also for cell proliferation and rapid growth of the endosperm. Between 7 and 10 DAF a change in gene activities from active to passive transport mechanisms was observed. Expression of micronutrient transporter and an array of aquaporins arose with the beginning of the storage phase. In accordance, intracellular changes have been observed in ETCs at 12 DAF. The cytoplasm of ETCs seems to be generally reduced compared to earlier stages, possibly this structural modifications might be associated with the shift to passive modes of transport. In summary, observed changes might be related to the switch in caryopsis development during the intermediate phase between 6 and 10 DAF where a metabolic and transcriptional reconfiguration indicates the transition of the endosperm into a storage accumulating organ (Sreenivasulu et al., 2006). The beginning of the accumulation process coincides with the switch from maternal to filial control of grain development and this might be also reflected in the changing patterns of transporter gene activity.

## IDENTIFICATION OF SIGNALS REGULATING ENDOSPERM TRANSFER CELL SPECIFICATION AND DIFFERENTIATION

### TISSUE-SPECIFIC 454 TRANSCRIPTOME SEQUENCING IDENTIFIED TCS PHOSPHORELAYS AS A MAJOR SIGNAL TRANSDUCTION PATHWAY IN ETCs

To identify new sequence information putatively involved in early differentiation of barley ETCs, 454 transcriptome sequencing of the differentiating ETC region from the syncytial stage until functionality has been performed (3–7 DAF). Tissues were isolated by laser-assisted microdissection and the transcriptome was analyzed by pyro-sequencing. Surprisingly, about 40% (17,028) of the generated contigs were not present in barley EST databases and represent ETC-specific sequences (Thiel et al., 2012b). Screening the data set for signaling components uncovered an intriguingly high amount of transcripts encoding elements of the two-component signaling (TCS) system to be specifically expressed in this endosperm region. Forty genes probably being part of the TCS were identified in the ETC transcriptome during the

narrow time period of 4 days, thereby covering all components and subfamilies of the TCS system (**Figure 3A**). The TCS represents an ancient signal transduction pathway firstly discovered in bacteria and has previously been shown to be co-opted by eukaryotic organisms, like fungi and plants, whereas in animals and humans this signaling route does not exist. In plants, the TCS persists of a multi-step phosphorelay involving phosphorylation of His and Asp residues of proteins in a modular arrangement and thereby, transmits a signal from the membrane to the nucleus to modulate cellular responses (Schaller et al., 2008). TCS phosphorelays have been shown to be implicated in the perception of external signals, such as sensing of nutrient availability, abiotic stresses, and to regulate various aspects of plant development (Sakakibara et al., 1998; Leibfried et al., 2005; Mizuno, 2005; Chefedor et al., 2006; Kim et al., 2006; Riefler et al., 2006). Information about implications in developmental programs of plants is largely related to cytokinin signaling (Schaller et al., 2008), but interactions with signaling pathways of other hormones, like ethylene, abscisic acid (ABA)

or auxins, are indicated by several studies (Hass et al., 2004; Wohlbach et al., 2008; Kakani and Peng, 2011; Scharein and Groth, 2011).

As presented in the phylogenetic tree in **Figure 3Aa** three types of histidine kinase (HK) transcripts were found in barley ETCs: six putative ethylene receptors characterized by a GAF domain, two putative cytokinin receptors with an emblematic CHASE domain and three classical HKs. Six genes encode histidine-containing phosphotransfer proteins (HPts) which act as intermediates in multi-step phosphorelays by converting signals from HKs to response regulators. Among them, three elements with conserved His residues and three pseudo-HPts are transcriptionally activated in ETCs. Response regulators (RRs) execute the signal output of the signal transduction pathway by activating downstream target genes. Three subclasses of RRs have been identified in the ETC transcriptome: three type-A and four type-C RRs which are solely composed of a receiver (REC) domain with short N- and C-terminal extensions and 11 sequences encoding B-type RR elements (Thiel et al., 2012b).

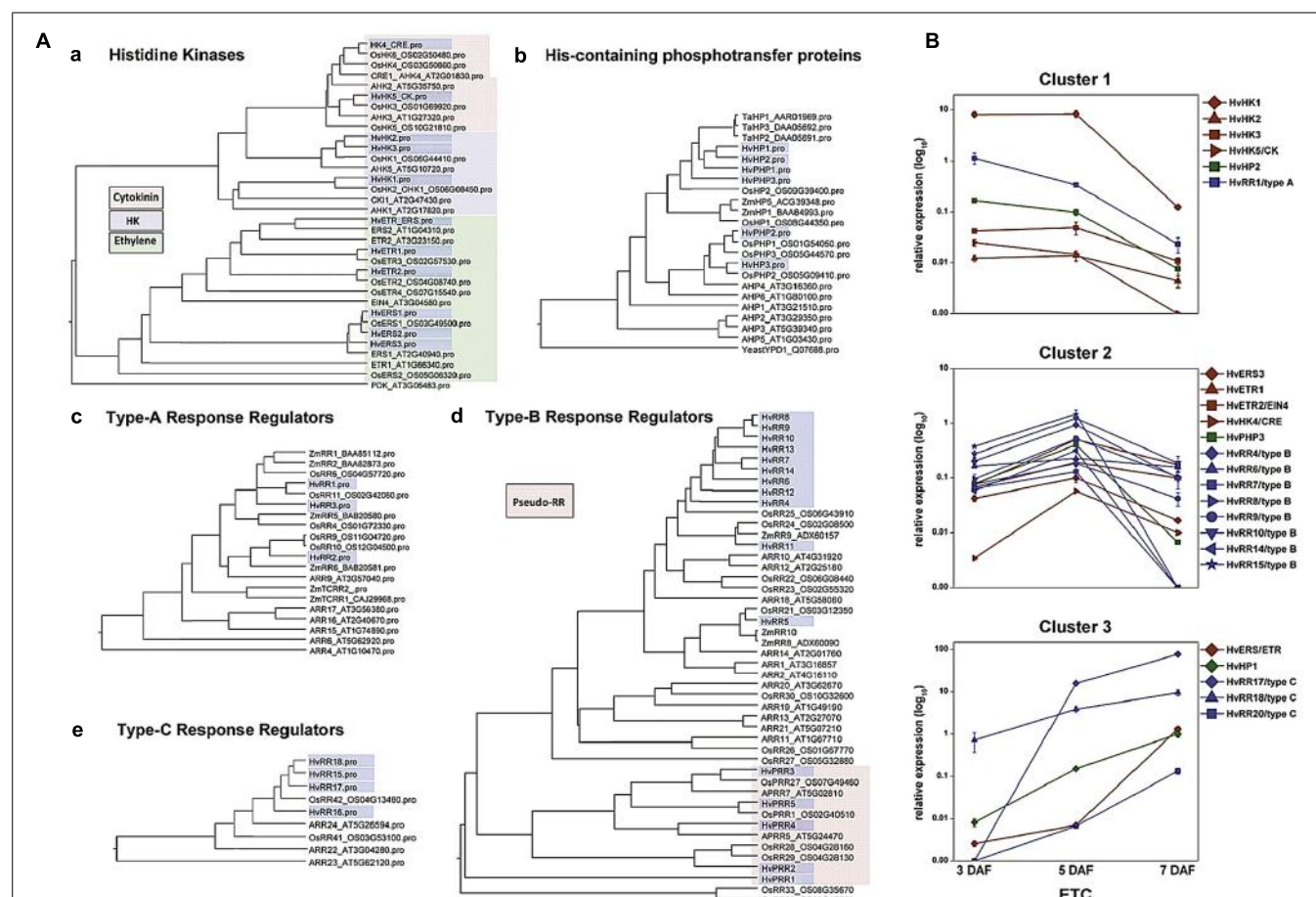


**FIGURE 3 |** Phylogenetic relationship of TCS elements from barley, *Arabidopsis* and rice and expression profiles of selected genes in barley ETCs. **(A)** Barley sequences are highlighted by blue boxes. **(a)** Histidine kinases, colors indicate different subgroups. *Arabidopsis* PDK was used as outgroup. **(b)** Hpt elements, protein sequences of *Z. mays* and *T. aestivum* were additionally included in the alignment. Yeast Hpt protein YPD1 was used

as outgroup. **(c–e)** Type-A, -B, -C response regulators, amino acid sequences of selected maize response regulators were included in the alignment. **(B)** Expression profiles of barley TCS elements in ETCs as determined by qRT-PCR analyses. Expression profiles of candidate genes were grouped by clusters. [Images are reproduced from Thiel et al. (2012b) with permission of PLoS org.]

Type-B RRs are structurally differing from other RRs as they contain long C-terminal extensions with a MYB-like DNA binding domain, suggesting that they act themselves as transcription factors (Imamura et al., 1999). The fact that to a great extent TCS sequences were not present in public EST databases supports the specificity for small distinct tissue regions, like differentiating ETCs, and subsequently, indicates an outstanding role for the TCS in intrinsic developmental programs of these cells.

Pioneering work toward a role for TCS phosphorelays in differentiation of maize BETCs came from Muñiz et al. (2006, 2010). They showed a specific transcript accumulation of *ZmTCR1* and -2 in the BETL layer and verified a physical interaction between both proteins with the phospho-intermediate ZmHP2. By qRT-PCR analysis other elements putatively contributing to TCS phosphorelays in maize kernels have been identified but a specific localization of these TCS elements in BETCs has not been resolved so far. Transcript profiling of barley TCS elements in isolated ETCs by qRT-PCR identified clusters of co-expressed genes activated in a consecutive manner during development (Figure 3B). At 3 DAF just at the transition from the syncytial state to cellularization, the HK *HvHK1* is highly and exclusively expressed in the ETC region. Concomitantly *HvHP2* and the type-A response regulator *HvRR1* show an overlapping profile with a truncated expression at 5/7 DAF (cluster 1). After cellularization when cells have adopted ETC fate, several putative ethylene receptors, a HPt element (*HvPHP3*) and a suite of type-B RRs depict a characteristic peak of expression at 5 DAF (cluster 2). During progression of structural specification of ETCs another putative ethylene receptor is coordinatively expressed with *HvHP1* and two type-C RRs (*HvRR15/-16*), which both depict outstandingly high transcript levels (cluster 3). Assuming that genes sharing a common function and/or a functional relation are frequently transcriptionally co-ordinated, co-expression analysis of TCS elements pinpoints to a participation in specific phosphorelays activated at important crossroads of ETC development. The experimental design of analysis also provided information about the specificity of gene expression in ETCs related to other grain tissues: transcripts assigned to clusters 1 and 2 were almost found to be exclusively expressed in ETCs whereas transcripts of cluster 3 also depict a remarkable expression in other tissues of the grain (see Thiel et al., 2012b).

#### A CROSSTALK OF SPECIFIC TCS ELEMENTS AND ABA MIGHT REGULATE ETC CELLULARIZATION

Membrane-bound HKs are expected to play a key role in TCS-mediated signal transduction pathways as they perceive extracellular signals which are finally transmitted via the cytoplasm into the nucleus. The deciphered localization of such a receptor component at the exchange surface of maternal and filial tissues generally hints at a role in signal transmission between the mother plant and the filial tissues. Among the TCS elements transcriptionally activated in the ETC region before cellularization (see Figure 3B), a decisive role is anticipated for *HvHK1*, which is the only HK remarkably been expressed in the syncytial endosperm. *In situ* hybridization verified the expression of *HvHK1* at 3 DAF

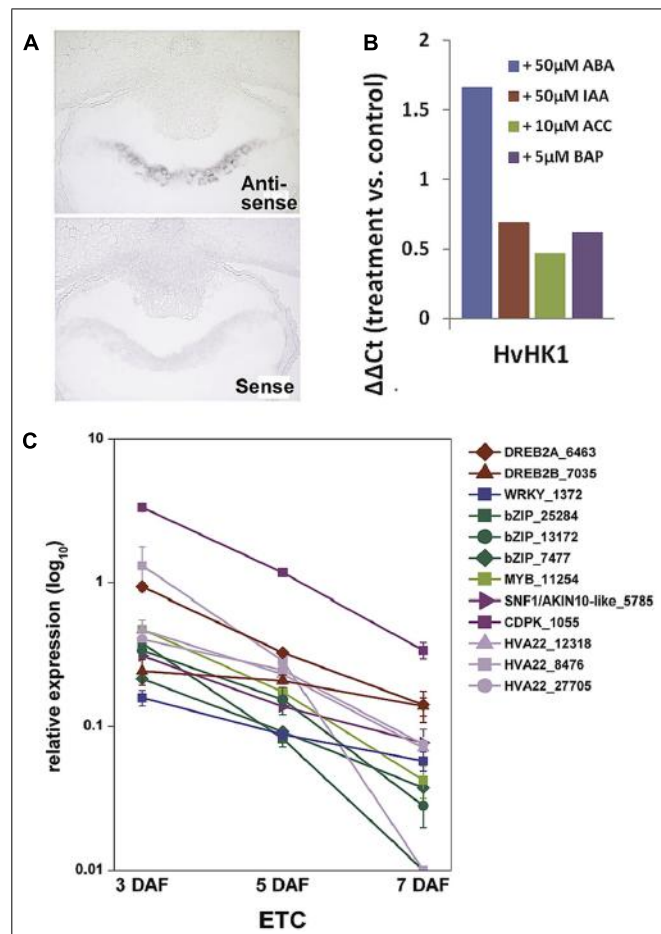


**FIGURE 4 | Transcript analyses of *HvHK1* and putatively interacting transcription factors. (A)** *In situ* hybridization specifies the expression of *HvHK1* in 3 DAF grains exclusively in the part of the cellularizing endosperm facing the nucellar projection. **(B)** Transcriptional response of *HvHK1* to hormones was analyzed by *in vitro* experiments. Grains were incubated in MS medium supplemented with the indicated concentrations of hormones for 16 h. The  $\Delta\Delta Ct$  value was calculated from qRT-PCR analysis and represents the  $\log_2$ -ratio compared to control conditions. **(C)** Expression profiles of putative interacting transcription factors and ABA signaling elements in ETCs. Transcript levels were determined by qRT-PCR analyses and relative expression is given in the  $\log_{10}$  scale. Transcripts numbers indicate the contig identifier in the 454 transcriptome assembly [Image in C is reproduced from Thiel et al. (2012b)].

exclusively in the part of the syncytium/cellularizing endosperm facing NP (Figure 4A). Interestingly, in the phylogenetic tree *HvHK1* clusters together with the *Arabidopsis* receptors AHK1 and Cytokinin Independent 1 (CKI1; Figure 3A). Genevestigator data show an expression of *AHK1* and *CKI1* in the chalazal endosperm (Zimmermann et al., 2004), which is one of the mitotic domains in the early syncytial endosperm positioned at the maternal-filial boundary of *Arabidopsis* seeds. In analogy to the ETC region, the chalazal endosperm facilitates nutrient transfer from the mother plant to the next generation (Boisnard-Lorig et al., 2001). AHK1 was initially identified as a plant osmosensor and thereby acting as a positive regulator of salt and drought

stress responses (Tran et al., 2007). By using single T-DNA insertion lines and AHK1 overexpression, AHK1 has previously been shown to positively affect ABA signaling and to enhance ABA biosynthesis in vegetative and seed tissues (Wohlbach et al., 2008). By *in vitro* incubation experiments with barley grains (4 DAF), a strong transcriptional response of *HvHK1* to external ABA was monitored; transcript levels increased to more than 3-fold (**Figure 4B**). To check if there are additional hints for ABA-mediated transcriptional regulation, we searched for conserved *cis*-regulatory motifs in the promoter regions of *HvHK1* and co-expressed TCS elements *HvHP2* and *HvRR1*. As now comprehensive information about the barley genome is available (<http://webblast.ipk-gatersleben.de/barley/viroblast.php>) promoter sequences 1 kb upstream of the predicted start codon were identified and analyzed for the occurrence of transcription factor binding sites. Promoter motifs known to be bound by transcription factors implicated in ABA signaling (ATHB, ABRE, DREB, MYC, MYB, and W-box) are highly abundant in the investigated promoter regions. The co-occurrence of *cis*-elements potentially interacting with ABA-related transcription factors reveals common mechanisms of transcriptional regulation by ABA (Thiel et al., 2012b). To encourage the role of putative interacting transcription factors, the ETC-specific 454 contigs were screened for candidate genes from these putative interaction partners. Transcript profiling by qRT-PCR revealed that three putative bZIP transcription factors, two putative DREB transcription factors (DREB2A, DREB2B), a MYB and a WRKY transcription factor, are highly expressed at 3 DAF (**Figure 4C**). Furthermore, three members of the HVA22 family, genes which are strongly induced by ABA (Shen et al., 2001), as well as candidate genes operating as positive regulators on the ABA signaling pathway (CDPK, SNF1-related kinase) depict the same profile. In summary, profiles of ABA signaling elements and transcription factors support the idea that ABA regulates transcriptional networks involved in ETC cellularization in a crosstalk with the phosphorelay genes *HvHK1*, *HvHP2*, and *HvRR1*. Protein-DNA binding studies would be helpful to verify transactivation of the phosphorelay genes by ABA-related transcription factors as suggested by the results. The identification of transcription factors transcriptionally activating phosphorelay genes with a proposed role in ETC specification would expand the knowledge about ABA-regulated signaling cascades in a fundamentally important process of seed development. The idea that ABA affects early endosperm development of seeds is supported by other studies in *Arabidopsis* and rice. Transcriptome analyses of the developing rice endosperm (Xue et al., 2012) and the proliferating *Arabidopsis* endosperm at the syncytial stage (Day et al., 2008) revealed a pronounced expression of ABA biosynthesis and signaling genes during early endosperm differentiation. The studies correspond to results obtained from the analysis of the barley endosperm mutant *seg8* for which defects in cellularization of ETCs have been attributed to altered ABA levels (Sreenivasulu et al., 2010). The study implies a role for ABA in cell cycle regulation during early endosperm development. Related to the function of potentially ABA-regulated TCS elements, which expression disappears after ETC cellularization, a possible role for the maintenance of the coenocyte and/or the switch to cellularization can be concluded for *HvHK1*, *HvHP2*, and *HvRR1*.

## PHOSPHORELAYS MIGHT BE INVOLVED IN ETHYLENE SIGNAL TRANSDUCTION AND REGULATE ESTABLISHMENT OF TRANSFER CELL STRUCTURE

Information about implications of the TCS in developmental programs of plants is largely related to cytokinin signaling in *Arabidopsis* (Schaller et al., 2008). However, elements of a subgroup of HKs (ETR/ERS) have been identified as ethylene receptors and negative regulators of the ethylene response, but the contribution of downstream phosphorelay elements in ethylene signal transduction has been discussed controversially. Previous results hinted at an implication of specific HPt and RR elements in ethylene signal transduction. Urao et al. (2000) detected physical interactions between the ethylene receptor ETR1 and three HPt intermediates as well as interactions of them with type-A response regulators. By genetic analysis, it was concluded that type-B response regulator ARR2 mediates ethylene responses and its transcription factor activity is likely to be regulated by an ETR1-initiated phosphorelay (Hass et al., 2004). More recently, an interaction of ETR1 with the HPt protein AHP1 has been evidenced by fluorescence polarization. Using this method the authors additionally confirmed that the affinity of the ETR1-AHP1 complex is tightly regulated by ethylene (Scharein and Groth, 2011). qRT-PCR profiling of TCS elements in ETCs revealed transcriptional activation of different putative ethylene receptors with concomitant downstream elements after cellularization (clusters 2 and 3, **Figure 3B**). Data of co-expressed TCS elements in barley ETCs between 5 and 7 DAF allow the assumption that type-B and type-C RRs, respectively, participate in ethylene receptor-initiated phosphorelays. An interesting fact is that the MYB-related transcription factor ZmMRP-1 (Gomez et al., 2009) and just lately, two MYB-related genes (Chinnappa et al., 2013) have been identified as transcriptional “master switches” regulating wall ingrowth deposition in BETCs of maize kernels and phloem parenchyma TCs in *Arabidopsis*, respectively. The high number of barley type-B RRs with a MYB-like DNA binding domain and their specific expression in ETCs after cellularization (5 DAF) imply a role for MYB domain-containing proteins as regulatory components in transcriptional networks controlling wall ingrowth development.

Supporting data for a key role of ethylene in barley ETC development came from microarray analysis of developing ETCs. High transcriptional activity of the key enzymes in ethylene biosynthesis, S-adenosylmethionine (SAM) synthase and ACC oxidase, particularly at 5 DAF indicates a burst in ethylene production after cellularization of ETCs, which is followed by an upregulation of ethylene signaling elements at 7 DAF or later stages. Confirmed players in ethylene signal transduction are ethylene receptors, ethylene insensitive 3 (EIN3) and EIL (EIN3-like) transcription factors operating upstream of ERF1/EREBP1 transcription factors. The combination of metabolite analysis with transcriptional activities gave further indications for an activated methylation (Yang) cycle in ETCs, which might provide the ethylene precursor SAM. Pronounced expression of genes encoding enzymes involved in methionine and SAM recycling correlate to changing levels of the metabolic intermediates cysteine, isoleucine, and methionine between 5 and 10 DAF (Thiel et al., 2012a). Considering the findings that ethylene signaling directs initiation of TC morphology in *V. faba* cotyledons and application of ACC

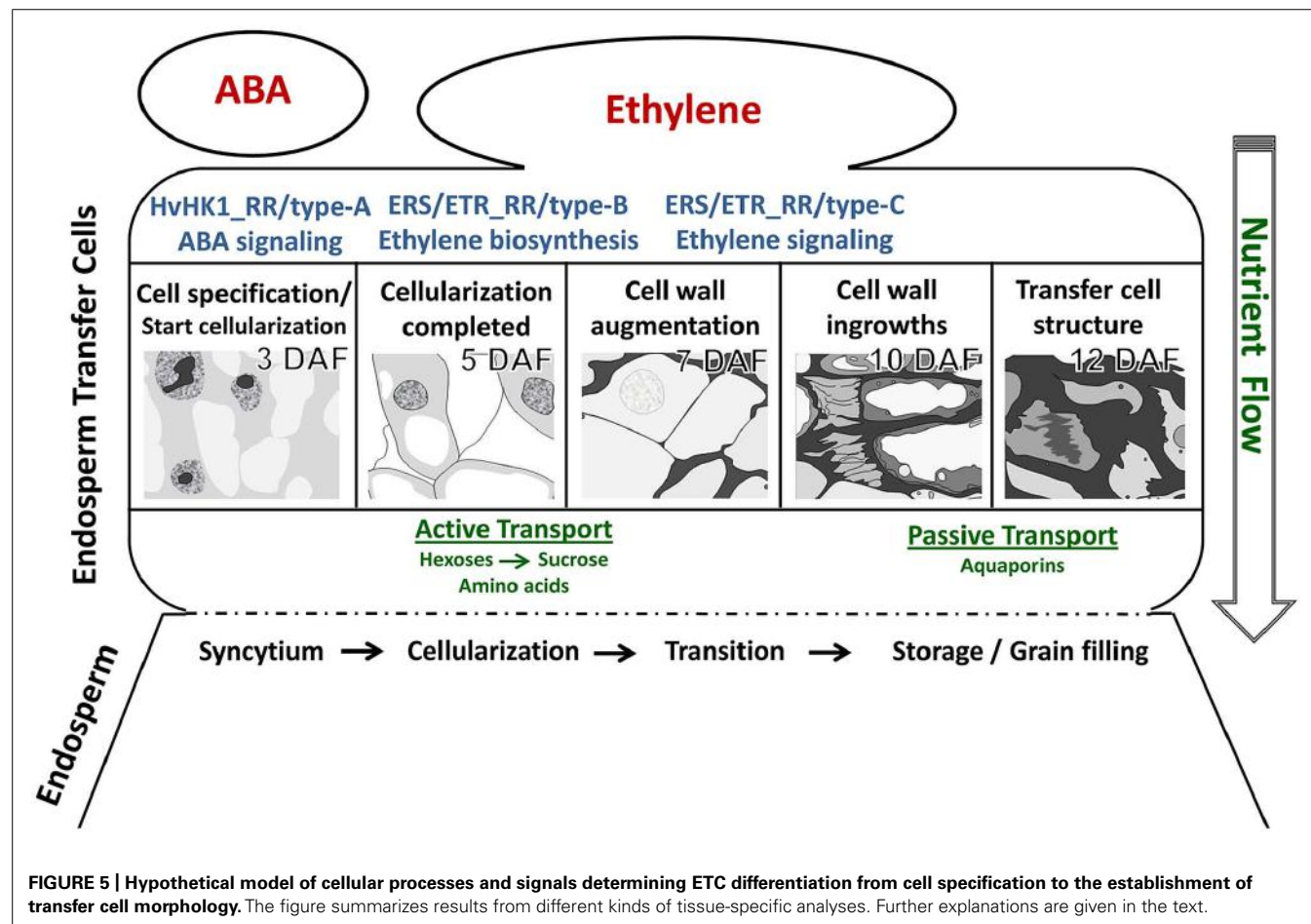
induces formation of wall ingrowths in tomato roots (Schikora and Schmidt, 2002; Dibley et al., 2009), high expression of ethylene biosynthesis and signaling genes in barley ETCs hints at an implication of ethylene in the formation of wall ingrowths. An important question is whether the downstream phosphorelay elements (HvHPts and HvRRs from B-and C-type) co-regulated with HvETR/ERS elements are part of ethylene receptor-initiated phosphorelays and/or if they interact with downstream elements in ethylene signal transduction. Protein-protein interaction studies could confirm specific interactions between TCS elements in ethylene receptor-initiated phosphorelays and known ethylene signaling elements as suggested by co-expression analysis.

## CONCLUSIONS AND FUTURE DIRECTIONS

Recent technological developments in providing access to specific cellular regions or even single cells have advanced our understanding of differentiation processes occurring inside an organ or in specific tissues. LM-based methods have brought knowledge gains about developmental programs involved in differentiation processes of ETCs in barley grains. Insights into ETC differentiation as discussed in this review are schematically represented in **Figure 5**. Global transcriptome analysis highlighted activated pathways in cellular differentiation and cell wall metabolism which could be related to transport mechanisms (active→passive) into

the endosperm. A decisive role for ABA in ETC specification and for ethylene as an inductive compound for cell wall modification was hypothesized. Expression of ABA-related transcription factors and signaling elements just at the onset of cellularization as well as transcriptional regulation of *HvHK1* pinpoints to early ABA influences on cell specification which might be perceived by *HvHK1*. Ethylene biosynthesis is clearly stimulated in ETCs after cellularization (5 DAF) in correspondence to transcriptionally activated ethylene receptor-initiated phosphorelays. Potential ERS/ETR-phosphorelays involve type-B RRs at 5 DAF whereas during further ETC differentiation other RR elements (type-C subgroup) might contribute to ethylene signaling pathways. Changing phosphorelay elements during the establishment of TC anatomy is accompanied by the upregulation of downstream elements on the ethylene signal transduction pathway. Accordingly, a cascade of ethylene biosynthesis in ETCs and successive ethylene regulation might be responsible for structural modifications of ETCs which in turn are linked to altered modes of transport.

The discovery of signals determining ETC differentiation in barley grains also represents the starting point for further investigations. Functional studies *in planta* by modulating the expression of identified candidate genes will help to advance our understanding about the importance of TCS pathways for



ETC and endosperm development. The verification of postulated interactions between phosphorelay elements and putative intersections with ABA and ethylene signaling pathways would emerge new aspects of hormonal regulation in crop seed development.

## ACKNOWLEDGMENTS

I would like to thank Uta Siebert for excellent assistance in microdissection-related work, Twan Rutten and Michael Melzer for microscopic analysis of barley ETC development, David Riewe for GC-MS analysis of metabolites from microdissected tissues and Julian Hollmann from CAU Kiel and Uwe Scholz for processing of 454 sequencing data. I am also grateful to Winfriede Weschke, Hans Weber, and Thorsten Schnurbusch for critical reading of the manuscript and helpful discussions. I wish to thank Karin Lipfert and Heike Ernst for graphical artwork. This work was supported by Deutsche Forschungsgemeinschaft (We 1608/5-1, 1608/8-1).

## REFERENCES

- Adriunas, F. A., Zhang, H. M., Weber, H., McCurdy, D. W., Offler, C. E., and Patrick, J. W. (2011). Glucose and ethylene signaling pathways converge to regulate trans-differentiation of epidermal transfer cells in *Vicia narbonensis* cotyledons. *Plant J.* 68, 987–998. doi: 10.1111/j.1365-313X.2011.04749.x
- Barrerao, C., Royo, J., Grijota-Martinez, C., Faye, C., Paul, W., Sanz, S., et al. (2009). The promoter of ZmMRP-1, a maize transfer cell-specific transcriptional activator, is induced at solute exchange surfaces and responds to transport demands. *Planta* 229, 235–247. doi: 10.1007/s00425-008-0823-0
- Bollenbeck, F., and Seiffert, U. (2008). “Fast registration-based automatic segmentation of serial section images for high-resolution images for high-resolution 3-D plant seed modeling,” in *Proceedings of the Fifth IEEE Symposium on Biomedical Imaging 2008*, Washington, DC, 352–355.
- Boisnard-Lorig, C., Colon-Carmona, A., Bauch, M., Hodge, S., Doerner, P., Bancharé, E., et al. (2001). Dynamic analyses of the expression of the HISTONE:YFP fusion protein in *Arabidopsis* show that syncytial endosperm is divided in mitotic domains. *Plant Cell* 13, 495–509.
- Brown, R. C., Lemmon, B. E., Stone, B. A., and Olsen, A. O. (1997). Cell wall (1–3) and (1–3,1–4)-beta-glucans during the early grain development in rice (*Oryza sativa* L.). *Planta* 202, 414–426. doi: 10.1007/s004250050145
- Chefdor, F., Benedetti, H., Depierreux, C., Delmotte, F., Morabito, D., and Carpin, S. (2006). Osmotic stress sensing in *Populus*: components identification of a phosphorelay system. *FEBS Lett.* 580, 77–81. doi: 10.1016/j.febslet.2005.11.051
- Chen, L.-Q., Qu, X.-Q., Hou, B.-H., Sosso, D., Osorio, S., Fernie, A. R., et al. (2012). Sucrose efflux mediated by SWEET proteins as a key step for phloem transport. *Science* 335, 207–211. doi: 10.1126/science.1213351
- Cheng, W. H., Taliercio, E. W., and Chourey, P. S. (1996). The Miniature1 seed locus of maize encodes a cell wall invertase required for normal development of endosperm and maternal cells in the pedicel. *Plant Cell* 8, 971–983. doi: 10.1105/tpc.8.6.971
- Chinnappa, K. S. A., Nguyen, T. T. S., Hou, J., Wu, Y., and McCurdy, D. W. (2013). Phloem parenchyma transfer cells in *Arabidopsis* – an experimental system to identify transcriptional regulators of wall ingrowth formation. *Front. Plant Sci.* 4:102. doi: 10.3389/fpls.2013.00102
- Costa, L. M., Yuan, J., Rouster, J., Paul, W., Dickinson, H., Jose, F., et al. (2012). Maternal control of nutrient allocation in plant seeds by genomic imprinting. *Curr. Biol.* 22, 160–165. doi: 10.1016/j.cub.2011.11.059
- Day, R. C., Herridge, R. P., Ambrose, B. A., and Macknight, R. C. (2008). Transcriptome analysis of proliferating *Arabidopsis* endosperm reveals biological implications for the control of syncytial division, cytokinin signaling, and gene expression regulation. *Plant Physiol.* 148, 1964–1984. doi: 10.1104/pp.108.128108
- Deneka, M., Neeft, M., and Van der Sluijs, P. (2003). Regulation of membrane transport by rab GTPases. *Crit. Rev. Biochem. Mol. Biol.* 38, 121–142. doi: 10.1080/713609214
- Doan, D. N., Linnestadt, C., and Olsen, O. A. (1996). Isolation of molecular markers from the barley endosperm coenocyte and the surrounding nucellus cell layers. *Plant Mol. Biol.* 31, 877–886. doi: 10.1007/BF00019474
- Dibley, S. J., Zhou, Y., Adriunas, F. A., Talbot, M. J., Offler, C. E., Patrick, J. W., et al. (2009). Early gene expression programs accompanying trans-differentiation of epidermal cells of *Vicia faba* cotyledons into transfer cells. *New Phytol.* 182, 863–877. doi: 10.1111/j.1469-8137.2009.02822.x
- Gomez, E., Royo, J., Guo, Y., Thompson, R., and Hueros, G. (2002). Establishment of cereal endosperm expression domains: identification and properties of a maize transfer cell-specific transcription factor, ZmMRP-1. *Plant Cell* 14, 599–610. doi: 10.1105/tpc.010365
- Gomez, E., Royo, J., Muniz, L., Sellam, O., Paul, W., Gerentes, D., et al. (2009). The maize transcription factor myb-related protein-1 is a key regulator of the differentiation of transfer cells. *Plant Cell* 21, 2022–2035. doi: 10.1105/tpc.108.065409
- Gruis, D., Guo, H., and Selinger, D. (2006). Surface position, not signaling from surrounding maternal tissues, specifies aleurone epidermal cell fate in maize. *Plant Physiol.* 141, 1771–1780. doi: 10.1104/pp.106.080945
- Gutierrez-Marcos, J. F., Costa, L. M., Biderre-Petit, C., Khbaya, B., O’Sullivan, D. M., Wormald, M., et al. (2004). Maternally expressed gene1 is a novel maize endosperm transfer cell-specific gene with a maternal parent-of-origin pattern of expression. *Plant Cell* 16, 1288–1301. doi: 10.1105/tpc.019778
- Hass, C., Lohrmann, J., Albrecht, V., Sweere, U., Hummel, F., Yoo, S. D., et al. (2004). The response regulator 2 mediates ethylene signaling and hormone signal integration in *Arabidopsis*. *EMBO J.* 23, 3290–3302. doi: 10.1038/sj.emboj.7600337
- Hunter, P. R., Craddock, C. P., Di Benedetto, S., Roberts, L. M., and Frigerio, L. (2007). Fluorescent reporter proteins for the tonoplast and the vacuolar lumen identify a single vacuolar compartment in *Arabidopsis* cells. *Plant Physiol.* 145, 1371–1382. doi: 10.1104/pp.107.103945
- Imamura, A., Hanaki, N., Nakamura, A., Suzuki, T., Taniguchi, M., Kiba, T., et al. (1999). Compilation and characterization of *Arabidopsis thaliana* response regulators implicated in His-Asp phosphorelay signal transduction. *Plant Cell Physiol.* 40, 733–742. doi: 10.1093/oxfordjournals.pcp.a029600
- Jauh, H. Y., Phillips, T. E., and Rogers, J. C. (1999). Tonoplast intrinsic protein isoforms as markers for vacuolar functions. *Plant Cell* 11, 1867–1882. doi: 10.1105/tpc.11.10.1867
- Kakani, A., and Peng, Z. (2011). ARR5 and ARR6 mediate tissue specific cross-talk between auxin and cytokinin in *Arabidopsis*. *Am. J. Plant Sci.* 2, 549–553. doi: 10.4236/ajps.2011.24065
- Kim, H. J., Ryu, H., Hong, S. H., Woo, H. R., Lim, P. O., Lee, I. C., et al. (2006). Cytokinin-mediated control of leaf longevity by AHK3 through phosphorylation of ARR2 in *Arabidopsis*. *Proc. Natl. Acad. Sci. U.S.A.* 103, 814–819. doi: 10.1073/pnas.0505150103
- Kohl, S., Hollmann, J., Blattner, F. R., Radchuk, V., Andersch, F., Steuernagel, B., et al. (2012). A putative role for amino acid permeases in sink-source communication of barley tissues elicited from RNA-seq. *BMC Plant Biol.* 12:154. doi: 10.1186/1471-2229-12-154
- Leibfried, A., To, J. P., Busch, W., Stehling, S., Kehle, A., Demar, M., et al. (2005). WUSCHEL controls meristem function by direct regulation of cytokinin-inducible response regulators. *Nature* 438, 1172–1175. doi: 10.1038/nature04270
- Li, S., Zhou, X., Huang, Y., Zhu, L., Zhang, S., Zhao, Y., et al. (2013). Identification and characterization of the zinc-regulated transporters, iron-regulated transporter-like protein (ZIP) gene family in maize. *BMC Plant Biol.* 13:114. doi: 10.1186/1471-2229-13-114
- McCurdy, D. W., Patrick, J. W., and Offler, C. E. (2008). Wall ingrowth formation in transfer cells: novel examples of localized wall deposition in plant cells. *Curr. Opin. Plant Biol.* 11, 653–661. doi: 10.1016/j.pbi.2008.08.005
- Mizuno, T. (2005). Two-component phosphorelay signal transduction systems in plants: from hormone responses to circadian rhythms. *Biosci. Biotechnol. Biochem.* 69, 2263–2276. doi: 10.1271/bbb.69.2263
- Muñiz, L. M., Royo, J., Gómez, E., Barrero, C., Bergareche, D., Hueros, G., et al. (2006). The maize transfer cell-specific type-A response regulator ZmTCR-1 appears to be involved in intercellular signaling. *Plant J.* 48, 17–27. doi: 10.1111/j.1365-313X.2006.02848.x
- Muñiz, L. M., Royo, J., Gómez, E., Baudot, G., Paul, W., Hueros, G., et al. (2010). Atypical response regulators expressed in the maize endosperm transfer cells link canonical two component system and seed biology. *BMC Plant Biol.* 10:84. doi: 10.1186/1471-2229-10-84

- Offler, C. E., Liet, E., and Sutton, E. G. (1997). Transfer cell induction in cotyledons of *Vicia faba* L. *Protoplasma* 200, 51–64. doi: 10.1007/BF01280734
- Olsen, O. A. (2001). Endosperm development: cellularization and cell fate specification. *Annu. Rev. Plant Physiol. Plant Mol. Biol.* 52, 233–267. doi: 10.1146/annurev.arplant.52.1.233
- Riefler, M., Novak, O., Strnad, M., and Schmülling, T. (2006). *Arabidopsis* cytokinin receptor mutants reveal functions in shoot growth, leaf senescence, seed size, germination, root development, and cytokinin metabolism. *Plant Cell* 18, 40–54. doi: 10.1105/tpc.105.037796
- Sakakibara, H., Suzuki, M., Takei, K., Deji, A., Taniguchi, M., and Sugiyama, T. (1998). A response-regulator homologue possibly involved in nitrogen signal transduction mediated by cytokinin in maize. *Plant J.* 14, 337–344. doi: 10.1046/j.1365-313X.1998.00134.x
- Schaller, G. E., Kieber, J. J., and Shiu, S.-H. (2008). Two-component signaling elements and histidyl-aspartyl phosphorelays. *Arabidopsis Book* 6:e0112. doi: 10.1199/tab.0112
- Scharein, B., and Groth, G. (2011). Phosphorylation alters the interaction of the *Arabidopsis* phosphotransfer protein AHP1 with its sensor kinase ETR1. *PLoS ONE* 6:e24173. doi: 10.1371/journal.pone.0024173
- Schikora, A., and Schmidt, W. (2002). Formation of transfer cells and H(+) -ATPase expression in tomato roots under P and Fe deficiency. *Planta* 215, 304–311. doi: 10.1007/s00425-002-0738-0
- Schuurmans, J. A., Van Dongen, J. T., Rutjens, B. P., Booman, A., Pieterse, C. M., and Borstlap, A. C. (2003). Members of the aquaporin family in the developing pea seed coat include representatives of the PIP, TIP, and NIP subfamilies. *Plant Mol. Biol.* 53, 633–645. doi: 10.1023/B:PLAN.0000019070.60954.77
- Shen, Q., Chen, C. N., Brands, A., Pan, S. M., and Ho, T. H. (2001). The stress- and abscisic acid induced barley gene HVA22: developmental regulation and homologues in diverse organisms. *Plant Mol. Biol.* 45, 327–340. doi: 10.1023/A:1006460231978
- Slewinsky, T. L. (2011). Diverse functional roles of monosaccharide transporters and their homologs in vascular plants: a physiological perspective. *Mol. Plant* 4, 641–662. doi: 10.1093/mp/srr051
- Sreenivasulu, N., Radchuk, V., Alawady, A., Borisjuk, L., Weier, D., Staroske, N., et al. (2010). De-regulation of abscisic acid contents causes abnormal endosperm development in the barley mutant seg8. *Plant J.* 64, 589–603. doi: 10.1111/j.1365-313X.2010.04350.x
- Sreenivasulu, N., Radchuk, V., Strickert, M., Miersch, O., Weschke, W., and Wobus, U. (2006). Gene expression patterns reveal tissue-specific signaling networks controlling programmed cell death and ABA-regulated maturation in developing barley seeds. *Plant J.* 47, 310–327. doi: 10.1111/j.1365-313X.2006.02789.x
- Talbot, M. J., Franceschi, V. R., McCurdy, D. W., and Offler, C. E. (2001). Wall ingrowth architecture in epidermal transfer cells of *Vicia faba* cotyledons. *Protoplasma* 215, 191–203. doi: 10.1007/BF01280314
- Talbot, M. J., Offler, C. E., and McCurdy, D. W. (2002). Transfer cell wall architecture: a contribution towards understanding localized wall deposition. *Protoplasma* 219, 197–209. doi: 10.1007/s007090200021
- Tauris, B., Borg, S., Gregersen, P. L., and Holm, P. B. (2009). A roadmap for zinc trafficking in the developing barley grain based on laser capture microdissection and gene expression profiling. *J. Exp. Bot.* 60, 1333–1347. doi: 10.1093/jxb/erp023
- Thiel, J., Müller, M., Weschke, W., and Weber, H. (2009). Amino acid metabolism at the maternal-filial boundary of young barley seeds: a microdissection-based study. *Planta* 230, 205–213. doi: 10.1007/s00425-009-0935-1
- Thiel, J., Weier, D., Sreenivasulu, N., Strickert, M., Weichert, N., Melzer, M., et al. (2008). Different hormonal regulation of cellular differentiation and function in nucellar projection and endosperm transfer cells – a microdissection-based transcriptome study of young barley grains. *Plant Physiol.* 148, 1436–1452. doi: 10.1104/pp.108.127001
- Thiel, J., Riewe, D., Rutten, T., Melzer, M., Friedel, S., Bollenbeck, F., et al. (2012a). Differentiation of endosperm transfer cells of barley – a comprehensive analysis at the micro-scale. *Plant J.* 71, 639–655. doi: 10.1111/j.1365-313X.2012.05018.x
- Thiel, J., Hollmann, J., Rutten, T., Weber, H., Scholz, U., and Weschke, W. (2012b). 454 transcriptome sequencing suggests a role for two-component signaling in cellularization and differentiation of barley endosperm transfer cells. *PLoS ONE* 7:e41867. doi: 10.1371/journal.pone.0041867
- Thompson, R. D., Hueros, G., Becker, H.-A., and Maitz, M. (2001). Development and function of transfer cells. *Plant Sci.* 160, 775–783. doi: 10.1016/S0168-9452(01)00345-4
- Tran, L. P., Urao, T., Qin, F., Maruyama, K., Kakimoto, T., Shinozaki, K., et al. (2007). Functional analysis of AHK1/ATHK1 and cytokinin receptor histidine kinases in response to abscisic acid, drought, and salt stress in *Arabidopsis*. *Proc. Natl. Acad. Sci. U.S.A.* 104, 20623–20628. doi: 10.1073/pnas.0706547105
- Urao, T., Miyata, S., Yamaguchi-Shinozaki, K., and Shinozaki, K. (2000). Possible His to Asp phosphorelay signaling in an *Arabidopsis* two-component system. *FEBS Lett.* 478, 227–232. doi: 10.1016/S0014-5793(00)01860-3
- Weschke, W., Panitz, R., Gubatz, S., Wang, Q., Radchuk, R., Weber, H., et al. (2003). The role of invertases and hexose transporters in controlling sugar ratios in maternal and filial tissues of barley caryopses during early development. *Plant J.* 33, 395–411. doi: 10.1046/j.1365-313X.2003.01633.x
- Wohlbach, D. J., Quirino, B. F., and Sussman, M. R. (2008). Analysis of the *Arabidopsis* histidine kinase ATHK1 reveals a connection between vegetative osmotic stress sensing and seed maturation. *Plant Cell* 20, 1101–1117. doi: 10.1105/tpc.107.055871
- Wu, B., Andersch, F., Weschke, W., Weber, H., and Becker, J. S. (2013). Diverse accumulation and distribution of nutrient elements in developing wheat grain studied by laser ablation inductively coupled plasma mass spectrometry imaging. *Metalomics* 5, 1276–1284. doi: 10.1039/c3mt00071k
- Xue, L. J., Zhang, J. J., and Xue, H. W. (2012). Genome-wide analysis of the complex transcriptional networks of rice developing seeds. *PLoS ONE* 7:e31081. doi: 10.1371/journal.pone.0031081
- Zhang, W. H., Zhou, Y., Dibley, K. E., Tyerman, S. D., Furbank, R. T., and Patrick, J. W. (2007). Nutrient loading of developing seeds. *Funct. Plant Biol.* 34, 314–331. doi: 10.1071/FP06271
- Zheng, Y., and Wang, Z. (2010). Current opinions on endosperm transfer cells in maize. *Plant Cell Rep.* 29, 935–942. doi: 10.1007/s00299-010-0891-z
- Zheng, Y., and Wang, Z. (2011). Contrast observation and investigation of wheat endosperm transfer cells and nucellar projection transfer cells. *Plant Cell Rep.* 30, 1281–1288. doi: 10.1007/s00299-011-1039-5
- Zhou, Y., Adriunas, F. A., Offler, C. E., McCurdy, D. W., and Patrick, J. W. (2010). An epidermal-specific ethylene signal cascade regulates trans-differentiation of transfer cells in *Vicia faba* cotyledons. *New Phytol.* 185, 931–943. doi: 10.1111/j.1469-8137.2009.03136.x
- Zimmermann, P., Hirsch-Hoffmann, M., Henning, L., and Gruissem, W. (2004). Genevestigator. *Arabidopsis* microarray database and analysis toolbox. *Plant Physiol.* 136, 2621–2632. doi: 10.1104/pp.104.046367
- Conflict of Interest Statement:** The author declares that the research was conducted in the absence of any commercial or financial relationships that could be construed as a potential conflict of interest.
- Received: 29 November 2013; accepted: 06 March 2014; published online: 26 March 2014.*
- Citation: Thiel J (2014) Development of endosperm transfer cells in barley. *Front. Plant Sci.* 5:108. doi: 10.3389/fpls.2014.00108*
- This article was submitted to Plant Physiology, a section of the journal *Frontiers in Plant Science*.*
- Copyright © 2014 Thiel. This is an open-access article distributed under the terms of the Creative Commons Attribution License (CC BY). The use, distribution or reproduction in other forums is permitted, provided the original author(s) or licensor are credited and that the original publication in this journal is cited, in accordance with accepted academic practice. No use, distribution or reproduction is permitted which does not comply with these terms.*



# Endosperm transfer cell-specific genes and proteins: structure, function and applications in biotechnology

Sergiy Lopato\*, Nikolai Borisjuk, Peter Langridge and Maria Hrmova

Australian Centre for Plant Functional Genomics, University of Adelaide, Glen Osmond, SA, Australia

**Edited by:**

Gregorio Hueros, Universidad de Alcalá, Spain

**Reviewed by:**

Michael G. Palmgren, University of Copenhagen, Denmark

Serena Varotto, University of Padova, Italy

**\*Correspondence:**

Sergiy Lopato, Australian Centre for Plant Functional Genomics, University of Adelaide, Waite Campus, Glen Osmond, SA 5064, Australia  
e-mail: sergiy.lopato@acpfu.edu.au

Endosperm transfer cells (ETC) are one of four main types of cells in endosperm. A characteristic feature of ETC is the presence of cell wall in-growths that create an enlarged plasma membrane surface area. This specialized cell structure is important for the specific function of ETC, which is to transfer nutrients from maternal vascular tissue to endosperm. ETC-specific genes are of particular interest to plant biotechnologists, who use genetic engineering to improve grain quality and yield characteristics of important field crops. The success of molecular biology-based approaches to manipulating ETC function is dependent on a thorough understanding of the functions of ETC-specific genes and ETC-specific promoters. The aim of this review is to summarize the existing data on structure and function of ETC-specific genes and their products. Potential applications of ETC-specific genes, and in particular their promoters for biotechnology will be discussed.

**Keywords:** endosperm transfer cells, biotechnology, invertase, lipid transfer protein, two-component system

## INTRODUCTION

Transfer cells are highly specialized plant cells responsible for the transport of solutes and nutrients from source to sink organs (Offler et al., 2003; Olsen, 2004). They can be found at many plant exchange surfaces, including phloem loading zones within the root, and unloading zones for transfer of nutrients to the endosperm in developing seeds. Endosperm transfer cells (ETC) have easily recognizable structural features, including an elongated shape and numerous cell wall in-growths, which greatly increase the surface area of the cell membrane and consequently enhance transport of solutes (Olsen, 2004). In maize seeds, transfer cells are located at the base of the endosperm. By contrast, in wheat and barley they are positioned along the crease (Figure 1; Olsen, 2004; Monjardino et al., 2013). Various molecular markers based on genes that are specifically or preferentially expressed in ETC, have been identified and isolated from maize, wheat, barley, and rice (Hueros et al., 1995, 1999a; Doan et al., 1996; Serna et al., 2001; Cai et al., 2002; Gutierrez-Marcos et al., 2004; Li et al., 2008; Kovalchuk et al., 2009). Initially, some of these markers were used by cytologists to localize ETC and determine their fate at different stages of grain development. For instance, it was discovered that ETC are not a part of maternal tissues, but rather a modification of part of the aleurone cell layer(s), which is located near to maternal vascular tissues. The identity of ETC is defined irreversibly during syncytium development and cellularization, the earliest stages of endosperm development (Costa et al., 2003; Olsen, 2004).

More recently, the function of some ETC-specific marker genes was elucidated, and their involvement in ETC differentiation and function established (Carlson et al., 2000; Weschke et al., 2003; Wang et al., 2008b; Muñiz et al., 2010). All currently known ETC-specific genes and those predominantly expressed in ETC cells, can be classified into one of the five groups (Table 1): (1) signal receptors and transducers, forming the basis of a two-component signaling system for ETC differentiation and development; (2)

transcriptional regulators and co-factors; (3) genes responsible for sugar conversion and transport; (4) genes encoding lipid transfer proteins (LTPs); and (5) genes encoding proteins with as yet unknown functions. Since the grain filling process is dependent on ETC structure and function, there is a high level of interest from biotechnologists in genes involved in the formation and function of ETC. This review will summarize current knowledge of the function of ETC-specific genes and the molecular structure of their products, focussing on commercially important grass species (i.e., maize, wheat, and barley), but also including relevant molecular evidence from the model plant *Arabidopsis*. Potential applications for some ETC-specific genes in genetic engineering for improved grain size, quality, and yield under favorable conditions and also under environmental stresses, will be discussed.

## TWO COMPONENT SIGNALING PLAYS AN IMPORTANT ROLE IN DIFFERENTIATION OF ETC

Two component signaling (TCS) was initially discovered in 1981 for bacteria (Hall and Silhavy, 1981), and its involvement in nearly all signal transduction events has been demonstrated. Existence of TCS in plants was revealed for the first time in 1996 (Kakimoto, 1996). The first type of TCS components described in plants are membrane-localized receptor histidine kinases (HK), responsible for the perception of signals transferred by ligand molecules, usually hormones. The binding of a ligand molecule leads to auto-phosphorylation of the receptor domain and intra-molecular transfer of the phosphoryl residue to the receiver domain of the HK (Hwang and Sheen, 2001). This is followed by phosphate transfer to a small soluble histidine phospho-transfer protein (HP), which is able to move to the nucleus. The structural characteristics of the AHK5<sub>RD</sub>-AHP1 complex from *Arabidopsis thaliana* (Bauer et al., 2013), suggest the process for transfer of the phosphoryl group from AHK5<sub>RD</sub> to AHP1 (Figure 2). HP proteins from maize (Sugawara et al., 2005), *Medicago truncatula* (Ruszkowski

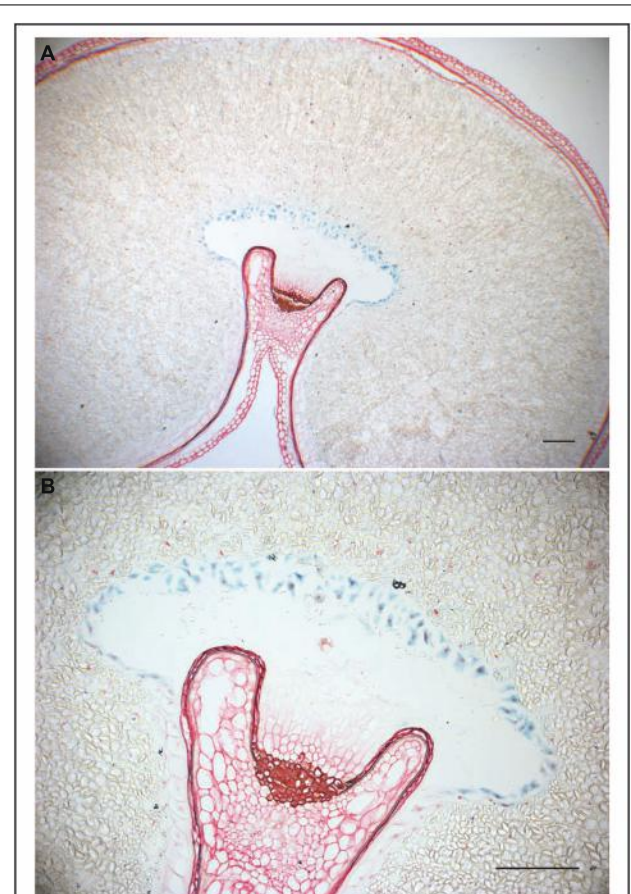


**FIGURE 1 | GUS expression in wheat grain directed by the ETC-specific *TdPR60* promoter.** (A) Histochemical GUS assay counterstained with safranin in 10  $\mu\text{m}$  thick transverse sections of transgenic wheat caryopsis at 31 DAP. (B) A detailed view on ETC at larger magnification. Bars = 200  $\mu\text{m}$ .

et al., 2013) and rice (Wesenberg et al., unpublished data, PDB 1YVI) superimposed over the AHP1 protein from *Arabidopsis* indicate that HP acceptor proteins from diverse plant species fold similarly, and that interfaces between HP and kinases are highly conserved (Figure 2). Further, comparison of the level of conservation of residues at the binding interface region of 22 HP proteins from 16 plant species including those from *Arabidopsis*, reveals a remarkably high level of preservation of architecture in HP proteins; in particular the spatial positions of a key His residue. It is therefore expected that the mode of action of the AHK5<sub>RD</sub>-AHP1 complex serves as a paradigm to understand the function of TCS in higher plants at the molecular level (Bauer et al., 2013). Analogous machineries of intermolecular phosphotransfers are likely to operate in both mono- and dicotyledonous plants. In the nucleus, HP activates type-B response regulators (RR), which are a subfamily of MYB transcription factors (TF). Members of this MYB subfamily in turn activate target genes, including genes encoding the type-A RR, which are usually negative regulators of hormone signaling pathways (Hwang and Sheen, 2001).

Two component signaling is involved in a range of plant developmental processes and responses to stresses and other stimuli, such as the development of meristems (Kim et al., 2006), maintenance of circadian rhythms (Mizuno, 2005), senescence (Riefler et al., 2006), phosphate and nitrogen availability responses (Sakakibara et al., 1998; Coello and Polacco, 1999; Takei et al., 2001, 2002), sulfur metabolism processes (Fernandes et al., 2009), responses to heavy metals (Srivastava et al., 2009), and other abiotic (Chefdor et al., 2006; Jain et al., 2008a; Karan et al., 2009) and biotic (Jolivet et al., 2007) stresses. Recently, many TCS components were identified in ETC, confirming ETC as the primary mediator of signal transduction between maternal tissue and developing grain (Muñiz et al., 2006, 2010; Thiel et al., 2012).

The first TCS components identified in cereal grains were the maize genes *Transfer Cell Response Regulators 1* and *2* (*ZmTCRR-1* and *ZmTCRR-2*; Table 1). These encode members of the type-A RR of the TCS, which are responsible for phospho-transfer-based signal transduction (Muñiz et al., 2006, 2010). The *TCRR* genes were found to be expressed exclusively in the ETC layer 8–14 days after pollination (DAP), when transfer-cell differentiation is most active. However, the *ZmTCRR-1* protein was also detected in conductive tissue deep inside the endosperm, where transcription of the gene was not observed (Muñiz et al., 2006). This finding suggests that TCS is involved in intercellular signal transduction. A possible role of TCRR proteins is to integrate external signals with seed developmental processes (Muñiz et al., 2006, 2010). The promoter of *ZmTCRR-1* was strongly *trans*-activated in heterologous systems by the transfer cell-specific TF *ZmMRP-1*, which is a MYB type TF (Muñiz et al., 2006, 2010; Gomez et al., 2009; Figure 3).

Recently, the ETC layer was isolated by laser micro-dissection and pressure catapulting (LMPC) from barley grains at different stages of development (Thiel et al., 2012). Sequence analysis of the barley ETC transcriptome revealed a large number of TCS components. Practically all known components of the TCS were identified and in some cases several types of each component were evident. For example, among the HK identified were six putative ethylene receptors, two putative cytokinin receptors and three HK of unknown function with high similarity to kinases from rice and *Arabidopsis* (Thiel et al., 2012). Six genes encoding HPs were also found to be expressed in the ETC layers. Two of these contained no His residue in the HP domain. All types (A, B, and C) of RRs were found in barley ETC. Three type-A RRs had higher levels of sequence similarity to rice RRs than to either ETC-specific *ZmTCRR-1* or *ZmTCRR-2* from maize (Muñiz et al., 2010), which cluster separately in phylogenetic analyzes. 11 sequences of type-B RRs and four isoforms of type-C RRs were also present in the barley ETC transcriptome (Thiel et al., 2012). The high number and high mRNA abundance of TCS components in developing ETC suggests that TCS is crucial for ETC development and consequently for grain filling.

## TRANSCRIPTIONAL REGULATION OF ETC FORMATION AND FUNCTION

*ZmMRP-1* is so far the only transfer cell-specific TF to have been identified and characterized in cereals (Table 1). It is proposed to

**Table 1 | Genes that are specifically or predominantly expressed in endosperm transfer cells\*.**

Plant	Gene name	Protein type	GenBank Accession	Suggested function**	Cited
Zea mays	<i>ZmTCRR-1</i>	Type-A response regulator	AM085299	Signal transduction	Muniz et al. (2006)
Zea mays	<i>ZmTCRR-2</i>	Type-A response regulator	Unavailable***	Signal transduction	Muniz et al. (2010)
Zea mays	<i>ZmNRP-1</i>	One-repeat MYB TF	AJ318518	Transcriptional activation of ETC/BETL-specific genes	Gómez et al. (2002)
Zea mays	<i>ZmMRP1-1</i>	C2H2 zinc finger protein	NM_001153367	Negative regulator of ZmMRP1	Royo et al. (2009)
Zea mays	<i>ZmMRP1-2</i>	C2H2 zinc finger protein	NM_001158398	Negative regulator of ZmMRP1	Royo et al. (2009)
Zea mays	<i>INCW2</i>	Cell-wall invertase	AF165180	Converting sucrose into glucose and fructose	Carlson et al. (2000)
<i>Sorghum bicolor</i>	<i>SbINCW</i>	Cell-wall invertase	EF177465 (partial CDS)	Converting sucrose into glucose and fructose	Jain et al. (2008b)
<i>Oriza sativa</i>	<i>GlF1</i>	Cell-wall invertase	EU095553	Converting sucrose into glucose and fructose	Wang et al. (2008a)
<i>Hordeum vulgare</i>	<i>HvCWN1/V1</i>	Cell-wall invertase	AJ534447	Converting sucrose into glucose and fructose	Weschke et al. (2003)
<i>Gossypium hirsutum</i>	<i>GhCWN1</i>	Cell-wall invertase	AI725433***	Converting sucrose into glucose and fructose	Wang and Ruan (2012)
<i>Hordeum vulgare</i>	<i>HvSF6FT7</i>	Sucrose:fructan 6-fructosyltransferase (soluble invertase)	X83233	Converting sucrose into glucose and fructose	Weschke et al. (2003)
<i>Hordeum vulgare</i>	<i>HvSTP1</i>	Hexose transporter	AJ534445	Importing hexoses into the endosperm	Weschke et al. (2003)
Zea mays	<i>MEG1</i>	LTP; defensin type	AY536121	Protection against pathogens	Gutiérrez-Marcos et al. (2004)
Zea mays	<i>BETL1</i>	LTP; defensin type	JO420076	Protection against pathogens	Hueros et al. (1995)
Zea mays	<i>BETL2 (BAP2)</i>	LTP	AJ133529	Signal transduction, protection against pathogens	Hueros et al. (1999a)
Zea mays	<i>BETL3</i>	LTP; defensin type	AJ133530	Protection against pathogens	Hueros et al. (1999a)
Zea mays	<i>BETL4</i>	LTP; Bowman-Birk family of $\alpha$ -amylase/trypsin inhibitors	AJ133531	Protection against insects and pathogens	Hueros et al. (1999a)
<i>Oriza sativa</i>	<i>OsPR9a</i>	LTP; defensin type	EU264060	Protection against insects and pathogens	Li et al. (2008)
<i>Hordeum vulgare</i>	<i>END1</i>	nsLTP	Z69631	Signal transduction, protection against pathogens	Doan et al. (1996)
<i>Oriza sativa</i>	<i>OsPR602</i>	nsLTP	EU264061	Signal transduction, protection against pathogens	Li et al. (2008)
<i>Triticum aestivum</i>	<i>TaPR60</i>	nsLTP	EU264062	Signal transduction, protection against pathogens	Kovalchuk et al. (2009)
<i>Oriza sativa</i>	<i>AL1</i>	Anthranilate N-hydroxycinnamoyl/benzoyltransferase	Os01g0382200 (Rice Annotation Project Database)	Function in plants is unknown	Kuwano et al. (2011)

\*Genes in the **Table 1** are arranged according to the group specification in the text.

\*\*Current knowledge of the function of ETC-specific genes is dependent on available data, and thus in some instances function of ETC-specific genes is speculative.

\*\*\*Sequence originates from a private cDNA collection.

\*\*\*\*The EST sequence used for cloning a full-length CDS. The full length CDS sequence was not provided by Wang and Ruan (2012).

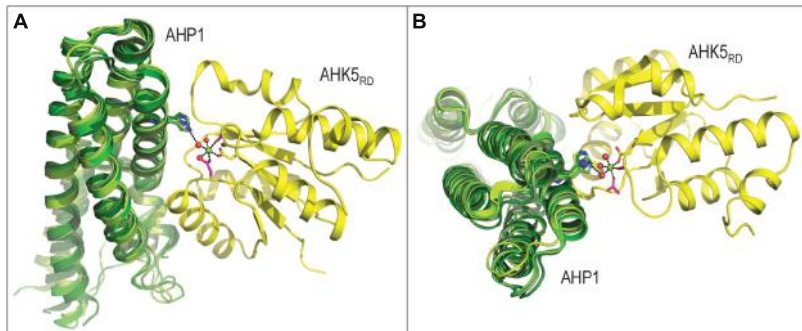


**FIGURE 2 | Three-dimensional structure of the AHK5<sub>RD</sub>-AHP1 complex from *Arabidopsis thaliana* (PDB 4EUK), consisting of the histidine-containing phosphotransfer (AHP1, green) and kinase (AHK5<sub>RD</sub>, yellow) region, is shown in two orthogonal orientations.** The structure of the complex in panel **A** is rotated by approximately 90 degrees to produce a view shown in panel **B**. The mechanism of intermolecular phosphotransfer mediated by the *Arabidopsis* AHK5<sub>RD</sub>-AHP1 complex. Maize ZmHP2 (PDB 1WN0, smudge green), *Medicago truncatula* MtHPT1 (PDB 3US6, limon green) and rice OsHPT (PDB 1YVI, forest green) are superposed

over the *Arabidopsis* AHP1. The His in AHP1 and Asp in AHK5<sub>RD</sub> residues that respectively donate and accept a phosphoryl group are shown in sticks in atomic green and yellow colors, respectively. The octahedral coordination geometry of Mg<sup>2+</sup> (green sphere) participating in the phosphotransfer reaction is indicated by black dashes (atomic distances between 1.9 Å and 2.0 Å), where Mg<sup>2+</sup> is coordinated by Asp from AHK5<sub>RD</sub>, three water molecules (red spheres) and two other residues (Asp and Cys) of AHK5<sub>RD</sub>. The distance of 3.4 Å between His from AHP1 and one of the water molecules is also shown.

Conservation:	5	5	5	5	5	5	59	5	5	
1IRZ:A	11	THELNKFLAAVDHLGVER---	AVPKKILDLMNVDKLT	RENVASHLQKF	RVALK	KVS---	64			
2AJE:A	17	SVAEVEALVQAVEKLGTR-	WRDVVKLCAFEDADHRTYV	LDKWKNTLVHT	AKISPQQR	76				
2CJJ:A	12	SAKENKAFAERALAVYDKDT	PDRWANVAR---	AVEGRTPEEVKKH	YEILVEDIKYIE	SGK	67			
ZmMRP-1	102	TTDEHRNFLRGLLEVGRGK-	WRNISK--YFVETRTPVQISSH	AKYFRRQE	TTEKQ	155				
Consensus ss:	hhhhhhhhhhhhhh				hhhhh	hh	hhhhhhhhhhhhhhhh			

**FIGURE 3 | Domain analyses of selected DNA binding proteins containing MYB domains that are involved in the two component system (TCS).** A multiple sequence alignment of ZmMRP-1 involved in TCS with three MYB domain-containing proteins ARR10-B of the GARP family from *Arabidopsis thaliana* (PDB 1IRZ, chain A), a telomeric repeat-binding protein from *Arabidopsis thaliana* (PDB 2AJE, chain A), and a MYB domain of the RAD transcription factor from *Antirrhinum majus* (PDB 2CJJ, chain A)

*majus* (PDB 2CJJ, chain A). Protein sequences were aligned with ProMals3D (Pei et al., 2008) and analysed for domain boundaries using ProDom (Bru et al., 2005). The predicted and consensus secondary structures (ss) are shown in red ( $\alpha$ -helices, h) and black (loops) types. Conservation of residues on a scale of 9–5 is shown at the top of the diagram. The absolutely conserved and similar residues are highlighted in brown and black, respectively.

play a central role in the regulatory pathways controlling transfer cell differentiation and function (Gómez et al., 2009). *ZmMRP-1* is a single-copy gene that encodes proteins with a MYB-related DNA binding domain (Figure 3) and a nuclear localization signal. Analysis of domain boundaries in the *ZmMRP-1* protein reveals the location of a MYB-like domain sequence (Figure 3). The MYB-like domain in *ZmMRP-1* shows significant similarity to secondary structural element distributions in known MYB domain-containing proteins, including ARR10-B of the GARP family from *A. thaliana* (Hosoda et al., 2002), a telomeric repeat-binding protein from *A. thaliana* (Sue et al., 2006) and a MYB domain of the RAD TF from *Antirrhinum majus* (Stevenson et al., 2006; Figure 3). In developing maize grain, *ZmMRP-1* transcript was detected in the cytoplasmic region of the basal endosperm coenocytes as early as 3 DAP. Because the transfer cell layer develops from this part of maize coenocytes, it is reasonable to propose a role for *ZmMRP-1* in ETC formation. However, the strongest *ZmMRP-1* expression was observed in transfer cell layers from 3 to 16 DAP and peaked at 11 DAP, when formation of ETC was already completed, suggesting an additional role of this TF in ETC function (Gómez et al., 2009).

To evaluate the level of conservation of ETC formation and function in different plant species, spatial expression patterns of *ZmMRP-1* were studied in transgenic lines of maize, *Arabidopsis*, tobacco and barley which were transformed with a *ZmMRP-1* promoter-GUS reporter construct (Barrero et al., 2009). GUS signal was detected in several plant organs in regions of active transport between source and sink tissues and at vascular connection sites between developing organs and the main plant vasculature. Promoter induction was observed in all tested species at early developmental stages of transport-to-sink tissues, including in the ETC layer (Barrero et al., 2009). Based on these results it was proposed that ETC differentiate in a similar way in diverse plant species, and that this differentiation is initiated by conserved induction signals. Using both *in planta* and yeast experiments it was demonstrated that *ZmMRP-1* promoter activity is modulated by different carbohydrates. Glucose was found to be the most effective inducer of the *ZmMRP-1* promoter (Barrero et al., 2009).

Several target genes of *ZmMRP-1* have been identified (Gómez et al., 2002; Costa et al., 2004; Gutierrez-Marcos et al., 2004; Barrero et al., 2006; Muñiz et al., 2006, 2010). The activation of BETL (*Basal Endosperm Transfer Layer*) gene promoters was

initially demonstrated by co-transformation of two constructs in tobacco protoplasts. In these experiments, constitutive expression of *ZmMRP-1* led to the activation of a co-transformed GUS gene driven by the promoter from the *Basal Endosperm Transfer Layer (BETL-1)* gene (Barrero et al., 2006). In whole plants, it was also shown that ectopic expression of *ZmMRP-1* under the control of the ubiquitin promoter in BETL-1:GUS transgenic maize led to activation of ETC-specific gene expression (Gómez et al., 2002). In a separate study, the promoter of *MATERNALLY EXPRESSED GENE1 (MEG1)* was found to be activated by ZmMRP-1, when the transcriptional *MEG1* promoter-GUS fusion construct and a transcriptional 35S:MRP1 construct were co-transformed into tobacco protoplasts (Costa et al., 2004; Gutierrez-Marcos et al., 2004). Since *MEG1* is expressed in maize basal transfer cells from 10 to 20 DAP, it can potentially be activated by ZmMRP-1 in maize plants. The promoter of the ETC-specific gene encoding a type-A RR, ZmTCRR-1, was also strongly activated in heterologous systems by ZmMRP-1 (Muñiz et al., 2006, 2010).

Interaction between ZmMRP-1 and the promoter of the transfer cell specific gene *BETL-1*, led to activation of the *BETL-1* promoter in various cell types (Barrero et al., 2006). Although the reporter construct containing the *BETL-1* promoter was silent in all tested types of cells when transformed alone, transient co-expression of ZmMRP-1 led to significant activation of the reporter gene. This suggests that ZmMRP-1 does not require the help of ETC-specific factors for promoter activation. The transient expression system was used to find specific *cis*-elements in the *BETL-1* promoter. A *cis*-element consisting of a 12 bp motif containing two consecutive repeats ( $2 \times$  TATCTC) was situated approximately 100 bp upstream of the TATA box of the *BETL-1* promoter. Specific binding of ZmMRP-1 to this *cis*-element was confirmed *in vitro* using electrophoretic mobility shift experiments (Barrero et al., 2006). Similar *cis*-elements were found in several other transfer cell-specific promoters and were designated as “transfer cell box” elements. However, the “transfer cell box” was not identified in ETC-specific promoters from wheat or rice (Li et al., 2008; Kovalchuk et al., 2009). In these species, a single copy of the TATCTC motif was found in a number of ETC-specific promoters, suggesting that there has been degeneration of transfer cell box sequences during evolution of some grass species. It cannot be excluded that ETC-specific expression of some genes is regulated by other, as yet unidentified TF(s), or at least requires the presence of other factors for specific interaction with promoter sequences.

It has been shown that ZmMRP-1 TF binds not only to gene promoters, but it may also bind other proteins (Royo et al., 2009). Two proteins were isolated in a yeast 2-hybrid screen using full length ZmMRP-1 as bait; these were designated as ZmMRP-1 Interactors 1 and 2 (ZmMRPI-1 and ZmMRPI-2; Table 1). Binding of ZmMRP-1 to ZmMRPI-1 and ZmMRPI-2 was confirmed *in planta* by co-localization of the proteins in transfer cell nuclei. ZmMRPI-1 and ZmMRPI-2 are very similar proteins, both belonging to the C(2)H(2) zinc finger protein subfamily of nuclear proteins. Members of this subfamily interact with MYB-related TF through their C-terminal conserved domains (Royo et al., 2009). In ZmMRPI-1 and ZmMRPI-2

proteins, a Zinc finger domain of the C2H2-type and a C-terminal DNA-binding domain are highly conserved both in disposition and in sequence identities at the amino acid level, which are 89 and 97% for the Zinc finger and DNA-binding domains, respectively (Figure 4). In both proteins the Zinc finger (Figure 4A) and C-terminal DNA-binding (Figure 4B) domains fold into  $\alpha$ -helices, and  $\beta$ -sheets, respectively. Although the full-length sequences of ZmMRPI-1 and ZmMRPI-2 share very high sequence identity (85%) and similarity (94%), analysis using the SMART database (Letunic et al., 2012) identified an ATPase, central region-like domain in ZmMRPI-1, but a glycoprotein E1-like domain and putative Raf-like Ras-binding domain in ZmMRPI-2 (Figure 4C). These domains were positioned in different locations of the protein sequences, reflecting localized differences in amino acid sequence that may be important for specific regulatory functions.

It was shown that MRPI proteins can modulate activation of ETC-specific promoters by interacting with ZmMRP-1 (Royo et al., 2009). In addition, the expression of *MRPI* genes in maize and *Arabidopsis* are found to be expressed at the same nutrient exchange surfaces, where the expression of *ZmMRP-1* has been previously detected. *MRPI*-orthologs genes have been identified in the rice and *Arabidopsis* genomes (Royo et al., 2009).

Although there are no reports of other types of TF which are specifically or predominantly expressed in ETC and participate in the regulation of ETC development and function, the existence of such TFs cannot be excluded. Most members of the HD-Zip IV TF subfamily, for example, are expressed in grain tissues (Yang et al., 2002; Javelle et al., 2011; Kovalchuk et al., 2012a), and are involved in regulation of LTP expression (Javelle et al., 2010; Lopato et al., unpublished data). It has been reported that at least three wheat LTPs (TaLtp7.2a, TaLtp9.1a, and TaLtp9.3e) are specifically expressed in the main vascular bundle of wheat scutellum (Boutrot et al., 2007), which plays a major role in sugar transport from endosperm to embryo during seed germination. Recently, it was demonstrated that the wheat HD-Zip IV TF TdGL9H1 is also predominantly expressed in the scutellar vascular bundle and thus is potentially a regulator of these LTPs (Kovalchuk et al., 2012b). Since several LTPs have been found to be specifically expressed in ETC layers (Hueros et al., 1995, 1999a; Doan et al., 1996; Li et al., 2008; Kovalchuk et al., 2009), it would be reasonable to predict that at least one member of HD-Zip IV subfamily is also specifically or predominantly expressed in ETC and involved in the transcriptional regulation of at least some ETC-specific LTPs.

## GENES RESPONSIBLE FOR SUGAR TRANSPORT TO ENDOSPERM

Sucrose is the main carbohydrate transported from photosynthetically active tissues to sinks such as root, flower, and seed (Ruan et al., 2010; Lemoine et al., 2013). However, sucrose does not enter in this form, but is converted into the hexoses glucose and fructose. These reactions are catalyzed by sugar invertases (INVs), which are reported also to have regulatory roles in plant growth and development (LeClere et al., 2008, 2010; Chourey et al., 2010). INVs can be classified into three groups according to their localisation in cells: vacuolar (VIN), cytoplasmic (CIN) and

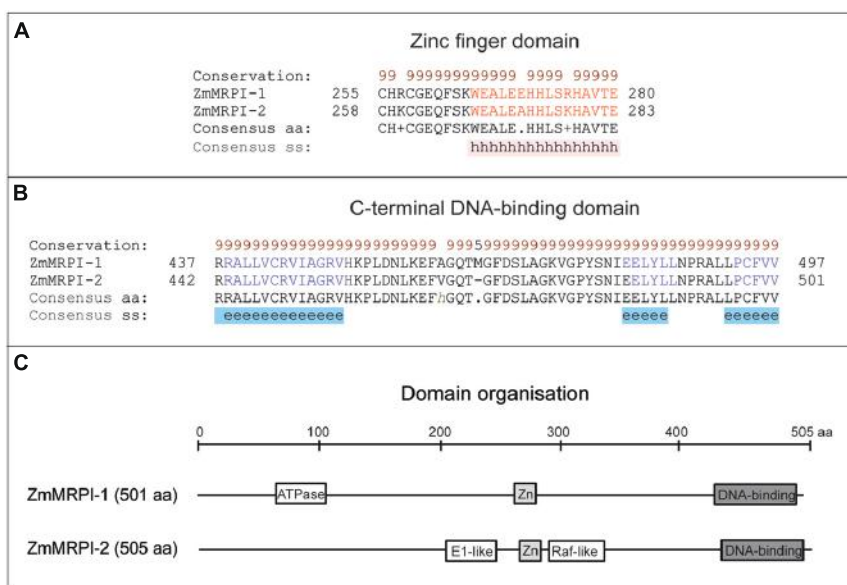


**FIGURE 4 | Domain analyses of ZmMRPI-1 and ZmMRPI-2 proteins involved in the two component system (TCS) contain a highly conserved Zinc finger domain in nearly the same location.** (A) A sequence alignment of the Zn finger domains, which fold into  $\alpha$ -helices. (B) A sequence alignment of the C-terminal DNA-binding domains, which fold into sheets. Protein sequences were aligned with ProMals3D (Pei et al., 2008) and analysed for domain boundaries using SMART (Letunic et al., 2012) and ProDom (Bru et al., 2005). The predicted and consensus secondary structures (ss) are shown in panels (A) and (B) in red ( $\alpha$ -helices, h), blue ( $\beta$ -sheets, e) and black (loops)

types. Conservation of residues (brown and black types) on a scale of 9–5 is shown at the top of the diagram. **(C)** Schematics of domain organization of ZmMRPI-1 and ZmMRPI-2, as analysed by SMART (Letunic et al., 2012) and ProDom (Bru et al., 2005). A position of the ATPase, central region-like domain is shown in ZmMRPI-1, while in ZmMRPI-2, glycoprotein E1-like and Raf-like Ras-binding domains are schematically represented. In both entries Zn finger (light gray) and C-terminal DNA-binding (dark gray) domains are also illustrated. The schematic is drawn to scale of 505 amino acid (aa) residues.

cell wall-bound or apoplastic (CWIN or INCW). Several studies have demonstrated that INCWs are the major type of INVs responsible for the delivery of hexoses to the developing seed (**Table 1**). Tight regulation of the delivery of hexoses by CWINs provides a mechanism for controlling cell division and even cell differentiation in developing kernels (Miller and Chourey, 1992; Weber et al., 1996). A positive correlation between seed development and the activity of INCWs has been observed in faba bean (Weber et al., 1995, 1996), maize (Cheng et al., 1996; Vilhar et al., 2002; Chourey et al., 2006), barley (Weschke et al., 2003; Sreenivasulu et al., 2004), rice (Hirose et al., 2002; Wang et al., 2008a), tomato (Zanor et al., 2009), and cotton (Wang and Ruan, 2012). In addition to INVs localized at the interface of sink organs, hexose transporters facilitate the import of hexoses into seed endosperm and other sinks (Bihmidine et al., 2013; reviewed in Slewinski, 2011).

## ETC-SPECIFIC CELL WALL-BOUND INVERTASES

Transfer cells are the gateway for sugar transport from maternal tissue to the endosperm. Sugar delivery in turn directly affects transfer cell formation. Mutants of the maize gene *Minature1* (*mn1*) show an anatomical lesion in the pedicel region and reduced size of the kernel (Lowe and Nelson, 1946; Miller and Chourey, 1992; Cheng et al., 1996). Kernel size is reduced due to reductions in both mitotic activity and cell size (Vilhar et al., 2002). *Minature1* encodes a cell wall invertase (INCW2) that was originally thought to be localized in the basal endosperm and

pedicel (Miller and Chourey, 1992; Cheng et al., 1996; Carlson et al., 2000). However, histochemical visualization of invertase activity in the maternal pedicel region revealed that *INCW2* is expressed exclusively in the ETC layer, and that the pedicel is served by the orthologs gene *INCW1* (Chourey et al., 2006).

Loss of *INCW2* function in the *mn1* mutant led to reduced size and number of the labyrinth-like wall-in-growths (WIGs) of ETC, a subsequent decrease in plasma membrane surface area and decline in ETC transport capacity, and consequently reduced grain filling (Kang et al., 2009). Analysis of intracellular structure by electron microscopy revealed that in the *mn1* mutant, WIGs in the ETC were stunted and the endoplasmic reticulum in these cells was swollen; Golgi density in the mutant ETC was reduced to 51% of the Golgi density in wild-type plants (Kang et al., 2009). *INCW2*-specific immunogold particles were detected in WIGs, the endoplasmic reticulum, Golgi stacks, and the trans-Golgi network in the ETC of wild-type plants, but were extremely rare in the ETC of the *mn1* mutant (Kang et al., 2009).

A recent study was undertaken to identify gene products that are metabolically regulated in ETC in response to invertase deficiency (Silva-Sanchez et al., 2013). Comparisons of soluble and cell wall-bound proteomes of the *mn1* mutant and wild-type (*Mn1*) plants revealed 131 differentially expressed proteins, which fell into two major groups: proteins related to carbohydrate metabolic and catabolic processes, or proteins involved in cell homeostasis (Silva-Sanchez et al., 2013).

Developing kernels of the *mn1* mutant also have drastically reduced auxin (IAA) levels (LeClere et al., 2008). The reduced IAA levels are due to decreased transcript abundance of the *ZmYucca1* (*ZmYuc1*) gene. This gene encodes flavin monooxygenase, a key enzyme in the IAA biosynthetic pathway (Chourey et al., 2010; LeClere et al., 2010). Using two different approaches it was shown that expression of *ZmYuc1* is regulated by sugar levels (LeClere et al., 2010). These data explain how sugar levels can influence auxin levels in seed, which in turn regulates specific aspects of seed development.

A similar role of INCW genes in seed development in rice has been reported (Wang et al., 2008b). Rice seed weight was increased by overexpression of the *GRAIN INCOMPLETE FILLING 1* (*GIF1*) gene that encodes a cell-wall invertase (Wang et al., 2008b). Interestingly, although expression under the native *GIF1* promoter increased grain size, ectopic expression of the *GIF1* gene under the 35S or rice *Waxy* promoters resulted in smaller grains. This observation illustrates that transgenic plant phenotypes depend on the spatial and temporal patterns of transgene expression.

A study of barley cell wall-bound invertase genes revealed an expression pattern similar to expression of maize *INCW2*. Two cell wall-bound invertase genes, *HvCWINV1* and *HvCWINV2*, were preferentially expressed in the maternal-basal endosperm boundary just before cellularization (Weschke et al., 2003). Transcripts of *HvCWINV1* were localized within the first row of endosperm cells, in the outermost area of the nucellar projection as well as in ETC before starch filling. *HvCWINV2* is expressed early in development, predominantly in the style region and later on in pericarp areas which transiently accumulate starch (Weschke et al., 2003).

Possible additional roles for INCWs have been revealed by examining spatial and temporal expression of the *GhCWIN1* gene in cotton seeds during very early seed development, from just before fertilization to the beginning of starch accumulation in the endosperm (Wang and Ruan, 2012). The dynamics of *GhCWIN1* expression suggest an involvement of INSWs in regulating endosperm nuclear division, embryonic provascular formation and differentiation of ETC (Wang and Ruan, 2012).

#### ETC-SPECIFIC CELL SOLUBLE INVERTASES

A barley gene encoding the soluble acid invertase enzyme, sucrose:fructan 6-fructosyltransferase (*HvSF6FT1*), shows similar temporal and spatial expression patterns to *HvCWINV2* (Weschke et al., 2003). *HvSF6FT1* is expressed in the inner cell layers of maternal pericarp above the dorsal cells, at 3 DAP. At 4 DAP the expression of *HvSF6FT1* is observed in the ventral pericarp and ETC. At 6 DAP, expression of this gene is limited to the ETC layers (Weschke et al., 2003). *HvSF6FT1* transcript levels and acid soluble invertase activity were found to be highest in the maternal pericarp 1–2 days after flowering (DAF). *HvSF6FT1* is strongly expressed in regions flanking the main vascular bundle and to a lesser extent in filial ETC, which continues until grain maturity (Weschke et al., 2003).

#### AN ETC-SPECIFIC HEXOSE TRANSPORTER

Regions of the developing barley grain associated with *HvCWINV1* expression are also associated with expression of a hexose

transporter, HvSTP1 (Weschke et al., 2003; **Table 1**). HvSTP1 is expressed at a very low level within the pericarp, but much more highly in the syncytial endosperm at 3 DAF and in ETC at 7 DAF. The temporal and spatial association of expression of HvSTP1 and INVs suggests that hexoses released by INVs within the endosperm cavity are transferred by the transporter to the liquid part of the mitotically active endosperm (Weschke et al., 2003). HvSTP1 is a large membrane protein of 743 amino acid residues with up to 10 trans-membrane  $\alpha$ -helices, as assessed by hydrophobic cluster analysis (HCA; Callebaut et al., 1997) and PRED-TMR (Pasquier et al., 1999; **Figure 5A**). Our topological analysis shows that HvSTP1 harbors a large intracellular module rich in hydrophilic residues that are positioned approximately in the middle of an  $\alpha$ -helical bundle (**Figure 5B**).

Thus, the activity of cell wall INVs establishes a sucrose concentration gradient between maternal symplast and endosperm apoplast by hydrolysis of sucrose to fructose and glucose moieties. Subsequently, an ETC-specific hexose transporter facilitates the import of hexoses into the endosperm (Miller and Chourey, 1992; Cheng et al., 1996; Weschke et al., 2003).

#### ETC-SPECIFIC LIPID TRANSFER PROTEINS

##### PLANT NON-SPECIFIC LIPID TRANSFER PROTEINS

Non-specific lipid transfer proteins (nsLTPs) have been found in a broad range of tissues from plants, animals and fungi (Crain and Zilversmit, 1980; Tai and Kaplan, 1985; Kader, 1996; Ng et al., 2012). The term “non-specific” indicates that LTPs can bind with phospholipids or their derivatives of broad specificity (Ostergaard et al., 1993). In plants, nsLTPs form multigenic families of structurally related proteins with low levels of protein sequence identity. All plant nsLTPs are originally translated as precursor proteins and contain hydrophobic signal peptides of different length, which are subsequently proteolytically processed by endopeptidases. The enzymes responsible for the processing of precursors remain largely unknown but are likely to be members of the subtilase group of Ser proteases (Murphy et al., 2012). The precise place and role of signal peptide processing of nsLTPs is also unknown. However, in one example it was shown that signal peptide processing takes place in microsomal membranes (Bernhard et al., 1991). It is not yet clear whether the proteolytic cleavage of a signal peptide also occurs in other types of membranes.

Plant nsLTPs usually have a molecular mass between 6.5 and 10.5 kDa and an isoelectric point ranging between 8.5 and 12 (Jose-Estanyol et al., 2004). Each mature nsLTP sequence usually contains a characteristic 8-cysteine residue motif: Cys<sub>1</sub>-Xn-Cys<sub>2</sub>-Xn-Cys<sub>3</sub>Cys<sub>4</sub>-Xn-Cys<sub>5</sub>Xcys<sub>6</sub>-Xn-Cys<sub>7</sub>-Xn-Cys<sub>8</sub>. Plant nsLTPs were initially classified into two types, based on their size and localization (Kader, 1996). Later, a new classification based on the analysis of a large number of nsLTPs sequences was proposed, to include nine types (I–IX) of nsLTPs (Boutrot et al., 2008). Genome-wide analysis revealed 49 *Arabidopsis*, 52 rice and 156 wheat nsLTPs (Boutrot et al., 2008). Recently, the first plant nsLTP database (nsLTPDB<sup>1</sup>) was constructed, which

<sup>1</sup><http://140.114.98.10/ltp/>

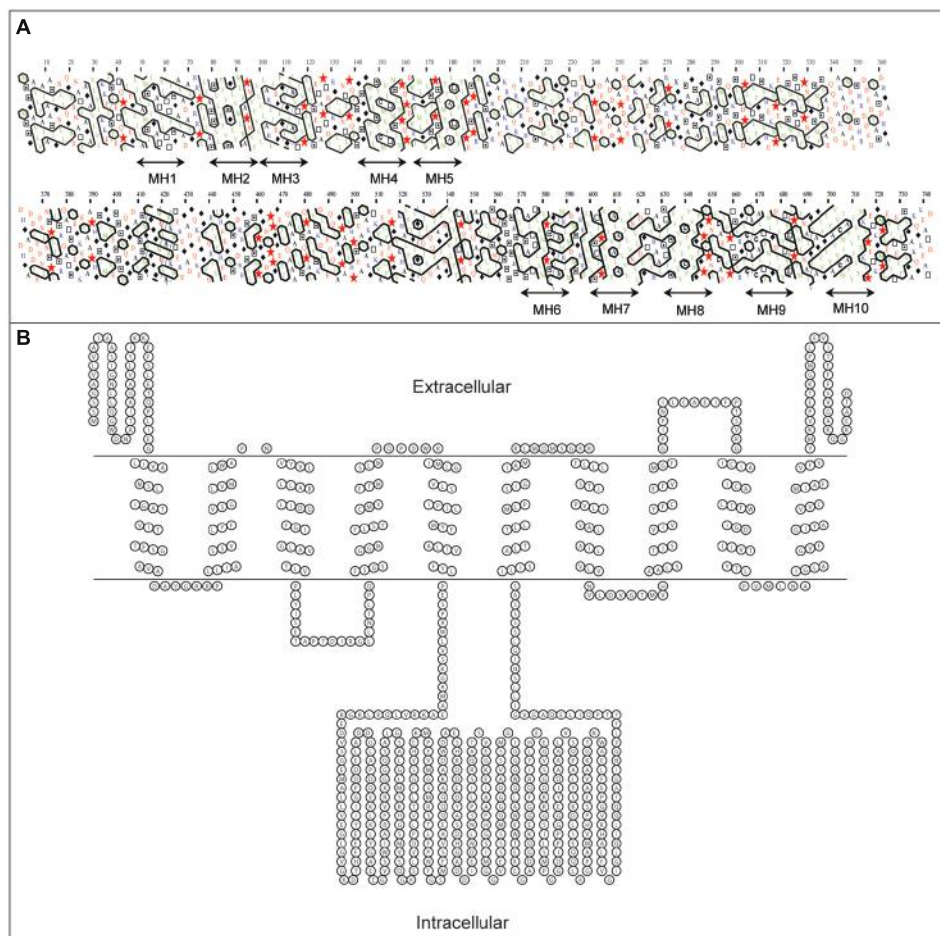


**FIGURE 5 | Secondary structure analyses of a barley hexose transporter HvSTP1. (A)** A bi-dimensional hydrophobic cluster analysis (HCA) plot (Callebaut et al., 1997). Positions of 10 membrane helices MH1–MH10 are marked by arrowed lines. Proline residues are shown as red stars, glycine residues as black diamonds, serine residues are empty squares and threonine residues are shown as squares containing a black dot in the center. Negatively charged residues are

colored in red and positively charged residues are in blue. Other residues are shown by their single amino acid letter codes. The amino acid numbers are read from the top to the bottom of the plots (in duplicate) in a left to right direction. **(B)** A topology model predicted by PRED-TMR algorithm (Pasquier et al., 1999). The intracellular and extracellular positions of individual domains are shown. The topology map was drawn with TOPO (<http://www.sacs.ucsf.edu/TOPO/topo.html>).

initially contained 595 nsLTPs from 121 different species. This database includes information about LTP sequence, protein structure, relevant references and also some biological data (Wang et al., 2012).

Plant nsLTPs are involved in embryogenesis (Sterk et al., 1991), defense against bacterial and fungal pathogens (Molina and Garcia-Olmedo, 1993; Molina et al., 1993; Hendriks et al., 1994; Lindorff-Larsen and Winther, 2001), symbiosis (Krause et al., 1994; Pii et al., 2009), plant response to environmental stresses (White et al., 1994; Liu et al., 2000; Cameron et al., 2006) and in the delivery of waxes to cuticle (Hendriks et al., 1994; Lindorff-Larsen and Winther, 2001; Lee et al., 2009). It has also been postulated that nsLTPs can associate with hydrophobic cell wall compounds and disrupt or facilitate cell wall extension (Nieuwland et al., 2005). A role in these very diverse functions is based on the ability of nsLTPs to carry a broad range of hydrophobic molecules such as fatty acids or fatty acid derivatives (Garcia-Olmedo et al., 1995). LTPs

can catalyze the exchange of lipids between natural and artificial membranes *in vitro* (Helmkamp, 1986; Wirtz and Gadella, 1990; Kader, 1996). A role of nsLTPs in intracellular lipid transfer has also been proposed (Miquel et al., 1988) but not yet proven. Existing knowledge suggests that LTPs are secreted from cells into the extracellular (cell wall) space (Serna et al., 2001; Yeats and Rose, 2008). Precise mechanisms of uploading, delivery to membranes and cuticle, and unloading of lipidic molecules by LTPs remain unclear.

#### LTP GENES SPECIFICALLY OR PREDOMINANTLY EXPRESSED IN ETC

Most nsLTP genes show very specific spatial patterns of expression, and several ETC-specific genes encoding different nsLTPs have been identified in developing kernels (Hueros et al., 1995, 1999b; Doan et al., 1996; Cai et al., 2002; Gutierrez-Marcos et al., 2004; Li et al., 2008; Kovalchuk et al., 2009; **Table 1**). Four types of nsLTPs are found in maize BETL. BETL-1 and BETL-3 show

sequence homology to defensin-like proteins; BETL-2 has no homologous sequences; and BETL-4 shares some homology with the Bowman-Birk family of  $\alpha$ -amylase/trypsin inhibitors (Hueros et al., 1995, 1999b). Members of these protein families have been shown to inhibit the growth of fungi and bacteria (Broekaert et al., 1997). Defensins and probably other types of LTPs can alter the permeability of fungal plasma membranes and hence may act as regulators of transport through plant cellular membranes (Thompson et al., 2001). Proteolytic processing and secretion into adjacent maternal tissue of BETL-2 (also named BAP2) protein was demonstrated by immunolocalization in different grain tissues (Serna et al., 2001). A gene with sequence similarity to *BETL-3*, *OsPR9a*, has been found in rice. However, *OsPR9a* expression is not restricted to ETC, but was also detected in some rice floral tissues (Li et al., 2008).

Expression of BETL-1 and BETL-2 proteins was found to be strongly reduced in the maize *reduced grain filling1* (*rgf1*) mutant, which also showed decreased uptake of sugars in endosperm cells at 5–10 DAP and changes in pedicel development (Maitz et al., 2000). The *rgf1* mutant is morphologically similar to the *mni1* mutant; it causes up to 70% reduction of grain filling in maize. Starch accumulation (but not synthesis) is reduced in *rgf1* kernels. Therefore, the *Rgf1* gene, which has not been identified, may be involved in sugar sensing or transport in ETC (Maitz et al., 2000).

Expression of at least some ETC-specific genes is under maternal control. One such gene, *Maternally Expressed Gene1* (*MEG1*), encodes a LTP which bears structural similarity to defensins (Gutierrez-Marcos et al., 2004). *MEG1* is expressed exclusively in the BETL cells of maize endosperm and has a parent-of-origin expression pattern during early stages of endosperm development. However, at later stages of endosperm development it shows biallelic expression. The product of this gene is glycosylated and localizes to the labyrinthine in-growths of the walls of transfer cells (Gutierrez-Marcos et al., 2004).

Another class of ETC-specific nsLTP genes was identified in the barley transfer cell domain of the endosperm coenocyte. The gene was designated *Endosperm 1* (*END1*; Doan et al., 1996). The expression pattern of the barley *END1* gene and its ortholog from wheat were studied using *in situ* hybridization (Doan et al., 1996; Drea et al., 2005). Before cellularization *END1* transcripts accumulate mainly in the coenocyte above the nucellar projection, and after cellularization in the ventral endosperm over the nucellar projection. At 8 DAP and later, a low level of *END1* expression can be detected in the ETC and the adjacent starchy endosperm (Doan et al., 1996). The function of *END1* remains unknown. The expression of the wheat *END1* homologue, designated *TaPR60*, was studied using transgenic wheat, barley, and rice stably transformed with a gene promoter-GUS fusion construct (Kovalchuk et al., 2009). In wheat and barley, *TaPR60* is expressed predominantly in ETC and in the adjacent starchy endosperm. However, in rice the expression pattern of *TaPR60* was rather different, suggesting that the regulatory mechanisms for ETC-specific expression in rice are different to wheat and barley (Kovalchuk et al., 2009). A molecular model of the *TaPR60* protein lacking its N-terminal hydrophobic peptide, constructed using the crystal structure of a non-specific LTP from *Prunus persica* as a template (Figure 6), indicates the likely positions of a

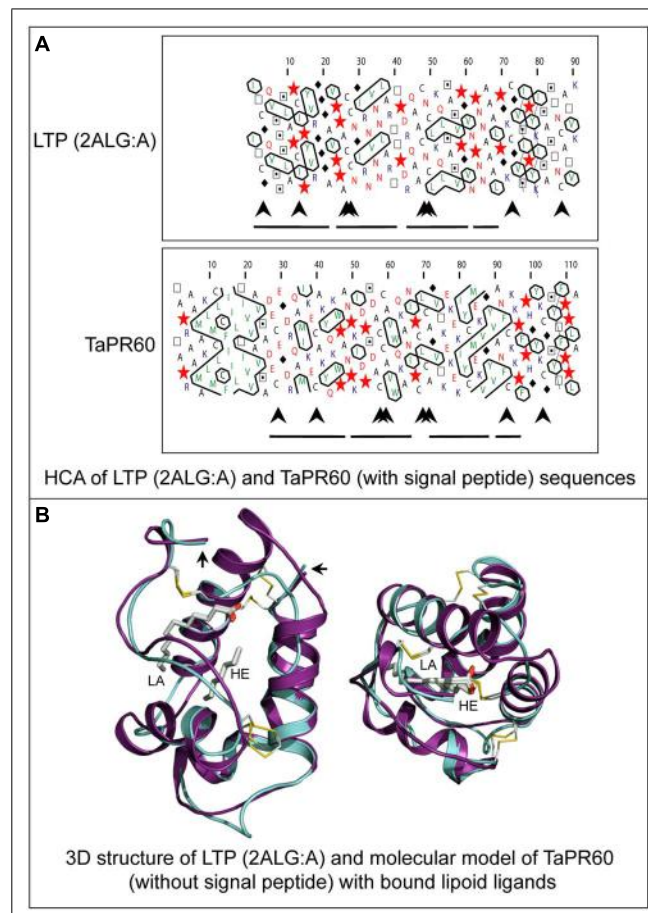


**FIGURE 6 | Structural molecular modeling of the TaPR60 lipid transfer protein. (A)** HCA of a non-specific lipid transfer protein (LTP) from *Prunus persica* (PDB 2ALG:A) and of TaPR60. Positions of N-terminal hydrophobic signal peptide (large arrow), four paired conserved cysteines (arrowheads) and  $\alpha$ -helices (lines) are marked. **(B)** Superposition of the TaPR60 model (cyan) on the template crystal structure of 2ALG:A (magenta) showing distribution of the secondary structural elements. A root-mean-square-deviation value for 69 structurally equivalent residues is 1.5 Å over the C $\alpha$  backbone positions. The dispositions of bound lauric acid (LA; left) and heptane (HE; right), in cpk colors internalized in protein cavities, and the positions of four invariant disulfide bridges (yellow) are also shown. The right-hand-side and left-hand-side arrows indicate N- and C-terminal parts of both proteins, respectively. The Figure was modified from Kovalchuk et al. (2009).

fatty acid (lauric acid) and lipid-mimicking molecule (heptane). These are enclosed in the central cavity of a triple  $\alpha$ -helical bundle of TaPR60. Modeling supports the hypothesis that TaPR60 is involved in binding and transfer of lipid molecules. It was also shown that the cavity of TaPR60 retains its shape both with and without the hydrophobic signal peptide (Kovalchuk et al., 2009). Therefore, TaPR60 could potentially enclose the lipid and lipid-like molecule(s) in the cavity during precursor processing and secretion. One of the possible functions of TaPR60 could be in mediation of lipid delivery to or through a membrane (Kovalchuk et al., 2009). Similar findings were reported for a closely related protein, TdPR61, isolated from durum wheat (*T. durum*; Kovalchuk et al., 2012a).

Expression directed by the promoter of a rice homologue of the *END1* gene, *OsPR602*, was studied in transgenic rice and barley. In rice, the promoter of *OsPR602* was active in ETC and above the ETC in several layers of the starchy endosperm cells. However, *GUS* reporter gene expression was also detected in the maternal vascular tissue adjacent to ETC and vascular tissue of the lemma and palea (Li et al., 2008). Surprisingly, in barley the promoter of *OsPR602* was activated only in ETC and adjacent layers of starchy endosperm and the temporal and spatial patterns of *GUS* expression were perfectly correlated with the expression of the *END1* gene from barley and *TaPR60* from wheat (Doan et al., 1996; Kovalchuk et al., 2009). These data again suggest possible differences in ETC-specific gene regulation between barley and rice.

The most probable roles of *END1*-like proteins in ETC are regulation of cell wall-ingrowth extension, formation of cellular membranes, lipid transfer to endosperm and/or defense from bacterial and fungal pathogens transported from maternal tissues.

### OTHER ETC-SPECIFIC GENES

Recently, a new ETC-specific gene, *AL1*, was isolated from rice (Kuwano et al., 2011; **Table 1**). The gene encodes a putative anthranilate N-hydroxycinnamoyl/benzoyltransferase and is expressed in the dorsal aleurone layer adjacent to the main vascular bundle. In rice, transfer cells are differentiated in this region. The role of this gene in plants remains unknown.

With the advent of new technologies for tissue/cell-specific transcriptome and proteome analysis (Thiel et al., 2012; Silva-Sánchez et al., 2013) it is expected that further genes with ETC-specific or predominant expression of novel function will be identified.

### POTENTIAL APPLICATIONS OF ETC-SPECIFIC GENES AND THEIR PROMOTERS FOR IMPROVEMENT OF GRAIN QUALITY AND YIELD

It is a well-documented that grain development in crops occurs under saturated supply of assimilates, which indicates that transportation of those nutrients from plant maternal tissues to embryo and endosperm is the main yield limiting factor (Borrás et al., 2004; Bihmidine et al., 2013). Therefore, manipulating the nutrients transport in order to increase grain sink strength is expected to lead to increased yield (Reynolds et al., 2009). Considering the role of ETC as a principal gateway regulating flux of nutrient precursors for endosperm filling, there is a huge, yet un-realized potential for engineering this gateway to increase grain yield and improve endosperm composition: quantity and quality of carbohydrates, proteins, lipids and micronutrients.

The importance of TCS for ETC development and the likely consequential involvement of TCS components in grain development, make this group of genes interesting tools for engineering or modifying grain quality and yield. Furthermore, involvement of TCS components in response to major abiotic stresses such as drought (Le et al., 2011; Kang et al., 2012), high salinity (Karan et al., 2009), and cold stress (Jeon et al., 2010) have been demonstrated. Although many genes representing the major components of TCS were recently identified in the barley ETC layer (Thiel et al.,

2012), their function and responsiveness to environmental stresses and stimuli are largely unknown. Most of the existing studies on TCS-based cytokinin and ethylene signaling have been done in the model plant *A. thaliana*. Although studies have recently expanded to a broader range of plant species, there is still very little known about TCS function in cereals and specifically in grain development (Hellmann et al., 2010). Therefore, it is still too early to design or even predict possible applications of specific grain-related TCS genes in breeding and molecular genetics projects.

There are similar problems for biotechnologists interested in manipulating the transcriptional regulation of ETC development and function. Only one TF, *ZmMRP-1*, has been demonstrated to regulate ETC function (Gómez et al., 2002). Observations that *ZmMRP-1* regulate several ETC-specific genes makes this TF a promising target. However, characterisation of transgenic plants with up- or down-regulated *ZmMRP-1* has not been reported. It may be that ectopic, constitutive overexpression of *ZmMRP-1* or silencing of this gene leads to significant pleiotropic changes in plant development or is lethal. It would be particularly interesting to express this gene under an ETC-specific promoter that is regulated by *ZmMRP-1*. This could lead to higher levels of *ZmMRP-1* as a result of feed-back loop activation of the promoter. Higher levels of *ZmMRP-1* could potentially enhance and/or extend in time the activation of target ETC-genes, and consequently further increase the development of cell wall-ingrowths (to increase cell membrane surface) and levels of ETC-specific proteins responsible for transport of lipids and sugars, hopefully culminating in increased efficacy of ETC function. An alternative to overexpression of *ZmMRP-1* could be manipulation of levels of *ZmMRP-1* regulators, the MRPI proteins.

The best studied and currently most promising ETC-related genes for the engineering of grain quality and yield, and particularly for grain yield under stress conditions, are genes of sucrose synthases, INVs, and hexose transporters. There are considerable data on the structure and function of these genes (Weschke et al., 2000; Xu et al., 2012). Some of these genes are either specifically or predominantly expressed in ETC and tissues adjacent to ETC layers in barley (Weschke et al., 2000), sorghum (Jain et al., 2008b), cotton (Wang and Ruan, 2012), maize (Chourey et al., 2012; Liu et al., 2012), and rice (Wang et al., 2008a). Improvement of grain size and yield by overexpression of a hexose transporter has not been reported. Recent reports of the effects of sucrose synthase and cell wall-bound invertase overexpression, however, are astonishing (Wang et al., 2008a; Xu et al., 2012; Li et al., 2013). For example, overexpression of a potato sucrose synthase gene in transgenic cotton reduced seed abortion and increased the seed fresh weight by about 30% compared to the seed weight of control plants (Xu et al., 2012). Constitutive overexpression of the *Mn1* gene from *Arabidopsis*, rice and maize in transgenic maize significantly increased invertase activities in leaves and developing seeds and dramatically improved grain yield through enlarged ears, and increased grain size and number (Li et al., 2013). Total starch content in transgenic kernels was also increased.

It is interesting however, that ectopic expression of cell wall-bound INVs does not always produce an expected positive effect

on grain size and yield. For example, ectopic expression of the *GIF1* gene under 35S or rice *Waxy* promoters resulted in smaller grains, while overexpression of *GIF1* driven by its native promoter increased grain production (Wang et al., 2008a). The incorrect spatial or temporal expression of sugar INVs and hexose transporters can potentially lead to re-arrangement of auxin levels in grain tissues and consequential changes in auxin gradient. Decreased auxin levels impair development of ETC and other parts of endosperm (Bernardi et al., 2012). Therefore, knowing and considering the cascade of events induced by hormones during early stages of grain development is important for making correct decisions on spatial and temporal expression of genes, which can directly or indirectly influence auxin concentrations.

Another way to increase invertase activity, while maintaining the original spatial patterns of invertase gene expression, is in silencing invertase inhibitors (Rausch and Greiner, 2004). Silencing of invertase inhibitors in transgenic tomato plants resulted in an increased seed weight and increased levels of hexoses in fruit (Jin et al., 2009). Inhibitor(s) of ETC-specific INVs have not been reported, but if such inhibitor(s) exist, tissue-specific silencing of these gene(s) would be interesting to test.

It would also be interesting to express genes of sucrose synthase, invertase, and hexose transporters simultaneously, using stacking constructs and clever selection of suitable promoters. A simpler approach could be the tissue specific overexpression of a TF which co-ordinately regulates a group of sugar production and transport genes. It was recently reported that overexpression of the soybean *GmZIP123* gene in transgenic *Arabidopsis* not only enhanced lipid accumulation in *Arabidopsis* seeds, but also up-regulated expression of two sucrose transporter genes and three cell-wall invertase genes by directly binding to their promoters. This in turn significantly increased levels of sucrose and both hexoses in seeds of transgenic plants compared to seeds of control plants (Song et al., 2013).

## CONCLUSIONS AND FUTURE PERSPECTIVES

ETC are highly specialized cells responsible for the delivery of signals and nutrients from maternal tissues to the developing endosperm. Large numbers of ETC-specific genes and genes predominantly expressed in ETC have been isolated and characterized from important cereal crop species and other plants during the last decade. Surprisingly, the most of identified genes fall into just four of the five groups. These four groups of genes are involved in signal transduction and/or transcriptional regulation in ETC. Genes from two groups are directly involved in transport of sugars and lipids to the endosperm. Because of the significance of ETC for grain development, ETC-specific genes and their promoters are important targets for the generation of transgenic crop plants with improved seed size and quality characteristics. The overexpression of ETC-specific *INCW* genes in transgenic rice and maize provides the first example of targeting ETC-specific genes for the manipulation of grain characteristics. However, a better understanding of the roles of ETC-specific genes encoding regulatory proteins is required for the correct application of these genes for grain biotechnology.

## ACKNOWLEDGMENTS

This work was supported by the Grains Research and Development Corporation, Government of South Australia, and by grant LP120100201 from the Australian Research Council to Maria Hrmova and Sergiy Lopato. We wish to thank Dr Nataliya Kovalchuk for providing us with pictures for the **Figure 1** and Dr Julie Hayes for critically reading the manuscript.

## REFERENCES

- Barrera, C., Muniz, L. M., Gomez, E., Hueros, G., and Royo, J. (2006). Molecular dissection of the interaction between the transcriptional activator ZmMRP-1 and the promoter of BETL-1. *Plant Mol. Biol.* 62, 655–668. doi: 10.1007/s11103-006-9047-5
- Barrera, C., Royo, J., Grijota-Martinez, C., Faye, C., Paul, W., Sanz, S., et al. (2009). The promoter of ZmMRP-1, a maize transfer cell-specific transcriptional activator, is induced at solute exchange surfaces and responds to transport demands. *Planta* 229, 235–247. doi: 10.1007/s00425-008-0823-0
- Bauer, J., Reiss, K., Veerabagu, M., Heunemann, M., Harter, K., and Stehle, T. (2013). Structure-function analysis of *Arabidopsis thaliana* histidine kinase AHK5 bound to its cognate phosphotransfer protein AHP1. *Mol. Plant* 6, 959–970. doi: 10.1093/mp/sss126
- Bernardi, J., Lanubile, A., Li, Q. B., Kumar, D., Kladnik, A., Cook, S. D., et al. (2012). Impaired auxin biosynthesis in the defective endosperm18 mutant is due to mutational loss of expression in the ZmYuc1 gene encoding endosperm-specific YUCCA1 protein in maize. *Plant Physiol.* 160, 1318–1328. doi: 10.1104/pp.112.204743
- Bernhard, W. R., Thoma, S., Botella, J., and Somerville, C. R. (1991). Isolation of a cDNA clone for spinach lipid transfer protein and evidence that the protein is synthesized by the secretory pathway. *Plant Physiol.* 95, 164–170. doi: 10.1104/pp.95.1.164
- Bihmidine, S., Hunter, C. T. III, Johns, C. E., Koch, K. E., and Braun, D. M. (2013). Regulation of assimilate import into sink organs: update on molecular drivers of sink strength. *Front. Plant Sci.* 4:177. doi: 10.3389/fpls.2013.00177
- Borrás, L., Slafer, G. A., and Otegui, M. E. (2004). Seed dry weight response to source–sink manipulations in wheat, maize and soybean: a quantitative reappraisal. *Field Crops Res.* 86, 131–146. doi: 10.1016/j.fcr.2003.08.002
- Boutrot, F., Chantret, N., and Gautier, M. F. (2008). Genome-wide analysis of the rice and *Arabidopsis* non-specific lipid transfer protein (nsLtp) gene families and identification of wheat nsLtp genes by EST data mining. *BMC Genomics* 9:86. doi: 10.1186/1471-2164-9-86
- Boutrot, F., Meynard, D., Guiderdoni, E., Joudrier, P., and Gautier, M. F. (2007). The *Triticum aestivum* non-specific lipid transfer protein (TaLtp) gene family: comparative promoter activity of six TaLtp genes in transgenic rice. *Planta* 225, 843–862. doi: 10.1007/s00425-006-0397-7
- Broekaert, W. F., Cammue, B. P., De Bolle, M., Thevissen, K., De Samblanx, G. W., and Osborn, R. (1997). Antimicrobial peptides from plants. *Crit. Rev. Plant Sci.* 16, 297–323. doi: 10.1080/07352689709701952
- Bru, C., Courcelle, E., Carrere, S., Beausse, Y., Dalmar, S., and Kahn, D. (2005). The ProDom database of protein domain families: more emphasis on 3D. *Nucleic Acids Res.* 33, D212–D215. doi: 10.1093/nar/gki034
- Cai, G., Faleri, C., Del Casino, C., Hueros, G., Thompson, R. D., and Cresti, M. (2002). Subcellular localisation of BETL-1, -2 and -4 in *Zea mays* L. endosperm. *Sex. Plant Reprod.* 15, 85–98. doi: 10.1007/s00497-002-0141-9
- Callebaut, I., Labesse, G., Durand, P., Poupon, A., Canard, L., Chomilier, J., et al. (1997). Deciphering protein sequence information through hydrophobic cluster analysis (HCA): current status and perspectives. *Cell Mol. Life Sci.* 53, 621–645. doi: 10.1007/s0018005005082
- Cameron, K. D., Teece, M. A., and Smart, L. B. (2006). Increased accumulation of cuticular wax and expression of lipid transfer protein in response to periodic drying events in leaves of tree tobacco. *Plant Physiol.* 140, 176–183. doi: 10.1104/pp.105.069724
- Carlson, S. J., Shanker, S., and Chourey, P. S. (2000). A point mutation at the Miniature1 seed locus reduces levels of the encoded protein, but not its mRNA, in maize. *Mol. Gen. Genet.* 263, 367–373. doi: 10.1007/s004380051180
- Chefdor, F., Benedetti, H., Depierreux, C., Delmotte, F., Morabito, D., and Carpin, S. (2006). Osmotic stress sensing in *Populus*: components identification of a phosphorelay system. *FEBS Lett.* 580, 77–81. doi: 10.1016/j.febslet.2005.11.051

- Cheng, W. H., Taliercio, E. W., and Chourey, P. S. (1996). The Miniature1 seed locus of maize encodes a cell wall invertase required for normal development of endosperm and maternal cells in the pedicel. *Plant Cell* 8, 971–983.
- Chourey, P. S., Jain, M., Li, Q. B., and Carlson, S. J. (2006). Genetic control of cell wall invertases in developing endosperm of maize. *Planta* 223, 159–167. doi: 10.1007/s00425-005-0039-5
- Chourey, P. S., Li, Q. B., and Cevallos-Cevallos, J. (2012). Pleiotropy and its dissection through a metabolic gene Miniature1 (Mn1) that encodes a cell wall invertase in developing seeds of maize. *Plant Sci.* 184, 45–53. doi: 10.1016/j.plantsci.2011.12.011
- Chourey, P. S., Li, Q. B., and Kumar, D. (2010). Sugar-hormone cross-talk in seed development: two redundant pathways of IAA biosynthesis are regulated differentially in the invertase-deficient miniature1 (mn1) seed mutant in maize. *Mol. Plant* 3, 1026–1036. doi: 10.1093/mp/ssq057
- Coello, P., and Polacco, C. J. (1999). ARR6, a response regulator from *Arabidopsis*, is differentially regulated by plant nutritional status. *Plant Sci.* 143, 211–220. doi: 10.1016/S0168-9452(99)00033-3
- Costa, L. M., Gutierrez-Marcos, J. F., Brutnell, T. P., Greenland, A. J., and Dickinson, H. G. (2003). The globby1-1 (glo1-1) mutation disrupts nuclear and cell division in the developing maize seed causing alterations in endosperm cell fate and tissue differentiation. *Development* 130, 5009–5017. doi: 10.1242/dev.00692
- Costa, L. M., Gutierrez-Marcos, J. F., and Dickinson, H. G. (2004). More than a yolk: the short life and complex times of the plant endosperm. *Trends Plant Sci.* 9, 507–514. doi: 10.1016/j.tplants.2004.08.007
- Crain, R. C., and Zilversmit, D. B. (1980). Net transfer of phospholipid by the nonspecific phospholipid transfer proteins from bovine liver. *Biochim. Biophys. Acta* 620, 37–48. doi: 10.1016/0005-2760(80)90182-4
- Doan, D. N., Linnestad, C., and Olsen, O. A. (1996). Isolation of molecular markers from the barley endosperm coenocyte and the surrounding nucellus cell layers. *Plant Mol. Biol.* 31, 877–886. doi: 10.1007/BF00019474
- Drea, S., Leader, D. J., Arnold, B. C., Shaw, P., Dolan, L., and Doonan, J. H. (2005). Systematic spatial analysis of gene expression during wheat caryopsis development. *Plant Cell* 17, 2172–2185. doi: 10.1105/tpc.105.034058
- Fernandes, J., Tavares, S., and Amancio, S. (2009). Identification and expression of cytokinin signaling and meristem identity genes in sulfur deficient grapevine (*Vitis vinifera* L.). *Plant Signal. Behav.* 4, 1128–1135. doi: 10.4161/psb.4.12.9942
- Garcia-Olmedo, F., Molina, A., Segura, A., and Moreno, M. (1995). The defensive role of nonspecific lipid-transfer proteins in plants. *Trends Microbiol.* 3, 72–74. doi: 10.1016/S0966-842X(90)88879-4
- Gómez, E., Royo, J., Guo, Y., Thompson, R., and Hueros, G. (2002). Establishment of cereal endosperm expression domains: identification and properties of a maize transfer cell-specific transcription factor, ZmMRP-1. *Plant Cell* 14, 599–610. doi: 10.1105/tpc.010365
- Gomez, E., Royo, J., Muniz, L. M., Sellam, O., Paul, W., Gerentes, D., et al. (2009). The maize transcription factor myb-related protein-1 is a key regulator of the differentiation of transfer cells. *Plant Cell* 21, 2022–2035. doi: 10.1105/tpc.108.065409
- Gutierrez-Marcos, J. F., Costa, L. M., Biderre-Petit, C., Khbayla, B., O'Sullivan, D. M., Wormald, M., et al. (2004). Maternally expressed gene1 is a novel maize endosperm transfer cell-specific gene with a maternal parent-of-origin pattern of expression. *Plant Cell* 16, 1288–1301. doi: 10.1105/tpc.019778
- Hall, M. N., and Silhavy, T. J. (1981). Genetic analysis of the major outer membrane proteins of *Escherichia coli*. *Annu. Rev. Genet.* 15, 91–142. doi: 10.1146/annurev.ge.15.120181.000515
- Hellmann, E., Gruhn, N., and Heyl, A. (2010). The more, the merrier: cytokinin signaling beyond *Arabidopsis*. *Plant Signal. Behav.* 5, 1384–1390. doi: 10.4161/psb.5.11.13157
- Helmkamp, G. M. J. (1986). Phospholipid transfer proteins: mechanism of action. *J. Bioenerg. Biomembr.* 81, 71–91. doi: 10.1007/BF00743477
- Hendriks, T., Meijer, E. A., Thoma, S., Kader, J.-C., and de Vries, S. C. (1994). “The carrot extracellular lipid transfer protein EP2: quantitative aspects with respect to its putative role in cutin synthesis,” in *Plant Molecular Biology*, Vol. H 81, eds G. Coruzzi and P. Puigdomènech (Berlin: Springer), 85–94.
- Hirose, T., Takano, M., and Terao, T. (2002). Cell wall invertase in developing rice caryopsis: molecular cloning of OsCIN1 and analysis of its expression in relation to its role in grain filling. *Plant Cell Physiol.* 43, 452–459. doi: 10.1093/pcp/pcf055
- Hosoda, K., Imamura, A., Katoh, E., Hatta, T., Tachiki, M., Yamada, H., et al. (2002). Molecular structure of the GARP family of plant Myb-related DNA binding motifs of the *Arabidopsis* response regulators. *Plant Cell* 14, 2015–2029. doi: 10.1105/tpc.002733
- Hueros, G., Royo, J., Maitz, M., Salamini, F., and Thompson, R. D. (1999a). Evidence for factors regulating transfer cell-specific expression in maize endosperm. *Plant Mol. Biol.* 41, 403–414. doi: 10.1023/A:1006331707605
- Hueros, G., Gomez, E., Cheikh, N., Edwards, J., Weldon, M., Salamini, F., et al. (1999b). Identification of a promoter sequence from the BET1 gene cluster able to confer transfer-cell-specific expression in transgenic maize. *Plant Physiol.* 121, 1143–1152. doi: 10.1104/pp.121.4.1143
- Hueros, G., Varotto, S., Salamini, F., and Thompson, R. D. (1995). Molecular characterization of BET1, a gene expressed in the endosperm transfer cells of maize. *Plant Cell* 7, 747–757. doi: 10.1105/tpc.7.6.747
- Hwang, I., and Sheen, J. (2001). Two-component circuitry in *Arabidopsis* cytokinin signal transduction. *Nature* 413, 383–389. doi: 10.1038/35096500
- Jain, M., Tyagi, A. K., and Khurana, J. P. (2008a). Differential gene expression of rice two-component signaling elements during reproductive development and regulation by abiotic stress. *Funct. Integr. Genomics* 8, 175–180. doi: 10.1007/s10142-007-0063-6
- Jain, M., Chourey, P. S., Li, Q. B., and Pring, D. R. (2008b). Expression of cell wall invertase and several other genes of sugar metabolism in relation to seed development in sorghum (*Sorghum bicolor*). *J. Plant Physiol.* 165, 331–344. doi: 10.1016/j.jplph.2006.12.003
- Javelle, M., Klein-Cosson, C., Vernoud, V., Boltz, V., Maher, C., Timmermans, M., et al. (2011). Genome-wide characterization of the HD-ZIP IV transcription factor family in maize: preferential expression in the epidermis. *Plant Physiol.* 157, 790–803. doi: 10.1104/pp.111.182147
- Javelle, M., Vernoud, V., Depege-Fargeix, N., Arnould, C., Oursel, D., Domergue, F., et al. (2010). Overexpression of the epidermis-specific homeodomain-leucine zipper IV transcription factor Outer Cell Layer1 in maize identifies target genes involved in lipid metabolism and cuticle biosynthesis. *Plant Physiol.* 154, 273–286. doi: 10.1104/pp.109.150540
- Jeon, J., Kim, N. Y., Kim, S., Kang, N. Y., Novak, O., Ku, S. J., et al. (2010). A subset of cytokinin two-component signaling system plays a role in cold temperature stress response in *Arabidopsis*. *J. Biol. Chem.* 285, 23371–23386. doi: 10.1074/jbc.M109.096644
- Jin, Y., Ni, D. A., and Ruan, Y. L. (2009). Posttranslational elevation of cell wall invertase activity by silencing its inhibitor in tomato delays leaf senescence and increases seed weight and fruit hexose level. *Plant Cell* 21, 2072–2089. doi: 10.1105/tpc.108.063719
- Jolivet, K., Grenier, E., Bouchet, J. P., Esquibet, M., Kerlan, M. C., Caromel, B., et al. (2007). Identification of plant genes regulated in resistant potato *Solanum sparsipilum* during the early stages of infection by *Globodera pallida*. *Genome* 50, 422–427. doi: 10.1139/G07-015
- Jose-Estanyol, M., Gomis-Ruth, F. X., and Puigdomenech, P. (2004). The eight-cysteine motif, a versatile structure in plant proteins. *Plant Physiol. Biochem.* 42, 355–365. doi: 10.1016/j.plaphy.2004.03.009
- Kader, J. C. (1996). Lipid-transfer proteins in plants. *Annu. Rev. Plant Physiol. Plant Mol. Biol.* 47, 627–654. doi: 10.1146/annurev.arplant.47.1.627
- Kakimoto, T. (1996). CKI1, a histidine kinase homolog implicated in cytokinin signal transduction. *Science* 274, 982–985. doi: 10.1126/science.274.5289.982
- Kang, B. H., Xiong, Y., Williams, D. S., Pozueta-Romero, D., and Chourey, P. S. (2009). Miniature1-encoded cell wall invertase is essential for assembly and function of wall-in-growth in the maize endosperm transfer cell. *Plant Physiol.* 151, 1366–1376. doi: 10.1104/pp.109.142331
- Kang, N. Y., Cho, C., Kim, N. Y., and Kim, J. (2012). Cytokinin receptor-dependent and receptor-independent pathways in the dehydration response of *Arabidopsis thaliana*. *J. Plant Physiol.* 169, 1382–1391. doi: 10.1016/j.jplph.2012.05.007
- Karan, R., Singla-Pareek, S. L., and Pareek, A. (2009). Histidine kinase and response regulator genes as they relate to salinity tolerance in rice. *Funct. Integr. Genomics* 9, 411–417. doi: 10.1007/s10142-009-0119-x
- Kim, H. J., Ryu, H., Hong, S. H., Woo, H. R., Lim, P. O., Lee, I. C., et al. (2006). Cytokinin-mediated control of leaf longevity by AHK3 through phosphorylation of ARR2 in *Arabidopsis*. *Proc. Natl. Acad. Sci. U.S.A.* 103, 814–819. doi: 10.1073/pnas.0505150103

- Kovalchuk, N., Smith, J., Pallotta, M., Singh, R., Ismagul, A., Eliby, S., et al. (2009). Characterization of the wheat endosperm transfer cell-specific protein TaPR60. *Plant Mol. Biol.* 71, 81–98. doi: 10.1007/s11103-009-9510-1
- Kovalchuk, N., Wu, W., Eini, O., Bazanova, N., Pallotta, M., Shirley, N., et al. (2012a). The scutellar vascular bundle-specific promoter of the wheat HD-Zip IV transcription factor shows similar spatial and temporal activity in transgenic wheat, barley and rice. *Plant Biotechnol. J.* 10, 43–53. doi: 10.1111/j.1467-7652.2011.00633.x
- Kovalchuk, N., Smith, J., Bazanova, N., Pyvovarenko, T., Singh, R., Shirley, N., et al. (2012b). Characterization of the wheat gene encoding a grain-specific lipid transfer protein TdPR61, and promoter activity in wheat, barley and rice. *J. Exp. Bot.* 63, 2025–2040. doi: 10.1093/jxb/err409
- Krause, A., Sigrist, C. J., Dehning, I., Sommer, H., and Broughton, W. J. (1994). Accumulation of transcripts encoding a lipid transfer-like protein during deformation of nodulation-competent *Vigna unguiculata* root hairs. *Mol. Plant Microbe Interact.* 7, 411–418. doi: 10.1094/MPMI-7-0411
- Kuwano, M., Masumura, T., and Yoshida, K. T. (2011). A novel endosperm transfer cell-containing region-specific gene and its promoter in rice. *Plant Mol. Biol.* 76, 47–56. doi: 10.1007/s11103-011-9765-1
- Le, D. T., Nishiyama, R., Watanabe, Y., Mochida, K., Yamaguchi-Shinozaki, K., Shinozaki, K., et al. (2011). Genome-wide expression profiling of soybean two-component system genes in soybean root and shoot tissues under dehydration stress. *DNA Res.* 18, 17–29. doi: 10.1093/dnaregs/dsq032
- LeClerc, S., Schmelz, E. A., and Chourey, P. S. (2008). Cell wall invertase-deficient miniature1 kernels have altered phytohormone levels. *Phytochemistry* 69, 692–699. doi: 10.1016/j.phytochem.2007.09.011
- LeClerc, S., Schmelz, E. A., and Chourey, P. S. (2010). Sugar levels regulate tryptophan-dependent auxin biosynthesis in developing maize kernels. *Plant Physiol.* 153, 306–318. doi: 10.1104/pp.110.155226
- Lee, S. B., Go, Y. S., Bae, H. J., Park, J. H., Cho, S. H., Cho, H. J., et al. (2009). Disruption of glycosylphosphatidylinositol-anchored lipid transfer protein gene altered cuticular lipid composition, increased plastoglobules, and enhanced susceptibility to infection by the fungal pathogen *Alternaria brassicicola*. *Plant Physiol.* 150, 42–54. doi: 10.1104/pp.109.137745
- Lemoine, R., La Camera, S., Atanassova, R., Dedaldechamp, F., Allario, T., Pourtau, N., et al. (2013). Source-to-sink transport of sugar and regulation by environmental factors. *Front. Plant Sci.* 4:272. doi: 10.3389/fpls.2013.00272
- Letunic, I., Doerks, T., and Bork, P. (2012). SMART 7: recent updates to the protein domain annotation resource. *Nucleic Acids Res.* 40, D302–D305. doi: 10.1093/nar/gkr931
- Li, B., Liu, H., Zhang, Y., Kang, T., Zhang, L., Tong, J., et al. (2013). Constitutive expression of cell wall invertase genes increases grain yield and starch content in maize. *Plant Biotechnol. J.* 11, 1080–1091. doi: 10.1111/pbi.12102
- Li, M., Singh, R., Bazanova, N., Milligan, A. S., Shirley, N., Langridge, P., et al. (2008). Spatial and temporal expression of endosperm transfer cell-specific promoters in transgenic rice and barley. *Plant Biotechnol. J.* 6, 465–476. doi: 10.1111/j.1467-7652.2008.00333.x
- Lindorff-Larsen, K., and Winther, J. R. (2001). Surprisingly high stability of barley lipid transfer protein, LTP1, towards denaturant, heat and proteases. *FEBS Lett.* 488, 145–148. doi: 10.1016/S0014-5793(00)02424-8
- Liu, H. C., Creech, R. G., Jenkins, J. N., and Ma, D. P. (2000). Cloning and promoter analysis of the cotton lipid transfer protein gene Ltp3. *Biochim. Biophys. Acta* 1487, 106–111. doi: 10.1016/S1388-1981(00)00072-X
- Liu, Y. H., Cao, J. S., Li, G. J., Wu, X. H., Wang, B. G., Xu, P., et al. (2012). Genotypic differences in pod wall and seed growth relate to invertase activities and assimilate transport pathways in asparagus bean. *Ann. Bot.* 109, 1277–1284. doi: 10.1093/aob/mcs060
- Lowe, J., and Nelson, O. E. (1946). Miniature seed: a study in the development of a defective caryopsis in maize. *Genetics* 31, 525–533.
- Maitz, M., Santandrea, G., Zhang, Z., Lal, S., Hannah, L. C., Salamini, F., et al. (2000). rgf1, a mutation reducing grain filling in maize through effects on basal endosperm and pedicel development. *Plant J.* 23, 29–42. doi: 10.1046/j.1365-313x.2000.00747.x
- Miller, M. E., and Chourey, P. S. (1992). The maize invertase-deficient miniature-1 seed mutation is associated with aberrant pedicel and endosperm development. *Plant Cell* 4, 297–305. doi: 10.1105/tpc.4.3.297
- Miquel, M., Block, M. A., Joyard, J., Dorne, A. J., Dubacq, J. P., Kader, J. C., et al. (1988). Protein-mediated transfer of phosphatidylcholine from liposomes to spinach chloroplast envelope membranes. *Biochim. Biophys. Acta* 937, 219–228. doi: 10.1016/0005-2736(88)90244-1
- Mizuno, T. (2005). Two-component phosphorelay signal transduction systems in plants: from hormone responses to circadian rhythms. *Biosci. Biotechnol. Biochem.* 69, 2263–2276. doi: 10.1271/bbb.69.2263
- Molina, A., and Garcia-Olmedo, F. (1993). Developmental and pathogen-induced expression of three barley genes encoding lipid transfer proteins. *Plant J.* 4, 983–991. doi: 10.1046/j.1365-313X.1993.04060983.x
- Molina, A., Segura, A., and Garcia-Olmedo, F. (1993). Lipid transfer proteins (nsLTPs) from barley and maize leaves are potent inhibitors of bacterial and fungal plant pathogens. *FEBS Lett.* 316, 119–122. doi: 10.1016/0014-5793(93)81198-9
- Monjardino, P., Rocha, S., Tavares, A. C., Fernandes, R., Sampaio, P., Salema, R., et al. (2013). Development of flange and reticulate wall ingrowths in maize (*Zea mays* L.) endosperm transfer cells. *Protoplasma* 250, 495–503. doi: 10.1007/s00709-012-0432-4
- Muñiz, L. M., Royo, J., Gomez, E., Barrero, C., Bergareche, D., and Hueros, G. (2006). The maize transfer cell-specific type-A response regulator ZmTCRR-1 appears to be involved in intercellular signalling. *Plant J.* 48, 17–27. doi: 10.1111/j.1365-313X.2006.02848.x
- Muñiz, L. M., Royo, J., Gomez, E., Baudot, G., Paul, W., and Hueros, G. (2010). A typical response regulators expressed in the maize endosperm transfer cells link canonical two component systems and seed biology. *BMC Plant Biol.* 10:84. doi: 10.1186/1471-2229-10-84
- Murphy, E., Smith, S., and De Smet, I. (2012). Small signaling peptides in *Arabidopsis* development: how cells communicate over a short distance. *Plant Cell* 24, 3198–3217. doi: 10.1105/tpc.112.099010
- Ng, T. B., Cheung, R. C., Wong, J. H., and Ye, X. (2012). Lipid-transfer proteins. *Biopolymers* 98, 268–279. doi: 10.1002/bip.22098
- Nieuwland, J., Feron, R., Huisman, B. A., Fasolino, A., Hilbers, C. W., Derkens, J., et al. (2005). Lipid transfer proteins enhance cell wall extension in tobacco. *Plant Cell* 17, 2009–2019. doi: 10.1105/tpc.105.032094
- Offler, C. E., McCurdy, D. W., Patrick, J. W., and Talbot, M. J. (2003). Transfer cells: cells specialized for a special purpose. *Annu. Rev. Plant Biol.* 54, 431–454. doi: 10.1146/annurev.arplant.54.031902.134812
- Olsen, O. A. (2004). Nuclear endosperm development in cereals and *Arabidopsis thaliana*. *Plant Cell* 16(Suppl.), S214–S227. doi: 10.1105/tpc.017111
- Ostergaard, J., Vergnolle, C., Schoentgen, F., and Kader, J. C. (1993). Acyl-binding/lipid-transfer proteins from rape seedlings, a novel category of proteins interacting with lipids. *Biochim. Biophys. Acta* 1170, 109–117. doi: 10.1016/0005-2760(93)90059-I
- Pasquier, C., Promponas, V. J., Palaios, G. A., Hamodrakas, J. S., and Hamodrakas, S. J. (1999). A novel method for predicting transmembrane segments in proteins based on a statistical analysis of the SwissProt database: the PRED-TMR algorithm. *Protein Eng.* 12, 381–385. doi: 10.1093/protein/12.5.381
- Pei, J., Kim, B. H., and Grishin, N. V. (2008). PROMALS3D: a tool for multiple protein sequence and structure alignments. *Nucleic Acids Res.* 36, 2295–2300. doi: 10.1093/nar/gkn072
- Pii, Y., Asteegno, A., Peroni, E., Zaccardelli, M., Pandolfini, T., and Crimi, M. (2009). The *Medicago truncatula* N5 gene encoding a root-specific lipid transfer protein is required for the symbiotic interaction with *Sinorhizobium meliloti*. *Mol. Plant Microbe Interact.* 22, 1577–1587. doi: 10.1094/MPMI-22-12-1577
- Rausch, T., and Greiner, S. (2004). Plant protein inhibitors of invertases. *Biochim. Biophys. Acta* 1696, 253–261. doi: 10.1016/j.bbapap.2003.09.017
- Reynolds, M., Foulkes, M. J., Slafer, G. A., Berry, P., Parry, M. A., Snape, J. W., et al. (2009). Raising yield potential in wheat. *J. Exp. Bot.* 60, 1899–1918. doi: 10.1093/jxb/erp016
- Riefler, M., Novak, O., Strnad, M., and Schmülling, T. (2006). *Arabidopsis* cytokinin receptor mutants reveal functions in shoot growth, leaf senescence, seed size, germination, root development, and cytokinin metabolism. *Plant Cell* 18, 40–54. doi: 10.1105/tpc.105.037796
- Royo, J., Gomez, E., Barrero, C., Muniz, L. M., Sanz, Y., and Hueros, G. (2009). Transcriptional activation of the maize endosperm transfer cell-specific gene BETL1 by ZmMRP-1 is enhanced by two C2H2 zinc finger-containing proteins. *Planta* 230, 807–818. doi: 10.1007/s00425-009-0987-2
- Ruan, Y. L., Jin, Y., Yang, Y. J., Li, G. J., and Boyer, J. S. (2010). Sugar input, metabolism, and signaling mediated by invertase: roles in development, yield potential, and response to drought and heat. *Mol. Plant* 3, 942–955. doi: 10.1093/mp/ssq044

- Ruszkowski, M., Brzezinski, K., Jedrzejczak, R., Dauter, M., Dauter, Z., Sikorski, M., et al. (2013). *Medicago truncatula* histidine-containing phosphotransfer protein: structural and biochemical insights into the cytokinin transduction pathway in plants. *FEBS J.* 280, 3709–3720. doi: 10.1111/febs.12363
- Sakakibara, H., Suzuki, M., Takei, K., Deji, A., Taniguchi, M., and Sugiyama, T. (1998). A response-regulator homologue possibly involved in nitrogen signal transduction mediated by cytokinin in maize. *Plant J.* 14, 337–344. doi: 10.1046/j.1365-313X.1998.00134.x
- Serna, A., Maitz, M., O'Connell, T., Santandrea, G., Thevissen, K., Tienens, K., et al. (2001). Maize endosperm secretes a novel antifungal protein into adjacent maternal tissue. *Plant J.* 25, 687–698. doi: 10.1046/j.1365-313x.2001.01004.x
- Silva-Sanchez, C., Chen, S., Zhu, N., Li, Q. B., and Chourey, P. S. (2013). Proteomic comparison of basal endosperm in maize miniature1 mutant and its wild-type Mn1. *Front. Plant Sci.* 4:211. doi: 10.3389/fpls.2013.00211
- Slewiński, T. L. (2011). Diverse functional roles of monosaccharide transporters and their homologs in vascular plants: a physiological perspective. *Mol. Plant* 4, 641–662. doi: 10.1093/mp/ssp051
- Song, Q. X., Li, Q. T., Liu, Y. F., Zhang, F. X., Ma, B., Zhang, W. K., et al. (2013). Soybean GmZIP123 gene enhances lipid content in the seeds of transgenic *Arabidopsis* plants. *J. Exp. Bot.* 64, 4329–4341. doi: 10.1093/jxb/ert238
- Sreenivasulu, N., Altschmid, L., Radchuk, V., Gubatz, S., Wobus, U., and Weschke, W. (2004). Transcript profiles and deduced changes of metabolic pathways in maternal and filial tissues of developing barley grains. *Plant J.* 37, 539–553. doi: 10.1046/j.1365-313X.2003.01981.x
- Srivastava, S., Srivastava, A. K., Suprasanna, P., and D'Souza, S. F. (2009). Comparative biochemical and transcriptional profiling of two contrasting varieties of *Brassica juncea* L. in response to arsenic exposure reveals mechanisms of stress perception and tolerance. *J. Exp. Bot.* 60, 3419–3431. doi: 10.1093/jxb/erp181
- Sterk, P., Booij, H., Schellekens, G. A., Van Kammen, A., and De Vries, S. C. (1991). Cell-specific expression of the carrot EP2 lipid transfer protein gene. *Plant Cell* 3, 907–921. doi: 10.1105/tpc.3.9.907
- Stevenson, C. E., Burton, N., Costa, M. M., Nath, U., Dixon, R. A., Coen, E. S., et al. (2006). Crystal structure of the MYB domain of the RAD transcription factor from *Antirrhinum majus*. *Proteins* 65, 1041–1045. doi: 10.1002/prot.21136
- Sue, S. C., Hsiao, H. H., Chung, B. C., Cheng, Y. H., Hsueh, K. L., Chen, C. M., et al. (2006). Solution structure of the *Arabidopsis thaliana* telomeric repeat-binding protein DNA binding domain: a new fold with an additional C-terminal helix. *J. Mol. Biol.* 356, 72–85. doi: 10.1016/j.jmb.2005.11.009
- Sugawara, H., Kawano, Y., Hatakeyama, T., Yamaya, T., Kamiya, N., and Sakakibara, H. (2005). Crystal structure of the histidine-containing phosphotransfer protein ZmHP2 from maize. *Protein Sci.* 14, 202–208. doi: 10.1110/ps.041076905
- Tai, S. P., and Kaplan, S. (1985). Phospholipid transfer proteins in microorganisms. *Chem. Phys. Lipids* 38, 41–50. doi: 10.1016/0009-3084(85)90056-8
- Takei, K., Sakakibara, H., Taniguchi, M., and Sugiyama, T. (2001). Nitrogen-dependent accumulation of cytokinins in root and the translocation to leaf: implication of cytokinin species that induces gene expression of maize response regulator. *Plant Cell Physiol.* 42, 85–93. doi: 10.1093/pcp/pce009
- Takei, K., Takahashi, T., Sugiyama, T., Yamaya, T., and Sakakibara, H. (2002). Multiple routes communicating nitrogen availability from roots to shoots: a signal transduction pathway mediated by cytokinin. *J. Exp. Bot.* 53, 971–977. doi: 10.1093/jexbot/53.370.971
- Thiel, J., Hollmann, J., Rutten, T., Weber, H., Scholz, U., and Weschke, W. (2012). 454 Transcriptome sequencing suggests a role for two-component signalling in cellularization and differentiation of barley endosperm transfer cells. *PLoS ONE* 7:e41867. doi: 10.1371/journal.pone.0041867
- Thompson, R. D., Hueros, G., Becker, H., and Maitz, M. (2001). Development and functions of seed transfer cells. *Plant Sci.* 160, 775–783. doi: 10.1016/S0168-9452(01)00345-4
- Vilhar, B., Kladnik, A., Blejec, A., Chourey, P. S., and Dermastia, M. (2002). Cytomical evidence that the loss of seed weight in the miniature1 seed mutant of maize is associated with reduced mitotic activity in the developing endosperm. *Plant Physiol.* 129, 23–30. doi: 10.1104/pp.001826
- Wang, E., Wang, J., Zhu, X., Hao, W., Wang, L., Li, Q., et al. (2008a). Control of rice grain-filling and yield by a gene with a potential signature of domestication. *Nat. Genet.* 40, 1370–1374. doi: 10.1038/ng.220
- Wang, Y. Q., Wei, X. L., Xu, H. L., Chai, C. L., Meng, K., Zhai, H. L., et al. (2008b). Cell-wall invertases from rice are differentially expressed in Caryopsis during the grain filling stage. *J. Integr. Plant Biol.* 50, 466–474. doi: 10.1111/j.1744-7909.2008.00641.x
- Wang, H. W., Hwang, S. G., Karuppanapandian, T., Liu, A., Kim, W., and Jang, C. S. (2012). Insight into the molecular evolution of non-specific lipid transfer proteins via comparative analysis between rice and sorghum. *DNA Res.* 19, 179–194. doi: 10.1093/dnares/dss003
- Wang, L., and Ruan, Y. L. (2012). New insights into roles of cell wall invertase in early seed development revealed by comprehensive spatial and temporal expression patterns of GhCWIN1 in cotton. *Plant Physiol.* 160, 777–787. doi: 10.1104/pp.112.203893
- Weber, H., Borisjuk, L., Heim, U., Buchner, P., and Wobus, U. (1995). Seed coat-associated invertases of fava bean control both unloading and storage functions: cloning of cDNAs and cell type-specific expression. *Plant Cell* 7, 1835–1846.
- Weber, H., Buchner, P., Borisjuk, L., and Wobus, U. (1996). Sucrose metabolism during cotyledon development of *Vicia faba* L. is controlled by the concerted action of both sucrose-phosphate synthase and sucrose synthase: expression patterns, metabolic regulation and implications for seed development. *Plant J.* 9, 841–850. doi: 10.1046/j.1365-313X.1996.9060841.x
- Weschke, W., Panitz, R., Gubatz, S., Wang, Q., Radchuk, R., Weber, H., et al. (2003). The role of invertases and hexose transporters in controlling sugar ratios in maternal and filial tissues of barley caryopses during early development. *Plant J.* 33, 395–411. doi: 10.1046/j.1365-313X.2003.01633.x
- Weschke, W., Panitz, R., Sauer, N., Wang, Q., Neubohn, B., Weber, H., et al. (2000). Sucrose transport into barley seeds: molecular characterization of two transporters and implications for seed development and starch accumulation. *Plant J.* 21, 455–467. doi: 10.1046/j.1365-313X.2000.00695.x
- White, A. J., Dunn, M. A., Brown, K., and Hughes, M. A. (1994). Comparative analysis of genomic sequence and expression of a lipid transfer protein gene family in winter barley. *J. Exp. Bot.* 45, 1885–1892. doi: 10.1093/jxb/45.12.1885
- Wirtz, K. W., and Gadella, T. W. Jr. (1990). Properties and modes of action of specific and non-specific phospholipid transfer proteins. *Experientia* 46, 592–599. doi: 10.1007/BF01939698
- Xu, S. M., Brill, E., Llewellyn, D. J., Furbank, R. T., and Ruan, Y. L. (2012). Over-expression of a potato sucrose synthase gene in cotton accelerates leaf expansion, reduces seed abortion, and enhances fiber production. *Mol. Plant* 5, 430–441. doi: 10.1093/mp/sss090
- Yang, J. Y., Chung, M. C., Tu, C. Y., and Leu, W. M. (2002). OSTF1: a HD-GL2 family homeobox gene is developmentally regulated during early embryogenesis in rice. *Plant Cell Physiol.* 43, 628–638. doi: 10.1093/pcp/pcf076
- Yeats, T. H., and Rose, J. K. (2008). The biochemistry and biology of extracellular plant lipid-transfer proteins (LTPs). *Protein Sci.* 17, 191–198. doi: 10.1110/ps.073300108
- Zanor, M. I., Osorio, S., Nunes-Nesi, A., Carrari, F., Lohse, M., Usadel, B., et al. (2009). RNA interference of LIN5 in tomato confirms its role in controlling Brix content, uncovers the influence of sugars on the levels of fruit hormones, and demonstrates the importance of sucrose cleavage for normal fruit development and fertility. *Plant Physiol.* 150, 1204–1218. doi: 10.1104/pp.109.136598
- Conflict of Interest Statement:** The authors declare that the research was conducted in the absence of any commercial or financial relationships that could be construed as a potential conflict of interest.
- Received:** 21 November 2013; **accepted:** 07 February 2014; **published online:** 27 February 2014.
- Citation:** Lopato S, Borisjuk N, Langridge P and Hrmova M (2014) Endosperm transfer cell-specific genes and proteins: structure, function and applications in biotechnology. *Front. Plant Sci.* 5:64. doi: 10.3389/fpls.2014.00064
- This article was submitted to Plant Physiology, a section of the journal *Frontiers in Plant Science*.
- Copyright © 2014 Lopato, Borisjuk, Langridge and Hrmova. This is an open-access article distributed under the terms of the Creative Commons Attribution License (CC BY). The use, distribution or reproduction in other forums is permitted, provided the original author(s) or licensor are credited and that the original publication in this journal is cited, in accordance with accepted academic practice. No use, distribution or reproduction is permitted which does not comply with these terms.



# Two maize *END-1* orthologs, *BETL9* and *BETL9like*, are transcribed in a non-overlapping spatial pattern on the outer surface of the developing endosperm

Joaquín Royo<sup>1\*</sup>, Elisa Gómez<sup>1</sup>, Olivier Sellam<sup>2</sup>, Denise Gerentes<sup>2</sup>, Wyatt Paul<sup>2</sup> and Gregorio Hueros<sup>1</sup>

<sup>1</sup> Departamento Biomedicina y Biotecnología (Genética), Universidad de Alcalá, Madrid, Spain

<sup>2</sup> GM Trait Discovery, Biogemma – Centre de Recherche de Chappes, Chappes, France

**Edited by:**

David McCurdy, The University of Newcastle, Australia

**Reviewed by:**

Sergiy Lopato, Australian Centre for Plant Functional Genomics, Australia  
Jose Gutierrez-Marcos, University of Warwick, United Arab Emirates

**\*Correspondence:**

Joaquín Royo, Departamento Biomedicina y Biotecnología (Genética), Universidad de Alcalá, Campus Universitario, Alcalá de Henares-28870, Madrid, Spain  
e-mail: joaquin.royo@uah.es

In the course of a project aimed to isolate transfer cells-specific genes in maize endosperm we have identified the *BETL9* gene. *BETL9* encodes for a small protein very similar in sequence to the product of the barley transfer cell-specific gene *END-1*. Both *BETL9* and *END-1* proteins are lipid transfer proteins, but their function is currently unknown. *In situ* hybridization analysis confirms that the *BETL9* gene is exclusively transcribed in the basal endosperm transfer cell layer during seed development since 10 days after pollination. However, immunolocalization data indicates that the *BETL9* protein accumulates in the maternal placento-chalaza cells located just beside the transfer cell layer. This suggests that the *BETL9* protein should be transported to the maternal side to exert its, still unknown, function. In addition, we have identified a second maize gene very similar in sequence to *BETL9* and we have named it *BETL9like*. *In situ* hybridization shows that *BETL9like* is also specifically transcribed in the developing maize endosperm within the same time frame that *BETL9*, but in this case it is exclusively expressed in the aleurone cell layer. Consequently, the *BETL9* and *BETL9like* genes are transcribed in a non-overlapping pattern on the outer surface of the maize endosperm. The *BETL9* and *BETL9like* promoter sequences, fused to the GUS reporter gene, accurately reflected the expression pattern observed for the genes in maize. Finally, we have identified in the *Arabidopsis* genome a set of four genes orthologous to *BETL9* and *BETL9like* and analyzed the activity of their promoters in *Arabidopsis* transgenic plants carrying fusions of their promoter sequences to the GUS reporter. As in the case of the maize genes, the *Arabidopsis* orthologs showed highly complementary expression patterns.

**Keywords:** nsLTP, transfer cells, endosperm, aleurone, maize, *Arabidopsis*

## INTRODUCTION

Developing seeds are strong sinks for nutrients produced in the maternal plant. Since there are not symplastic connections between the maternal and filial tissues, the flow of nutrients required to sustain seed filling has to be carried through the apoplast, where solutes coming from the vascular system of the mother are discharged in the maternal side. In many species, the nutrients are uploaded from the apoplast by a specialized group of cells that differentiate as transfer cells in the outer surface of the developing seed, facing the maternal vascular terminals (reviewed in Royo et al., 2007). Transfer cells are characterized by numerous cell wall ingrowths that increase their surface area to enhance its nutrient uptake capacity (Pate and Gunning, 1972). In cereals, these transfer cells differentiate from the endosperm and their precise position and extension varies on the different species. In maize, the maternal vascular terminals are placed at the base of the developing seed and form a cup-shaped cushion. Nutrients discharged from the conducting vases must transverse several layers of crushed maternal cells, the placento-chalazal zone (Kladnik et al., 2004), in their way to the seed surface. There, the transfer cells are located as a continuous layer placed in front of the maternal

vascular terminals and interrupting the aleurone layer that covers the remaining surface of the seed (Thompson et al., 2001). They constitute the basal endosperm transfer cell layer (BETL). In wheat and barley, there is a vascular bundle running along the length of the grain and the nutrients are discharged, through modified maternal cells in the nucellar projection, to the endosperm cavity that extends along the seed, in parallel to the vascular bundle. From this cavity, nutrients are taken up by the endosperm transfer cells whereas the aleurone covers the remaining surface of the seed (Olsen, 1992; Royo et al., 2007). In rice, nutrients transported in the vascular bundle running along the length of the developing seed are not discharged to a cavity, but loaded symplastically into a layer of nucellar epidermal cells that covers most of the seed surface and it is of maternal origin. Therefore, nutrients from this nucellar tissue do not move to the apoplast facing the filial endosperm in a localized region and consequently there is no a distinct transfer cell layer differentiated from the aleurone (Bechtel and Pomeranz, 1977; Opara and Gates, 1981; Krishnan and Dayanandan, 2003). Nevertheless, the region of the aleurone facing the vascular bundle contains additional layers of cells and these cells possess a specific regulatory program, as evidenced by the expression of genes not

found in any other area of the aleurone (Li et al., 2008; Kuwano et al., 2011).

A growing number of genes expressed in the endosperm transfer cells have been identified during the last years. In maize there is already an extensive collection that includes genes named as *BETL1*, 2, 3, and 4 (Hueros et al., 1995, 1999) encoding for small cysteine-rich proteins. The product of the *BETL2* gene was renamed BAP-2 (basal layer antifungal protein 2) after its *in vitro* antifungal activity was demonstrated (Serna et al., 2001). *meg-1* (*maternally expressed gene1*) encodes for another small cysteine-rich protein that shows imprinting in their expression (Gutiérrez-Marcos et al., 2004). *ZmCKS* encodes for the enzyme CMP-KDO synthase involved in the activation of an important precursor for the synthesis of components of the cell wall pectins and, although not transfer cells specific, it is highly expressed in this tissue, probably to sustain the intensive remodeling of their cell walls during development (Royo et al., 2000). *ZmMRP-1* is a single-MYB domain transcription factor of the SHAQKYF class that controls the expression of several of the *BETL* genes (Gómez et al., 2002) and *meg-1* (Gutiérrez-Marcos et al., 2004) and it is a major determinant of the identity of the endosperm transfer cells (Gómez et al., 2009). *ZmTCRR-1* and *ZmTCRR-2* encode Type A response regulators that are probably involved in a signal transduction pathway important for the development of these cells and both genes are also transcriptionally regulated by *ZmMRP-1* (Muñiz et al., 2006, 2010).

In barley the *END-1* (*endosperm 1*) gene is expressed in the transfer cells facing the endosperm cavity (Doan et al., 1996) and it encodes for a non-specific lipid transfer protein (nsLTP). nsLTPs are a large family of proteins widely distributed across the plant kingdom that are able to bind lipids in a hydrophobic cavity stabilized by four disulphide bridges among a set of eight conserved cysteines in their primary sequence (reviewed in Yeats and Rose, 2008). Some of the nsLTPs genes are expressed in aleurone cells and could participate in the synthesis of extracellular cuticle layers (Boutrot et al., 2007), but a similar activity in transfer cells seems at odds with the active transport of nutrients circulating through these cells. Subsequently, it has been shown that other nsLTPs similar to *END-1* are expressed in transfer cells from wheat (Kovalchuk et al., 2009, 2012) and in the maternal nucellar cells covering the vascular bundles and the adjacent aleurone cells that are functionally equivalent in rice (Li et al., 2008). An alternative role in antipathogen defense has been hypothesized for nsLTPs, consistently with the emerging evidence suggesting that endosperm transfer cells control a delicate balance between the need to facilitate an intense transport and the need to impede the ingress of pathogens into the growing seed.

In this paper we describe the cloning and characterization of *BETL9*, a maize gene for a nsLTP highly related to *END-1* and its wheat and rice relatives. *BETL9* was cloned in the course of a screening for *BETL* genes and *in situ* hybridization confirmed that it is really specifically expressed in that tissue. We have found that there is a highly similar gene to *BETL9* in maize, that we named *BETL9like*. Surprisingly, *BETL9like* is expressed instead in the aleurone cells, *in situ* hybridization with specific probes for both genes showed that there is a sharp boundary between their expression domains that coincides with the border

between the BETL and aleurone regions of the endosperm. We have isolated proximal promoter regions for both genes that reproduce, in transgenic maize plants, the expression pattern of the endogenous genes. We have also isolated the promoter regions of the four *Arabidopsis* genes encoding for the nsLTPs most closely related to *BETL9* and *BETL9like* and studied their expression patterns in transgenic *Arabidopsis* plants carrying promoter-GUS constructs.

## RESULTS

### ISOLATION OF TWO LIPID TRANSFER GENES SPECIFICALLY EXPRESSED IN THE DEVELOPING MAIZE KERNEL

We have previously described (Balandin et al., 2005) a screening for genes specifically expressed in the basal halves of developing maize kernels, based on the method of Sokolov and Prokop (1994). In the course of this screening we isolated a cDNA clone containing an open reading frame for a 107 amino acids long nsLTP. Northern blot analysis indicated that the transcripts corresponding to this cDNA were only detectable in developing maize kernels as early as 11 days after pollination (DAP; the youngest time point used in these experiments) and only in RNA extracted from the lower halves of hand dissected kernels (Figure 1). In accordance with its expression pattern we have called this gene *BETL9*. Inspection of the Maize Genome Sequencing Project database reveals that this gene is located on chromosome 3 and has the identifier GRMZM2G0847413.

Analysis of the maize genome sequence database revealed the presence of a gene closely related to *BETL9* that we consequently named as *BETL9like*. A cDNA clone for *BETL9like* was isolated and Northern blot analysis indicated it was also specifically expressed in developing maize kernels, with a temporal pattern closely resembling that of *BETL9*. Its transcripts, however, were not restricted

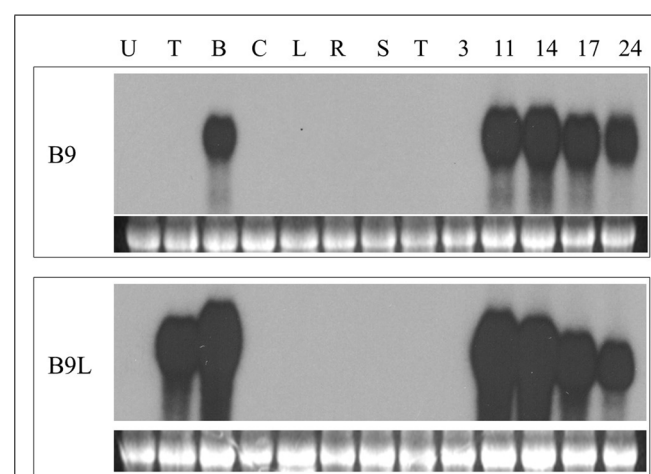


**FIGURE 1 | Northern blot analyses of the expression of *BETL9* and *BETL9like*.**

The probe used in each northern blot is indicated on the left. Each panel contains an EtBR picture of the ribosomal RNA to show equal loading. The tissues used as source of total RNA (10 µg per lane) were: U, unpollinated female flowers; T, upper part of 10 DAP kernels; B, lower part of 10 Dap kernels; C, coleoptiles; L, leaves; R, roots; S, silks; T, tassel (male flowers); 3, 11, 14, 17, and 24, complete kernels collected at the indicated developmental stage (in DAP).

to the basal halves of the kernels, the RNA from the upper halves of immature kernels showed an equally strong hybridization signal with the *BETL9like* probe (**Figure 1**). According to the Maize Genome Sequencing Project database this gene is located on chromosome 8 and has the identifier GRMZM2G091054.

Non-specific lipid transfer protein are an extensive group of related proteins widely distributed in the plant kingdom. Plant nsLTPs typically contain an N-terminal signal peptide and are characterized by an eight cysteine motif (8 CM) of the form: C-Xn-C-Xn-CC-Xn-CXC-Xn-C-Xn-C. The cysteine residues are engaged in the formation of four disulphide bonds that stabilize a hydrophobic cavity where phospholipids and other lipidic compounds can bind (Yeats and Rose, 2008). Consequently, the *in vivo* activity of nsLTPs is supposed to pivot on this ability to bind lipids. However, the actual physiological function of most of these proteins has not been determined. Based on sequence relationships among their rice, wheat and *Arabidopsis* members, plant ns-LTPs have been previously classified in nine groups (Boutrot et al., 2008; Wang et al., 2012) and according to this scheme *BETL9* and *BETL9like* belong to group VI. Edstam et al. (2011) classified the plant nsLTPs proteins using a different sorting scheme and included in their analysis sequences from non-flowering plants. In their scheme, nsLTPs of group VI are included in a wider type they named D. Type D nsLTPs appeared very early in evolution, shortly after the divergence of the first land plants.

Based on the Boutrot et al. (2008) and Wang et al. (2012) studies and our own search on sequence databases we have compiled the complete amino acid sequences of members of the group VI from several cereal species, along with the four members from *Arabidopsis* (**Figure 2A**). In the alignment shown in **Figure 2A** we include the two maize proteins BETL9 and BETL9like, but not the translation product of the AC194405.3\_FG009 gene. This gene, located on chromosome 8, contains the N-terminal half of a related protein, but its coding region is currently interrupted in the sequence databases by a region of poor sequence quality that makes impossible its precise identification. In **Figure 2A** we have also included the sequences of the proteins encoded by three classes of wheat genes: *TaLtpVIb* from *Triticum aestivum* (Boutrot et al., 2008) and the *T. aestivum* members of the two pairs of orthologous *T. aestivum* and *T. durum* genes *TaPR60* and *TdPR60* (Kovalchuk et al., 2009) and *TaPR61* and *TdPR61* (Kovalchuk et al., 2012). *TaPR61* corresponds to the wheat gene *TaLtpVI.a* described by Boutrot et al. (2008). We also include the four rice genes (Os01g58650, Os01g58660, Os10g05720, and Os11g29420) initially reported by Boutrot et al. (2008), and Os03g25350, added by Wang et al. (2012). Os01g58660 was cloned on the basis of its sequence similarity with *TaPR60* by Li et al. (2008), and named *OsPR602*. From barley we have included the product of *END-1* (Doan et al., 1996), located on chromosome 1H, and those from the genes HvMLOC62188, on chromosome 3HL, and HvMLOC63390, on chromosome 3H. Finally, we include four genes from *Sorghum bicolor*, two of them (Sb08g005340 and Sb08g005360) probably represent the product of a recent tandem duplication event, since they are highly similar and located in close proximity on chromosome 8. The same duplication event could have generated the nearby and very similar gene Sb08005345, but we do

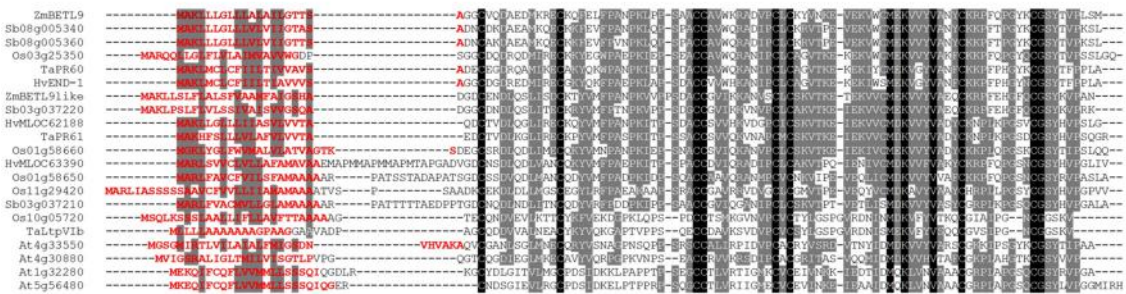
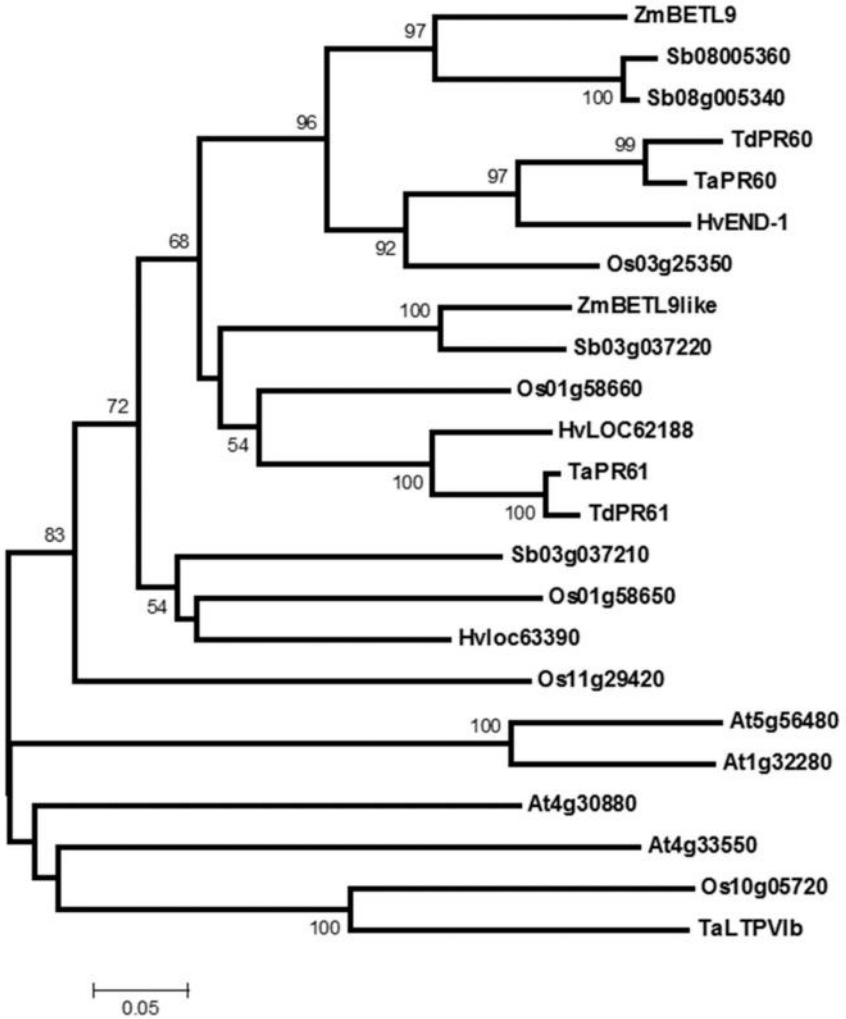
not include it here because it contains sequence alterations suggesting this might be a pseudogen. The other pair of sorghum genes (Sb03g37210 and Sb03g37220) are located in close proximity on chromosome 3, but their sequences are not as closely related as that of the genes on chromosome 8. Wang et al. (2012) included in group VI two additional genes from rice (Os11g03870) and *Arabidopsis* (At2g13295), but we discarded them here because their protein sequences do not have all the characteristic features of the members of group VI. These features are the presence of a valine and methionine residues located at positions -4 and -10, respectively, from cysteine at position 7 of the motif 8 CM, and a single intron interrupting their coding sequence 4 nt downstream of the codon for the last cysteine of the 8 CM motif.

Phylogenetic analysis based on the alignment of the sequences of the mature nsLTPs reveals the presence of two subgroups of proteins of cereal origin in type VI (**Figure 2B**). The first one includes BETL9 and the product of the barley gene *END-1* (Doan et al., 1996). *END-1* is expressed in the endosperm transfer cells that in the barley developing kernel are located over the nucellar projection running along the length of the grain. This subgroup also includes the products of the common and durum wheat endosperm transfer cell-specific genes *TaPR60* and *TdPR60* (Kovalchuk et al., 2009) as well as the protein from the rice gene Os03g25350 and from the two closely related sorghum genes located in close physical proximity on chromosome 8. Microarray database mining reveals that the Os03g25350 transcripts are abundant in spikelets and young seeds, but we do not have precise data about the pattern of expression of this gene. The second subgroup includes BETL9like, and the protein products of the genes HvMLOC62188 from barley, located on chromosome 3HL, Sb03g037220 from sorghum, Os01g58660 from rice and *TaPR61*, and *TdPR61* from common and durum wheat. The wheat genes are expressed in the endosperm transfer cells, but also in the aleurone, part of the starchy endosperm, the embryo surrounding region (ESR) and the developing embryo (Kovalchuk et al., 2012). Os01g58660 is expressed in the aleurone cells located in most close proximity to the maternal vascular bundles, and in the maternal tissues located between those vascular bundles and the seed surface (Li et al., 2008). The remaining proteins of cereal origin of this group VI do not form a well-supported clade and there is not much information about the expression patterns of their genes.

The protein products from the four *Arabidopsis* genes belonging to group VI (At1g32280, At4g30880, At4g33550, and At5g56480) do not cluster with the cereal ones. This separation between the proteins from *Arabidopsis* and cereal species inside a group is very common in the nsLTPs family and precludes identifying orthology relationships among them (Boutrot et al., 2008).

#### **IN SITU LOCALISATION OF THE BETL9 AND BETL9LIKE TRANSCRIPTS IN THE DEVELOPING MAIZE KERNEL**

*In situ* hybridization experiments were used to clarify the spatial discrepancies observed in the Northern blot analyses, see above, where *BETL9* was localized in the lower half of the kernels whereas *BETL9like* was found both in the upper and lower halves. Localisation of the *BETL9* and *BETL9like* transcripts was

**A****B**

**FIGURE 2 | Sequence analysis of the protein sequences of group VI nsLTPs. (A)** Alignment of type VI nsLTPs proteins from maize (ZmBETL9 and ZmBETL9like), sorghum (Sb03g037210, Sb03g037220, Sb08g005340, and Sb08005360), barley (HvEND-1, HvMLOC62188, and HvMLOC63390), rice (Os01g58650, Os01g58660, Os03g25350, Os10g05720, and Os11g29420), wheat (TaLtpVlb, TaPR60, and TaPR61), and *Arabidopsis* (At1g32280, At4g30880, At4g33550, and At5g56480). Sequences were aligned using ClustalW. Identical amino acids are in black boxes, similar amino acids in gray.

boxes. Signal peptides were predicted using SignalP 4.1 (Peterson et al., 2011) and their sequences are shown in red. **(B)** Phylogenetic relationships of the nsLTPs protein from type VI. The analysis is based on the alignment of the proteins shown in **A**, excluding the N-terminal signal peptides, plus the *Triticum durum* TdPR60 and TdPR61 proteins. The Neighbor-Joining tree was constructed using MEGA 5.2 with 1000 bootstrap replicates and the *p*-distance and pairwise deletion options. Only bootstrap values above 50% are shown.

determined in longitudinal sections of developing maize kernels using antisense probes corresponding to gene-specific regions of the cDNAs. *BETL9* transcripts are only present at the BETL (Figures 3A–E, TCL) whereas *BETL9like* transcripts are only at the aleurone cell layer covering the remaining outer surface of the developing endosperm (Figures 3G–N, AI). Both genes were readily detected as early as 5 DAP (Figures 3A,G). The transition between the transcription domains of both genes accurately reflects the transition between the characteristically elongated, cell wall ingrowths-covered transfer cells and the smaller, cubic, and symmetric aleurone cells. At the embryo pole, the aleurone consists of a single cell layer that forms a cavity enclosing the embryo, this layer is readily evidenced by the strong expression of the *BETL9like* marker. At the upper part of the seed (Figure 3M), the *BETL9like* marker seems to reflect the maturation stage of the aleurone cells, which at 16 DAP are still forming a three layers of cells that will evolve into a single cell layer at maturity. The hybridization signals appears in one, two, or three cell layers depending on the seed area analyzed. No transcripts were detected in the embryo, ESR or other parts of the seed and adjacent maternal tissues.

#### LOCALISATION OF THE BETL9 PROTEIN

An antibody was raised in rabbits against the BETL9 mature protein translated in *Escherichia coli*. The antibody specifically recognized a single protein of the expected molecular size for the mature BETL9 protein, 9.8 KDa, in crude protein extracts prepared from the basal halves of 14 DAP maize kernels (data not shown).

Inmunolocalization using this antibody against wax-embedded sections from 14 DAP kernels detected the BETL9 protein

exclusively at the placenta-chalazal region located on the maternal tissues of the pedicel (Figure 3F). This maternal region is facing the BETL, where *in situ* studies indicate the *BETL9* transcripts are accumulating. Almost no signal is detectable at the BETL cells suggesting that the BETL9 protein is efficiently exported from them into the apoplast in a polarized fashion.

Assuming that the *BETL9like* transcripts are efficiently translated, the absence of immunolocalization signal either at the aleurone or the tissues surrounding it, suggests that this antibody is indeed specific against the BETL9 protein and does not appreciably detect BETL9like protein molecules.

#### ACTIVITY OF THE BETL9 AND BETL9LIKE PROMOTERS IN TRANSGENIC MAIZE

The promoter regions located upstream of the *BETL9* (1911 base pairs, bp) and *BETL9like* (2229 bp) coding regions were isolated from the corresponding clones of a BAC library screened with the cDNA probes. These promoter regions were fused to the reporter GUS gene and used to produce stable transformed maize transgenic plants. At least three transgenic lines containing single locus insertion of the constructs were analyzed in detail in each case.

In the maize transgenic plants the pattern of GUS staining reproduced that obtained from *in situ* studies for both genes. The GUS signal was exclusively observed in developing seeds from 8 DAP until almost maturity in both cases but whereas in plants carrying the *BETL9* promoter the signal was only detected in the basal endosperm transfer cells (Figure 4A), in those with the *BETL9like* promoter the GUS staining was limited to the aleurone layer (Figure 4B). Consequently, these promoter regions are sufficient to explain the different expression patterns of both genes

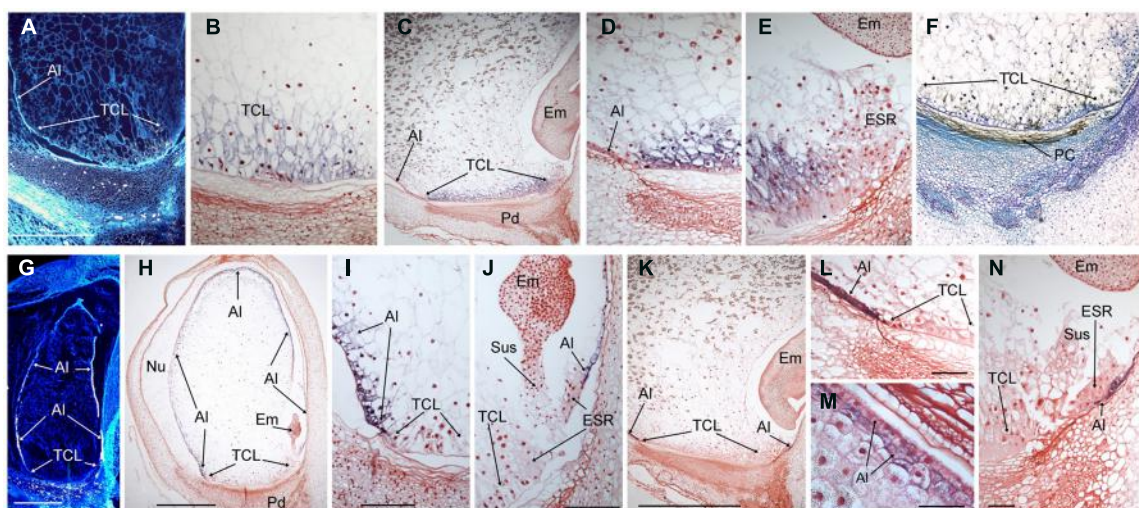


**FIGURE 3 | Expression analyses of the *BETL9* and *BETL9like* genes in developing maize kernels.** The expression of *BETL9* was analyzed by *in situ* hybridization with antisense RNA probes (A–E) or Immunolocalization (F) with a specific antisera. The expression of *BETL9like* was analyzed with an antisense RNA probe (G–N). RNA labeling was done with  $S^{35}$ -dUTP (A,G) or DIG-dUTP (B,E,H–N). Sections correspond to 5 DAP (A,G), 10 DAP (B,F,H–J), and 16 DAP (C–E,K–N).  $S^{35}$  hybridization signal appears as light

dots in the dark field microphotographs, DIG signal is visualized as a purple-black precipitate. For the immunolocalization positive signal s visualized as a brown-black precipitate. Sense and preimmune sera controls produced no signal and are not shown due to space constrains. TCL, transfer cell layer; AI, aleurone; Em, embryo; ESR, embryo surrounding region; Pd, pedicel; PC, Placenta-chalaza; Nu, nucella; Sus, suspensor. Bars mean 500  $\mu$ m in A,G; 1 mm in H,K and 50  $\mu$ m in I,J,L–N.

and post transcriptional processes are expected to be of minor importance in controlling it. The expression of the reporter constructs, as detected by histochemical staining, showed in both cases some delay when compared with the expression of the endogenous genes, although the difference in sensitivity between the GUS staining and the *in situ* hybridization might explain this discrepancy.

#### ACTIVITY OF THE PROMOTERS OF THE *Arabidopsis BETL9*-RELATED GENES IN TRANSGENIC *Arabidopsis* PLANTS

We have previously indicated that there are four *Arabidopsis* genes included in the group VI of nsLTPs (At1g32280, At4g30880, At4g33550, and At5g56480), but they do not cluster into either the *BETL9* or *BETL9like* subgroups. In the absence of clear phylogenetic relationships coming from the comparison of their sequences, analysis of their expression patterns could provide some insights into possible functional relationships between the *Arabidopsis* and cereal proteins. Consequently, we have isolated the promoter regions of the four genes by PCR amplification using forward and reverse primers designed from the sequence data at the *Arabidopsis* genomic sequence database. The resulting promoter regions were fused to the reporter GUS genes and used to obtain stable transgenic *Arabidopsis* plants. For each gene several

transgenic lines were analyzed and the results of the more representative ones are shown (Figure 5A; for a color-coded cartoon). The promoters of the four genes show distinct patterns of activity with a very limited overlapping. In mature plants the activity of the promoter of At1g32280 is restricted to a collar region in the transition zone between the stem and hypocotyl, the basal rosette node, and in the stipules around the branching points of the inflorescence stems. In young seedlings this promoter is, however, transiently active in the first developing pair of true leaves, where it marks only the proximal parts of the leave (Figure 5D). At5g56480 is also active in the rosette node, but not in the stipules and neither in any part of developing plantlets. The At4g30880 promoter is active in the hypocotyl both in seedlings (Figure 5B) and mature plants. The expression of the gene is especially strong at the borders of the hypocotyl, i.e., at the interfaces with stem or roots. There is also a weak activity in nectaries. The activity of the At4g33550 promoter extends along the vascular bundles of stems, leaves, and root in the mature plant and developing plantlets (Figure 5C), and it is also evident in the collar of vascular bundles located at the base of flowers and immature siliques, as well as in the branching points of the root.

In reproductive tissues, the promoter of At1g32280 is active in mature anthers, ovules, and developing seeds (both in embryo

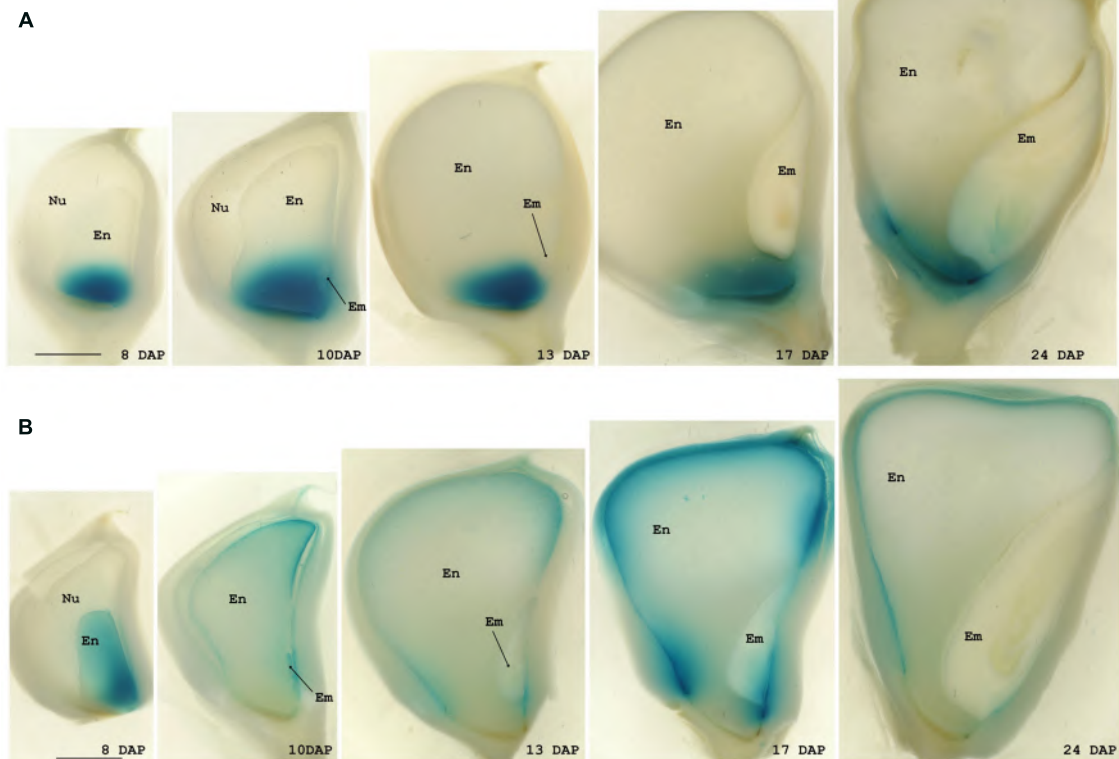
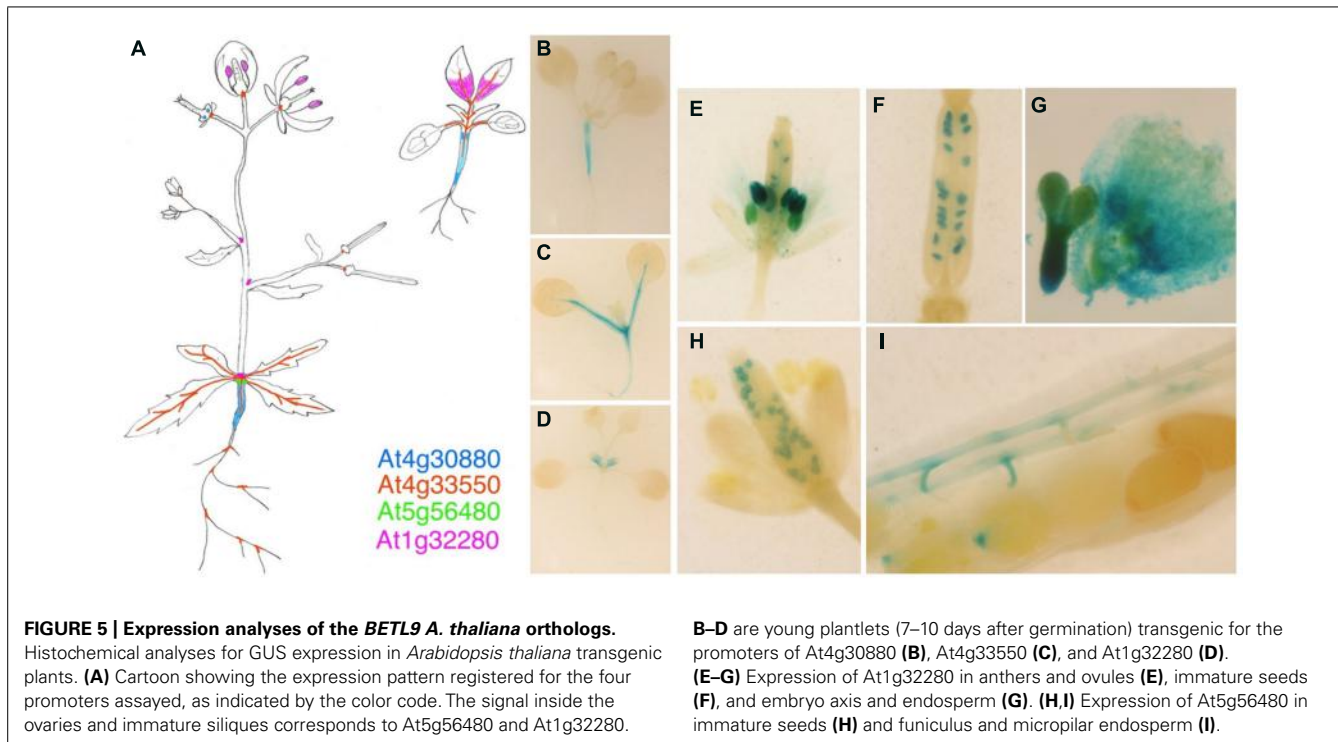


**FIGURE 4 | Expression analyses of the *BETL9* and *BETL9like* promoters.** Histochemical analyses for GUS expression in maize kernels. Positive expression is seen as a blue precipitated. The age of the kernels is indicated as days after pollination. The promoters

assayed are the *BETL9* promoter (A) and the *BETL9like* promoter (B), in the lower panel. En, endosperm; Em, embryo; Nu, nucella. The scale bars shown in the 8 DAP figures mean approximately 1 mm.



and endosperm, **Figures 5E–G**) whereas that of At4g30880 is only transiently active in the developing anthers of young flower buds. The promoter of At5g56480 is active in ovules, from the bud to the mature stages, in the funicular connections to the pod vasculature and in very young seeds at the micropilar side (**Figures 5H,I**) but it is not active in developing seeds.

## DISCUSSION

The most characteristic feature of the nsLTPs is their well proved capacity to bind lipidic compounds (Yeats and Rose, 2008) and, consequently, it is widely assumed that they are probably involved in the transport of those substances. On the other hand, nsLTPs have a conspicuous N-terminal signal peptide that presumably leads to their export out of the cell and makes rather unlikely their participation in the intracellular trafficking of lipids. For this reason, it has been suggested that nsLTPs would be involved in the transport of lipids to extracellular locations during the synthesis of structures such as the cuticle layer (Pyee et al., 1994; Lee et al., 2009). This role would be particularly likely for those nsLTPs genes predominantly expressed in epidermal cells of aerial parts of the plant because it is there where the cuticular layers are usually located. However, it should be reminded that in each plant species there is a great number of nsLTPs that presumably have diversified to perform distinct physiological functions, and to work in different parts of the plant body and during diverse developmental stages. Consequently, it would be very surprising to find a single nsLTPs *in vivo* function. Indeed, some nsLTPs have shown antimicrobial activity *in vitro* and the expression of their encoding genes is induced after pathogen infection, suggesting that they could be involved in defense against these invaders (Molina and Garcia-Olmedo, 1993, 1997; Guiderdoni et al., 2002; Gomès

et al., 2003). For those nsLTPs their defensive role would be acting like toxic weapons, but for the *Arabidopsis* DIR1 (defective in induced resistance1) nsLTP it would be carrying, or chaperoning, a still unknown systemic signal that triggers defensive responses in parts of the plant still free of the pathogen (Maldonado et al., 2002; Champigny et al., 2013). It is not known if other nsLTPs could also be involved in the transport of lipid signals, in defense or developmentally related signaling pathways. On the other hand, some nsLTPs from legume plants participate in the control of the symbiotic interactions between the host and its rhizobium partner during the nodulation process, likely acting as a positive signal for the rhizobium colonization (Pii et al., 2009), but their exact mechanism of action is unclear.

In this context, *BETL9* and *BETL9like* are an interesting case because they are a couple of very similar maize genes exclusively transcribed in developing seeds, more specifically at the two endosperm layers covering their surface: *BETL9* in the *BETL* and *BETL9like* in the aleurone. Both cell layers can be considered as the endosperm epidermis, marking the border between the seed and the enclosing maternal body. However, the *BETL* and aleurone have very different physiological activities in that border because whereas the aleurone layer functions as a classical barrier, the *BETL* is a place of very active nutrient uptake into the developing seed from the maternal vascular terminals located just in front of it. In fact, the *BETL* is the only exchange surface available for the developing maize seed because the rest of the endosperm is surrounded by a cuticle layer (Davis et al., 1990). Consequently, we suggest that this pair of similar genes could have diversified following an ancient duplication to carry out different functions in those two contiguous regions. *BETL9like* in the

synthesis of a cuticle, facilitating the establishment of an effective barrier surrounding the aleurone layer, and *BETL9* adopting a function more related to toxicity against pathogens trying to enter the seed along the same pathway that nutrients. That being the case, *BETL9* would add to the number of proteins expressed at the BETL with presumed or already proven anti pathogenic activity. *BETL1*, *BETL3*, and *meg-1* (Hueros et al., 1995, 1999; Gutiérrez-Marcos et al., 2004) genes code for proteins related to the antimicrobial peptides defensins. *BETL4* has some similarity to alpha-amylase/trypsin inhibitors (Thompson et al., 2001) and *BETL2* was renamed as BAP-2 (basal layer antifungal protein 2) after been demonstrated that it has antifungal activity *in vitro* (Serna et al., 2001). In addition, both *BETL1* and BAP2 proteins accumulate at the placenta-chalazal area, the maternal region that the nutrients coming from the maternal vascular terminals, and presumably also the pathogens, should cross before arriving to the BETL. In the case of *BETL9*, the availability of an antibody allowed us to show that also in this case the protein is exported from the BETL to the apoplast and extends through the placenta-chalazal region where its putative antipathogenic activity should be exerted (**Figure 3F**). Either this export is particularly efficient, or the *BETL9* protein molecules inside the BETL cells are not very stable because only traces of *BETL9* protein are detected inside the BETL (**Figure 3F**). Unfortunately, we do not have an antibody able to detect the *BETL9like* protein and we cannot discern if it remains around the cell walls of the aleurone cells where it is transcribed, as expected if it is involved in the synthesis of the cuticle covering them, or it expands across the maternal cells as *BETL9*. Another, more speculative, possibility would be that *BETL9* functions as a member of a signaling system between the seed and maternal tissues contributing to the coordinated development and location of the maternal vascular terminals and the BETL seed layer. We have already indicated that one nsLTP, the product of the *dir1 Arabidopsis* gene, is indeed involved in a signaling system. DIR1 protein belongs to group IV of nsLTPs according to the Boutrot et al. (2008) scheme, but groups IV and VI proteins were included in the wider Type D according to the classification scheme by Edstam et al. (2011), pointing to a relationship that could extend to their activities.

Independently of their putative physiological role, the expression patterns of *BETL9* and *BETL9like* genes provide us with a valuable material to study the mechanisms regulating differential gene activity between endosperm transfer cells and aleurone in maize. We have isolated proximal promoter regions of both genes that very closely recapitulate the expression patterns of the corresponding endogenous genes, in transgenic maize plants carrying promoter-GUS constructs (**Figure 4**). Consequently, these constructs could be used in the future to investigate the regulatory mechanisms determining BETL and aleurone specific expression. Unfortunately, there is still a very sparse knowledge about the transcription factors network regulating gene expression in the different maize endosperm domains. Conversely, the resulting scarcity of well characterized target sequences and their frequent ambiguity makes very difficult to get fruitful results only from sequence analysis. For this reason, we have attempted to complete the classical search for already characterized target motifs with a comparative approach in the sequence analysis of these

promoters, taking advantage of the availability of genomic data from sorghum. Sorghum is a closely related species to maize and we reason that the three sorghum genes that we have identified as orthologous to either *BETL9* or *BETL9like* (Sb08g005340 and Sb08g005360 for *BETL9* and Sb03g037220 for *BETL9like*; **Figure 2B**) would presumably have similar expression patterns to their maize counterparts and be regulated by related transcription factors, binding similar target sequences. A search for conserved short motifs in the sequences of 1 Kb of the maize and sorghum proximal promoters of the five genes using the MEME (Bailey and Elkan, 1994) and MAST (Bailey and Gribskov, 1998) tools reveals that *BETL9* and Sb08g005360 have a significant number of common sequence motifs. *BETL9like* and Sb03g037220 share a different group of motifs, as expected from the distinct expression patterns of the maize genes and their relationships with their sorghum relatives. Intriguingly, although the protein products of the Sb08g005340 and Sb08g005360 genes are almost identical, the promoter of Sb08g005340 has a different pattern of motifs. Since both genes are closely located in the same chromosome, this suggests they could have differed in their expression patterns after a recent duplication event that generated them, although only experimental data could validate this prediction. Meanwhile, we have taken advantage of our conserved motifs approach to focus our attention on the presence in the promoter of the *BETL9* and Sb08g005360 genes of several copies of the sequence TATCT, sometimes repeated in tandem, and positioned around 500 bp upstream of the start codon of the coding region. This conserved motif is highly related, but not identical, to the “transfer cell box,” the target of the transfer cell specific transcription factor ZmMRP-1 (Barrero et al., 2006). In the promoters of *BETL9like* and Sb03g037220 there are several copies of the motif TTGACACTTG located between 200 and 400 bp upstream of the position of the start codon, this motif is also present in the promoters of the wheat *TdPR61* and barley HvLOC62188 genes that belong to the same phylogenetic group (**Figure 2B**). The first half of this motif resembles the W box-like sequences that are closely related to the binding motifs for WRKY proteins, although functional studies indicate they are unlikely targets for these transcription factors (Ciolkowski et al., 2008). The second half is related to the CANNTG E-box element found in other seed-specific promoters (Stalberg et al., 1996). Finally, we have found in the promoters of both *BETL9* and *BETL9like* genes and their sorghum relatives, but not in Sb08g005340, the motif ACATGCAAC, related to the RY repeat present in the promoters of several seed specific genes in cereals and legumes (Baumlein et al., 1992). This set of differentially conserved motifs comprises promising targets to be validated during the experimental dissection of both promoters.

The phylogenetic relationships among the cereal nsLTP proteins belonging to group VI suggests that a duplication before the divergence of the maize, sorghum, barley, rice, and wheat lineages originated the *BETL9* and *BETL9like* clades leaving apart a less well defined group of sequences (**Figure 2B**). Current data (Doan et al., 1996; Li et al., 2008; Kovalchuk et al., 2009, 2012; this work) indicates that this split has been accompanied by a differentiation in their expression patterns. The members of both main clades are specifically expressed in seeds, but with some differences.

The genes of the *BETL9* clade from maize (**Figure 3**), the barley *END-1* (Doan et al., 1996) and the wheat *TdPR60* (Kovalchuk et al., 2009) have their expression restricted to the endosperm transfer cells. Endosperm transfer cells, although located in different physical arrangements in these species (Royo et al., 2007), share their position as entrance gates to the developing seed for nutrients coming from the maternal tissues. We do not have detailed data concerning the expression pattern of the rice member of this clade (Os03g25350), but the available information from microarray analysis is not incompatible with this scheme. On the other hand, the situation is not so homogenous in the *BETL9like* clade. The maize *BETL9like* gene is only expressed in the aleurone layer of the endosperm, and it is clearly silent in the transfer cells (**Figures 3** and **4**), but this clear-cut difference with the expression of its *BETL9* counterpart is not seen in the rice and wheat members of the clade. In rice there is not a distinct endosperm transfer cell layer, but the *OsPR602* (Os01g58660) expression is restricted to the aleurone cells located in closer proximity to the maternal vascular bundles that constitute their nearest equivalent (Li et al., 2008). Considering only this, the expression of *OsPR602* would be equivalent to that of the *BETL9* genes and not to the maize *BETL9like*. However, the promoter of *OsPR602* is also active in the maternal nucellar cells located in the pathway between the vascular bundles and the adjacent aleurone. This pattern contrasts with the expression of the typical rice transfer cell-like specific gene *AL1* (Kuwano et al., 2011) and indicates that *OsPR602* is not as specific as the *BETL9* genes. In addition, the wheat gene *TdPR61* (Kovalchuk et al., 2012) has also a wide expression pattern, including not only the aleurone, like the maize *BETL9like* gene, but the endosperm transfer cells, the ESR and the embryo, but not any maternal tissues surrounding the developing seed as in the case of *OsPR602*. Finally, the only source of information on the expression of the cereal genes of the group VI that cannot be clearly assigned to the *BETL9* or *BETL9like* clades comes from microarray experiments data for the three rice genes, and suggests that their transcripts are not restricted to developing seeds. On the absence of more precise data this could indicate that these genes have evolved to perform different physiological functions.

In conclusion, our current data indicates that in cereals there was a duplication and diversification of the genes encoding for the group VI nsLTPs leading to two clear subgroups, we have called them *BETL9* and *BETL9like* clades, that are mainly expressed in developing seeds, and a third one less well defined and studied. In maize the genes belonging to each of the two main subgroups have clearly different patterns of expression in the two endosperm domains covering the surface of the seed whereas in the other cereal species this spatial differentiation of the expression patterns is less clear. Aside from the cereal splits there are the four *Arabidopsis* genes belonging to group VI. As it is common in the other nsLTPs groups (Boutrot et al., 2008), the *Arabidopsis* proteins constitute a separate clade and it is not possible to establish an obvious correspondence between them and those from cereals. This suggests that the successive duplications leading to the current members in both groups of plant occurred after the divergence between the lineages leading to *Arabidopsis* and cereals. Data concerning the promoter activity of the four *Arabidopsis* genes (**Figure 5**) also support this notion because none of them have patterns reminiscent

of those found for the cereal genes. The *Arabidopsis* genes have clearly diversified their spatial and temporal patterns of expression, suggesting they have evolved different *in vivo* functions, in addition their expression is not restricted to seeds although some members are expressed in immature endosperm and embryo.

## MATERIALS AND METHODS

### PLANT MATERIAL

DNA, RNA, and biological samples were obtained from wild type (var. A69Y) or transgenic (var. A188) maize plants (*Zea mays*) grown in a glasshouse and from *Arabidopsis thaliana* var Col-0 grown under long-day conditions (18 h light/6 h darkness, 70% humidity, 21°C/18°C).

### MOLECULAR BIOLOGY METHODS

Standard DNA and RNA methods were carried following Sambrook et al. (1989) and as previously described (Hueros et al., 1995).

### BACTERIAL EXPRESSION, PURIFICATION OF THE BETL9 PROTEIN AND PREPARATION OF THE ANTISERUM

The mature *BETL9* coding sequence was generated by PCR from the cDNA clone by PCR, using primers which added suitable restriction sites. The PCR product was digested with the restriction enzymes Bam HI and BglII and cloned into the pQE60 expression vector (Qiagen GmbH) to yield pQE60-BETL9. The pQE60 vector provides a start codon followed by three aminoacids, which results in the addition at the N-terminus of four aminoacids (MGGS) to the first residue of the mature BETL9 protein. At the C-terminus, an extension of eight aminoacids (RSHHHHHH) are fused to the last aminoacid of the mature protein. The construct was transformed into *E. coli* strain M15 and protein overexpression and purification was done following the manufacturer's instructions under denaturing conditions. The purity of the protein was checked by SDS-PAGE electrophoresis and Coomassie blue staining. After desalting by dialysis in 0.1 M acetic acid, the protein was lyophilised, dissolved in distilled water, and used to immunize rabbits to obtain polyclonal sera.

### IN SITU HYBRIDISATION AND INMUNOLOCALIZATION

A69Y maize seeds were collected at different DAP and fixed in 4% paraformaldehyde, 0.1% glutaraldehyde in 0.1 M sodium phosphate buffer pH 7.2 for 12–24 h depending on the tissue volume. Samples were dehydrated and embedded in wax (Paraplast, Sigma) using xylol as solvent. Sections 10 μm thick were affixed to glass slides treated with 3-aminopropyltriethoxylane. Sections were deparaffinised in xylol and rehydrated through an ethanol series.

For the *in situ* hybridisation, DIG- or S<sup>35</sup>-labeled antisense and sense probes were synthesized using T3 and T7 polymerases (Boehringer Manheim) from linearised pBluescript SK<sup>+</sup> plasmids containing the *BETL9* and *BETL9like* cDNAs. Probes were partially hydrolysed with sodium carbonate. Sections were hybridized as previously described (Hueros et al., 1995), following the method of Cox and Goldberg (1988). For the detection of the hybridization signal a radiosensitive emulsion was used in

the case of S<sup>35</sup>-labeled probes. After film developing, the signal appears as dark spots that appear bright in dark-field microscopy. Sections were counterstained with calcofluor white and photographed under UV light. In the case of DIG-labeled probes the detection was done using an anti-DIG antibody coupled with alkaline phosphatase, after addition of the enzyme substrates (Roche-diagnostic) the signal was visualized as a black-purple precipitated. Sections were counterstained with saphranine-O (Sigma).

For the immunolocalization experiments, inhibition of endogenous peroxidase was carried out by incubating the sections in 0.3% v/v H<sub>2</sub>O<sub>2</sub> in 0.5% methanol for 10 min. Tissue was then washed in PBS and blocked with 10% normal donkey serum (Chemicon International) in PBS for 30 min at room temperature. Sections were incubated with anti-BETL9, anti-BETL9like, or preimmune sera diluted 1:200 in PBS for 2 h at room temperature. The immunoreaction was detected using horseradish peroxidase-coupled secondary antibody (Sigma) diluted 1:500 and 3'-diaminobenzidine (Sigma).

### PROMOTER ISOLATION, PLANT TRANSFORMATION, AND GUS ACTIVITY ASSAYS

Promoters of the maize BETL9 and BETL9like genes were obtained from BAC genomic clones. The promoter sequences were cloned as fusions to the GUS reporter gene in *Agrobacterium*-mediated plant transformation vectors. *Z. mays* plants of the variety A188 were transformed essentially as described by Ishida et al. (1996).

Promoters of the *Arabidopsis* genes were amplified by PCR from genomic DNA using primers designed according to the information present in the *Arabidopsis* genome sequence database. 1751, 1780, 1013, and 1001 bp of sequence upstream of the coding region start codon were amplified from the At1g32280, At4g30880, At4g33550, and At5g56480 genes, respectively. To prepare the *Arabidopsis* reporter lines, these promoter sequences were ligated upstream of the GUS reporter gene in the pBI101.3 plasmid (Clontech). *A. thaliana* Col-0 plants were transformed following the floral dip method as described by Clough and Bent (1998).

Expression of the GUS gene was detected by histochemical staining according to the method of Jefferson et al. (1987). Tissues were stained for GUS in a medium containing 0.5 mg/ml X-glucuronide (Duchefa), 0.5 mM K<sup>+</sup>-ferrocyanide, 0.5 mM K<sup>+</sup>-ferricyanide, 10 mM Na<sub>2</sub>EDTA, 50 mM phosphate buffer, pH 7, 0.1% Triton X-100, and 20% methanol.

### ACKNOWLEDGMENTS

This work was supported by grants from the Spanish Ministerio de Ciencia e Innovacion to Gregorio Hueros. (BIO2009-11856 and BIO2012-39822) and internal funds from Biogemma SAS.

### REFERENCES

- Bailey, T. L., and Elkan, C. (1994). "Fitting a mixture model by expectation maximization to discover motifs in biopolymers," in *Proceedings of the Second International Conference on Intelligent Systems for Molecular Biology* (Menlo Park, CA: AAAI Press), 28–36.
- Bailey, T. L., and Gribkov, M. (1998). Combining evidence using p-values: application to sequence homology searches. *Bioinformatics* 14, 48–54. doi: 10.1093/bioinformatics/14.1.48
- Balandin, M., Royo, J., Gómez, E., Muñiz, L. M., Molina, A., and Hueros, G. (2005). A protective role for the embryo surrounding region of the maize endosperm, as evidenced by the characterisation of ZmESR-6, a defensin gene specifically expressed in this region. *Plant Mol. Biol.* 58, 269–282. doi: 10.1007/s11103-005-3479-1
- Barrera, C., Muñiz, L. M., Gómez, E., Hueros, G., and Royo, J. (2006). Molecular dissection of the interaction between the transcriptional activator ZmMRP-1 and the promoter of BETL-1. *Plant Mol. Biol.* 62, 655–658. doi: 10.1007/s11103-006-9047-5
- Baumlein, H., Nagy, I., Villarroel, R., Inze, D., and Wobus, U. (1992). Cis-analysis of a seed protein gene promoter: the conservative RY repeat CAT-GCATG within the legumin box is essential for tissue-specific expression of a legumin gene. *Plant J.* 2, 233–239. doi: 10.1046/j.1365-313X.1992.t01-45-00999.x
- Bechtel, D. B., and Pomeranz, Y. (1977). Ultrastructure of the mature ungerminated rice (*Oryza sativa*) caryopsis. The caryopsis coat and the aleurone cells. *Am. J. Bot.* 64, 966–973. doi: 10.2307/2442251
- Boutrot, F., Chantret, N., and Gauchoer, M. F. (2008). Genome-wide analysis of the rice and *Arabidopsis* non-specific lipid transfer protein (nsLtp) gene families and identification of wheat nsLtp genes by EST data mining. *BMC Genomics* 9:86. doi: 10.1186/1471-2164/9/86
- Boutrot, F., Meynard, D., Guiderdoni, E., Joudrier, P., and Gautier, M. F. (2007). The *Triticum aestivum* non-specific lipid transfer protein (TaLtp) gene family: comparative promoter activity of six TaLtp genes in transgenic rice. *Planta* 225, 843–862. doi: 10.1007/s00425-006-0397-7
- Champigny, M. J., Isaacs, M., Carella, P., Faubert, J., Robert, P. R., and Cameron, R. K. (2013). Long distance movement of DIR1 and investigation of the role of DIR1-like during systemic acquired resistance in *Arabidopsis*. *Front. Plant Sci.* 4:230. doi: 10.3389/fpls.2013.00230
- Ciolkowski, I., Wanke, D., Birkenbihl, R. P., and Somssich, I. E. (2008). Studies on DNA-binding selectivity of WRKY transcription factors lend structural clues into WRKY-domain function. *Plant Mol. Biol.* 68, 81–92. doi: 10.1007/s11103-008-9353-1
- Clough, S. J., and Bent, A. F. (1998). Floral dip: a simplified method for *Agrobacterium*-mediated transformation of *Arabidopsis thaliana*. *Plant J.* 16, 735–743. doi: 10.1046/j.1365-313X.1998.00343.x
- Cox, K. H., and Goldberg, R. B. (1988). "Analysis of plant gene expression," in *Plant Molecular Biology: A Practical Approach*, ed. C. H. Shaw (Oxford: IRL Press), 1–35.
- Davis, R. W., Smith, J. D., and Cobb, B. G. (1990). A light and electron microscope investigation of the transfer cell region of maize caryopses. *Can. J. Bot.* 68, 471–479. doi: 10.1139/b90-063
- Doan, D., Linnestad, C., and Olsen, O.-A. (1996). Isolation of molecular markers from the barley endosperm coenocyte and the surrounding nucellus cell layers. *Plant Mol. Biol.* 31, 877–886. doi: 10.1007/BF00019474
- Edstam, M. M., Viitanen, L., Salminen, T. A., and Edqvist, J. (2011). Evolutionary history of the non-specific lipid transfer proteins. *Mol. Plant* 4, 947–964. doi: 10.1093/mp/ssr019
- Gómez, E., Royo, J., Guo, Y., Thompson, R. D., and Hueros, G. (2002). Establishment of cereal endosperm expression domains: identification and properties of a maize transfer cell-specific transcription factor, ZmMRP-1. *Plant Cell* 14, 599–610. doi: 10.1105/tpc.010365
- Gómez, E., Royo, J., Muñiz, L. M., Sellam, O., Wyatt, P., Gerentes, D., et al. (2009). The maize transcription factor myb-related protein-1 is a key regulator of the differentiation of transfer cells. *Plant Cell* 21, 2022–2035. doi: 10.1105/tpc.108.065409
- Gomès, E., Sagot, E., Gaillard, C., Laquaitaine, L., Poinsot, B., Sanejouand, Y. H., et al. (2003). Non-specific lipid-transfer protein genes expression in grape (*Vitis sp.*) cells in response to fungal elicitor treatments. *Mol. Plant Microbe Interact.* 16, 456–464. doi: 10.1094/MPMI.2003.16.5.456
- Guiderdoni, E., Cornero, M. J., Vignols, F., García-Garrido, J. M., Lescot, M., Tharreau, D., et al. (2002). Inducibility by pathogen attack and developmental regulation of the rice Ltp1 gene. *Plant Mol. Biol.* 49, 683–699. doi: 10.1023/A:1015595100145
- Gutiérrez-Marcos, J. F., Costa, L., Biderre-Petit, C., Khbaya, B., O'Sullivan, D., Wormald, M., et al. (2004). Maternally expressed gene1 is a novel maize endosperm transfer cell-specific gene with a maternal parent-of-origin pattern of expression. *Plant Cell* 16, 1288–1301. doi: 10.1105/tpc.019778
- Hueros, G., Royo, J., Maitz, M., Salamini, F., and Thompson, R. D. (1999). Evidence for factors regulating transfer cell-specific expression in maize endosperm. *Plant Mol. Biol.* 41, 403–414. doi: 10.1023/A:1006331707605

- Hueros, G., Varotto, S., Salamini, F., and Thompson, R. D., (1995). Molecular characterization of BET1, a gene expressed in the endosperm transfer cells of maize. *Plant Cell* 7, 747–757. doi: 10.1105/tpc.7.6.747
- Jefferson, R. A., Kavanagh, T. A., and Bevan, M. (1987). GUS fusions: beta-glucuronidase as a sensitive and versatile gene fusion marker in higher plants. *EMBO J.* 6, 3901–3907.
- Kladnik, A., Chamusco, K., Dermastia, M., and Chourey, P. (2004). Evidence of programmed cell death in post-phloem transport cells of the maternal pedicel tissue in developing caryopsis of maize. *Plant Physiol.* 136, 3572–3581. doi: 10.1104/pp.104.045195
- Kovalchuk, N., Smith, J., Bazanova, N., Pyvovarenko, T., Singh, R., Shirley, N., et al. (2012). Characterization of the wheat gene encoding a grain-specific lipid transfer protein TdPR61, and promoter activity in wheat, barley and rice. *J. Exp. Bot.* 63, 2025–2040. doi: 10.1093/jxb/err409
- Kovalchuk, N., Smith, J., Pallotta, M., Singh, R., Ismagul, A., Eliby, S., et al. (2009). Characterization of the wheat endosperm transfer cell-specific protein TaPR60. *Plant Mol. Biol.* 71, 81–98. doi: 10.1007/s11103-009-9510-1
- Krishnan, S., and Dayanandan, P. (2003). Structural and histochemical studies on grain filling in the caryopsis of rice (*Oryza sativa* L.). *J. Biosc.* 28, 455–469. doi: 10.1007/BF02705120
- Kuwano, M., Masamura, T., and Yoshida, K. T. (2011). A novel endosperm transfer cell-containing region-specific gene and its promoter in rice. *Plant Mol. Biol.* 76, 47–56. doi: 10.1007/s11103-011-9765-1
- Lee, S. B., Go, Y. S., Bae, H. J., Park, J. H., Cho, S. H., Cho, H. J., et al. (2009). Disruption of glycosylphosphatidylinositol-anchored lipid transfer protein gene altered cuticular lipid composition, increased plastoglobules, and enhanced susceptibility to infection by the fungal pathogen *Alternaria brassicicola*. *Plant Physiol.* 150, 42–54. doi: 10.1104/pp.109.137745
- Li, M., Singh, R., Bazanova, N., Milligan, A. S., Shirley, N., Langridge, P., et al. (2008). Spatial and temporal expression of endosperm transfer cell-specific promoters in transgenic rice and barley. *Plant Biotechnol. J.* 6, 465–476. doi: 10.1111/j.1467-7652.2008.0033.x
- Maldonado, A. M., Doerner, P., Dixon, R. A., Lamb, C. J., and Cameron, R. K. (2002). A putative lipid transfer protein involved in systemic resistance signalling in *Arabidopsis*. *Nature* 419, 399–402. doi: 10.1038/nature00962
- Molina, A., and García-Olmedo, F. (1993). Developmental and pathogen-induced expression of three barley genes encoding lipid transfer proteins. *Plant J.* 4, 983–991. doi: 10.1046/j.1365-313X.1993.04060983.x
- Molina, A., and García-Olmedo, F. (1997). Enhanced tolerance to bacterial pathogens caused by the transgenic expression of barley lipid transfer protein LTP2. *Plant J.* 12, 669–675. doi: 10.1046/j.1365-313X.1997.00605.x
- Muñiz, L., Royo, J., Gómez, E., Barrero, C., Bergareche, D., and Hueros, G. (2006). The maize transfer cell-specific type-A response regulator ZmTCRR-1 appears to be involved in intercellular signalling. *Plant J.* 48, 17–27. doi: 10.1111/j.1365-313X.2006.02848.x
- Muñiz, L., Royo, J., Gómez, E., Baudot, G., Wyatt, P., and Hueros, G. (2010). Atypical response regulators expressed in the maize endosperm transfer cells link canonical two component systems and seed biology. *BMC Plant Biol.* 10:84. doi: 10.1186/1471-2229-10-84
- Olsen, O.-A. (1992). Histo-differentiation and molecular biology of developing cereal endosperm. *Seed Sci. Res.* 2, 117–131. doi: 10.1017/S0960258500001240
- Oparka, K. J., and Gates, P. (1981). Transport of assimilates in the developing caryopsis of rice (*Oryza sativa*): ultrastructure of the pericarp vascular bundle and its connections with the aleurone layer. *Planta* 151, 561–572. doi: 10.1007/BF00387436
- Pate, J. S., and Gunning, B. E. S. (1972). Transfer cells. *Annu. Rev. Plant Physiol.* 23, 173–196. doi: 10.1146/annurev.pp.23.060172.001133
- Peterson, T. N., Brunak, S., von Heijne, G., and Nielsen, H. (2011). SignalP 4.0: discriminating signal peptides from transmembrane regions. *Nat. Methods* 8, 785–786. doi: 10.1038/nmeth.1701
- Pii, Y., Astegno, A., Peroni, E., Zaccardelli, M., Pandolfini, T., and Crimi, M. (2009). The *Medicago truncatula* N5 gene encoding a root-specific lipid transfer protein is required for the symbiotic interaction with *Sinorhizobium meliloti*. *Mol. Plant Microbe Interact.* 22, 1577–1587. doi: 10.1094/MPMI-22-12-1577
- Pyee, J., Yu, H., and Kolattukudy, P. E. (1994). Identification of a lipid transfer protein as the major protein in the surface wax of broccoli (*Brassica oleracea*) leaves. *Arch. Biochem. Biophys.* 311, 460–468. doi: 10.1006/abbi.1994.1263
- Royo, J., Gómez, E., and Hueros, G. (2000). A maize homologue of the bacterial CMP-3-deoxy-D-manno-2-octulosonate (KDO) synthetases. *J. Biol. Chem.* 275, 24993–24999. doi: 10.1074/jbc.M905750199
- Royo, J., Gómez, E., and Hueros, G. (2007). “Transfer cells,” in *Plant Cell Monographs (8): Endosperm Development and Molecular Biology*, ed. O.-A. Olsen (Berlin: Springer Verlag), 73–89.
- Sambrock, J., Fritsch, F. F., and Maniatis, T. (1989). *Molecular Cloning: a Laboratory Manual*, 2nd Edn. New York, NY: Cold Spring Harbor Laboratory Press.
- Serna, A., Maitz, M., O’Connell, T., Santandrea, G., Thevissen, K., Tienens, K., et al. (2001). Maize endosperm secretes a novel antifungal protein into adjacent maternal tissues. *Plant J.* 25, 687–698. doi: 10.1046/j.1365-313x.2001.01004.x
- Sokolov, B. P., and Prokrop, D. J. (1994). A rapid and simple PCR-based method for isolation of cDNAs from differentially expressed genes. *Nucl. Acids Res.* 25, 4009–4015. doi: 10.1093/nar/22.19.4009
- Stalberg, K., Ellerstrom, M., Ezcurra, I., Ablov, S., and Rask, L. (1996). Disruption of an overlapping E-box/ABRE motif abolished high transcription of the napA storage-protein promoter in transgenic *Brassica napus* seeds. *Planta* 199, 515–519. doi: 10.1007/BF00195181
- Thompson, R. D., Hueros, G., Becker, H., and Maitz, M. (2001). Development and functions of seed transfer cells. *Plant Sci.* 160, 775–783. doi: 10.1016/S0168-9452(01)00345-4
- Wang, H. W., Hwang, S.-G., Karuppanapandian, T., Liu, A., Kim, W., and Jang, C. S. (2012). Insight into the molecular evolution of non-specific lipid transfer proteins via comparative analysis between rice and sorghum. *DNA Res.* 19, 179–194. doi: 10.1093/dnares/dss003
- Yeats, T. H., and Rose, J. K. C. (2008). The biochemistry and biology of extracellular plant lipid-transfer proteins (LTPs). *Protein Sci.* 17, 191–198. doi: 10.1110/ps.073300108

**Conflict of Interest Statement:** The authors declare that the research was conducted in the absence of any commercial or financial relationships that could be construed as a potential conflict of interest.

**Received:** 16 January 2014; **paper pending published:** 23 February 2014; **accepted:** 15 April 2014; **published online:** 06 May 2014.

**Citation:** Royo J, Gómez E, Sellam O, Gerentes D, Paul W and Hueros G (2014) Two maize END-1 orthologs, BETL9 and BETL9like, are transcribed in a non-overlapping spatial pattern on the outer surface of the developing endosperm. *Front. Plant Sci.* 5:180. doi: 10.3389/fpls.2014.00180

This article was submitted to Plant Physiology, a section of the journal Frontiers in Plant Science.

Copyright © 2014 Royo, Gómez, Sellam, Gerentes, Paul and Hueros. This is an open-access article distributed under the terms of the Creative Commons Attribution License (CC BY). The use, distribution or reproduction in other forums is permitted, provided the original author(s) or licensor are credited and that the original publication in this journal is cited, in accordance with accepted academic practice. No use, distribution or reproduction is permitted which does not comply with these terms.



# A comparative glycoproteome study of developing endosperm in the hexose-deficient *miniature1* (*mn1*) seed mutant and its wild type *Mn1* in maize

Cecilia Silva-Sanchez<sup>1</sup>, Sixue Chen<sup>1,2</sup>, Jinxi Li<sup>1</sup> and Prem S. Chourey<sup>3,4\*</sup>

<sup>1</sup> Proteomics, Interdisciplinary Center for Biotechnology Research, University of Florida, Gainesville, FL, USA

<sup>2</sup> Department of Biology, UF Genetics Institute, University of Florida, Gainesville, FL, USA

<sup>3</sup> United States Department of Agriculture, Agricultural Research Service, Center for Medical, Agricultural and Veterinary Entomology, Gainesville, FL, USA

<sup>4</sup> Department of Agronomy, University of Florida, Gainesville, FL, USA

**Edited by:**

Gregorio Hueros, Universidad de Alcalá, Spain

**Reviewed by:**

Serena Varotto, University of Padova, Italy

Gregorio Hueros, Universidad de Alcalá, Spain

**\*Correspondence:**

Prem S. Chourey, United States Department of Agriculture, Agricultural Research Service, 1600 SW 23rd Drive, Gainesville, FL 32608, USA  
e-mail: prem.chourey@ars.usda.gov

In maize developing seeds, transfer cells are prominently located at the basal endosperm transfer layer (BETL). As the first filial cell layer, BETL is a gateway to sugars, nutrients and water from mother plant; and anchor of numerous functions such as sucrose turnover, auxin and cytokinin biosynthesis/accumulation, energy metabolism, defense response, and signaling between maternal and filial generations. Previous studies showed that basal developing endosperms of *miniature1* (*mn1*) mutant seeds lacking the *Mn1*-encoded cell wall invertase II, are also deficient for hexose. Given the role of glucose as one of the key sugars in protein glycosylation and proper protein folding; we performed a comparative large scale glycoproteome profiling of total proteins of these two genotypes (*mn1* mutant vs. *Mn1* wild type) using 2D gel electrophoresis and glycosylation/total protein staining, followed by image analysis. Protein identification was done by LC-MS/MS. A total of 413 spots were detected; from which, 113 spots matched between the two genotypes. Of these, 45 showed >20% decrease/increase in glycosylation level and were selected for protein identification. A large number of identified proteins showed decreased glycosylation levels in *mn1* developing endosperms as compared to the *Mn1*. Functional classification of proteins, showed mainly of post-translational modification, protein turnover, chaperone activities, carbohydrate and amino acid biosynthesis/transport, and cell wall biosynthesis. These proteins and activities were related to endoplasmic reticulum (ER) stress and unfolded protein response (UPR) as a result of the low glycosylation levels of the mutant proteins. Overall, these results provide for the first time a global glycoproteome profile of maize BETL-enriched basal endosperm to better understand their role in seed development in maize.

**Keywords:** seed development, gene expression, sugar metabolism, transfer cells, maize

## INTRODUCTION

The *mn1* mutation in maize is associated with a loss of 70% seed weight at maturity due to a loss-of-function mutation at the *Mn1* locus that codes for the endosperm-specific cell wall invertase 2 (INCW2). The INCW2 protein is entirely localized in basal endosperm transfer cell layer (BETL), a major if not the sole gateway for the intake of sugars and nutrients from maternal cells into the filial tissue (Miller and Chourey, 1992; Cheng et al., 1996). Homozygous *mn1* mutant is not lethal presumably due to a residual low level of the cell wall invertase (CWI) activity encoded by another homolog, *Incw1* (Chourey et al., 2006). A BETL in developing maize seed is composed of two to three strata of highly specialized transfer cells (Davis et al., 1990; Kang et al., 2009), marked by a hallmark feature of labyrinth-like proliferation of cell wall called wall-in-growths (WIGs) in plants (Offler et al., 2003; Vaughn et al., 2007; Ruan et al., 2010). The INCW2 protein is immunolocalized to the *Mn1* WIGs, and the *mn1* mutant is associated with stunted WIG development due to the INCW2

deficiency (Kang et al., 2009). Sucrose hydrolysis is clearly a major physiological function of the *Mn1*-encoded INCW2 in the BETL and there is evidence that metabolically released hexoses, not exogenous, are critical as a driving force in assimilate movement between maternal and filial cells (Cheng and Chourey, 1999). As expected from the INCW2-deficiency, the *mn1* basal endosperm shows greatly reduced levels of glucose, fructose and sorbitol; and increased levels of sucrose relative to the *Mn1* developing seeds (LeClere et al., 2010; Chourey et al., 2012).

Glycoproteins (GPs) have one or more covalently attached glycan (oligosaccharide, often with the presence of glucose) moieties. Nearly all N-linked GPs are believed to be secretory proteins, which are associated with numerous functions, including stress tolerance and cell-cell communication in development. Proteins entering the secretory pathway are marked by signal peptides; 17% of all proteins in *Arabidopsis* have predicted signal peptides and, 33% of these have at least one trans-membrane domain associated with the endoplasmic reticulum (ER). Addition of

*N*-glycans to the proteins occurs as a co-translational modification at the ER and then transported through secretory pathway to the cell surface in a traffic process mediated mostly by the Golgi complex (Vitale and Boston, 2008; Liu and Howell, 2010). The ER is suggested to be a nursery where newly synthesized secretory proteins are properly decorated, modified, de-decorated (deglycosylated), finally properly folded and assembled prior to exit to their final destination (Vitale and Boston, 2008). Quality Control (QC) in this entire process is highly critical. Improperly folded proteins in the ER are causal to the so called ER-stress that is associated with unfolded protein response (UPR)—a signal transduction pathway that is well studied in mammalian and yeast cells. Recent studies in plants suggest that QC, ER stress, and UPR play an important role in biotic/abiotic stress and seed development (Liu and Howell, 2010).

The most detailed studies of GPs in maize developing endosperm have been on the storage protein zein, stored in ER-derived protein bodies (Vitale and Boston, 2008; Arcalis et al., 2010). However, there is no such information on the GPs in the BETL, a cell type not associated with storage functions in seed development. Here we report the first detailed profile of the GPs in the basal endosperm using LC-MS/MS approach, a pre-eminent tool for identification and quantitative characterization of GPs (Ruiz-May et al., 2012). Comparative GP profiles of the BETL enriched proteins of the *mn1* relative to the *Mn1* revealed potential changes due to both the hexose deficiency.

## EXPERIMENTAL PROCEDURES

### PLANT MATERIALS AND CHEMICALS

Immature maize (*Zea mays* L.) kernels wild type (*Mn1*) and *miniature 1* mutant (*mn1*) in the W22 inbred line were harvested at 12 days after pollination (DAP). All plants were grown in the field and were self- or -sib-pollinated. At the time of harvest, kernels were individually excised from the ear with a paring knife, taking care to include undamaged base (pedicel) of each kernel. Excised kernels were flash frozen in liquid nitrogen and stored at  $-80^{\circ}\text{C}$  until analysis. We used the basal 1/3 end of the endosperm because it is enriched for the BETL cells, the sole site of the *Mn1* expression and also a major zone for sucrose turn-over reactions, as previously discussed (LeClere et al., 2008; Silva-Sánchez et al., 2013). All chemicals were purchased from Fisher Scientific Inc., USA unless otherwise stated.

### TOTAL PROTEIN EXTRACTION

Soluble proteins were extracted from the one-third lower part of maize kernels according to a method reported by Hurkman and Tanaka (1986) with minor modifications. The frozen kernels were ground into fine powder in a pre-chilled mortar and pestle. A total of 3 mL of extraction buffer (0.1 M Tris HCl pH 8.8, 10 mM EDTA, 0.2 M DTT, 0.9 M sucrose) and 3 mL of saturated phenol were added to homogenize the sample. To extract proteins, samples were constantly agitated for 2 h at room temperature. The mixture was then centrifuged at  $5000 \times g$  for 10 min at  $4^{\circ}\text{C}$ . The top clear phenol phase was removed and collected in a fresh tube. The remaining pellet was re-extracted with 3 mL buffered phenol solution and centrifuged again to recover the

top clear phenol phase and combined with the previous fraction. The supernatant was precipitated with five volumes of ice cold 0.1 M ammonium acetate in 100% methanol overnight and centrifuged at  $20000 \times g$  for 20 min at  $4^{\circ}\text{C}$ . The supernatant was discarded and the pellet was washed twice with 0.1 M ammonium acetate in 100% methanol, then washed twice with cold 80% acetone and finally with 70% of ethanol. The pellet was solubilized in isoelectric focusing (IEF) buffer (7 M urea, 2 M thiourea, 4% (w/v) CHAPS and 40 mM DTT). The samples were treated with benzonase (Novagen, Gibbstown, NJ) for 30 min and then centrifuged at 34,000 rpm for 30 min at  $15^{\circ}\text{C}$  using an ultracentrifuge (Optima TLX ultracentrifuge, Beckman Coulter). Supernatant was collected and 50  $\mu\text{L}$  aliquots were kept at  $-80^{\circ}\text{C}$  until use.

### TWO DIMENSIONAL GEL ELECTROPHORESIS, PROTEIN STAINING AND IMAGING ANALYSIS

Protein samples were quantified using an EZQ protein quantitation kit (Invitrogen, CA, USA). Protein extracts of 500  $\mu\text{g}$  each were mixed with 0.2% of ampholytes (pH 3–10) and loaded onto an 18 cm Immobilized pH gradient (IPG) strips (pH range 3–10 NL) (GE healthcare, CA, USA), followed by overnight rehydration at room temperature. IEF was conducted on an Ettan IPGphor3 system (GE Healthcare, CA, USA) using the following conditions: 200 V for 30 min, then ramping to 500 V for 30 min, and finally to 10,000 V for 1 h. The voltage was held at 10,000 V until 85,000 Vh were reached in order to ensure complete separation and focusing of the proteins. After IEF, the strips were equilibrated for 15 min in equilibration buffer (6 M urea, 75 mM Tris-HCl pH 8.8, 29.3% glycerol, 2% SDS, 0.002% bromophenol blue) containing 2% DTT, and for another 15 min in equilibration buffer containing 2.5% iodoacetamide. The IPG strips were placed onto 18 cm 12.5% SDS gels (Jule Biotechnologies INC, Milford, CT, USA). Electrophoresis was run at 15 W for 5 h. A total of three replicate 2-DE experiments were conducted for each sample.

After gel electrophoresis, staining with a glycoprotein-specific stain Pro-Q Emerald fluorescent dye was performed according to manufacturer's instructions (Invitrogen, CA, USA). Images were acquired using the Investigator ProPic unit equipped with a UV light-box (Genomics solutions, MI, USA). Then, the gels were destained and restained with a total protein dye Sypro Ruby following manufacturer's instructions (Invitrogen, CA, USA). Images were acquired with the Investigator ProPic unit. Spot detection, matching and quantification across the replicate gels of wild type and mutant samples, were done using a Progenesis Samespot Software (Non-linear Dynamics, CA, USA). The function of automatic spot detection and matching was used, followed by manual inspection. Protein experimental molecular weights were calculated using a CandyCane™ molecular mass standard (Invitrogen, CA, USA) separated in a separate lane on the 2D gels, and the experimental isoelectric points were determined based on IPG strip specifications. Normalized spot volumes were used to determine the quantitative changes of glycosylated/total protein ratios and total protein levels. ANOVA test was used to determine the statistical significance.

## PROTEIN IDENTIFICATION USING LIQUID CHROMATOGRAPHY

### TANDEM MS (LC-MS/MS)

Selected 2D gel spots were excised using an Investigator ProPic robot (Genomics Solutions Inc., USA) and digested with trypsin as previously described (Sheffield et al., 2006). The lyophilized peptides were resuspended in 15  $\mu$ L of loading buffer (3% acetonitrile, 0.1% acetic acid, 0.01% trifluoroacetic acid) and loaded onto a C18 capillary trap cartridge (LC Packings, USA) and then separated on a 15 cm nanoflow analytical C18 column (PepMap 75  $\mu$ m id, 3  $\mu$ m, 100  $\text{\AA}$ ) at a flow rate of 300 nL/min on a nanoLC ultra 1D plus system (ABSciex, USA). Solvent A composition was 3% acetonitrile (ACN) v/v, 0.1% acetic acid v/v; whereas solvent B was 97% ACN v/v, 0.1% acetic acid v/v. Peptide separation was performed with a linear gradient from 3 to 40% of solvent B for 20 min, followed by an increasing to 90% of solvent B in 5 min and hold for 5 min (Zhu et al., 2010). The eluted peptides were directly sprayed into an LTQ Orbitrap XL mass spectrometer (Thermo Scientific Inc., Bremen, Germany). MS2 spectra were acquired in a data-dependent mode. An Orbitrap full MS scan (resolution:  $3 \times 10^4$ , mass range 400–1800 Da) was followed by 10 MS2 scans in the ion trap, which were performed via collision induced dissociation on the top 10 most abundant ions. Isolation window for ion selection was 3 Da. Normalized collision energy was set at 28%. Dynamic exclusion time was 20 s (Li et al., 2012a). The acquired mass spectra were searched against a Uniprot Zea mays database (62,860 entries, Jan-04-2013) using Mascot 2.2 search engine (<http://www.matrixscience.com>) with the following parameters: tryptic peptides with 1 missed cleavage site, mass tolerance of precursor ion of 10 ppm and MS/MS ion of 0.8 Da, fixed carbamidomethylation of cysteine, variable

methionine oxidation, asparagine and glutamine deamination. Unambiguous identification was done using Scaffold software V 3.0 (Proteome Software, OR, USA).

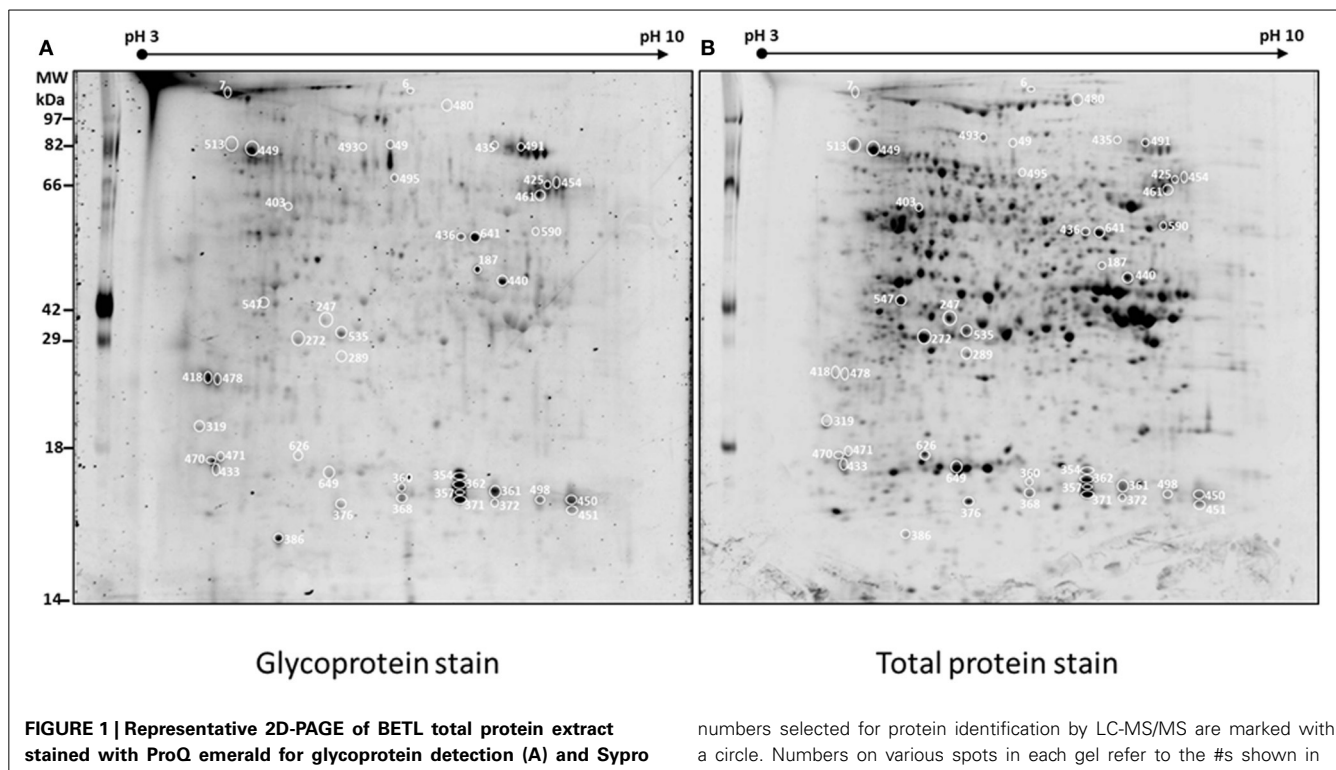
### BIOINFORMATICS ANALYSIS

Functional classification of the proteins was done according to the clusters of orthologous groups for eukaryotic complete genomes (KOG) (<ftp://ftp.ncbi.nih.gov/pub/COG/KOG/>) (Tatusov et al., 2003) and the prediction of subcellular localization was done using a Plant-mPLoc tool (<http://www.csbio.sjtu.edu.cn/bioinf/plant-multi/>) (Chou and Shen, 2010). The identified proteins were submitted to an N-Glycosite tool for glycosylation site analysis (<http://www.hiv.lanl.gov/content/sequence/GLYCOSITE/glycosite.html>) (Zhang et al., 2004). Prediction of the N-terminal presequences: chloroplast transit peptide (cTP), mitochondrial targeting peptide (mTP) and secretory pathway signal peptide (SP) was done using the TargetP 1.1 tool (<http://www.cbs.dtu.dk/services/TargetP/>) (Emanuelsson et al., 2000).

## RESULTS AND DISCUSSION

### TWO DIMENSIONAL GEL ANALYSIS, PROTEIN IDENTIFICATION AND GLYCOPROTEIN (GP) DETECTION

In order to determine the differences in glycosylation patterns of BETL between the wild type (WT) and the mutant (M), total protein extracts were prepared from the one-third lower part of maize kernels. For each sample, three biological replicates/gels were performed. The gels were stained with ProQ Emerald for glycoproteins, and then for total protein detection with Sypro Ruby stain. **Figure 1** shows representative images of gels stained for potential glycoproteins and total proteins. A total



of 413 spots were detected in the four gels of the three replicates (**Supplemental Figure 1**) representing the wild type and mutant endosperm extracts; of these, 254 spots with *p*-values smaller than 0.05 based on ANOVA test were selected for further analysis.

Glycosylation of each protein spot was evaluated by their staining intensity with the GP stain that was normalized by the intensity of total protein stain (G/TP) for both WT and the mutant samples. Normalized glycosylation ratios are represented as  $M_{(G/TP)}/WT_{(G/TP)}$  in **Table 1**. A total of 113 protein spots matched between the wild type and mutant gels, are shown in **Supplemental Table 1**. There are 45 spots (**Figure 1**) showing more than 20% increase or decrease in the normalized glycosylation level. Interestingly, only 4% of the 113 spots matched between WT and M showed increased GP ratios when comparing to the WT, while 36% showed decreased ratios (**Supplemental Table 1**).

**Figure 2** shows four representative spots with dynamic changes in normalized glycosylation levels (G/TP). The majority of proteins have decreased glycosylation ratio that is calculated by  $M_{(G/TP)}/WT_{(G/TP)}$ ; as demonstrated by spots 357 and 436 in **Figure 2** with ratios of 0.69 and 0.71, respectively. Only four spots showed 20% increased glycosylation in the mutant compared to the wild type. The spot 547 in **Figure 2** is one of those proteins with glycosylation levels in the mutant being more than two-fold of those in the wild type. This indicates the relationship between glycosylation and protein abundance is complex. **Figure 2** also includes an example of a protein, spot 185, with the glycosylation ratio of 0.97 that represented no significant change in glycosylation (**Supplemental Table 1**) in the two genotypes.

The 45 spots from the wild type and the mutant were excised and subjected to trypsin digestion and LC-MS/MS analysis. After database search using Mascot, the data were filtered in Scaffold software, and protein identification was considered valid if it had an overall 99% confidence and at least three unique peptides with 95% confidence. A total of 35 spots showed 69 comparable protein identifications between the WT and the M (**Table 1**). Some spots such as 272, 436, and 449 yielded multiple protein identifications due to the overlapping nature of proteins with similar molecular weights and isoelectric points (pIs). Several proteins were also reported by Zhu et al. (2006) in a similar proteomic study of root elongation zone in maize. Conversely, the same proteins were identified from multiple spots, e.g., spots 425, 454, and 461 as subtilisin-like protease, spots 357, 362, and 371 as Rhicadhesin receptor, and spots 440 and 449 as ER luminal binding protein. Differential post-translational modifications may account for these isoforms (Satoh et al., 2002). Alternative splicing is known to create multiple RNAs from a single gene that increase the proteome diversity. In maize, 19.2% of the total expressed genes are reported to be alternatively spliced (Barbazuk et al., 2008); thus various protein isoforms encoded by the same gene or its homologs may have alternative sizes and/or pIs.

Although nearly all the identified proteins (**Table 1**) exhibited close correlations between experimental and reported pIs, some did show discrepancy between the experimental molecular weights and theoretical molecular weights (e.g., spots 376, 454, and 493). These variations can be attributable to several factors, such as the lack of full length cDNA sequences or misannotation

for these proteins; some of the cDNA sequences may have different splicing or degraded products, and post-translational modifications like glycosylation, which can also alter the molecular weights. Out of the 69 proteins presented in **Table 1**, 39 have been reported to be glycosylated.

## FUNCTIONAL CLASSIFICATION

Functional classification of the identified proteins (**Table 1**) was performed according to the clusters of orthologous groups for eukaryotic complete genomes (KOG, Tatusov et al., 2003). Thirteen different categories were found: (I) Post-translational modification, protein turnover, chaperone functions; (II) carbohydrate metabolism and transport; (III) Amino acid metabolism and transport; (IV) Energy production and conversion; (V) Translation; (VI) RNA processing and modification; (VII) Nucleotide metabolism and transport; (VIII) Signal transduction; (IX) Coenzyme metabolism; (X) Secondary metabolites biosynthesis, transport and catabolism; (XI) Defense mechanisms; (XII) General functional prediction only; (XIII) No KOG related; as shown in **Figure 3A**.

Category I (Post-translational modification, protein turnover, chaperone functions) was the most represented category that included 15 proteins such as ER luminal binding protein (spots 440 and 449, **Table 1**), glutathione transferase (spot 362), heat shock proteins (spots 449 and 513), proteasome subunits (spots 376 and 433), chaperone proteins (spot 449), vignain (spot 440), subtilisin like protease (spots 454, 461, and 425), and WD repeat (spot 491). Interestingly, all proteins represented in the 10 spots are glycosylated as reported previously in other organisms (**Table 1**, the last column for the references); however, all showed reduced normalized glycosylation ratio except for the heat shock protein 70 (spot 513) with a ratio of 1.19. These spots showed a total protein ratio,  $M_{(TP)}/WT_{(TP)}$ , of 1.0 or slightly higher (**Table 1**), suggesting that the reduced glycosylation in the mutant was not associated with the reduced abundance of these proteins.

Protein glycosylation is accomplished when the lipid (dolichol)-linked oligosaccharide transfers the carbohydrate-containing structure ( $\text{Glc}_3\text{Man}_9\text{GlcNAc}_2$ ) to nascent peptides in the ER (Howell, 2013). Several studies have shown that the glucose residues on the lipid linked oligosaccharide facilitate the *in vitro* transfer of the oligosaccharide to the protein although it is not an absolute requirement (Kornfeld and Kornfeld, 1985). Cells starved of glucose or in energy deprivation state fail to produce  $\text{Glc}_3\text{Man}_9\text{GlcNAc}_2\text{-P-P-Dol}$ ; instead, they accumulate  $\text{Man}_9\text{GlcNAc}_2$  lipid linked species that were associated with the decrease in protein glycosylation in thyroid slices (Spiro et al., 1983). The accumulation of defective saccharide-lipid linked carrier upon different stresses varies according to cell type. In the BETL region of the *mn1* mutant kernels, the low glucose content may lead to defective or low levels of the dolichol-linked oligosaccharide causing a reduction of the normal glycosylation process associated as a general trend of low glycosylation ratios when compared with the WT.

**Table 1** depicts proteins with a high total protein ratio when comparing to the wild type, including heat shock proteins (spots

**Table 1 | Glycoproteins identified in wild type (*Mn1*) and mutant *mn1-1* BETL protein extracts.**

#	Accession number	Name	pl	MW	$M_{(G/TP)}/W_{(G/TP)}$	$M_{(TP)}/W_{(TP)}$	# Unique peptides		# N-glyco sites	SP	LOC	References	
							E	T	WT	M			
49 493	C0P0D6 B6TX01	Uncharacterized protein Glycoside hydrolase, family 28	5.77 5.68	7.26 6.16	87.29 85.53	56.24 49.74	0.45 0.52	0.88 1.02	7 3	5 3	2 10	0.14 0.38	M Tawde and Freimuth, 2012
	B7ZKJ2	Similar to Zinc finger protein-like from <i>Oryza sativa</i> (O5YL5)	6.79	48.15				0.99	7	10	3	0.95	S Bykova et al., 2006
454	C0HF77	Similar to Subtilisin-like protease from <i>Zea mays</i> (B6U0R8)	8.11	8	65.86	82.63	0.56				1	0.05	Overath et al., 2012
376	B4FNK1	Similar to Proteasome subunit beta type from <i>Zea mays</i> (B6TGL3)	5.5	5.45	16.10	40.51	0.61	1.63	13	10			
471 433	B4FRC8 B6T504	Fruit protein PKIVI52 Proteasome subunit alpha type	4.91 4.85	6.62 4.72	17.51 17.38	31.61 25.95	0.62 0.64	1.52 1.73	7 8	6 9	0 0	0.00 0.05	C Overath et al., 2012
495	B8A2E9	Similar to 2-isopropylmalate synthase B from <i>Zea mays</i> (B6SWN1)	5.78	6.59	71.07	68.68	0.65	1.49	9	3	4	0.00	C
C4J6J7		Similar to Phosphoribosylaminoimidazole carboxylase aipases-subunit, putative from <i>Ricinus communis</i> (B9S7H9)	6.59		68.71				5	7	2	0.00	C
362	O9ZP62	Glutathione transferase III (A)	6.47	5.96	16.45	23.92	0.67	1.99	3	3	1	0.31	Boušová et al., 2011
	B4FY73	Similar to Rhicadhesin receptor from <i>Zea mays</i> (B6TKE1)	6.57		22.82				8	8	1	0.96	S Gucciardo et al., 2007
451	B4FUJ3	Germin-like protein subfamily 1 member 17	8.37	6.4	16.22	24.60	0.67	1.45	3	3	1	0.95	S Gucciardo et al., 2007
461	C0HF77	Similar to Subtilisin-like protease from <i>Zea mays</i> (B6U0R8)	7.92	8	65.56	82.63	0.67	1.08	6	14	3	0.95	S Bykova et al., 2006
418	B4FVS8	Protein phosphatase 2C isoform epsilon	4.82	4.7	24.14	30.66	0.67	1.76	4	3	1	0.11	Alonso et al., 2004
	B6TU39	Peroxidase 2	4.85		34.96				3	5	1	0.03	Spadiut et al., 2012
361	B4FUJ3	Germin-like protein subfamily 1 member 17	6.94	6.4	16.51	24.60	0.67	2.26	3	3	1	0.95	S Gucciardo et al., 2007
491	O9LLB8	Exoglucanase	7.4	6.54	88.18	64.61	0.69	1.27	6	9	5	0.81	S Grevesse et al., 2003

(Continued)

**Table 1 | Continued**

#	Accession number	Name	pI		MW		$M_{(G/TP)/WT_{(G/TP)}}$		$M_{(TP)/WT_{(TP)}}$		# Unique peptides		SP	LOC	References
			E	T	E	T	WT	M	WT	M	WT	M			
COPD60		Similar to WD-repeat protein, putative from <i>Ricinus communis</i> (B9SSV2)	6.48		72.51				3	7	4	4	0.19		
COP3S2		Similar to Protein TOC75, chloroplastic from <i>Oryza sativa</i> (Q84Q83)	7.64		91.63				18	12	5	5	0.00	C	
436	C0PPA1	Adenylosuccinate synthetase, chloroplastic	6.52	6.68	52.76	51.96	0.69	0.69	9	7	2	2	0.02	C	Beránek et al., 2001
	B6TBZ8	Alanine aminotransferase 2	6.23		53.03				6	7	1	1	0.09		Xue et al., 2012
	B4FQk0	Similar to Monodehydroascorbate reductase from <i>Zantedeschia aethiopica</i> (O9SPM2)	8.65		53.77				3	13	0	0	0.00	M	
		Undeleted legumin-1	6.2		52.83				10	15	1	1	0.77	S	Arcalis et al., 2010
	Q948.8	6-phosphogluconate dehydrogenase, decarboxylating	6.3		54.17				4	3	1	1	0.07	C	
	B6TX10	Geminin-like protein subfamily 1 member 17	7.75	6.4	16.36	24.60	0.70	2.45	3	4	1	1	0.95	S	Gucciardo et al., 2007
498	B4FUT3	Similar to putative lipase from <i>Hordeum vulgare</i> (A1C0L3)	5.52	6.49	27.03	39.67	0.70	2.02	4	6	1	1	0.97	S	Romdhane et al., 2012
535	C0HHC3	ER luminal binding protein	5.08	5.1	85.53	73.08	0.71	3.67	16	7	1	1	0.90	S	Denecke et al., 1991
449	B4FW90	Heat shock protein1	5.07		70.88				16	21	4	4	0.13		Koles et al., 2007
	B7ZZ42	Similar to DnaK-type molecular chaperone hsp70-rice from <i>Oryza sativa</i> (Q53NM9)	5.1		71.16				9	9	5	5	0.07		Porras et al., 2005
	B6S269	Heat shock cognate 70 kDa protein 2	5.05		71.14				4	3	4	4	0.07		Koles et al., 2007.
	C0PF13	Similar to Alpha-N-arabinofuranosidase A from <i>Zea mays</i> (B6TB9)	5.2		74.85				6	10	3	3	0.02		Koseki et al., 2006
480	B6UOS1	Elongation factor 2	6.39	6	159.25	93.92	0.71	1.12	13	4	3	3	0.09		Solórzano et al., 2012
	C0HER4	Similar to Putative aconitase hydratase 1 from <i>Sorghum bicolor</i> (Q1KS80)	5.76		74.31				11	15	3	3	0.10		
641	Q948.8	Undeleted legumin-1	6.66	6.2	52.33	52.83	0.71	0.88	15	10	1	1	0.77	S	Arcalis et al., 2010
371	B6UGQ9	Rhicadhesin receptor	6.47	6.57	16.27	22.83	0.72	2.01	5	9	1	1	0.97	S	Gucciardo et al., 2007
440	B4FW90	ER luminal binding protein	7.08	5.1	42.29	73.08	0.74	1.06	3	3	1	1	0.90	S	Denecke et al., 1991

(Continued)

**Table 1 | Continued**

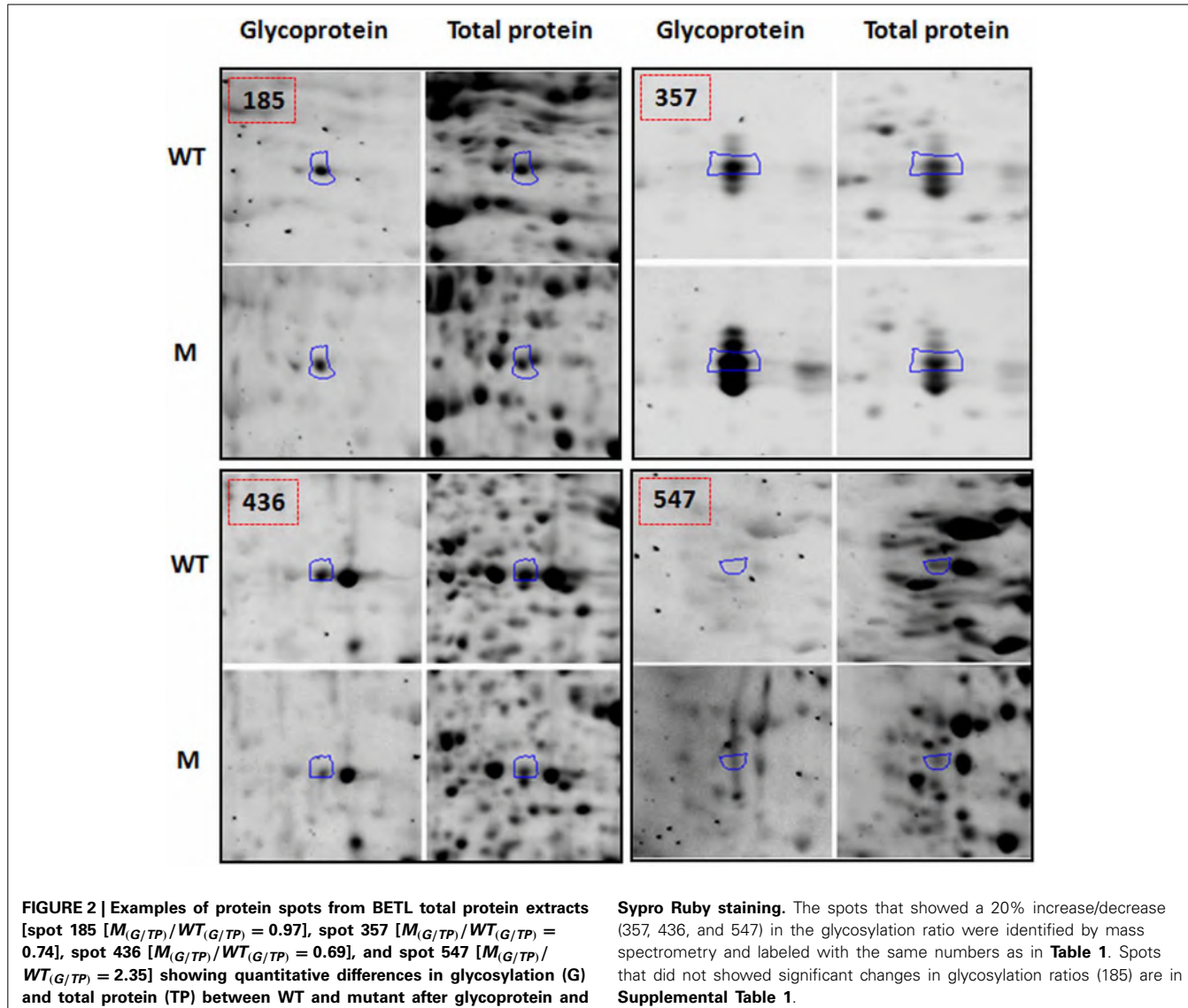
#	Accession number	Name	pI		MW		$M_{(G/TP)}/WT_{(G/TP)}$	$M_{(TP)}/WT_{(TP)}$	# Unique peptides	# N-glyco sites	SP	LOC	References
			E	T	E	T			WT	M			
B4FUE0	P9329	GTP-binding protein PTD004	6.3		44.24				3	8	2	0.07	
	B6TM9	Alcohol dehydrogenase class-3	6.37		40.77				3	4	1	0.15	
	B6UGQ9	Vigrain	6.47	6.57	40.90				9	8	1	0.99	S
357		Rhicadhesin receptor	6.47	6.57	22.83	0.74	1.83	6	7	1	0.97	S	
425	B4GON0	Glucose-6-phosphate isomerase	7.73	6.96	62.24	0.75	1.16	15	15	4	0.15	S	
	C0HF77	Similar to Subtilisin-like protease from Zea mays (B6U0R8)	8	8	82.63			14	14	3	0.95	S	
272	B4FNIM4	60S acidic ribosomal protein P0	5.27	5.19	26.68	0.77	1.58	12	11	1	0.52	Zhou et al., 2007	
	B6TP93	Fructokinase-2	5.34		34.49			18	22	0	0.41		
478	B4FWV31	Protein phosphatase 2C isoform epsilon	4.9	4.76	35.53			8	12	3	0.13	Lu, 2008	
		Glycine-rich RNA-binding protein 7	4.9	4.76	31.21	0.78	1.39						
319	B6TR84	Glycine-rich RNA-binding protein 7	4.73	4.87	25.11	0.78	1.11	6	8	2	0.07	M	
187	C0P558	Similar to Heterogeneous nuclear ribonucleoprotein A3-like protein 2 from <i>Zea mays</i> (B6TV58)	6.7	8.46	44.91	0.79	1.50	9	7	0	0.06		
	B4FLA2	Similar to Chorismate synthase from <i>Sorghum bicolor</i> (C5WQV1)	7.64		47.07			4	4	2	0.00	C	
	B4FLJ3	Isocitrate dehydrogenase [NADP]	6.57		46.10			4	4	3	0.15		
435	B7ZYR3	Uncharacterized protein Q9LLB8	6.92	6.3	89.35	0.79	2.03	5	5	2	0.01	C	
		Exoglucanase	6.54		64.61			4	3	5	0.81	S	
	C4J692	Similar to Protein TOC75, chloroplastic from <i>Oryza sativa</i> (Q84Q83)	6.91		73.86			7	5	4	0.10	M	
649	P12863	Triosephosphate isomerase, cytosolic APx1-Cytosolic Ascorbate Peroxidase	5.46	5.52	26.89	0.79	1.06	5	11	2	0.05	Love and Hanover, 2005	
	B6UB73	Triosephosphate isomerase	5.65		27.39			4	9	0	0.04		
626	B6SMQ5	Similar to Protein MYG1, putative from <i>Ricinus communis</i> (B9RY58)	5.28	5.5	17.36	0.80	0.94	7	11	2	0.09	Love and Hanover, 2005	
247	B6TS23	Protein Z	5.43	5.6	42.16	0.80	0.93	3	4	1	0.01	C	
	C06509	Caffeic acid 3-O-methyltransferase	5.48		39.57			13	10	1	0.30	Spiro, 2002	
	B4FTN5	Similar to Protein MYG1, putative from <i>Ricinus communis</i> (B9RY58)	6.02		42.70			5	4	3	0.01	M	

(Continued)

**Table 1 | Continued**

#	Accession number	Name	pI			MW			$M_{(G/TP)}/M_{(WT_{(TP)})}$			$M_{(TP)}/M_{(WT)}$			# Unique peptides	# N-glyco sites	SP	LOC	References	
			E	T	T	E	T	T	WT	WT	WT	WT	WT	WT	WT					
513	B8A3D0	Similar to Chloroplast heat shock protein 70 from <i>Penisetum americanum</i> (A4ZYQ0)	4.96	4.84	87.29	66.47	1.19		1.08	16	10		6	0.05		Koles et al., 2007				
	B6UFFB3	Stromal 70 kDa heat shock-related protein		5.08		74.67				9	29		6	0.01	C	Koles et al., 2007				
590	B7ZX15	Similar to Putative diphosphate-fructose-6-phosphate 1-phosphotransferase from <i>Oryza sativa</i> (Q6Z522)	7.73	8.23	54.66	58.19	1.19		0.91	6	3		3	0.03	M					
	B4FBF4	Serine hydroxymethyltransferase	6.84		51.60					14	8		1	0.13						
	B6T7Q7	Serine hydroxymethyltransferase		8.6		56.53				6	9		2	0.02	M					
403	C0P2V1	Similar to Leucine aminopeptidase 2, chloroplastic from <i>Oryza sativa</i> (Q6K669)	5.22	5.62	61.20	28.37	1.48		0.76	5	4		3	0.13	Matsuhashita-Morita et al., 2011					
	B4F8W6	Similar to UTP-glucose-1-phosphate uridylyltransferase from Zea mays (B6T4R3)		5.3		52.09				4	5		2	0.16	Eimert et al., 1996					
	B4FDA9	Similar to UTP-glucose-1-phosphate uridylyltransferase from Zea mays (B6T4R3)		5.23		52.18				20	16		2	0.13	Eimert et al., 1996					
547	B9TSV1	Glutamine synthetase	5.12	5.25	35.39	39.31	2.35		1.01	4	6		3	0.15	Shin and Park, 2004					
	B6TMW7	Transaminase/ transferase, transferring nitrogenous groups		5.07		43.53				4	6		0	0.12						
	B6TS21	Succinyl-CoA ligase beta-chain	5.99		45.19					8	4		0	0.01	M					

pI-isoelectric point, MW-molecular weight, E-experimental observation, T-reported value,  $M_{(G/TP)}/M_{(WT_{(TP)})}$ -normalized glycosylation ratio,  $M_{(TP)}/M_{(WT)}$ -total protein fold change, #Unique peptides-number of unique peptides identified in MS, #N-glyco sites-number of predicted N-X-S or N-X-T glycosylation motifs, X is any amino acid except proline (<http://www.hiv.lanl.gov/content/sequence/GLYCCSITE/glycosite.html>), SP-Signal peptide prediction (<http://www.cbs.dtu.dk/services/TargetP/>), M-mitochondrion, C-chloroplast, S-secretory pathway

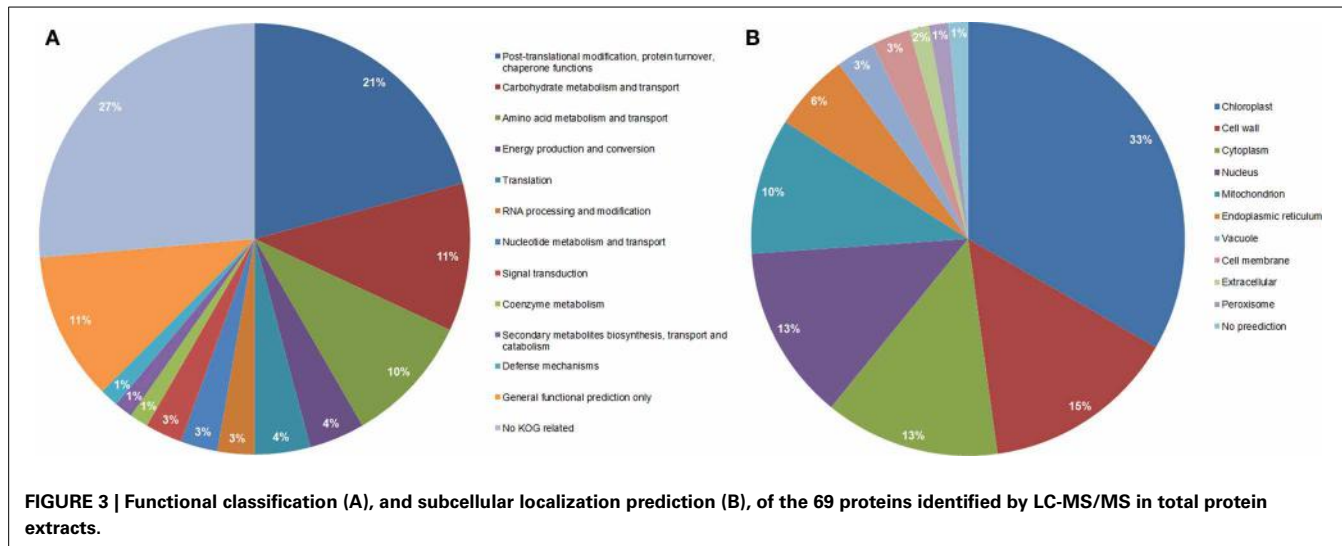


449 and 513), glutathione transferase III (spot 362) and proteasome (spots 376 and 433). Proteomic studies in developing seeds of *Brassica campestris* L reported that 23.4% of the total proteins are involved in protein processing and degradation (Li et al., 2012b).

One of the main protein folding machineries in protein processing is the *N*-glycan dependent folding pathway (Howell, 2013). After the Glc<sub>3</sub>Man<sub>9</sub>GlcNAc<sub>2</sub> core is transferred to the nascent polypeptide by the oligosaccharide transferase (OST), the Glc α-1, 2, and α-1,3 are removed by the glucosidase I and II, then calreticulin/calnexin along with protein disulfide isomerase (PDI) help in the proper folding of the protein. Folded proteins are released by glucosidase which cleaves off the last glucose α-1,3 and are finally secreted. Proteins that are not properly folded are sensed by UDP-glucose:glycoprotein glucosyltransferase, and they can be reglycosylated to reenter the calreticulin/calnexin mediated folding cycle; where *N*-glycosylation plays an important role in the endoplasmic reticulum quality control (ERQC).

We hypothesized that ER stress was induced in the BETL region due to the observed low protein *N*-glycosylation, and since *N*-glycans are recognized along several steps in the folding process of proteins, low *N*-glycosylation may lead to accumulation of unfolded/misfolded proteins that triggers the UPR response to mitigate the ER stress. These observations are consistent with Howell (2013) that UPR in plants is associated with upregulation of genes involved in protein folding and endoplasmic reticulum associated degradation (ERAD).

We observed four Hsp1 and Hsp70 proteins (spots 449 and 513); some with a high protein ratio in the *mn1* mutant kernels when compared with the WT; these proteins are reported to be involved in protein targeting to the mitochondria and chloroplasts (Kriechbaumer et al., 2012), along with ER luminal binding proteins (spots 440 and 449), proposed to be involved in protein body assembly within the ER (Li et al., 2012b), supporting the hypothesis of ER stress and UPR process as a response of the defective glycosylation process occurring in the BETL region.



In addition to UPR response, the degradation of proteins via the ubiquitination-mediated pathway is an important mechanism in plant growth and development, and is responsible for the degradation of abnormal peptides and short-lived cellular regulators; controlling many processes that allow rapid response to intracellular signals (Sadanandom et al., 2012). This pathway is also related the ERAD by sensing glycoproteins that fail to fold into a native state. The alpha mannosidase interfere the reglucosylation cycles and removes the  $\alpha$ -1,6 linked mannose from the core oligosaccharide linked to a glycoprotein. The mannose trimmed glycoprotein is recognized by a series of luminal proteins such as Lectin OS9 and HRD3 and then exported to the cytosol to be degraded via ubiquitinilation mediated pathway (Howell, 2013). The observation of proteasome subunit alpha and beta (spots 433 and 376 respectively) in a high total protein ratio in the *mn1* mutant compared to the WT kernels suggest that *mn1* kernels are undergoing ER stress due to low concentration of glucose in the BETL region.

A correlation between ER stress and programed cell death (PCD) is also described in plants (Zuppini et al., 2004). PCD occurs when internal contents of a cell are engulfed in the vacuole, leading to the tonoplast rupture and release of vacuolar hydrolytic enzymes. The tonoplast rupture is mediated by vacuolar processing enzymes that have caspase-like activity (Howell, 2013). Along with the observed proteins related to ER stress, UPR, and ERAD processes, we found that the subtilisin-like protease (spots 425, 454, and 461) also have a reported caspase-like activity (Vartapetian et al., 2011). This protein showed a low normalized glycosylation level and no change in the total protein ratio in the *mn1* mutant compared to the WT, suggesting that ER stress might regulate PCD through under-glycosylation in the *mn1* mutant BETL region. Overall, the reduced glycosylation levels of many of the above proteins may also affect diverse metabolic and cellular functions in developing seeds.

Carbohydrate catabolism and transport, the second most represented group in the functional classification (Figure 3A), is composed of eight proteins in the glycolysis pathway, pentose

pathway, fructose and mannose metabolism and starch synthesis (spots 272, 403 with two proteins, 425, 436, 590, 626, and 649). The enzymes that participate in glycolysis pathway showed low ratios of glycosylation in the *mn1* mutant when compared to WT and no change in the total protein ratio (Table 1). Several glycolytic enzymes among other protein/enzymes are reported to be modified by O-GlcNAc in various systems (Love and Hanover, 2005). The enzymes that participate in glycolysis are of special interest, due to the greatly reduced levels of hexoses resulting from the INCW2-deficiency in the BELT region of the mutant.

One of the proteins involved in carbohydrate catabolism is glucose-6-phosphate-isomerase (spot 425). It catalyzes the conversion of glucose-6-phosphate to fructose 6-phosphate, an important step in the hexoamine biosynthetic pathway. We observed that the glycosylation ratio of glucose-6-phosphate-isomerase was reduced ( $\approx 0.76$ ) and the total protein ratio was nearly the same ( $\approx 1.16$ ), suggesting that its enzymatic function and activity may be modulated through glycosylation. Cells can sense the level of a product, UDP-GlcNAc, in the hexoamine biosynthetic pathway as an indication of the level of glucose, the precursor that is used in the same pathway (Love and Hanover, 2005). Because glucose-6-phosphate-isomerase is an essential enzyme in the hexoamine biosynthetic pathway, we hypothesize that it plays an important role in maintaining the homeostasis in the cells in terms of nutrient levels in the *mn1* kernel. Further studies are needed in the characterization of this particular protein and its role in regulatory pathways.

Triosephosphate isomerase (spot 649) that catalyzes the interconversion of glyceraldehyde-3-phosphate to dihydroxyacetone phosphate was found in cytosolic and plastid isoforms with the same trend in glycosylation and total protein abundance as the glycolytic enzymes, in which glycosylation level goes down while the total protein level doesn't change significantly. For fructose and mannose metabolism, fructokinase-2 (spot 272) was found with a low glycosylation ratio but a high ratio in total protein ( $\approx 1.5$ ); while diphosphate-fructose-6-phosphate 1-phototransferas (spot 590) was found with a high ratio of

glycosylation ( $\approx 1.2$ ) and no significant change in the total protein ratio. The 6-phosphogluconate dehydrogenase (spot 436), a decarboxylating enzyme, participates in the pentose phosphate pathway (PPP) and was found with low ratios for both glycosylation and total protein. Significantly, Spielbauer et al. (2013), reported a subset of chloroplast-localized PPP enzymes to be not only present in endosperm amyloplasts but are also critical for starch and oil biosynthesis in developing seeds. The UTP-glucose-1-phosphate uridylyltransferase (spot 403) is responsible for synthesis and pyrophosphorylation of UDP-glucose, a key precursor of carbohydrate formation (including sucrose, cellulose, starch, glycogen and  $\beta$ -glucan biosynthesis). This protein showed one of the highest ratios in glycosylation but had a reduced ratio in total protein level. UGPase is highly abundant in cell wall membrane in barley and it is speculated to have a role in providing UDP-glucose for biosynthesis of cell wall components, including  $\beta$ -glucans and cellulose (Eimert et al., 1996).

Amino acid metabolism and transport was the third most important category in functional classification. There were six proteins involved in amino acid metabolism; 2-isopropylmalate synthase, alanine aminotransferase, chorismate synthase, serine hydroxymethyltransferase, transaminase and glutamine synthetase (spots 495, 436, 187, 590, and 547 for last two proteins). The first three enzymes showed a low glycosylation ratio but 2-isopropylmalate synthase and chorismate synthase had a high protein abundance ratio (Table 1). The last three enzymes had high glycosylation ratios but did not change in protein levels, which suggests that glycosylation may play a role in the regulation of these enzymes. In rice seed development proteomics studies, Deng et al. (2013) observed a correlation between the accumulation of proteins involved in protein synthesis and turnover, protein folding and amino acid metabolism, in early stages of rice seed development, indicating an active turnover of proteins during early development stages; as observed in our work.

#### SUBCELLULAR LOCATION OF THE IDENTIFIED PROTEINS

When observing the subcellular location prediction of the common proteins between the wild type and the mutant (Figure 3B), the chloroplast was the most represented with a 33% contribution of the total proteins identified, followed by the cell wall proteins (15%) and cytoplasm (13%). The chloroplast protein group consists of a very wide spectrum of different proteins that are involved in energy production and conversion, amino acid metabolism and transport, nucleotide metabolism and transport, carbohydrate metabolism and transport, and post-translational modification-protein turnover-chaperone functions.

All cell wall associated proteins showed low glycosylation level in the *mn1* mutant compare to the WT, as expected. The cell wall group was composed of 10 proteins; three subtilisin-like proteases that have post-translational modification, protein turnover, and chaperone functions (spots 425, 454, and 461) did not show any significant change in their total protein ratio. The other seven proteins did not belong to any KOG related group and were germinin-like proteins (GLPs), rhicadhesin receptor, and alpha-N-arabinofuranosidase A (spots 357, 361, 362, 371, 449, 451, and 498). It has been reported that about 40% of all known GLPs are cell wall proteins; and all GLPs contain N-terminal secretory

sequences that relate them strongly to the cell wall/extracellular matrix targeting (Breen and Bellgard, 2010). GLPs have been studied as defense molecules in different plant species, conditions and diseases due to their high resistance to protease, heat, SDS and extreme pH. Several reports identified GLPs in diverse environmental conditions, such as salt, aluminum, drought stresses, fungal pathogen attacks, bacteria and virus infections (Breen and Bellgard, 2010). A special class of GLPs that is almost exclusively found in cereals is characterized by an oxalate oxidase (OXO) activity; meanwhile, a barley GLP reported by Bernier and Berna (2001) presents a different ADP glucose enzyme activity that leads to the hypothesis of its involvement in the control of metabolic flow toward starch, cell wall polysaccharides, glycoproteins and glycolipids in plants (Rodríguez-López et al., 2001). In addition, Gucciardo et al. (2007) isolated a pea GLP that showed similarity in its N-terminus with a rhicadhesin receptor. The GLP mRNA was expressed in non-conventional locations for rhicadhesin receptors such as in nodules and the expanding cells adjacent to the nodule meristem and in the nodule epidermis. This protein is demonstrated to have a superoxide dismutase activity and show resistance to high temperature among other stresses (Breen and Bellgard, 2010). All GLP proteins showed an increased protein ratio in the *mn1* mutant kernel, suggesting an upregulation due to the stress caused by the glucose-deficiency in BETL region.

Eight proteins of cytosolic location (spots 362, 403, 418, 425, 440, 480, 491, and 547) are described in Table 1 and Figure 3B were found in the experiment. These proteins have a variety of functions such as amino acid metabolism and transport; carbohydrate metabolism and transport; post-translational modification, protein turnover, chaperone functions; secondary metabolites biosynthesis; transport and catabolism; and translation. Glutathione transferase III(A), peroxidase 2, and a like-WD-repeat protein (spots 362, 418, and 491; respectively) showed low normalized glycosylation level but an increase in the total protein ratio. These proteins are related to oxidative stress. In a previous study (Silva-Sánchez et al., 2013), proteins related to glutathione metabolism were up-regulated, in the *mn1* kernels, suggesting a potential redox regulation by glutathione. Elongation factor 2, alcohol dehydrogenase class-3 and glucose-6-phosphate isomerase (spots 425, 440, and 480; respectively) showed a low normalized glycosylation level and nearly no change in their total protein ratio. These observations suggest that their regulation may be mediated through their glycosylation. A protein similar to UTP-glucose-1-phosphate uridylyltransferase (UGPUT) from *Zea mays* (B6T4R3, spot 403) showed a high normalized glycosylation ratio ( $\approx 1.48$ ) but a low total protein ratio ( $\approx 0.76$ ). This protein plays an important role in the biosynthesis of cell wall polysaccharides as well as in the synthesis of the carbohydrate moiety for glycolipid and glycoproteins (Kleczkowski et al., 2004). Glutamine synthetase (GS) (spot 547) showed the highest level of normalized glycosylation ( $\approx 2.35$ ) but no change in total protein ratio ( $\approx 1.01$ ). Cytosolic GS participate in seed development by assimilating ammonium in sink tissues probably through the asparagine catabolism as a possible source of ammonium (Bernard and Habash, 2009). The high glycosylation levels of UGPUT and GS suggest a complex mode of post-translational

regulation in the plant. It is interesting to add that glycosylation of cytosolic proteins has been reported previously. Haltiwanger et al. (1992) described that several cytoplasmic and nuclear proteins undergo O-glycosylation, which is highly dynamic in nature and is known to response to various stimuli in the media, in a similar way to phosphorylation responses. These processes are thus far well known in yeast or animal models (Spiro, 2002; Love and Hanover, 2005) although there is some research done in plants (Thornton et al., 1999; Love and Hanover, 2005 and references there in).

#### N-GLYCOSYLATION PREDICTION AND SECRETORY PATHWAY

For all of the proteins present in **Table 1**, we predicted the number of probable N-glycosylation sites based on the N-X-S, N-X-T, or NX[ST]Z motifs, where X can be any amino acid residues except proline using the *N*-glycosite tool (Zhang et al., 2004). A total of 48 proteins showed at least one predicted N-glycosylation site in their sequence. Those proteins that did not show any predicted N-glycosylation sites potentially have other types of unusual or rare glycosylation or are not studied/reported as glycoproteins yet. Although some proteins that showed at least one predicted N-glycosylation site, they may have been reported with other types of glycosylation. For example, the proteasome alpha subunit (spot 433) has been reported to be O-glycosylated in mouse (Overath et al., 2012); elongation factor 2 (spot 480) is an O-glycosylated protein in human cervical cancer cells (Solórzano et al., 2012), triosaphosphate isomerase (Spots 626 and 649) (Love and Hanover, 2005); and protein Z showed O-glycosylation in human plasma (Spiro, 2002). O-glycosylation occurs in a great variety of proteins that are involved in key nuclear and cytoplasmic activities. Similar to phosphorylation, O-GlcNAc modification occurs on Ser or Thr residues. O-GlcNAc is interchangeable with phosphorylation. These two modifications have similar roles in biological functions as well. O-GlcNAc modification is associated to a variety of regulatory activities such as carbohydrate metabolism, signaling, transcription and translation, and stress response (Love and Hanover, 2005).

In order to investigate whether the proteins are related to the secretory pathway and have the potential of being glycosylated or not, the identified proteins from the 45 spots in **Table 1** were subjected to signal peptide prediction using the TargetP tool (Emanuelsson et al., 2000). According to the prediction, 17 proteins showed the highest scores for SP and have signal peptides. Examples of these proteins included rhicadhesin receptor (spots 357, 362, and 371), ER luminal binding protein (spots 440 and 449), GLP's (spots 361, 451, and 498), subtilisin-like protease (spots 425, 454, and 461). Many of these proteins are cell wall proteins or membrane proteins and are known to be glycosylated (Denecke et al., 1991; Bykova et al., 2006; Koseki et al., 2006; Gucciardo et al., 2007). For proteins with relative low scores for signal peptide prediction, eight proteins were assigned to mitochondria while 10 were located in the chloroplasts. The majority of these proteins have not been reported as glycoproteins. For the proteins that were not assigned neither to mitochondria or chloroplast; the low score on the SP prediction could indicate that these proteins have no classical secretion signal (Radhamony and Theg, 2006), and may follow so-called unconventional secretion

based on alternative models of secretion independent of ER and Golgi route (Zhang and Schekman, 2013).

#### CONCLUSIONS

The study of glycosylated proteins in the total protein extracts of BETL from wild type and the *mn1* mutant revealed the deficiency of the mutant in the glycosylation process. The identified proteins that participate actively in post-translational modifications, protein turnover and chaperone functions may indicate the ER stress and UPR in the mutant due to the defective glycosylation processes. Carbohydrate metabolism related proteins showed in general low glycosylation ratios, suggesting that their enzymatic functions and activities may be regulated by the glycosylation levels through the hexosamine pathway. Low glycosylation ratios were also found in cell wall proteins of the mutant, which represent most of the plant defense proteins and structural protein-crosslink. More studies are needed to fully understand the mechanism underlying protein glycosylation, sugar sensing and plant survival.

#### ACKNOWLEDGMENTS

We thank Mr. Q-B Li and Mrs Ran Zheng for excellent technical assistance, and Drs B-H Kang and B. Rathinasabapathi for critical review of the manuscript.

#### SUPPLEMENTARY MATERIAL

The Supplementary Material for this article can be found online at: <http://www.frontiersin.org/journal/10.3389/fpls.2014.00063/abstract>

**Supplemental Figure 1 | Overview of glycoprotein stain (A,B) vs. total protein stain (C,D) of wild type (A,C) and mutant (B,D).**

**Supplemental Table 1 | Selection of spots to be analyzed by mass spectrometry.** Spots in bold showed a significant variation of 20% and were chosen for mass spectrometry. GLY/G and TP stand for glycoproteins and total proteins.

#### REFERENCES

- Alonso, A., Sasin, J., Bottini, N., Friedberg, I., Friedberg, I., Osterman, A., et al. (2004). Protein tyrosine phosphatases in the human genome. *Cell* 117, 699–711. doi: 10.1016/j.cell.2004.05.018
- Arcalis, E., Stadtmann, J., Marcel, S., Drakakaki, G., Winter, V., Rodriguez, J., et al. (2010). The changing fate of a secretory glycoprotein in developing maize endosperm. *Plant Physiol.* 153, 693–702. doi: 10.1104/pp.109.152363
- Barbazuk, W. B., Fu, Y., and McGinnis, K. M. (2008). Genome-wide analysis of alternative splicing in plants: opportunities and challenges. *Genome Res.* 18, 1381–1392. doi: 10.1101/gr.053678.106
- Beránek, M., Drsata, J., and Palicka, V. (2001). Inhibitory effect of glycation on catalytic activity of alanine aminotransferase. *Mol. Cell. Biochem.* 218, 35–39. doi: 10.1023/A:1007280913732
- Bernard, S. M., and Habash, D. Z. (2009). The importance of cytosolic glutamine synthetase in nitrogen assimilation and recycling. *New Phytol.* 182, 608–620. doi: 10.1111/j.1469-8137.2009.02823.x
- Bernier, F., and Berna, A. (2001). Germins and germin-like proteins: plant do-all proteins. But what do they do exactly? *Plant Physiol. Biochem.* 39, 545–554. doi: 10.1016/S0981-9428(01)01285-2
- Boušová, I., Průchová, Z., Trnková, L., and Drsata, J. (2011). Comparison of glycation of glutathione S-transferase by methylglyoxal, glucose or fructose. *Mol. Cell. Biochem.* 357, 323–330. doi: 10.1007/s11010-011-0903-5
- Breen, J., and Bellgard, M. (2010). Germin-like proteins (GLPs) in cereal genomes: gene clustering and dynamic roles in plant defence. *Funct. Integr. Genomics.* 10, 463–476. doi: 10.1007/s10142-010-0184-1

- Bykova, N. V., Rampitsch, C., Krokhin, O., Standing, K. G., and Ens, W. (2006). Determination and characterization of site-specific *N*-glycosylation using MALDI-Qq-TOF tandem mass spectrometry: case study with a plant protease. *Anal. Chem.* 78, 1093–1103. doi: 10.1021/ac0512711
- Cheng, W. H., and Chourey, P. S. (1999). Genetic evidence that invertase-mediated release of hexoses is critical for appropriate carbon partitioning and normal seed development in maize. *Theor. Appl. Genet.* 98, 485–495. doi: 10.1007/s001220051096
- Cheng, W. H., Taliercio, E. W., and Chourey, P. S. (1996). The Miniature1 seed locus of maize encodes a cell wall invertase required for normal development of endosperm and maternal cells in the pedicel. *Plant Cell* 8, 971–983.
- Chou, K. C., and Shen, H. B. (2010). Plant-mPLoc: a top-down strategy to augment the power for predicting plant protein subcellular localization. *PLoS ONE* 5:e11335. doi: 10.1371/journal.pone.0011335
- Chourey, P. S., Jain, M., Li, Q. B., and Carlson, S. J. (2006). Genetic control of cell wall invertase in developing endosperm of maize. *Planta* 223, 159–167. doi: 10.1007/s00425-005-0039-5
- Chourey, P. S., Li, Q. B., and Cevallos-Cevallos, J. (2012). Pleiotropy and its dissection through a metabolic gene *Miniature1* (*Mn1*) that encodes a cell wall invertase in developing seeds. *Plant Sci.* 184, 45–53. doi: 10.1016/j.plantsci.2011.12.011
- Davis, R. W., Smith, J. D., and Cobb, B. G. (1990). A light and electron-microscope investigation of the transfer cell region of maize caryopses. *Can. J. Bot.* 68, 471–479. doi: 10.1139/b90-063
- Denecke, J., Goldman, M. H., Demolder, J., Seurinck, J., and Boterman, J. (1991). The tobacco luminal binding protein is encoded by a multigene family. *Plant Cell* 3, 1025–1035.
- Deng, Z. Y., Gong, C. Y., and Wang, T. (2013). Use of proteomics to understand seed development in rice. *Proteomics* 13, 1784–1800. doi: 10.1002/pmic.201200389
- Eimert, K., Villand, P., Kilian, A., and Kleczkowski, L. A. (1996). Cloning and characterization of several cDNAs for UDP-glucose pyrophosphorylase from barley (*Hordeum vulgare*) tissues. *Gene* 170, 227–232. doi: 10.1016/0378-1199(95)00873-X
- Emanuelsson, O., Nielsen, H., Brunak, S., and von Heijne, G. (2000). Predicting subcellular localization of proteins based on their N-terminal amino acid sequence. *J. Mol. Biol.* 300, 1005–1016. doi: 10.1006/jmbi.2000.3903
- Grevesse, C., Lepoivre, P., and Jijakli, M. H. (2003). Characterization of the exoglucanase-encoding gene *PaEXG2* and study of its role in the biocontrol activity of *Pichia anomala* strain K. *Phytopathology* 93, 1145–1152. doi: 10.1094/PHYTO.2003.93.9.1145
- Gucciaro, S., Wisniewski, J. P., Brewin, N. J., and Bornemann, S. (2007). A germin-like protein with superoxide dismutase activity in pea nodules with high protein sequence identity to a putative rhicadhesin receptor. *J. Exp. Bot.* 58, 1161–1171. doi: 10.1093/jxb/erl282
- Haltiwanger, R. S., Kelly, W. G., Roquemore, E. P., Blomberg, M. A., Dong, L. Y., Kreppel, L., et al. (1992). Glycosylation of nuclear and cytoplasmic proteins is ubiquitous and dynamic. *Biochem. Soc. Trans.* 20, 264–269.
- Howell, S. H. (2013). Endoplasmic reticulum stress responses in plants. *Annu. Rev. Plant Biol.* 64, 477–499. doi: 10.1146/annurev-arplant-050312-120053
- Hurkman, W. J., and Tanaka, C. K. (1986). Solubilization of plant membrane proteins for analysis by two-dimensional gel electrophoresis. *Plant Physiol.* 81, 802–806. doi: 10.1104/pp.81.3.802
- Kang, B. H., Xiong, Y., Williams, D. S., Pozueta-Romero, D., and Chourey, P. S. (2009). Miniature1-encoded cell wall invertase is essential for assembly and function of wall-in-growth in the maize endosperm transfer cell. *Plant Physiol.* 151, 1366–1376. doi: 10.1104/pp.109.142331
- Kleczkowski, L. A., Geisler, M., Ciereszko, I., and Johansson, H. (2004). UDP-glucose pyrophosphorylase. An old protein with new tricks. *Plant Physiol.* 134, 912–918. doi: 10.1104/pp.103.036053
- Koles, K., Lim, J. M., Aoki, K., Porterfield, M., Tiemeyer, M., Wells, L., et al. (2007). Identification of N-glycosylated proteins from the central nervous system of *Drosophila melanogaster*. *Glycobiology* 17, 1388–1403. doi: 10.1093/glycob/cwm097
- Kornfeld, R., and Kornfeld, S. (1985). Assembly of asparagine-linked oligosaccharides. *Annu. Rev. Biochem.* 54, 631–664. doi: 10.1146/annurev.bi.54.070185.0003215
- Koseki, T., Miwa, Y., Mese, Y., Miyanaga, A., Fushinobu, S., Wakagi, T., et al. (2006). Mutational analysis of N-glycosylation recognition sites on the biochemical properties of *Aspergillus kawachii* alpha-L-arabinofuranosidase 54. *Biochim. Biophys. Acta* 1760, 1458–1464. doi: 10.1016/j.bbagen.2006.04.009
- Kriechbaumer, V., von Löffelholz, O., and Abell, B. M. (2012). Chaperone receptors: guiding proteins to intracellular compartments. *Protoplasma* 249, 21–30. doi: 10.1007/s00709-011-0270-9
- LeClere, S., Schmelz, E. A., and Chourey, P. S. (2008). Cell wall invertase-deficient miniature 1 kernels have altered phytohormone levels. *Phytochemistry* 69, 692–699. doi: 10.1016/j.phytochem.2007.09.011
- LeClere, S., Schmelz, E. A., and Chourey, P. S. (2010). Sugar levels regulate tryptophan-dependent auxin biosynthesis in developing maize kernels. *Plant Physiol.* 153, 306–318. doi: 10.1104/pp.110.155226
- Li, J., Ferraris, J. D., Yu, D., Singh, T., Izumi, Y., Wang, G., et al. (2012a). Proteomic analysis of high NaCl-induced changes in abundance of nuclear proteins. *Physiol. Genomics* 44, 1063–1071. doi: 10.1152/physiolgenomics.00068.2012
- Li, W., Gao, Y., Xu, H., Zhang, Y., and Wang, J. (2012b). A proteomic analysis of seed development in *Brassica campestris* L. *PLoS ONE* 7:e50290. doi: 10.1371/journal.pone.0050290
- Liu, J. X., and Howell, S. H. (2010). Endoplasmic reticulum protein quality control and its relationship to environmental stress responses in plants. *Plant Cell* 22, 2930–2942. doi: 10.1105/tpc.110.078154
- Love, D. C., and Hanover, J. A. (2005). The hexosamine signaling pathway: deciphering the “O-GlcNAc code.” *Sci. STKE* 2005, re13. doi: 10.1126/stke.3122005re13
- Lu, G. (2008). *Regulation of Local Signaling by Type 2c Protein Phosphatases*. Dissertations, Academic, UCLA, Molecular Cellular, and Integrative Physiology, 66–67.
- Matsushita-Morita, M., Tada, S., Suzuki, S., Hattori, R., Marui, J., Furukawa, I., et al. (2011). Overexpression and characterization of an extracellular leucine aminopeptidase from *Aspergillus oryzae*. *Curr. Microbiol.* 62, 557–564. doi: 10.1007/s00284-010-9744-9
- Miller, M. E., and Chourey, P. S. (1992). The maize invertase-deficient miniature-1 seed mutation is associated with aberrant pedicel and endosperm development. *Plant Cell*, 4, 297–305.
- Müntz, K. (1996). Proteases and proteolytic cleavage of storage proteins in developing and germinating dicotyledonous seeds. *J. Exp. Botany* 47, 605–622. doi: 10.1093/jxb/47.5.605
- Offler, C. E., McCurdy, D. W., Patrick, J. W., and Talbot, M. J. (2003). Transfer cells: cells specialized for a special purpose. *Annu. Rev. Plant Biol.* 54, 431–454. doi: 10.1146/annurev.aplant.54.031902.134812
- Overath, T., Kuckelkorn, U., Henklein, P., Strehl, B., Bonar, D., Kloss, A., et al. (2012). Mapping of O-GlcNAc sites of 20 s proteasome subunits and Hsp90 by a novel biotin-cystamine tag. *Mol. Cell Proteomics* 11, 467–477. doi: 10.1074/mcp.M111.015966
- Porras, F., Urrea, F., Ortiz, B., Martínez-Cairo, S., Bouquelet, S., Martínez, G., et al. (2005). Isolation of the receptor for the *Amaranthus leucocarpus* lectin from human T lymphocytes. *Biochim. Biophys. Acta* 1724, 155–162. doi: 10.1016/j.bbagen.2005.03.014
- Radhamony, R. N., and Theg, S. M. (2006). Evidence for an ER to Golgi to chloroplast protein transport pathway. *Trends Cell. Biol.* 16, 385–387. doi: 10.1016/j.tcb.2006.06.003
- Rodríguez-López, M., Baraja-Fernández, E., Zandueta-Criado, A., Moreno-Bruna, B., Muñoz, F. J., Akazawa, T., et al. (2001). Two isoforms of a nucleotide-sugar pyrophosphatase/phosphodiesterase from barley leaves (*Hordeum vulgare* L.) are distinct oligomers of hvglp1, a germin-like protein. *FEBS Lett.* 490, 44–48.
- Romdhan, I. B., Fendri, A., Frikha, F., Gargouri, A., and Belghith, H. (2012). Purification, physico-chemical and kinetic properties of the deglycosylated *Talaromyces thermophilus* lipase. *Int. J. Biol. Macromol.* 51, 892–900. doi: 10.1016/j.ijbiomac.2012.06.034
- Ruan, Y. L., Jin, Y., Yang, Y. J., Li, G. J., and Boyer, J. S. (2010). Sugar input, metabolism, and signaling mediated by invertase: roles in development, yield potential, and response to drought and heat. *Mol. Plant.* 3, 942–955. doi: 10.1093/mp/ssq044
- Ruiz-May, E., Thannhauser, T. W., Zhang, S., and Rose, J. K. C. (2012). Analytical technologies for identification and characterization of the plant N-glycoproteome. *Front. Plant Sci.* 3:150. doi: 10.3389/fpls.2012.00150
- Sadanandom, A., Bailey, M., Ewan, R., Lee, J., and Nelis, S. (2012). The ubiquitin-proteasome system: central modifier of plant signalling. *New Phytol.* 196, 13–28. doi: 10.1111/j.1469-8137.2012.04266.x

- Satoh, K., Takeuchi, M., Oda, Y., Deguchi-Tawarada, M., Sakamoto, Y., Matsubara, K., et al. (2002). Identification of activity-regulated proteins in the postsynaptic density fraction. *Genes Cells* 7, 187–197. doi: 10.1046/j.1356-9597.2001.00505.x
- Sheffield, J., Taylor, N., Fauquet, C., and Chen, S. (2006). The cassava (*Manihot esculenta* Crantz) root proteome: protein identification and differential expression. *Proteomics* 6, 1588–1598. doi: 10.1002/pmic.200500503
- Shin, D., and Park, C. (2004). N-terminal extension of canine glutamine synthetase created by splicing alters its enzymatic property. *J. Biol. Chem.* 279, 1184–1190. doi: 10.1074/jbc.M309940200
- Silva-Sánchez, C., Chen, S., Zhu, N., Li, Q.-B., and Chourey, P. S. (2013). Proteomic comparison of basal endosperm in maize *miniature1* mutant and its wild-type *Mn1*. *Front. Plant Sci.* 4:211. doi: 10.3389/fpls.2013.00211
- Solórzano, C., Angel Mayoral, M., de los Angeles, C. M., Berumen, J., Guevara, J., Raúl Chávez, F., et al. (2012). Overexpression of glycosylated proteins in cervical cancer recognized by the *Machaerocereus eruca* agglutinin. *Folia Histochem. Cytophiol.* 50, 398–406. doi: 10.5603/FHC.2012.0054
- Spadiut, O., Rossetti, L., Dietzsch, C., and Herwig, C. (2012). Purification of a recombinant plant peroxidase produced in *Pichia pastoris* by a simple 2-step strategy. *Protein Expr. Purif.* 86, 89–97. doi: 10.1016/j.pep.2012.09.008
- Spielbauer, G., Li, L., Romisch-Margl, L., Do, T., Fouquet, R., Fernie, A. R., et al. (2013). Chloroplast-localized 6-phosphogluconate dehydrogenase is critical for maize starch accumulation. *J. Exp. Bot.* 64, 2231–2242. doi: 10.1093/jxb/ert082
- Spiro, R. G. (2002). Protein glycosylation: nature, distribution, enzymatic formation, and disease implications of glycopeptide bonds. *Glycobiology* 12, 43R–56R. doi: 10.1093/glycob/12.4.43R
- Spiro, R. G., Spiro, M. J., and Bhoyroo, V. D. (1983). Studies on the regulation of the biosynthesis of glucose-containing oligosaccharide-lipids. Effect of energy deprivation. *J. Biol. Chem.* 258, 9469–9476.
- Tatusov, R. L., Fedorova, N. D., Jackson, J. D., Jacobs, A. R., Kiryutin, B., Koonin, E. V., et al. (2003). The COG database: an updated version includes eukaryotes. *BMC Bioinformatics* 4:41. doi: 10.1186/1471-2105-4-41
- Tawde, M. D., and Freimuth, P. (2012). Toxic misfolding of *Arabidopsis* cellulases in the secretory pathway of *Pichia pastoris*. *Protein Expr. Purif.* 85, 211–217. doi: 10.1016/j.pep.2012.08.009
- Thornton, T. M., Swain, S. M., and Olszewski, N. E. (1999). Gibberellin signal transduction presents ellipsis the SPY who O-GlcNAc'd me. *Trends Plant Sci.* 4, 424–428. doi: 10.1016/S1360-1385(99)01485-5
- Vartapetian, A. B., Tuzhikov, A. I., Chichkova, N. V., Taliantsky, M., and Wolpert, T. J. (2011). A plant alternative to animal caspases: subtilisin-like proteases. *Cell Death Differ.* 18, 1289–1297. doi: 10.1038/cdd.2011.49
- Vaughn, K. C., Talbot, M. J., Offler, C. E., and McCurdy, D. W. (2007). Wall ingrowths in epidermal transfer cells of *Vicia faba* cotyledons are modified primary walls marked by localized accumulations of arabinogalactan proteins. *Plant Cell Physiol.* 48, 159–168. doi: 10.1093/pcp/pcl047
- Vitale, A., and Boston, R. S. (2008). Endoplasmic reticulum quality control and the unfolded protein response: insights from plants. *Traffic* 9, 1581–1588. doi: 10.1111/j.1600-0854.2008.00780.x
- Xue, Y. L., Miyakawa, T., Sawano, Y., and Tanokura, M. (2012). Cloning of genes and enzymatic characterizations of novel dioscorin isoforms from *Dioscorea japonica*. *Plant Sci.* 183, 14–19. doi: 10.1016/j.plantsci.2011.10.021
- Zhang, M., Gaschen, B., Blay, W., Foley, B., Haigwood, N., Kuiken, C., et al. (2004). Tracking global patterns of N-linked glycosylation site variation in highly variable viral glycoproteins: HIV, SIV, and HCV envelopes and influenza hemagglutinin. *Glycobiology* 14, 1229–1246. doi: 10.1093/glycob/cwh106
- Zhang, M., and Schekman, R. (2013). Unconventional secretion, unconventional solutions. *Scienc* 340, 559–561. doi: 10.1126/science.1234740
- Zhou, H., Liu, Y., Chui, J., Guo, K., Shun, Q., Lu, W., et al. (2007). Investigation on glycosylation patterns of proteins from human liver cancer cell lines based on the multiplexed proteomics technology. *Arch. Biochem. Biophys.* 459, 70–78. doi: 10.1016/j.abb.2006.10.027
- Zhu, J., Chen, S., Alvarez, S., Asirvatham, V. S., Schachtman, D. P., Wu, Y., et al. (2006). Cell wall proteome in the maize primary root elongation zone. I. Extraction and identification of water-soluble and lightly ionically bound proteins. *Plant Physiol.* 140, 311–325. doi: 10.1104/pp.105.070219
- Zhu, M., Simons, B., Zhu, N., Oppenheimer, D. G., and Chen, S. (2010). Analysis of abscisic acid responsive proteins in *Brassica napus* guard cells by multiplexed isobaric tagging. *J. Proteomics* 73, 790–805. doi: 10.1016/j.jprot.2009.11.002
- Zuppini, A., Navazio, L., and Mariani, P. (2004). Endoplasmic reticulum stress-induced programmed cell death in soybean cells. *J. Cell Sci.* 117, 2591–2598. doi: 10.1242/jcs.01126
- Conflict of Interest Statement:** The authors declare that the research was conducted in the absence of any commercial or financial relationships that could be construed as a potential conflict of interest.
- Received:** 07 August 2013; **accepted:** 07 February 2014; **published online:** 26 February 2014.
- Citation:** Silva-Sánchez C, Chen S, Li J and Chourey PS (2014) A comparative glycoproteome study of developing endosperm in the hexose-deficient *miniature1* (*mn1*) seed mutant and its wild type *Mn1* in maize. *Front. Plant Sci.* 5:63. doi: 10.3389/fpls.2014.00063
- This article was submitted to Plant Physiology, a section of the journal *Frontiers in Plant Science*.
- Copyright © 2014 Silva-Sánchez, Chen, Li and Chourey. This is an open-access article distributed under the terms of the Creative Commons Attribution License (CC BY). The use, distribution or reproduction in other forums is permitted, provided the original author(s) or licensor are credited and that the original publication in this journal is cited, in accordance with accepted academic practice. No use, distribution or reproduction is permitted which does not comply with these terms.



# A PCR-based forward genetics screening, using expression domain-specific markers, identifies mutants in endosperm transfer cell development

Luis M. Muñiz<sup>1</sup>, Elisa Gómez<sup>1</sup>, Virginie Guyon<sup>2</sup>, Maribel López<sup>1</sup>, Bouchaib Khbaya<sup>2</sup>, Olivier Sellam<sup>2</sup>, Pascual Pérez<sup>2</sup> and Gregorio Hueros<sup>1\*</sup>

<sup>1</sup> Departamento Biomedicina and Biotecnología (Genética), Universidad de Alcalá, Alcalá de Henares, Spain

<sup>2</sup> GM Trait Discovery, Biogemma, Centre de Recherche de Chappes, Chappes, France

**Edited by:**

David McCurdy, The University of Newcastle, Australia

**Reviewed by:**

Serena Varotto, University of Padova, Italy

Johannes Thiel, Leibniz Institute of Plant Genetics and Crop Plant Research (IPK), Germany

**\*Correspondence:**

Gregorio Hueros, Departamento Biomedicina and Biotecnología (Genética), Universidad de Alcalá, Campus Universitario, Alcalá de Henares-28870, Spain  
e-mail: gregorio.hueros@uah.es

Mutant collections are an invaluable source of material on which forward genetic approaches allow the identification of genes affecting a wide variety of biological processes. However, some particular developmental stages and morphological structures may resist analysis due to their physical inaccessibility or to deleterious effects associated to their modification. Furthermore, lethal mutations acting early in development may escape detection. We have approached the characterization of 101 maize seed mutants, selected from a collection of 27,500 visually screened Mu-insertion lines, using a molecular marker approach based on a set of genes previously ascribed to different tissue compartments within the early developing kernel. A streamlined combination of qRT-PCR assays has allowed us to preliminary pinpoint the affected compartment, establish developmental comparisons to WT siblings and select mutant lines with alterations in the different compartments. Furthermore, clusters of markers co-affected by the underlying mutation were identified. We have analyzed more extensively a set of lines presenting significant variation in transfer cell-associated expression markers, and have performed morphological observations, and immunolocalization experiments to confirm the results, validating this approach as an efficient mutant description tool.

**Keywords:** transfer cells, development, aleurone, mutant, gene expression

## INTRODUCTION

The angiosperm seed is a complex structure evolutionarily designed to attain protection of the forming embryo, resist desiccation, facilitate its dispersal and nurture the new plant before it obtains sufficient photosynthetic ability for self-support. The synchronized formation of tissular domains and activation of their different functions presents a very interesting scenario for developmental studies (Berger, 2003), as plant seeds are easy to obtain in great numbers in a controlled manner, dissection and structure observation is easy, and similar developmental patterns are implemented with little variation by very different plant species. A number of works have described the architecture and development of the seed (Wobus and Weber, 1999; Boisnard-Lorig et al., 2001; Thompson et al., 2001). Among these, the maize seed has received particular attention due to its economic value and widespread cultivation (Timmermans et al., 2004). It is the result of a double fertilization event which produces two isolated compartments differing in ploidy level but otherwise genetically identical, the embryo and the endosperm. The endosperm develops from the fusion of one sperm nucleus with the central cells of the embryo sac, producing a triploid syncytial tissue which follows a nuclear type of development (Kiesslbach, 1949). Few days after pollination, active cell division yields to a differentiation process that results in four specialized tissues within the endosperm (Olsen, 2001; Consonni et al., 2005; Scanlon and

Takacs, 2008): the starchy endosperm, which accumulates nutrients for seedling nutrition after germination; the ESR, presumably involved in nutrient transfer from the mother plant to the embryo and its protection (Balandín et al., 2005); the basal endosperm transfer layer (BETL), located right under the starchy endosperm and opposite to the placenta-chalaza, where it facilitates solute uptake and secretes defensive peptides onto the seed-mother plant interface (Serna et al., 2001; Olsen, 2004); and the aleurone, a peripheral layer of nearly cubical cells which participates in substrate mobilization upon germination of the embryo (Bommert and Werr, 2001) and covers the entire surface of the endosperm except for the BETL.

Forward genetics is a time-proven, reliable strategy to identify genes involved in the regulation of biological processes. Providing researchers with a collection of individuals on which to perform phenotypic screenings and amenable to an easy search for the causative gene has been the goal of an increasing number of mutant collections in several biological systems (*Arabidopsis*; Alonso et al., 2003; maize; Walbot, 2000; rice; An et al., 2005; *Drosophila*; Bellen et al., 2004; *Caenorhabditis*; Barstead and Moerman, 2006; mouse; Adams et al., 2004...). The study of early developmental processes or tissue differentiation through mutant screening poses however some problems, like the reduced size and accessibility of some tissues and the loss of individuals bearing defects deleterious for organ/tissue organization in early

stages (Warren and Fishman, 1998). Technologies able to detect and quantify markers for development and function in minute samples and/or in a fast, simple manner may open the possibility to scrutinize tissue organization and functionality in a reliable way (Borisjuk et al., 1998), thus facilitating the identification of interesting mutants. Genes expressed in a tissue-specific manner are thus excellent candidates as tools to detect mutations affecting cell fate and organ determination.

Genetic determinants and markers for the endosperm differentiated tissues have been described along the years (Opsahl-Ferstad et al., 1997; Bonello et al., 2000; Becraft, 2001; Gómez et al., 2002). Many of these genes have been shown to be intimately associated to the presence/function of a specific cell type and may provide an unequivocal beacon of its presence or state of development. Additionally, genes with known expression kinetics along tissue differentiation may allow pinpointing precisely the moment when a given mutation is relevant for tissue identity or function. To test the feasibility of a molecular-based analysis of the maize seed as mutant-screening tool, we have analyzed 101 maize mutant lines showing alterations in the kernel development via a streamlined combination of qRT-PCR tests. We have described the molecular effect of the mutations in each line on kernel formation, pinpointed the affected cell types according to the expression patterns, and validated the results by performing histological descriptions and immunolocalization of sibling kernels, confirming this approach as an efficient mutant screening tool.

## MATERIALS AND METHODS

### PLANT MATERIAL

One hundred and one maize lines showing monogenic segregation for mutations affecting kernel development were selected from a collection of 27,500 Mutator-mutagenized maize lines (Martin et al., 2006). Wild type (WT) and mutant sibling kernels were dissected out from segregating ears once they could be unambiguously distinguished (in most cases between 13 and 15 DAP). Kernels were immediately frozen in liquid N<sub>2</sub> and stored at -80°C until they were used for RNA extraction.

### RNA EXTRACTION

RNA was extracted from 2 WT and 2 mutant kernels for each line using the FastRNA® Pro System (Bio101) with minor modifications to the manufacturer's protocol. Briefly, frozen seeds were crushed in liquid nitrogen and immediately mixed with lysis buffer. After completing the extraction and prior to quantitation, the RNA solutions were frozen at -80°C and centrifuged to precipitate starch.

### qRT-PCR DESIGN

At least one of the primers selected for each gene spanned an intron site in the genomic DNA, to avoid amplification of contaminating DNA in the RNA preparations. Primer couples were designed to amplify short cDNA sequences to maximize the efficiency of the PCR reactions.

The qRT-PCR reactions were performed in an ABI-PRISM-7000 instrument using the Power SYBR Green One-Step RT-PCR Master Mix, both from Applied Biosystems, and 20 ng of total

RNA as template. Reactions were checked for specificity by visual inspection of melting curves and relative expression values were calculated using the  $\Delta\Delta Ct$  method, normalizing to the *ZmFKBP-66* gene Ct in the same sample and comparing the WT/mutant pairs.

### IMMUNOLOCALIZATION AND HISTOLOGY

Seeds kept at -80°C were hand dissected whilst frozen and immediately fixed in 0.1 M phosphate buffer pH 7.2 plus 4% paraformaldehyde, 0.1% glutaraldehyde. Samples were then dehydrated in an ethanol series and embedded in Paraplast (Sigma). Sections 8  $\mu$ m thick were attached to sylanized glass slides. Slides were deparaffinised with xylene (Dimethyl-benzene) and then rehydrated in an ethanol series. Endogenous peroxidase activity was deactivated by incubation in 0.3% hydrogen peroxide for 20 min. Sections were then blocked with 2% normal donkey serum for 2 h at room temperature (RT) and reacted with antiBETL1 or antiBETL2 antisera, or the corresponding pre-sera at 1:500 dilution. Reacted primary antibodies were detected with biotin-conjugated anti-rabbit goat antibody diluted 1:750 (Sigma) and then with Extravidin-peroxidase (Sigma) solution at 1:800 dilution. Finally, positive reaction was developed using SIGMAFAST™ DAB with Metal Enhancer (Sigma) until a gray-black precipitate was clearly visible on the sera-reacted slides. The sections were stained post-detection with 0.025 % Azure B in phosphate buffer pH4 for 3 min, washed in abundant distilled water, mounted in DEPEX and photographed as described in Muñiz et al. (2006).

## RESULTS

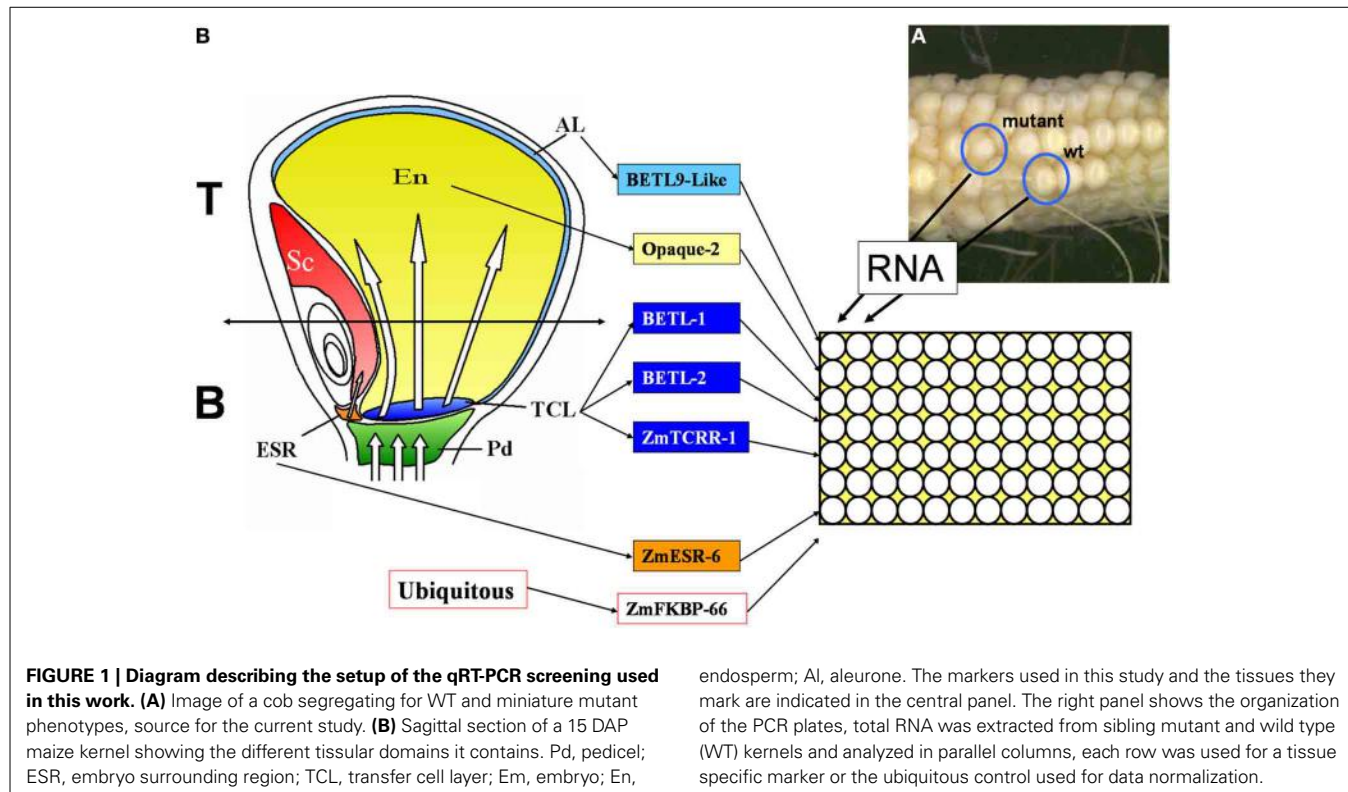
### COLLECTION OF RNA FROM WILD TYPE AND MUTANT SIBLING DEVELOPING KERNELS

A visual screening among 25,000 maize lines of a *Mu* transposon-mutagenized collection allowed identification of 600 lines showing alterations in the development of the endosperm. These lines were classified as *min* (miniature) or *udve* (undeveloped with embryo) (Figure 1A). F2 seeds from 101 mutant lines were planted in the field to produce the material used in the present work. Immature cobs were opened for visual inspection starting at 13 days after pollination (13 DAP). In most cases WT and mutant kernels could be unambiguously distinguished in segregating ears 13–15 DAP. Kernels were collected at the youngest possible distinctive developmental stage, frozen in liquid nitrogen and stored at -80°C.

On average, 200  $\mu$ g total RNA was obtained from the WT kernels and 80  $\mu$ g from the mutant kernels, although wide variation was observed for the mutant samples among the different lines. The quality of the RNA was analyzed by formaldehyde-gel electrophoresis of aliquots of 3  $\mu$ g (not shown); only samples showing intact ribosomal RNA species were used for real time PCR.

### DESIGN OF REAL TIME PCR ASSAYS FOR DEVELOPING ENDOSPERM EXPRESSION DOMAIN SPECIFIC MARKERS

Marker genes were selected for different expression domains within the developing endosperm (see Figure 1B for a graphical representation of the domains analyzed). The expression pattern of all the markers used in this study has been characterized in



detail, including *in situ* hybridization studies. The list includes 4 markers for the transfer cell layer: *BETL-1* and *BETL-2* (Hueros et al., 1999), *ZmTCRR-1* (Muñiz et al., 2006), and *ZmMRP-1* (Gómez et al., 2002, 2009); 1 marker for the embryo surrounding region: *ZmESR-6* (Balandín et al., 2005); 1 marker for the aleurone: *BETL-9like* (our group, see Royo et al., under review) and 1 marker for the starchy endosperm: *Opaque-2* (the expression of the gene was analyzed by *in situ* hybridization in Dolfini et al., 1992). As an internal control for data normalization, we selected the ubiquitously expressed gene *ZmFKBP-66* (Hueros et al., 1999). Different primer sets were tested for each gene (data not shown) until a primer pair was identified (Table 1) satisfying the following criteria: 1. No PCR product was amplified from 50 ng genomic DNA, using the same PCR conditions designed for the real time RT-PCR assays, 2. In the absence of PCR product, no primer dimers were formed, and 3. The efficiency of the amplification, as determined by the standard curve method, was similar for all genes, and approached 1 (not shown).

The ability of the selected primer pairs to detect domain specific expression was tested in real time RT-PCR experiments using as template total RNA extracted from the upper (Top in Figure 1B) or lower (Bottom in Figure 1B) halves of WT kernels collected at 10 DAP. As shown in Figure 1B, the upper part of the kernels does not contain transfer cells and very little embryo surrounding region, whilst both the upper and lower halves should contain roughly equivalent amounts of aleurone and starchy endosperm tissues.

Consistent with the distribution of tissues within the seed, the results (Figure 2) showed a higher accumulation of transcript in

the bottom samples, with a difference of over 1 order of magnitude, for the transfer cell and ESR specific markers. Equivalent amounts of transcript were detected, however, in Top and Bottom for the aleurone and starchy endosperm specific markers.

#### REAL TIME PCR ANALYSES

For the real time PCR analyses of the selected lines, the scheme outlined in Figure 1 was followed. We designed an analysis setup for pairs of total RNA samples from immature WT and mutant sibling kernels in parallel columns of 12 × 8 well PCR plates. PCR primers specific for the seven tissue-specific markers and the ubiquitous control were distributed in each of the 8 rows of the plate (see the schematics in Figure 1B). The analyses of the expression data for the WT kernels from the 101 lines (Figure 3A), shows that the markers expression level ranges from highly expressed (*BETL-1*, *BETL-2*, and *BETL-9like*) to very lowly expressed (*ZmMRP-1*), encompassing nearly two orders of magnitude. The expression levels of *ZmTCRR-1*, *ZmESR-6*, and *Opaque-2* were intermediate between the other two groups. The variation in the expression level of the markers among the WT samples from different lines was moderate, and very likely reflects differences in the maturation stage of the different ears at the time the kernels were collected. The low expression level found for *ZmMRP-1* could compromise the sensitivity of the WT/mutant comparisons and we therefore decided not to include this marker among the primary criteria for selection of putative transfer cell mutant lines.

A pooled comparison of the effect of the different mutations on the expression of the markers reflects a wide range of variation

**Table 1 | Summary of primers used in the transcriptomic analysis.**

Gene	Amplicon size (bp)	Primers (5'-3')	Expression domain
BETL-1	93	CAGCACAATCGTCGCGCTT TTCTGGGTTCCCGATGC*AGC	Transfer cells
BETL-2	115	TGCACGCACAACAAGTG*GGC AGCATGGCCCGTCGTCAATT	Transfer cells
ZmMRP-1	120	GACTACAGATGAGCACAG*GAATTTC GCATGGCTAGAGATCTGCA	Transfer cells
ZmTCRR-1	106	ATTGGAATTCTTAGATGCG*AAC CGATTC*CTTCACTTCCCTAA	Transfer cells
ZmESR-6	90	GCCATAACCATGCCGTCT TGCAGACGCATCCATTG*CGA	ESR
BETL-9like	283	CTATGTTGCCATAGGCTCTCATGC GCTGGAACCTTGTAGC*TTCCG	Aleurone
Opaque-2	158	AGAACTGGAGGACCAG*GTAGC CCTCTCCCATCTTCAC*CTTA	Starchy endosperm
ZmFKBP-66	117	GGGTGCTGTTGAAG*TCA GCAATAA*CTTCCTCTCATCG	Ubiquitous

The table presents gene name, expected amplicon size, primer sequence and represented tissue domain. The asterisks indicate the intron/exon boundary.

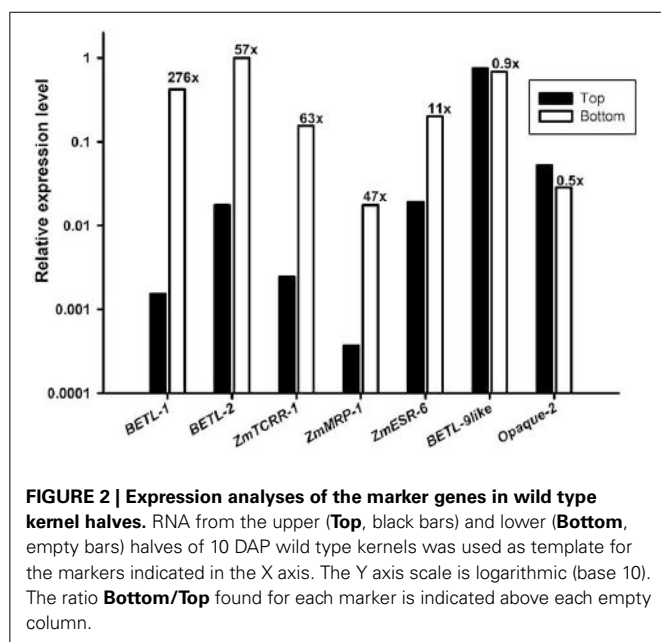


**FIGURE 2 | Expression analyses of the marker genes in wild type kernel halves.** RNA from the upper (**Top**, black bars) and lower (**Bottom**, empty bars) halves of 10 DAP wild type kernels was used as template for the markers indicated in the X axis. The Y axis scale is logarithmic (base 10). The ratio **Bottom/Top** found for each marker is indicated above each empty column.

among the lines and among markers (Figure 3B). The analysis of the structure of this variation indicates that most lines show only a moderate decrease in the expression of the domain markers. As a result, the median values for the different markers' WT/mutant ratio are below 5, being as low as 1.16 in the case of *ZmESR-6*. This gene and *ZmMRP-1* display the lowest median WT/mutant

variation, possibly confirming the aforementioned discrimination limit for lowly expressed genes. In the case of *ZmESR-6*, which has a higher expression than *ZmMRP-1*, the limited extension of its expression domain at this stage may contribute to the low WT/mutant ratio found. On the other hand, in a small number of lines the expression ratio WT/mutant for certain markers indicated a variation of several orders of magnitude (note the long error bars in Figure 3B for *BETL-1*, -2, *ZmTCRR-1*, and *BETL-9*). Most probably, in these lines the mutation has altered the early differentiation of a certain cell type leading to a significant reduction of the expression levels of the corresponding markers.

The expression ratios were converted into color variations to visualize the expression patterns of the different markers and lines (Figure 4), the lines were then ordered according to the WT/mutant ratio displayed for *BETL-2* and *ZmTCRR-1* (the numeric values the figure is based on are supplied as Supplementary Table S1). These markers were chosen as first and second hierarchical parameters for the evaluation of the lines, regarding the putative absence of the TC domain, as both of them were reliably measurable by qRT-PCR. In this way, 11 lines (labeled in red in Figure 4), with differing severity in the alteration of the TC marker expression levels, were selected for further characterization. Surprisingly, in the case of *BETL-1* no expression could be detected in 36% of the lines in either WT or mutant kernels. This result discarded the expression data recorded for this marker as the primary parameter for the selection of candidate lines and suggest that the expression of this marker might be influenced by environmental factors.

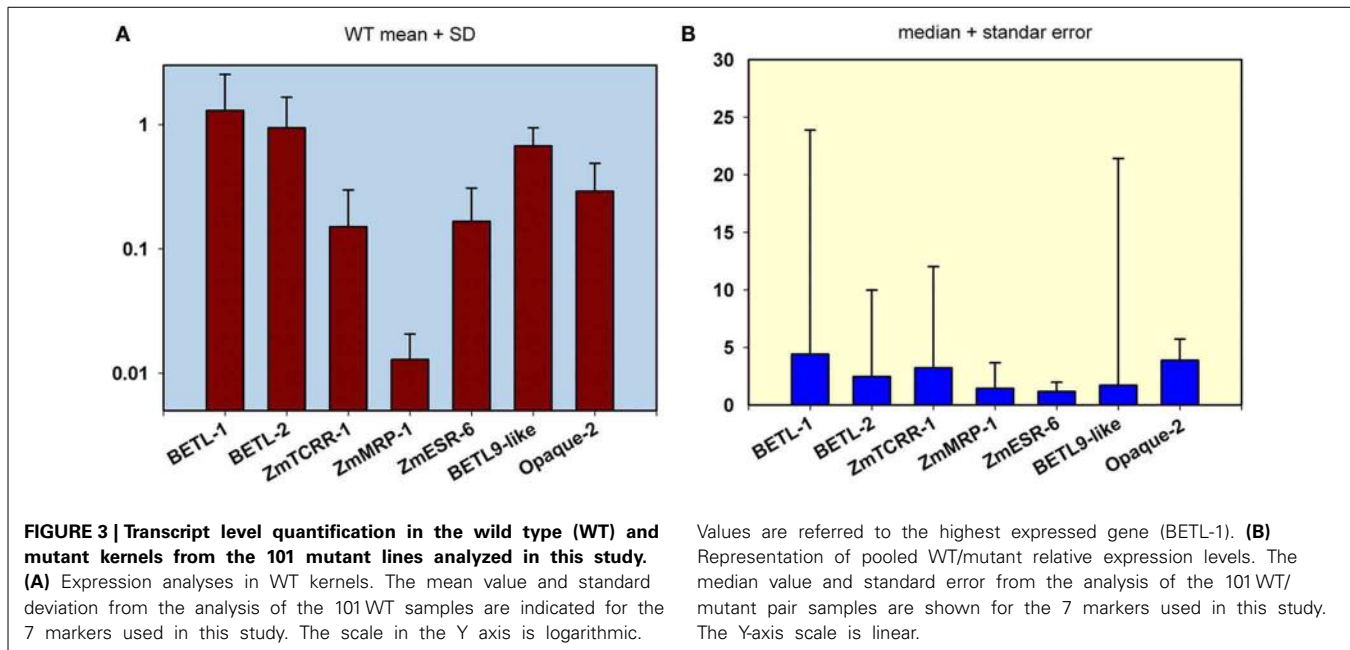
For 29 lines, no significant difference in the expression level of the markers in the WT and mutant samples was found. The remaining 72 lines showed a WT/mutant ratio >5 for at least one of the markers (Figure 4).

When the aleurone and transfer cell specific markers were examined, only 10 (for *BETL-9like*) or 30 (for *BETL-2*) lines showed a ratio WT/mutant higher than 5, although this ratio reached levels above two orders of magnitude in particular cases. This contrasts with the situation observed for *Opaque2*, which showed a ratio >5 in 42 (58%) of the lines showing any variation, and was the only marker affected in 25 cases. The decrease in the expression of the *Opaque2* marker in the mutant kernels was, however, moderate; for the majority (31 lines) the ratio WT/mutant ranged between 5 and 10 and was never higher than 30. The ESR marker showed the least affection, with WT/mutant ratios higher than 5 only in 6 cases and a quite moderate range from 5 to 11 fold.

The 11 lines selected were then rechecked by qRT-PCR on RNA extracted from sibling seeds. The qRT-PCR analyses showed the results of line C1282 were not reproducible on the new RNA samples (no significant differences were found in this round of tests, not shown), and the line was removed from subsequent studies.

#### HISTOLOGY AND IMMUNOANALYSES OF SELECTED LINES

As a way to obtain an anatomical perspective of the effect of the mutations under study, investigate what their effect on seed structure is, and validate the qRT-PCR analysis' ability to predict specific tissue alterations we prepared optical microscopy sections

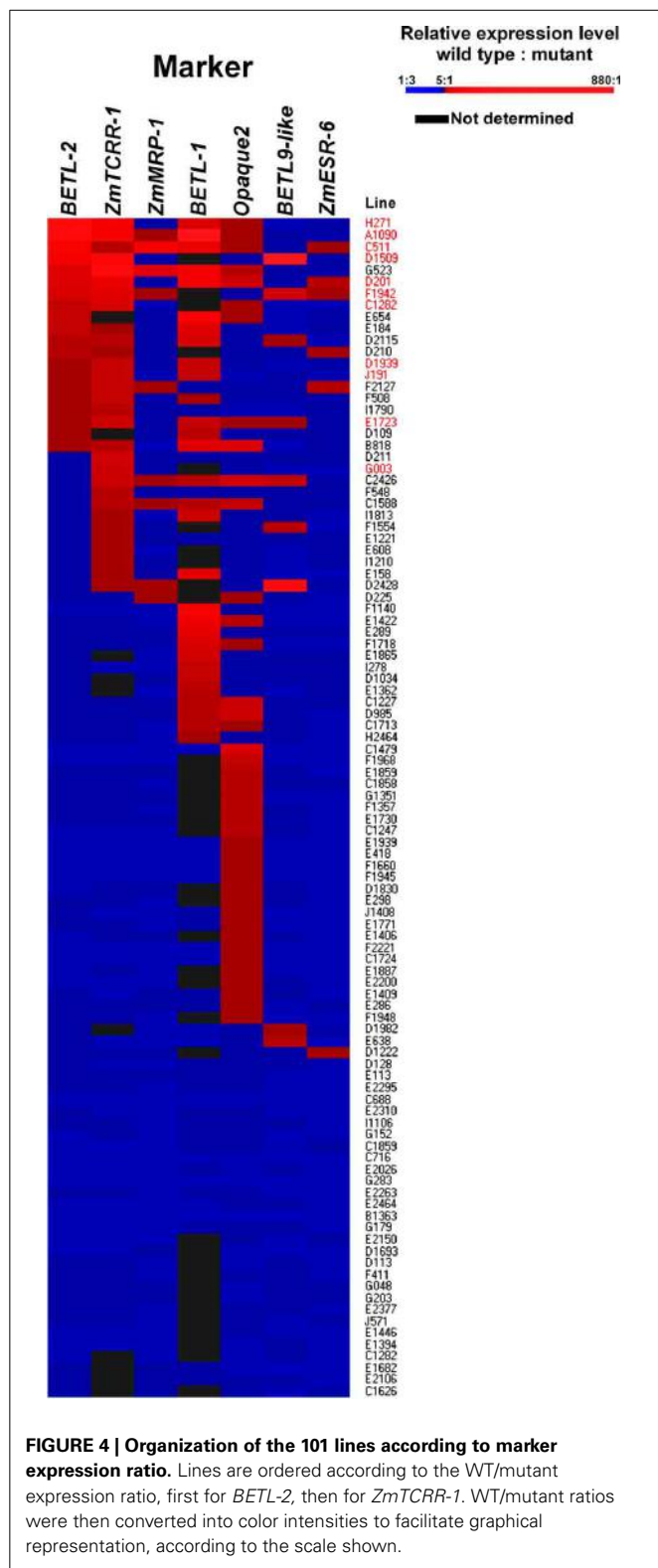


of 15 DAP WT and mutant seeds for histological observation. Additionally, we performed immunolocalization of several TC specific proteins to check correspondence between transcript and protein levels and examine protein localization in this compartment. We used polyclonal sera generated against recombinant BETL-1 or BETL-2 peptides. These proteins are secreted from the transfer cells to the placenta-chalaza, forming a continuous layer in the seed-mother plant interface (Hueros et al., 1995; Serna et al., 2001), so potentially they offer an indication of the tissue's ability to perform some of its functions. As expected, both antibodies labeled the transfer cell area and the pedicel directly opposite to the TC in sections of 15 DAP WT seeds (Figure 7, top left panel). Only BETL-1 on A1090 is shown). We provide now a summary of the results for each mutant line focusing on three aspects: macroscopic alterations and size, transfer cell domain markers (both gene expression and protein accumulation) and histological features:

**A1090:** The 15 DAP endosperm is highly reduced in size relative to the WT, which at this stage replaces the nucella almost completely (Figure 5, panel 1). The surface of the endosperm, where the aleurone is located, is formed by differentially stained cells which are much altered in appearance; these cortical cells are flattened and interspersed with starchy endosperm cells. Accumulation of starch in the central endosperm is not significantly affected, together with the general appearance of the storage cells, although their size is somewhat smaller (Figure 6, panel 1). The cells at the base of the endosperm, where the transfer layer should be, are also flat and miss their characteristic cell wall ingrowths (Figure 7, panel 1). In summary, in this line all the superficial cells seem to have adopted a similar fate, different from storage cells but without distinctive features of aleurone and transfer cells, although resembling an immature aleurone layer. The qRT-PCR analysis of this line shows severe

decreases in markers for the TCs and mild reductions in those for aleurone and starchy endosperm. The immunodetection of TC marker peptides in 15 DAP kernels reveals, in agreement with the qRT-PCR results, a very low signal from BETL-1 and -2 from the basal endosperm in mutant seeds, while they are readily detectable in WT siblings (Figure 7, panel 1: only BETL-1 detection is shown). In this line TC molecular markers faithfully reflected the histological alterations, while the degree of modification of other altered markers (*Opaque-2*, *ZmESR-6*, *ZmMRP-1*, or *BETL9-like*) did not correlate so well with the anatomy.

**C0511:** In this line kernel size is much reduced and nucellar tissue still occupies most of the caryopsis (Figure 5, panel 2). Starch deposition is much delayed in the peripheral endosperm when compared to WT, although this difference is not so significant in central endosperm at this stage. Tissue organization within the endosperm is lax, the storage cells being the only clearly recognizable structure. There are, however, patches of aleurone-like cells, with a cubical or prismatic morphology, which surround the starchy endosperm (Figure 6, panel 2). The transfer cells are absent or not properly developed for morphological recognition (Figure 7, panel 2). The transcript levels for transfer cell and ESR genes in this line are reduced between 1 and 2 orders of magnitude in mutant kernels, and aleurone and endosperm markers are also reduced, indicating a general underdevelopment of the seed. The strong sub-expression of *ZmMRP-1* might explain the down-regulation of the TC markers under its transcriptional control, and strongly corresponds with the severe alterations in the transfer cell identity. The immunological detection of BETL-2 shows an irregularly distributed signal at the basal cells and none at the pedicel of the mutant, while the immunostaining is strong in WT material (Figure 7, panel 2). In this line the molecular characterization reflects the anatomical events quite faithfully, as the



basal endosperm markers' severe alteration and the endosperm *Opaque-2* reduction are validated by the absence or erroneous development of transfer cells and an apparent delay or arrest in storage tissue function.

**D1509:** The morphological study of mutant seeds shows that their size is less reduced than in other mutants in this work, with the endosperm occupying about half of the nucellar space (**Figure 5**, panel 3). Apical and basal poles are clearly defined, although the internal endosperm organization is quite lax. Subaleuronal starch accumulation, visible in WT kernels is absent in the mutant, although the internal endosperm seems well-differentiated. It can be clearly distinguished from peripheral tissues, which in the case of the aleurone shows a flattened, collapsed appearance and stains more intensely than the inner cells (**Figure 6**, panel 3). Likewise, the transfer cells are not organized in a "palisade" layer, but rather as a flat, discontinuous row of dense cytoplasm-containing cells, compressed by the internal endosperm, which occasionally invades the layer. The intermediate, elongated transmitting cells seem to be absent in the mutant (**Figure 7**, panel 3). qRT-PCR analysis of this line shows acute differences between WT and mutant kernels regarding *ZmTCRR-1*, *BETL-2*, and *BETL-9like*, which suggest abnormalities in the outermost endosperm layers (*BETL-1* was not analyzed in this material as apparently the line lacks this gene). The TC master regulator, *ZmMRP-1*, is however, less affected than its targets, suggesting an independent cause for their down-regulation. *Opaque-2* and *ZmESR-6* are reduced to a minor extent (about 4 and 5 times, respectively). The immunolocalization of BETL markers (*BETL-2*, as the line doesn't show any detectable *BETL-1* expression) shows a strong signal in the transfer layer and the underlying pedicel of WT individuals, while it is much reduced in the mutant, matching the RNA expression data (**Figure 7**, panel 3). The molecular definition of the mutant is consistent with its tissular appearance, anticipating the superficial disorders that can be found under optical microscopy.

**H0271:** Morphologically, the mutant endosperms are small in size (about 1/3 of the WT at this stage) and elongated in shape, reminding of a younger developmental point (**Figure 5**, panel 4). The embryo encapsulation within the endosperm is still clearly observed (inset in panel 4) and the tissue seems disorganized and mixed with both the starchy endosperm and extended aleurone around the embryo. The starchy endosperm is quite similar in both genotypes, in the central area as well as in the periphery, with very little starch present. Storage cells are however smaller in the mutant. The aleurone layer is flattened and the cells show a dense cytoplasm, except those on the outer germlinal surface which show a more rounded, and regular shape (**Figure 6**, panel 4). The transfer cell layer is apparently missing or totally altered in its morphology, as the cells in this area are irregular in shape and devoid of cell wall ingrowths (**Figure 7**, panel 4). The expression analysis of this line indicates a severe reduction in TC transcripts (from 24 times for *BETL-1* to almost 150 for *BETL-2*) in the mutant kernels, while other regional markers are only slightly affected (this is the case of *ZmESR-6*, which is reduced by approximately 50% in the mutant) or even elevated. The immunological study shows no detection of *BETL-1* peptide (not shown). However, in contrast to the extremely low RNA levels, accumulation of *BETL-2* can be detected at the basal endosperm and pedicel (**Figure 7**, panel 4). The apparent disagreement in *BETL-2* transcript and

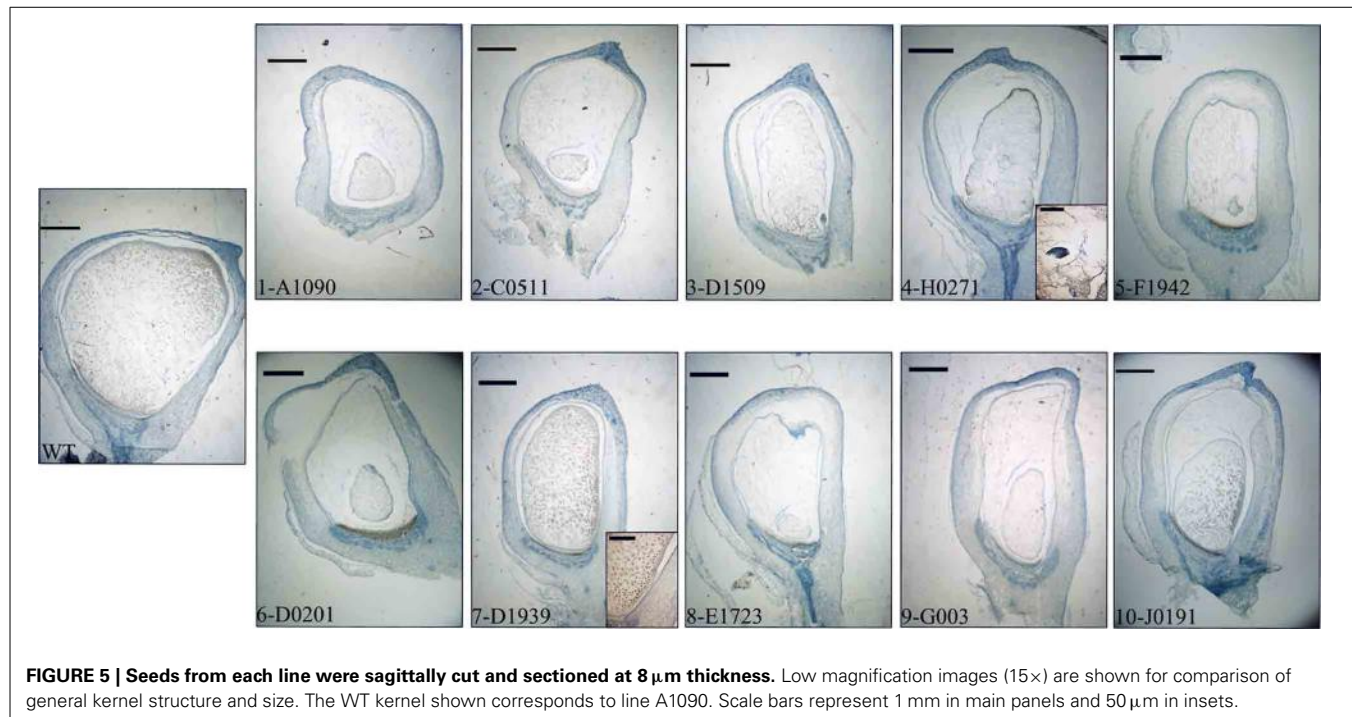


**FIGURE 5 | Seeds from each line were sagittally cut and sectioned at 8  $\mu\text{m}$  thickness.** Low magnification images (15 $\times$ ) are shown for comparison of general kernel structure and size. The WT kernel shown corresponds to line A1090. Scale bars represent 1 mm in main panels and 50  $\mu\text{m}$  in insets.

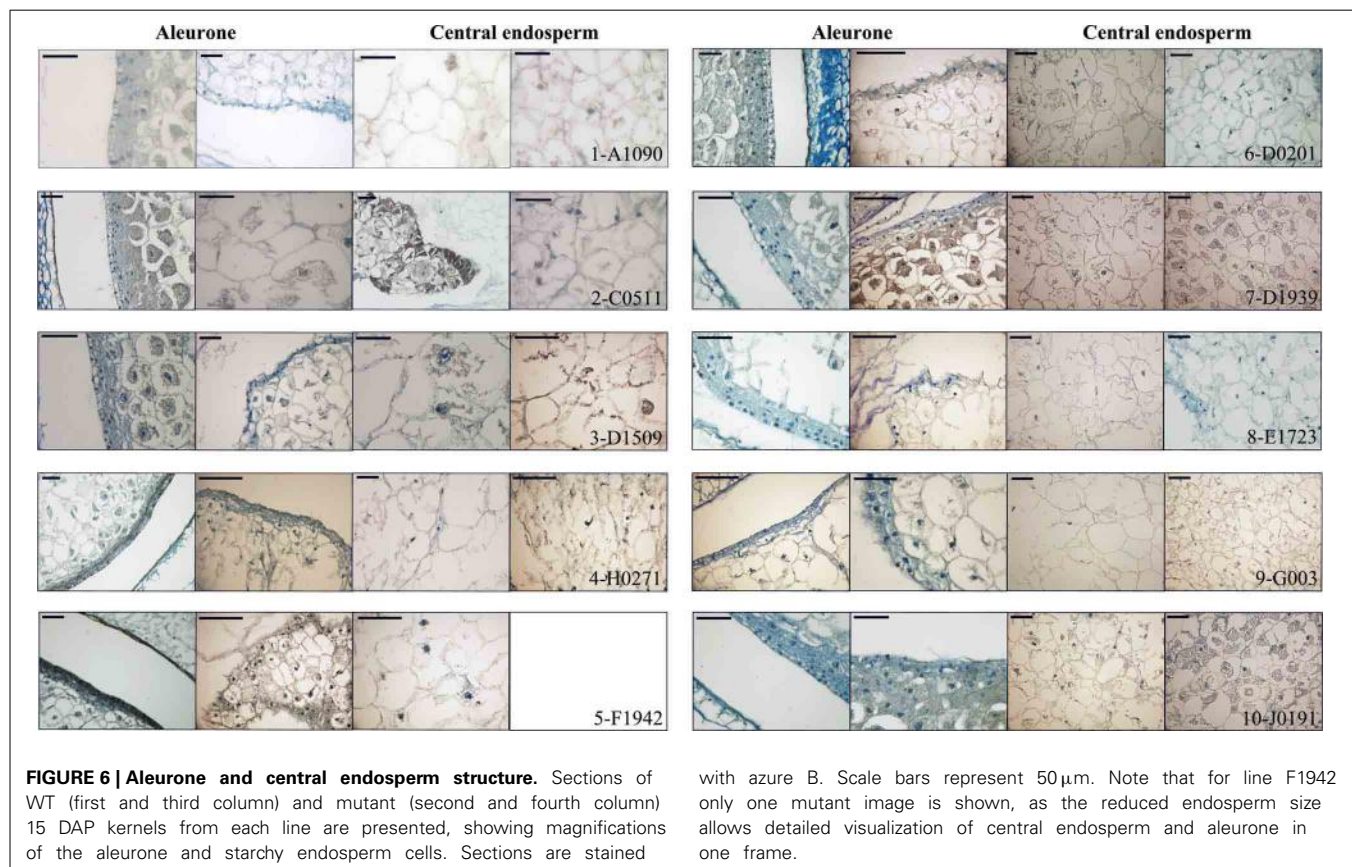


**FIGURE 6 | Aleurone and central endosperm structure.** Sections of WT (first and third column) and mutant (second and fourth column) 15 DAP kernels from each line are presented, showing magnifications of the aleurone and starchy endosperm cells. Sections are stained with azure B. Scale bars represent 50  $\mu\text{m}$ .

Note that for line F1942 only one mutant image is shown, as the reduced endosperm size allows detailed visualization of central endosperm and aleurone in one frame.

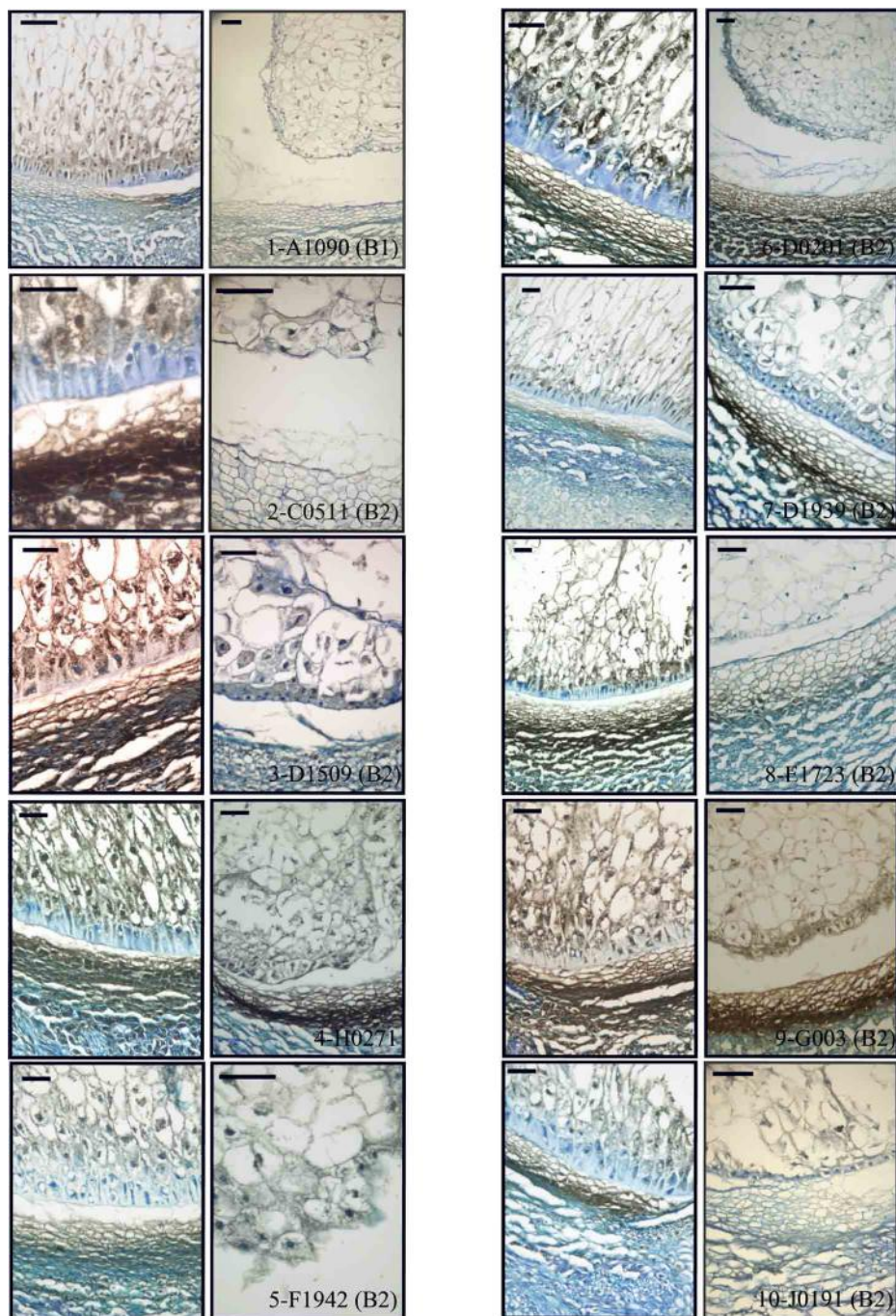


**FIGURE 7 | Basal endosperm structure and immunodetection of BETL peptides.** Sections of WT (first and third column) and mutant (second and fourth column) were reacted with antiBETL1 or antiBETL2 and counterstained with azure B. Scale bars represent 50  $\mu$ m.

protein accumulation levels notwithstanding, the transfer cell developmental alteration visible under the microscope was in fact detected by the molecular tests.

**F1942:** The mutant endosperm is reduced to a minute fraction of the normal size (in fact the smallest one of the mutant lines), being formed by only a few tens of poorly differentiated cells that seem randomly organized (**Figure 5**, panel 5). The mutant

central “starchy endosperm” cells are bigger and more regular in size than the peripheral ones (**Figure 6**, panel 5). The endosperm surface is not cytologically regular, and internal cells occasionally occupy it. There are no obvious aleurone or transfer cell layer and no starch deposition can be found. All tissue markers (except *BETL-1*, which is not detectable in WT kernels either) are down to a certain extent in the mutant kernels of

this line, from 4.5-fold for *Opaque-2* to over 30-fold for *BETL-2*, indicating a general alteration in development. Anti-*BETL-2* labels the whole periphery of the endosperm, concentrating on cells of small size and flat or elongated structure (**Figure 7**, panel 5), although the signal is weak and almost indistinguishable from general background. The line's extensive abnormalities reflect well on the molecular results, although the expression analysis does not directly indicate the severity of the alterations, when compared to other lines.

**D0201:** The size of the mutant endosperm at 15 DAP is about one-third of the WT sibling, with a pear-shaped morphology (**Figure 5**, panel 6). The aleurone is deformed with occasional invasion from the internal cells, and there is no apparent starch accumulation in the subaleurone or in the small cells that constitute the central endosperm (**Figure 6**, panel 6). The transfer layer showed a strikingly bi-phenotypic morphology in this mutant. The cell layer is composed by thick-walled WT-looking transfer cells at the germinal half, and storage type-looking cells at the abgerminal end. Cells in this area are irregular in shape, not corresponding in morphology to neither aleurone nor transfer cells (**Figure 7**, panel 6). The expression analysis of the mutant kernels shows reduced expression of all marker genes, except for *ZmMRP-1* and *BETL-9like*, the aleurone transcript. The detection of *BETL-2* in this line showed signal in the pedicel cup, as expected, but only in the germinal half of the transfer layer and less intense than in the WT (**Figure 7**, panel 6). A lower magnification is shown to include the pedicel in the mutant). In summary, the altered morphology of the mutant seed is reflected on the expression analysis.

**D1939:** This line displays a remarkable difference with the other lines analyzed. The endosperm size is fairly normal in this line, about 2/3 of the WT, with a clear morphological differentiation between starchy endosperm and superficial cells (**Figure 5**, panel 7). However, the starch deposition pattern appears altered; the central endosperm accumulates more starch than the WT, and this extends to the subaleurone, especially along the germinal and abgerminal sides of the endosperm instead of the characteristical upper dominance typical of WT kernels at this stage (**Figure 6**, panel 7; inset in **Figure 5**, panel 7). The surface of the endosperm is formed by a layer of nearly flattened cells which become slightly more prismatic in the transfer area, acquiring also engrossed cell walls. These cells lack, however, the characteristic wall ingrowths expected in transfer elements, and they resemble an engrossed aleurone or an intermediate state between aleurone and transfer cell fate. The conductive tissue immediately over the transfer area lacks its typical centripetally elongated shape and invaginations, and is morphologically indistinguishable from the upper endosperm area (**Figure 7**, panel 7). Expression abnormalities in the mutant focus on the transfer cell markers, and in a relatively moderate manner (from 14-fold in *BETL-1* to 1.6-fold for *ZmMRP-1*) while other areas show less effect (just 3.3 times for *Opaque-2*), and the marker for aleurone cell fate, *BETL-9like*, is in fact unregulated over 3 times. The expression analysis would in summary indicate a state of mild alteration or developmental delay for the mutants, affecting specially the base of the endosperm in this line (as compared to others in the collection).

The immunolocalization of *BETL-1* and -2 shows agreeing results, with no detectable signal from *BETL-1* and a faint one, mostly in the pedicel from *BETL-2* (*BETL-2* is shown in **Figure 7**, panel 7). As suggested by the molecular study, most the alterations focus at the transfer cells, while the aleurone and starchy endosperm look relatively unaffected.

**E1723:** The anatomical appearance of the mutant seeds is deeply affected in this line. The endosperm is reduced to a small mass of cells which doesn't cover the whole pedicel surface and shows no defined polarity (**Figure 5**, panel 8). There is no apparent tissue organization, as the whole mass is formed by storage cells diminishing in diameter close to the surface of the endosperm, where many cells are collapsed (**Figure 6**, panel 8). The mutant seeds displayed significant downregulation of the markers under study, with the exception of *ZmMRP-1* and *ZmESR-6*, although the WT/mutant ratios are lower than for other lines in this work. The values range from 18 (*ZmTCRR-1*) to 3.6 times (*ZmESR-6*). The immunological markers tested in this mutant are either undetectable (*BETL-1*) or faint and limited to the areas where the protein accumulates at higher levels in WT seeds (*BETL-2* at the pedicel, **Figure 7**, panel 8). The developmental alterations in this line were correctly predicted by the molecular analysis, although their severity is much greater than what can be found in other lines with greater WT/mutant expression ratios.

**G003:** As in other mutants in this study, the endosperm is reduced in size (about 1/3 of the WT), although its general axial organization is normal (**Figure 5**, panel 9). Tissular domains are clearly differentiated and occupy their regular positions, with the periphery being clearly distinguishable from the central endosperm. The cells in this tissue are smaller in the mutant, and show lower or no starch deposition. The aleurone is formed by a layer of 1–3 thick cells that become wider over the upper endosperm portion. The walls of these cells are more intensely stained than those in the WT, possibly indicating a greater thickness (**Figure 6**, panel 9). The transfer cells, conversely, seem to have a thinner, less stained than WT appearance, and their shape varies from stretched to almost round (see **Figure 7**, panel 9). The area on top of them, the transmitting tissue, is indistinguishable from the starchy endosperm, while the WT displays the characteristical axial elongation in this area. The analysis of domain markers in this line shows that the mutant individuals do not differ much from the WT as far as the ESR (*ZmESR-6* ratio approx. 0.7), the aleurone (*BETL-9like* ratio approx. 1) and the starchy endosperm (*Opaque-2* ratio approx. 2.9) are concerned. The transfer cell markers are affected by the mutation to a different extent, as *BETL-2* is slightly down-regulated (about 3 times) and *ZmTCRR-1* is down by over one order of magnitude (17.5). *BETL-1* expression is hardly detectable in this line. *ZmMRP-1*, the transcription factor that regulates the expression of *BETL-1*, -2 and *ZmTCRR-1* is also slightly down-regulated. The immunolocalization experiments showed that *BETL-2* accumulation concentrates mainly at the pedicel, with a patchy location at the endosperm base (**Figure 7**, panel 9). This mutant line presents a comparatively mild phenotype, as could be expected from the molecular analysis, in which only *ZmTCRR-1* indicated alterations in the transfer cell area.

**J0191:** The endosperm size is reduced approximately by half in the mutant, and the starch deposition pattern within the endosperm differs significantly from the WT, as abundant starch granules accumulate at the germinal side and extend into the central endosperm (**Figure 5**, panel 10). In fact starch storage seems more advanced in the mutant, as the cells are more densely filled with granules. The cells in peripheral positions display a thick cell wall all around the endosperm, although they differ in shape; the basal cells are rectangular, almost cubical in front of the phloem terminals, and display a dense cytoplasm. The cells in the aleurone layer are flattened along the whole layer. The adgerminal subaleurone displays a dense cytoplasm, filled with starch (**Figure 6**, panel 10). The main effect at the transcriptional level of this line's mutation shows on the transfer cell markers, which are down regulated between 7 and 15 times (**Figure 4**), pointing at an altered development of the transfer cell area. Other transcriptional domains are relatively unaffected, as values for *ZmESR-6* and *Opaque-2* are even higher in mutant seeds than in WT, while the aleurone marker is down-regulated only twice. *BETL-2* is detected at both the basal endosperm layer and the pedicel, although significantly reduced in quantity. The signal at the endosperm is limited to the tissue immediately above the altered TCs, while the WT kernel shows abundant signals at the pedicel and the basal endosperm (**Figure 7**, panel 10). The overall mutant appearance in this line is fairly regular, with the exception of an apparent increase in starch accumulation. This observation, together with the increased *Opaque-2* expression suggest an advanced development for the storage tissue, while the transfer cells appear underdeveloped and not fully differentiated from the aleurone.

## DISCUSSION

Large mutant collections in a variety of model organisms are a powerful tool to understand the impact of the genetic component in the functional biology of the individual. However, as phenotype scoring is the access gate to the study of the underlying genetic mechanism (Hotz et al., 2006), a comprehensive and thorough screening process becomes the key to their use. Analyzing or even finding phenotypes related to the process or tissue of interest is especially difficult when these are not easily accessible to assay (Kielczewska and Vidal, 2006). A wide variety of approaches has been used, from classical bare-eye observation (Kuromori et al., 2006) to complex functional *in vivo* and *in vitro* assays (Burrack and Higgins, 2007). The development of molecular tools at high throughput scale has allowed to include metabolome (Benning, 2004), proteome and transcriptome analysis as a part of a mutant's phenotypic description (Domoney et al., 2006). The availability and variety of markers greatly facilitates the isolation and study of new mutant lines, although their development and design may be cumbersome (Guitton et al., 2004). It is not unrealistic to expect that markers based on genes with developmentally regulated expression in a given tissue or cell type are somehow involved in determining its identity (Li and Wurtzel, 1998; Kubo et al., 2005); thus, the growing information about gene expression timing and localization collected in the bibliography and public databases allows to design directed transcriptomic screens to

study particular processes or tissues, even when these are not easily accessible. This work has a dual purpose: we have designed and tested a molecular kit for the screening of a maize seed mutant collection and the dissection of mutant phenotypes affecting seed development, based on a set of genes previously identified as specific of particular kernel compartments. Secondly, we report the characterization at the molecular and histological levels of a series of maize mutants displaying seed phenotypes.

The transcripts used to "label" the transfer cell area, embryo surrounding region and aleurone have been isolated and described by our group, and detailed data exist about their expression site, developmental regulation and in some instances functional hierarchy. *ZmESR-6* encodes a defensin-like peptide that has shown antimicrobial activity in *in vitro* test (Balandín et al., 2005). *BETL-1* and -2 have currently no known function, although *BETL-2* may also be involved in seed defense, as *in vitro* tests have shown bactericidal properties for the peptide (Serna et al., 2001). *ZmTCRR-1* shows sequence similarity to plant response regulators and is proposed to participate in signal transduction in the seed (Muñiz et al., 2006). The three TC transcripts have been shown to be transcriptionally regulated by *ZmMRP-1*, a R1 MYB-type transcription factor which is expressed in the developing kernel since early stages and whose activity suffices to confer transfer cell features to aleurone cells (Gómez et al., 2002, 2009). *ZmBETL-9like* encodes a peptide of unknown function which is expressed along the aleurone layer, complementing the surfacial expression pattern of its paralog *ZmBETL-9* (see Royo et al., under review). Together with *Opaque-2*, isolated over 16 years ago, they may constitute a valuable set of tools to describe the anatomical and developmental state of the maize kernel and predict the alterations to be found within the seed structure. We validated their use as indicators of presence/state of development of a specific tissue in qRT-PCR by comparing the relative values obtained in the analysis of upper (formed by aleurone and starchy endosperm) and lower (aleurone, starchy endosperm, transfer cells and ESR) halves of WT seeds. Previous studies through Northern blot and *in situ* hybridization have shown that these BETL and ESR transcripts are undetectable by these techniques in the upper endosperm, while aleurone and starchy endosperm markers distribute approximately evenly (Hueros et al., 1999; Gómez et al., 2002; Balandín et al., 2005; Muñiz et al., 2006; Dolfini et al., 2007). The differences in the values obtained are in all cases in agreement with previous data, showing over 1 order of magnitude difference in their accumulation in bottom over the top half for the basal specific genes, while those expressed in the aleurone and starchy endosperm are roughly comparable in both samples. The value of the bottom/top ratio is highly dependent on the abundance of the different transcripts, as the quantification threshold of bottom-specific genes for the top samples is always close to the detection limit of the technique. This highlights an otherwise expected technical consideration: genes with low expression levels display a lower sensitivity for mutant discrimination in this strategy, as the screening is based on the comparison of expression strength in WT and prospective mutants.

Once the design of the qRT-PCR experiment was set, it allowed for the rapid transcriptomic screening of over 100 lines for markers representing 4 compartments within the endosperm. The fact

that no expression for *BETL-1* was detectable in up to 1/3 of the lines can be explained by the genetic structure of the mutant collection, which comes from a number of crossings of different Mu-bearing maize parents. A variation in the number of *BETL-1* loci among maize lines, probably due to active transposable elements at their location, was already described in Hueros et al. (1999).

The application of the directed transcriptomic screening to WT individuals from the mutant collection showed very minor variations in the expression of the different markers, supporting their use as reliable indicators of WT structure. In 29 lines (28.7% of the analyzed genotypes) none of the markers presented alterations. Pending a morphological study of these lines, (which is beyond the scope of the present paper) this would point to an origin of the macroscopic phenotype (*min* or *udve*) not associated to significant identity alterations in the endosperm domains studied. Alternatively, a different set of marker genes might be able to detect alterations in these tissues that have gone undetected in our panel. If this is the case, fine-tuning the identity of the markers or increasing their number and their relevance for the tissue or developmental event under study may yield a higher correlation between the molecular and microscopical approaches. In our case, we screened the starchy endosperm using a marker essential for its storage function, and the transfer layer with four markers. The hierarchical relationship among *ZmMRP-1* and the other TC transcripts might however limit the range of exploration, and more diverse, independent markers might be desirable.

The analysis of WT vs. mutant seeds showed that the transcriptional alterations were under 1 order of magnitude for most of the lines, although significant outliers could be found. These severely altered lines are potentially of great interest to study the effect of certain cell type alteration or absence on the seed development. The highest variation (not including *BETL-1* due to the aforementioned reason) was found in *BETL-9like* expression, which was reduced only slightly in most of the lines but displayed strong reductions of up to 885 times in others (Figure 4).

The transcriptome analysis allowed clustering of the 101 maize lines in quantitative categories based on the degree of alteration of the different markers (Figure 4). We have found, as expected, significant correlations in the reductions of the different TC markers, indicating that the mutations found in the collection disrupt the tissue's developmental program in early stages. However, as most of these genes reach their peak expression around 11 DAP, it would be highly informative to have an earlier marker to pinpoint more precisely the developmental effect of the mutation. This adds in fact a new analytical power to the quantitative molecular dissection in cases where a number of genes affecting a given process or tissue are known. The expression analysis of a set of selected genes might show in which point of development the case under study is affected, by determining the earliest gene with altered expression. Our analysis also shows that for these particular mutant phenotypes (miniature and undeveloped with embryo), *Opaque-2* is the most commonly affected marker, which is coherent as the most conspicuous feature in both cases is a reduced seed size, and this is mainly the result of starchy endosperm growth. The analysis

of the mutant collection points to a developmental organization along the top/bottom axis and surface/center gradient (Gruis et al., 2006), as most of the lines significantly affected in the ESR also display a TC molecular phenotype (5 out of 6), and transfer cell defects are present in 7 of the 9 aleurone-affected mutants. The marker for central endosperm fate, on the other hand, behaves quite independently from other seed areas, as only 16 of the 41 *Opaque-2*-altered lines show TC, ESR, or aleurone defects.

The transcriptional analysis has allowed us to select lines displaying transcriptional defects in the transfer cell markers to a varying extent (H0271, D1939, J191, G003), surface tissues (D1509) or TC plus starchy endosperm (A1090, C0511, D0201, F1942, E1723), and rechecked the marker expression using qRT-PCR on independent seeds (not shown). Both analysis showed good correspondence, except for line C1282. This may be the result of differences in developmental state of the tested material or incorrect phenotyping.

The anatomical analysis of mutant seeds combined to immunolocalization allowed us to further check and refine the description of each of the mutants. However, caution must be exercised when interpreting the immunolocalization results quantitatively; the technical features of this analysis preclude proper comparison between samples, as WT and mutant seeds have been processed on different slides. The goals of our immunological study are offering an anatomical perspective of the mutants to complement the expression results, and ascertaining whether transfer cell-specific peptides can still be detected in morphologically altered seeds.

All the lines showing only transfer cell marker alterations (H0271, D1939, J191, and G003) display a reduced endosperm size with a generally conserved seed architecture. The transfer cells are misshaped, with a cubical appearance reminiscent of aleurone tissue. This suggests that although the central/peripheral organization is retained, the mutations in these lines affect determination of transfer cell identity, causing an arrest/redirection of the developmental program to another surface cell type. A similar effect was found in the *emp4-1* mutant, in which *VPI* expression can be found in the basal area (Gutierrez-Marcos et al., 2007). The effect of these basal alterations on the overall endosperm size might reflect a deficient uptake of nutrients and a concomitant delay in development (Dolfini et al., 2007).

Mutant kernels of the line D1509 present altered "surface" markers (both transfer cell and aleurone) in ranges from 50 to almost 900 times WT/mutant values. An exception is made of the ESR cells, for which the WT accumulation is just a bit over 4 times the mutant value. The directed transcriptome analysis offers a relatively accurate portrait of the seed's appearance, as in this line both the immunological markers and anatomical analysis indicate a relatively normal internal structure and seed size (albeit slightly reduced) with surface alterations, which include invasion of the periphery by starchy endosperm tissue. This phenotype is similar to *crinkly4* (Becraft et al., 1996) or *cp2-o12* (Becraft and Asuncion-Crabb, 2000), and suggests the mutated gene is involved in surface differentiation. An increasing number of genes have been shown to affect aleurone and general surface specification in maize, uncovering identity mechanisms based on

the proper membrane localization and recycling of kinase-type receptors and signal processors (Becraft and Asuncion-Crabb, 2000; Kessler et al., 2002), whose effect is aleurone-specific at the cellular level but affects the whole seed development. The size reduction, common to the previously commented category, indicates the relevance of the surface tissues to properly complete endosperm filling (Dolfini et al., 2007). A point of further interest in these lines is the mutation's effect on other plant epidermal tissues, as common developmental routes have been discovered along the years (Lid et al., 2004). As germination is often compromised in *udve* mutants, embryo rescue approaches may be necessary to determine whether the mutation affects later stages of the plant life cycle (Gutiérrez-Marcos et al., 2007).

Five lines in our analysis showed a severe developmental phenotype, with reduced size, complete disorganization of the storage tissue and starch location, and loss of histological identity. This phenomenon of tissue malformation has been previously associated to a misregulation of cell division (Consonni et al., 2005). Such an extent of alteration suggests that genes acting early in the seed development might be affected, as cell identity proceeds in a clonal manner from the coenocyte phase (Becraft, 2001; Olsen, 2001). *Baseless1*, a maternal effect gene acting in the embryo sac causes alterations in the transfer cell layer position and structure, as well as a general disorganization of the endosperm and delay in embryo development since very early stages, which are visually detectable around 10 DAP (Gutiérrez-Marcos et al., 2006). The molecular analysis we used is especially suitable for the detection of this kind of early-effect mutations, provided a set of suitable markers is available. A feature shared by all the lines is a greater tissue differentiation in the germinal area, where both aleurone and transfer cells display more resemblance to their WT counterparts. This is in agreement with a gradual differentiation and maturation of the seed tissues along several axes, as previously proposed by other authors (Becraft and Asuncion-Crabb, 2000).

As a whole, a wide array of processes are candidates to be mutated in this material as the kernel development is affected by external signals, nutrient availability, positional cues and genetic factors, all acting coordinately along time (Berger, 2003; Consonni et al., 2005; Brugiére et al., 2008). Additionally, gene dosage and imprinting affect tissue specification as well (Gehring et al., 2004; Gutiérrez-Marcos et al., 2006).

We believe the PCR-based strategy proposed here is a valuable tool for the early detection and initial characterization of mutants affecting seed development. The availability of genes specifically expressed in different kernel domains and developmental stages allows to describe, from a transcriptomic point of view, the anatomical effect of a mutation even when direct observation of the affected tissues is not feasible (Verza et al., 2005; Laudencia-Chingcuanco et al., 2006). The use of a sensitive technique such as qRT-PCR permits the application of a panel of expression-based markers to determine whether a given cell type/tissular domain is functioning or developing properly, simultaneously quantifying the extent of the alteration, if any. This use of genes discovered by transcriptomic approaches to be tissue or development-specific further extends the array of tools that can be applied in forward genetics programs.

## ACKNOWLEDGMENTS

This work was supported by grants from the Spanish Ministerio de Ciencia e Innovacion to Gregorio Hueros (Gen2006-27783-E and BIO2012-39822) and internal funds from Biogemma SAS.

## SUPPLEMENTARY MATERIAL

The Supplementary Material for this article can be found online at: <http://www.frontiersin.org/journal/10.3389/fpls.2014.00158/abstract>

## REFERENCES

- Adams, D. J., Biggs, P. J., Cox, T., Davies, R., van der Weyden, L., Jonkers, J., et al. (2004). Mutagenic insertion and chromosome engineering resource (MICER). *Nat Genet.* 36, 867–871. doi: 10.1038/ng1388
- Alonso, J. M., Stepanova, A. N., Leisse, T. J., Kim, C. J., Chen, H., Shinn, P., et al. (2003). Genome-wide insertional mutagenesis of *Arabidopsis thaliana*. *Science* 301, 653–657. doi: 10.1126/science.1086391
- An, G., Jeong, D., Jung, K., and Lee, S. (2005). Reverse genetic approaches for functional genomics of rice. *Plant Mol. Biol.* 59, 111–123. doi: 10.1007/s11103-004-4037-y
- Balandín, M., Royo, J., Gómez, E., Muñiz, L. M., Molina, A., and Hueros, G. (2005). A protective role for the embryo surrounding region of the maize endosperm, as evidenced by the characterisation of *ZmESR-6*, a defensin gene specifically expressed in this region. *Plant Mol. Biol.* 58, 269–282. doi: 10.1007/s11103-005-3479-1
- Barstead, R. J., and Moerman, D. G. F. (2006). “*C. elegans* deletion mutant screening,” in *C. elegans Methods and Applications*, ed K. Strange (Totowa, NJ: Humana Press), 51–58. doi: 10.1385/1597451517
- Becraft, P. W. (2001). Cell fate specification in the cereal endosperm. *Semin. Cell Dev. Biol.* 12, 387–394. doi: 10.1006/scdb.2001.0268
- Becraft, P. W., and Asuncion-Crabb, Y. (2000). Positional cues specify and maintain aleurone cell fate in maize endosperm development. *Development* 127, 4039–4048.
- Becraft, P. W., Stinard, P. S., and McCarthy, D. R. (1996). Crinkly4: a TNFR-like receptor kinase involved in maize epidermal differentiation. *Science* 273, 1406–1409. doi: 10.1126/science.273.5280.1406
- Bellen, H. J., Levis, R. W., Liao, G., He, Y., Carlson, J. W., Tsang, G., et al. (2004). The BDGP gene disruption project: single transposon insertions associated with 40% of *Drosophila* genes. *Genetics* 167, 761–781. doi: 10.1534/genetics.104.026427
- Benning, C. (2004). Genetic mutant screening by direct metabolite analysis. *Anal. Biochem.* 332, 1–9. doi: 10.1016/j.ab.2004.04.040
- Berger, F. (2003). Endosperm: the crossroad of seed development. *Curr. Opin. Plant Biol.* 6, 42–50. doi: 10.1016/S1369526602000043
- Boisnard-Lorig, C., Colon-Carmona, A., Bauch, M., Hodge, S., Doerner, P., Bancharel, E., et al. (2001). Dynamic analyses of the expression of the histone::yfp fusion protein in *Arabidopsis* show that syncytial endosperm is divided in mitotic domains. *Plant Cell* 13, 495–509. doi: 10.1105/tpc.13.3.495
- Bommert, P., and Werr, W. (2001). Gene expression patterns in the maize caryopsis: clues to decisions in embryo and endosperm development. *Gene* 271, 131–142. doi: 10.1016/S0378-1119(01)00503-0
- Bonello, J. F., Opsahl-Ferstad, H., Perez, P., Dumas, C., and Rogowsky, P. M. (2000). ESR genes show different levels of expression in the same region of maize endosperm. *Gene* 246, 219–227. doi: 10.1016/S0378-1119(00)00088-3
- Borisjuk, L., Walenta, S., Weber, H., Mueller-Klieser, W., and Wobus, U. (1998). High-resolution histographical mapping of glucose concentrations in developing cotyledons of *Vicia faba* in relation to mitotic activity and storage processes: glucose as a possible developmental trigger. *Plant J.* 15, 583–591. doi: 10.1046/j.1365-313X.1998.00214.x
- Brugiére, N., Humbert, S., Rizzo, N., Bohn, J., and Habben, J. E. (2008). A member of the maize isopentenyl transferase gene family, *Zea mays* isopentenyl transferase 2 (*ZmIPT2*), encodes a cytokinin biosynthetic enzyme expressed during kernel development. *Plant Mol. Biol.* 67, 215–229. doi: 10.1007/s11103-008-9312-x
- Burrack, L. S., and Higgins, D. E. (2007). Genomic approaches to understanding bacterial virulence. *Curr. Opin. Microbiol.* 10, 4–9. doi: 10.1016/j.mib.2006.11.004

- Consonni, G., Gavazi, G., and Dolfini, S. (2005). Genetic analysis as a tool to investigate the molecular mechanisms underlying seed development in maize. *Ann. Bot.* 96, 353–362. doi: 10.1093/aob/mci187
- Dolfini, S., Consonni, G., Viotti, C., Dal Pra, M., Saltini, G., Giulini, A., et al. (2007). A mutational approach to the study of seed development in maize. *J. Exp. Bot.* 58, 1197–1205. doi: 10.1093/jxb/erl290
- Dolfini, S., Landoni, M., Tonelli, C., Bernard, L., and Viotti, A. (1992). Spatial regulation in the expression of structural and regulatory storage-protein genes in Zea mays endosperm. *Dev. Genet.* 13, 264–276. doi: 10.1002/dvg.1020130404
- Domoney, C., Duc, G., Noel Ellis, T. H., Ferrández, C., Firnhaber, C., Gallardo, K., et al. (2006). Genetic and genomic analysis of legume flowers and seeds. *Curr. Opin. Plant Biol.* 9, 133–141. doi: 10.1016/j.pbi.2006.01.014
- Gehring, M., Choi, Y., and Fischer, R. L. (2004). Imprinting and seed development. *Plant Cell* 16, S203–S213. doi: 10.1105/tpc.017988
- Gómez, E., Royo, J., Guo, Y., Thompson, R., and Hueros, G. (2002). Establishment of cereal endosperm expression domains: identification and properties of a maize transfer cell-specific transcription factor, ZmMRP-1. *Plant Cell* 14, 599–610. doi: 10.1105/tpc.010365
- Gómez, E., Royo, J., Muñiz, L. M., Sellam, O., Paul, W., Gerentes, D., et al. (2009). The maize transcription factor myb-related protein-1 is a key regulator of the differentiation of transfer cells. *Plant Cell* 21, 2022–2035. doi: 10.1105/tpc.108.065409
- Gruis, D., Guo, H., Selinger, D., Tian, Q., and Olsen, O. A. (2006). Surface position, not signalling from surrounding maternal tissues, specifies aleurone epidermal cell fate in maize. *Plant Physiol.* 141, 898–909. doi: 10.1104/pp.106.080945
- Guitton, A. E., Page, D. R., Chambrier, P., Lionnet, C., Faure, J. E., Grossniklaus, U., et al. (2004). Identification of new members of fertilisation independent seed polycomb group pathway involved in the control of seed development in *Arabidopsis thaliana*. *Development* 131, 2971–2981. doi: 10.1242/dev.01168
- Gutiérrez-Marcos, J. F., Costa, L. M., and Evans, M. M. (2006). Maternal gametophytic *baseless1* is required for development of the central cell and early endosperm patterning in maize (*Zea mays*). *Genetics* 174, 317–329. doi: 10.1534/genetics.106.059709
- Gutierrez-Marcos, J. F., Para, M. D., Giulini, A., Costa, L. M., Gavazzi, G., Cordelier, S., et al. (2007). *empty pericarp4* encodes a mitochondrion-targeted pentatricopeptide repeat protein necessary for seed development and plant growth in maize. *Plant Cell* 19, 196–210. doi: 10.1105/tpc.105.039594
- Hotz, M., Pinto, L. H., and Takahashi, J. S. (2006). Large-scale mutagenesis and phenotypic screens for the nervous system and behaviour in mice. *Trends Neurosci.* 29, 233–240. doi: 10.1016/j.tins.2006.02.006
- Hueros, G., Gomez, E., Cheikh, N., Edwards, J., Weldon, M., Salamini, F., et al. (1999). Identification of a promoter sequence from the bet1 gene cluster able to confer transfer-cell-specific expression in transgenic maize. *Plant Physiol.* 121, 1143–1152. doi: 10.1104/pp.121.4.1143
- Hueros, G., Varotto, S., Salamini, F., and Thompson, R. D. (1995). Molecular characterization of *Bet1*, a gene expressed in the endosperm transfer cells of maize. *Plant Cell* 7, 747–757.
- Kessler, S., Seiki, S., and Sinha, N. (2002). *Xcl1* causes delayed oblique periclinal cell divisions in developing maize leaves, leading to cellular differentiation by lineage instead of position. *Development* 129, 1859–1869. doi: 10.1242/f1006325.78956
- Kielczewska, A., and Vidal, S. M. (2006). Enemy at the gates: forward genetics of the mouse antiviral response. *Curr. Opin. Immunol.* 18, 617–626. doi: 10.1016/j.coim.2006.07.009
- Kiesselsbach, T. A. (1949). *The Structure and Reproduction of Corn*. Cold Spring Harbor, NY: Cold Spring Harbor Laboratory Press.
- Kubo, M., Udagawa, M., Nishikubo, N., Horiguchi, G., Yamaguchi, M., Ito, J., et al. (2005). Transcription switches for protoxylem and metaxylem vessel formation. *Genes Dev.* 19, 1855–1860. doi: 10.1101/gad.1331305
- Kuromori, T., Wada, T., Kamiya, A., Yuguchi, M., Yokouchi, T., Imura, Y., et al. (2006). A trial of genome analysis using 4000 Ds-insertional mutants in gene-coding regions of *Arabidopsis*. *Plant J.* 47, 640–651. doi: 10.1111/j.1365-313X.2006.02808.x
- Laudencia-Chingcuanco, D. L., Stamova, B. S., Lazo, G. R., Cui, X., and Anderson, O. D. (2006). Analysis of the wheat endosperm transcriptome. *J. Appl. Genet.* 47, 287–302. doi: 10.1007/BF03194638
- Li, Z., and Wurtzel, E. T. (1998). The *ltk* gene family encodes novel receptor-like kinases with temporal expression in developing maize endosperm. *Plant Mol. Biol.* 37, 749–761. doi: 10.1023/A:1006012530241
- Lid, S. E., Al, R. H., Krekling, T., Meeley, R. B., Ranch, J., Opsahl-Ferstad, H., et al. (2004). The maize disorganized aleurone layer 1 and 2 (*dil1*, *dil2*) mutants lack control of the mitotic division plane in the aleurone layer of developing endosperm. *Planta* 218, 370–378. doi: 10.1007/s00425-003-1116-2
- Martin, A., Lee, J., Kichey, T., Gerentes, D., Zivy, M., Tatout, C., et al. (2006). Two cytosolic glutamine synthetase isoforms of maize are specifically involved in the control of grain production. *Plant Cell* 18, 3252–3274. doi: 10.1105/tpc.106.042689
- Muñiz, L. M., Royo, J., Gómez, E., Barrero, C., Bergareche, D., and Hueros, G. (2006). The maize transfer cell-specific type-A response regulator *ZmTCR-1* appears to be involved in intercellular signalling. *Plant J.* 48, 17–27. doi: 10.1111/j.1365-313X.2006.02848.x
- Olsen, O. A. (2001). Endosperm development: cellularization and cell fate specification. *Ann. Rev. Plant Physiol. Plant Mol. Biol.* 52, 233–267. doi: 10.1146/annurev.arplant.52.1.233
- Olsen, O. A. (2004). Nuclear endosperm development in cereals and *Arabidopsis thaliana*. *Plant Cell* 16, S214–S227. doi: 10.1105/tpc.017111
- Opsahl-Ferstad, H., Le Deunff, E., Dumas, C., and Rogowsky, P. M. (1997). *ZmESR*, a novel endosperm-specific gene expressed in a restricted region around the maize embryo. *Plant J.* 12, 235–246. doi: 10.1046/j.1365-313X.1997.12010235.x
- Scanlon, M. J., and Takacs, E. M. (2008). “Kernel biology,” in *Handbook of Maize: Its Biology*, eds J. L. Bennetzen and S. Hake (New York, NY: Springer), 121–144.
- Serna, A., Maitz, M., O’Connell, T., Santandrea, G., Thevissen, K., Tienens, K., et al. (2001). Maize endosperm secretes a novel antifungal protein into adjacent maternal tissue. *Plant J.* 25, 687–698. doi: 10.1046/j.1365-313X.2001.01004.x
- Thompson, R. D., Hueros, G., Becker, H. A., and Maitz, M. (2001). Development and functions of seed transfer cells. *Plant Sci.* 160, 775–783. doi: 10.1016/S0168-9452(01)00345-4
- Timmermans, M. C. P., Brutnell, T. P., and Becraft, P. W. (2004). The 46th annual maize genetics conference. Unlocking the secrets of the maize genome. *Plant Physiol.* 136, 2633–2640. doi: 10.1104/pp.104.048702
- Verza, N. C., Rezende e Silva, T., Cord Neto, G., Nogueira, F. T. S., Fisch, P. H., de Rosa, V. E., et al. (2005). Endosperm-preferred expression of maize genes as revealed by transcriptome-wide analysis of expressed sequence tags. *Plant Mol. Biol.* 59, 363–374. doi: 10.1007/s11103-005-8924-7
- Walbot, V. (2000). Saturation mutagenesis using maize transposons. *Curr. Opin. Plant Biol.* 3, 103–107. doi: 10.1016/S1369-5266(99)00051-5
- Warren, K. S., and Fishman, M. C. (1998). “Physiological genomics”: mutant screens in zebrafish. *Am. J. Physiol.* 275 (Heart Circ. Physiol. 44), H1–H7.
- Wobus, U., and Weber, H. (1999). Seed maturation: genetic programmes and control signals. *Curr. Opin. Plant Biol.* 2, 33–38. doi: 10.1016/S1369-5266(99)80007-7
- Conflict of Interest Statement:** The authors declare that the research was conducted in the absence of any commercial or financial relationships that could be construed as a potential conflict of interest.
- Received:** 12 February 2014; **accepted:** 06 April 2014; **published online:** 28 April 2014.
- Citation:** Muñiz LM, Gómez E, Guyon V, López M, Khbayá B, Sellam O, Pérez P and Hueros G (2014) A PCR-based forward genetics screening, using expression domain-specific markers, identifies mutants in endosperm transfer cell development. *Front. Plant Sci.* 5:158. doi: 10.3389/fpls.2014.00158
- This article was submitted to Plant Physiology, a section of the journal *Frontiers in Plant Science*.
- Copyright © 2014 Muñiz, Gómez, Guyon, López, Khbayá, Sellam, Pérez and Hueros. This is an open-access article distributed under the terms of the Creative Commons Attribution License (CC BY). The use, distribution or reproduction in other forums is permitted, provided the original author(s) or licensor are credited and that the original publication in this journal is cited, in accordance with accepted academic practice. No use, distribution or reproduction is permitted which does not comply with these terms.



# Lignification of developing maize (*Zea mays* L.) endosperm transfer cells and starchy endosperm cells

Sara Rocha<sup>1</sup>, Paulo Monjardino<sup>1\*</sup>, Duarte Mendonça<sup>1</sup>, Artur da Câmara Machado<sup>1</sup>, Rui Fernandes<sup>2</sup>, Paula Sampaio<sup>2</sup> and Roberto Salema<sup>2,3</sup>

<sup>1</sup> Departamento de Ciências Agrárias, Instituto de Biotecnologia e Bioengenharia - Centro de Biotecnologia dos Açores, Universidade dos Açores, Angra do Heroísmo, Portugal

<sup>2</sup> Instituto de Biologia Molecular e Celular, Universidade do Porto, Porto, Portugal

<sup>3</sup> Departamento de Biologia, Faculdade de Ciências, Universidade do Porto, Porto, Portugal

**Edited by:**

David McCurdy, The University of Newcastle, Australia

**Reviewed by:**

Mark Talbot, CSIRO Plant Industry, Australia

Arata Yoshinaga, Kyoto University, Japan

**\*Correspondence:**

Paulo Monjardino, Departamento de Ciências Agrárias, Instituto de Biotecnologia e Bioengenharia - Centro de Biotecnologia dos Açores, Universidade dos Açores, Rua Capitão João de Ávila, 9700-042 Angra do Heroísmo, Portugal  
e-mail: paulo@uac.pt

Endosperm transfer cells in maize have extensive cell wall ingrowths that play a key role in kernel development. Although the incorporation of lignin would support this process, its presence in these structures has not been reported in previous studies. We used potassium permanganate staining combined with transmission electron microscopy – energy dispersive X-ray spectrometry as well as acriflavine staining combined with confocal laser scanning microscopy to determine whether the most basal endosperm transfer cells (MBETCs) contain lignified cell walls, using starchy endosperm cells for comparison. We investigated the lignin content of ultrathin sections of MBETCs treated with hydrogen peroxide. The lignin content of transfer and starchy cell walls was also determined by the acetyl bromide method. Finally, the relationship between cell wall lignification and MBETC growth/flange ingrowth orientation was evaluated. MBETC walls and ingrowths contained lignin throughout the period of cell growth we monitored. The same was true of the starchy cells, but those underwent an even more extensive growth period than the transfer cells. Both the reticulate and flange ingrowths were also lignified early in development. The significance of the lignification of maize endosperm cell walls is discussed in terms of its impact on cell growth and flange ingrowth orientation.

**Keywords:** transfer cells, starchy cells, maize endosperm, lignin, flange ingrowths, reticulate ingrowths, cell growth analysis

## INTRODUCTION

Transfer cells are the first cells to differentiate in maize endosperm and their main purpose is to facilitate the flow of assimilates into the starchy cells. They are characterized by complex flange and reticulate wall ingrowths (Monjardino et al., 2013) that project several micrometers into the cytosol and maintain a consistent ultrastructure throughout development (Davis et al., 1990; Talbot et al., 2002; Offler et al., 2003; McCurdy et al., 2008; Monjardino et al., 2013). The starchy cells are the most abundant cells in the endosperm. They predominantly accumulate starch and protein starting 12–14 days after pollination (DAP) and continuing until physiological maturity (Young and Gallie, 2000; Monjardino et al., 2005; Prioul et al., 2008). They undergo programmed cell death during endosperm development (Young and Gallie, 2000), but nevertheless withstand severe desiccation and maintain their tightly-arranged starch granules and protein bodies.

Lignification is associated with several traits in plants, including the structural integrity of the cell wall, secondary growth of vascular tissues, the strength of the stem and root (Boerjan et al., 2003), resistance to fungi (Ride, 1975; Xu et al., 2011), the prevention of autolytic cell wall degradation (O'Brien, 1970), and the gravitropic response of trees (Donaldson et al., 2010). Lignins are the second most abundant polymers in plants (after cellulose) and comprise phenolic heteropolymers resulting from the oxidative coupling of the three *p*-hydroxycinnamyl alcohols:

*p*-coumaryl, coniferyl and sinapyl (Lewis and Yamamoto, 1990; Dixon et al., 2001). The polymerization of *p*-hydroxyphenyl, guaiacyl, and syringyl monomers via carbon–carbon and ether linkages is mediated by free radicals (Nadji et al., 2009; Liu, 2012; Zhang et al., 2012).

Lignin has been suggested to be present in the ingrowths of transfer cells adjacent to sieve elements of basal nodes of the perennial *Valeriana officinalis* plants (Gaymann and Lörcher, 1990), using toluidine blue stain to detect it. In addition Heide-Jørgensen and Kuijt (1994) have detected lignin in transfer cells situated between the root xylem elements of *Triphysaria* sp. plants and their hosts with phloroglucinol. However, other studies using the periodic-Schiff reaction with alcian blue or with toluidine stains failed to detect lignification in transfer cells compared to xylem cells in the nodes of *Trifolium repens* and *Trollius europaeus* (Gunning and Pate, 1974). Furthermore, lignin was not detected with phloroglucinol in *Vicia faba* cotyledon transfer cells (Vaughn et al., 2007), which have led to a general consensus that transfer cells are not lignified (Offler et al., 2003; McCurdy et al., 2008). However, these methods may not be sensitive enough to detect small amounts of lignin, e.g., phloroglucinol does not detect the early stages of lignification and a negative phloroglucinol reaction therefore does not necessarily confirm the absence of lignin (Kutscha and McOrmond, 1972; Müsel et al., 1997). It has been demonstrated that ferulic and *p*-coumaric acids, two precursors

of lignin, can esterify to lignin and to polysaccharides of the wall of the *Poaceae* (Harris and Hartley, 1976), including in tissues that give a negative phloroglucinol reaction. It is possible that may be the case in the endosperm transfer cells.

Potassium permanganate ( $\text{KMnO}_4$ ) is a general electron-dense staining agent for lignin, which works by oxidizing coniferyl groups. The permanganate anion is reduced to insoluble manganese dioxide ( $\text{MnO}_2$ ) which then precipitates, indicating the reaction site (Hepler et al., 1970; Bland et al., 1971; Kutscha and Gray, 1972; Xu et al., 2006; Ma et al., 2011). Ultrathin sections can be stained with  $\text{KMnO}_4$  to determine the distribution of lignin in woody cell walls (Donaldson, 1992; Grünwald et al., 2002; Coleman et al., 2004; Wi et al., 2005; Xu et al., 2006; Lee et al., 2007; Tao et al., 2009; Ma et al., 2011).

Scanning electron microscopy and transmission electron microscopy (TEM) can be used to generate backscattered electrons for energy dispersive X-ray spectrometry (EDS), and these techniques can be used to probe the results of  $\text{KMnO}_4$  staining (Stein et al., 1992; Xu et al., 2006; Ma et al., 2011). The greater the concentration of Mn revealed by TEM–EDS, the higher the lignin concentration (Xu et al., 2006), and these data can be used for the quantitative assessment of lignin distribution (Ma et al., 2011). Bland et al. (1971) and Hoffmann and Parameswaran (1976) found that  $\text{KMnO}_4$  can stain several amino acids and other cell wall components with acidic groups in addition to lignin, but their studies involved chemically-delignified plant material and acidic groups that are rare in native plant cell walls. However, fixatives such as glutaraldehyde can react with the aminoacids lysine, tyrosine, tryptophan, phenylalanine, histidine, cysteine, proline, serine, glycine, glycylglycine, and arginine (Migneault et al., 2004), therefore their reactivity to  $\text{KMnO}_4$  may be altered in fixed tissues. Coleman et al. (2004) highlighted the duration of  $\text{KMnO}_4$  staining, because excessive exposure can result in non-specific staining of the cell wall based on the potent oxidation activity of this chemical (Lawn, 1960).

Acriflavine is a fluorochrome that can detect low levels of lignin. The intensity of acriflavine fluorescence is proportional to the concentration of lignin, and the signal can be detected and quantified by confocal laser scanning microscopy (CLSM) (Donaldson et al., 2001; Coleman et al., 2004; Christiernin et al., 2005; Cho et al., 2008; Nakagawa et al., 2012) or epifluorescence microscopy (Donaldson and Bond, 2005).

Lignin can be extracted using solvents containing hydrogen peroxide ( $\text{H}_2\text{O}_2$ ), so the same method can be used for lignin detection (Xiang and Lee, 2000; Svitelska et al., 2004; Yao et al., 2006; Hejri and Saboora, 2009). This technique is often more useful when applied in combination with other detection strategies.

There are several methods that chemically extract and detect lignin from plant tissues that vary in sensitivity and specificity (Hatfield and Fukushima, 2005). Each methodology carries its specific constraints and one that is relevant to this study is the rather limited amount of tissue to be analyzed. The transfer cells are located in the placenta-chalazal region of the endosperm, their tissue often has a total volume of  $\sim 0.1 \text{ mm}^3$ , therefore even when large numbers of samples are pooled it may not be enough for most of the methods for lignin analysis. The acetyl bromide method combines the specificity, the sensitivity and the relatively

low requirement of plant tissue (Fukushima and Hatfield, 2001; Foster et al., 2010).

We determined the presence of lignin in developing transfer cells and starchy cells using two staining techniques:  $\text{KMnO}_4$  in conjunction with TEM–EDS and acriflavine in conjunction with CLSM. We also studied  $\text{H}_2\text{O}_2$ -treated samples by TEM and TEM–EDS. The lignin content of the walls was also determined by acetyl bromide method, we analyzed the growth of both types of cells, and determined the flange ingrowth orientation in transfer cells. Our results revealed that transfer cells become lignified during early development when undergoing active growth and the formation of cell wall ingrowths. Similar levels of lignification were observed in the reticulate and flange ingrowths and cell walls at mid-development stages. The cell walls of starchy cells also became lignified from early through late developmental stages.

## MATERIALS AND METHODS

### PLANT MATERIAL, GROWTH CONDITIONS, AND SAMPLING

Maize plants (inbred W64A) were cultivated and kernels were collected from 2009 to 2013 as previously described (Monjardino et al., 2013). At each sampling date, at least 30 kernels were collected from at least five different ears. We focused on the most basal endosperm transfer cells (MBETCs) and the starchy cells.

The temperature was recorded daily during early kernel development allowing the growing degree days (GDD) to be calculated according to the formula  $\text{GDD} = \Sigma (\text{ADT} - \text{BT})$ , where ADT is the average daily temperature and BT is the base temperature of  $10^\circ\text{C}$  (Gilmore and Rogers, 1958). Minimum temperatures  $<10^\circ\text{C}$  were adjusted to  $10^\circ\text{C}$ , and maximum temperatures  $>30^\circ\text{C}$  were adjusted to  $30^\circ\text{C}$ . The developmental stages were therefore described as DAP and references were made to GDD.

### TEM–EDS OF SAMPLES STAINED WITH $\text{KMnO}_4$

Kernels were selected at 6, 12, and 20 DAP (95–97.5, 190–192.5, and 315.5–318.5 GDD, respectively), and were sectioned with a razor blade, discarding most of the endosperm tissue except the basal and central endosperm regions. The tissues were fixed immediately in 4% glutaraldehyde containing 2% osmium tetroxide for 2 h. The fixed sections were dehydrated in acetone and progressively infiltrated in Spurr's resin for 8 days at room temperature (Monjardino et al., 2007) before polymerization at  $60^\circ\text{C}$ .

Ultrathin sections (40–60 nm) were prepared on a LKB 2188 NOVA Ultramicrotome (LKB NOVA) using diamond knives (Diatome). The sections were mounted on 400-mesh gold grids (Agar Scientific), stained with 1%  $\text{KMnO}_4$  for 2 min each, followed by eight washes in water, and examined under a JEOL JEM 1400 TEM equipped with an EDS Microanalysis System (Oxford Instruments). We analyzed MBETC and starchy cell walls, ingrowths and vesicles adjacent to the reticulate ingrowths (when visible). The areas were traced for the probe to raster and produce an integrated average of several thousand readings (Figures 1A–F). Areas of the sample that apparently did not contain any cell content were used as controls. The elements analyzed in the samples were C, O, Mn, Na, K, Ca, and Fe. The levels of each element were expressed in terms of the relative proportion in relation to the sum of the seven elements.

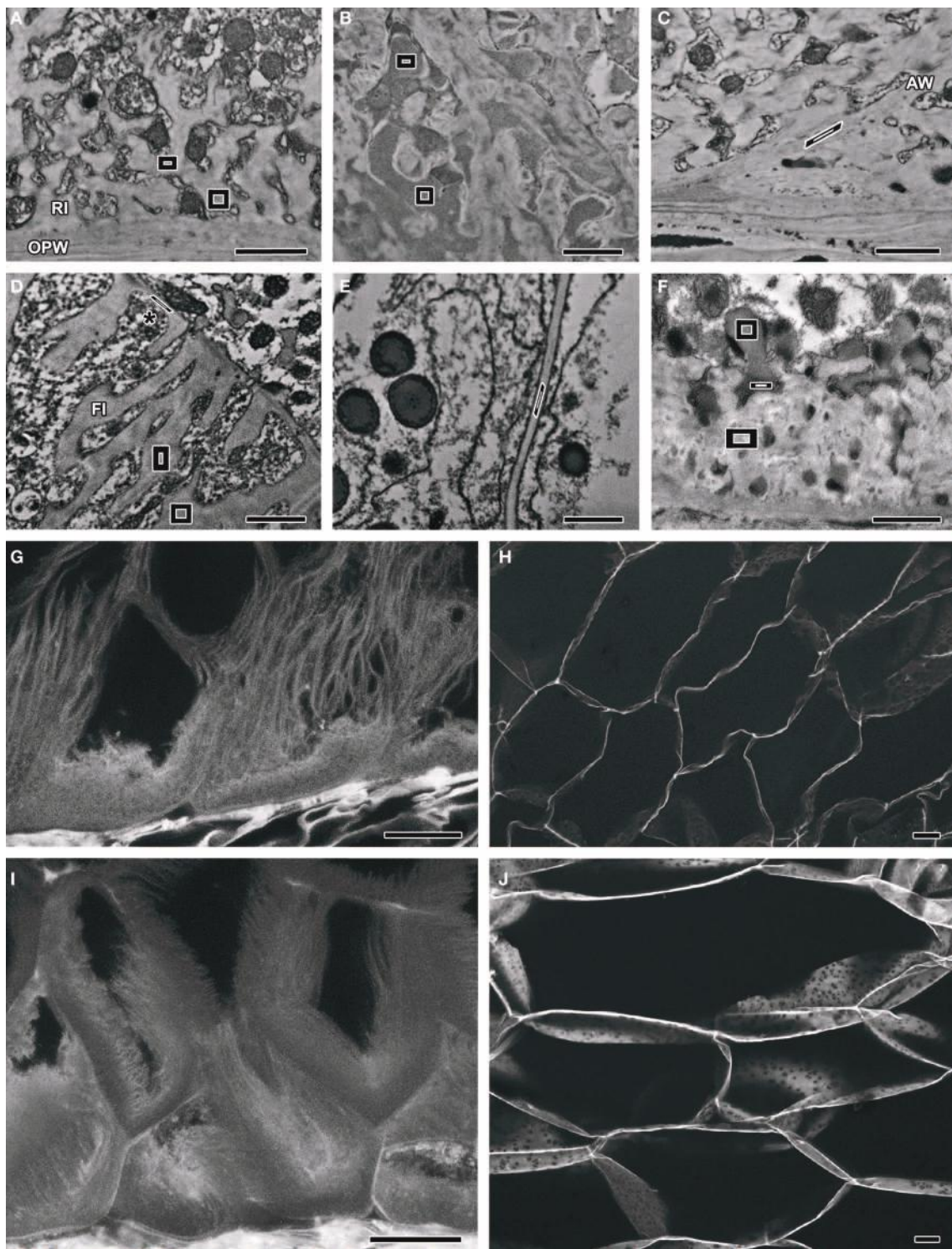


**FIGURE 1 | Images obtained by TEM-EDS (A–E) and TEM (F) of samples stained with KMnO<sub>4</sub>.** Polygons represent the boundaries of EDS readings in each sample. (G–J) CLSM images of acriflavine-stained samples. (A) MBETCs at 12 DAP – readings were obtained from the reticulate ingrowths. (B) MBETCs at 12 DAP – readings were obtained from vesicles adjacent to reticulate ingrowths. (C) MBETCs at 12 DAP – readings were obtained from anticalinal walls. (D) MBETCs at 20 DAP –

readings were obtained from flange ingrowths and inner periclinal walls (\*). (E) Starchy cells at 20 DAP – readings were obtained from the walls. (F) MBETCs at 6 DAP – readings were obtained from vesicles releasing their contents into reticulate ingrowths. (G) MBETCs at 9 DAP. (H) Starchy cells at 9 DAP. (I) MBETCs at 25 DAP. (J) Starchy cells at 25 DAP. AW, anticalinal wall; FI, flange ingrowth; OPW, outer periclinal wall; RI, reticulate ingrowth. Scale bars: (A–F) = 1 μm; (G–J) = 20 μm.

## TEM AND TEM-EDS FOLLOWING EXPOSURE TO H<sub>2</sub>O<sub>2</sub>

Kernels were selected at 5–20 DAP (69.5–77.5 to 284.0–287.5 GDD) and processed as described above. After mounting on 400-mesh gold grids, the ultrathin sections were treated with 4% H<sub>2</sub>O<sub>2</sub> for 15 or 60 min, followed by three washes in water. Images were captured using a Zeiss EM10 C TEM (Carl Zeiss) and were digitally recorded using a Gatan SC 1000 ORIUS CCD camera (Warrendale).

Ultrathin sections containing MBETCs of 6 DAP and 12 DAP kernels (97.5 and 191 GDD, respectively), were treated with 3% H<sub>2</sub>O<sub>2</sub> for 60 min, followed by eight washes in water, after which they were stained with 1% KMnO<sub>4</sub> for 2 min, followed by three washes in water, and examined under a JEOL JEM 1400 TEM equipped with an EDS Microanalysis System. The element analysis was conducted as described above. The percentage reduction of Mn deposition due to H<sub>2</sub>O<sub>2</sub> treatment was calculated by comparison to other ultrathin sections of the same samples that were only stained with 1% KMnO<sub>4</sub> for 2 min.

## CLSM WITH ACRIFLAVINE STAINING

Kernels were selected at 6, 9, and 25 DAP (92.0–92.5, 128–134.5, and 355.5–356.5 GDD, respectively), and sectioned longitudinally (70–100  $\mu\text{m}$  thicknesses) with a Leica VT 1200 vibratome (Leica Microsystems). The sections were stained with 0.0025% aqueous acriflavine for 10 min, followed by a 2-min wash in water, and coverslips were mounted with glycerol (adapted from Donaldson and Bond, 2005). Unstained sections were used as controls. The sections were visualized under a Zeiss CLSM 510 (Carl Zeiss) at an excitation wavelength of 488 nm and emission wavelengths of 505–550 nm and LP 615 nm for detection. The projected images were obtained from Z stacks at a resolution of 1024  $\times$  1024 pixels. The Z stacks contained 16–35 planes at 0.37- $\mu\text{m}$  intervals.

## LIGNIN DETERMINATION BY ACETYL BROMIDE METHOD

Kernels of 5, 10, and 15 DAP (61.5–77.5, 140–152.5, and 211–231 GDD, respectively), were dissected manually and the transfer cell and starchy cell tissues were collected separately, frozen in liquid nitrogen and stored at –80°C until further use. There was a particular concern in dissecting the transfer cell tissue in order to not include remnants of the nucellus, the pedicel and pericarp, and the embryo tissue. The starchy cells were collected from the central endosperm region. For each sampling at least 120 kernels were dissected and at least four samples were pooled in each replicate in order to have a minimum of 50 mg of dry matter for the extraction of wall material (Foster et al., 2010). The extraction of lignin was done according to the procedures of Fukushima and Hatfield (2001) and absorbance was measured at 280 nm by a double beam UV-Vis spectrophotometer Shimadzu UV-2401 PC (Shimadzu Corporation). The analysis was done on two replicates of transfer cells and starchy cells of 10 and 15 DAP kernels and on the pedicel and pericarp of 5 DAP kernels. Stems of *Populus nigra* L. were used as control. The percentage of acetyl bromide soluble lignin was determined using an appropriate coefficient (maize = 17.75 L g<sup>−1</sup> cm<sup>−1</sup>; *Populus nigra* = 18.21 L g<sup>−1</sup> cm<sup>−1</sup>) with the formula described in Foster et al. (2010).

## ANALYSIS OF GROWTH AND FLANGE INGROWTH ANGLE

For growth analysis, kernels at 4–35 DAP (62.0–65.5 to 515.5–522.0 GDD) were processed as described above for CLSM, but were stained with 0.01% calcofluor white (Monjardino et al., 2013). For flange ingrowth angle analysis, kernels at 6, 12, and 20 DAP (83.5–93, 168.0–177.5, and 284.0–287.5 GDD, respectively), were processed in the same manner. Sections were visualized under a Zeiss CLSM 510 at an excitation wavelength of 405 nm (UV diode laser) and an emission wavelength of 420–480 nm. The projected images were obtained from Z stacks at a resolution of 1024  $\times$  1024 pixels. The Z stacks contained 25–98 planes at 0.37- $\mu\text{m}$  intervals.

Cell areas (taken from two-dimensional CLSM images) were measured from an average of seven cells per kernel and 15 kernels per sampling date. Flange ingrowth angles were measured from an average of three cells per kernel and five kernels per sampling date. Cell areas were measured from contiguous MBETCs with Zeiss software LSM 510 4.0 SP1 using the “closed free-shape curve” feature from the “overlay toolbar.” Flange ingrowth angles in MBETCs were measured relative to the nearest anticinal wall using the “line” feature from the “overlay toolbar” in the same software.

All selected images were imported into Adobe Photoshop CS6 software (Adobe Systems) for presentation, and photomontages were produced using the same software.

## STATISTICAL ANALYSIS

A complete randomized model was used to analyze the TEM-EDS data, and ANOVA was carried out using Microsoft Excel. Means were compared using the Tukey multiple range test. For growth analysis, a regression survey was conducted using CurveExpert Professional software with GDD as the independent variable and cell area as the dependent variable. Among several tested models, the Richards sigmoidal function gave the best fit for MBETC growth analysis, whereas the logarithmic function gave the best fit for starchy cell growth analysis.

## RESULTS

### TEM-EDS ANALYSIS

Our TEM analysis highlighted some differences between reticulate ingrowths, vesicle content, anticinal walls, flange ingrowths, inner pericinal walls, and starchy cell walls, but without sufficient clarity to distinguish them (Figures 1A–F). However, the additional EDS quantification mode allowed us to measure the amount of Mn and thus to infer the pattern of lignin deposition. Manganese could be detected as early as 6 DAP, mainly in the reticulate ingrowths (Figure 1A) and vesicles (Figure 1B), and also to a lesser extent in the anticinal walls (Figure 1C), the flange ingrowths and inner pericinal walls (Figure 1D), and starchy cell walls (Figure 1E, Table 1). The reticulate ingrowths and vesicles contained significantly higher levels of Mn than the flange ingrowths, the anticinal walls and pericinal walls at 6 DAP, whereas at 12 DAP the reticulate ingrowths, vesicles and anticinal walls had significantly higher levels of Mn than the flange ingrowths, pericinal walls and starchy cell walls. At 20 DAP, there were no significant differences in Mn levels among the vesicles, ingrowths, and walls of the MBETCs and starchy cells. The Mn

**Table 1 | The average percentage concentration of elemental Mn in transfer cells and starchy cells at 6, 12, and 20 DAP determined by TEM-EDS.**

	6 DAP	12 DAP	20 DAP	P
Reticulate ingrowths	8.18 a <sup>1</sup> , A <sup>2</sup>	7.43 a <sup>1</sup> , A	7.84 a <sup>1</sup> , A	>0.05
Vesicles adjacent to reticulate ingrowths	9.35 a, A <sup>2</sup>	8.66 a, A	10.25 a, A	>0.05
Anticlinal walls next to the OPW <sup>§</sup>	6.00 a, B <sup>2</sup>	7.61 a, A	7.05 a, A	>0.05
Flange ingrowths	6.26 a, B <sup>2</sup>	5.53 a, B	6.48 a, A	>0.05
Periclinal walls	5.50 b, B <sup>2</sup>	4.98 b, B	7.69 a, A	0.02
Starchy cell walls	—	3.35 a, C	5.68 a, A	>0.05
Control	0.63 a, C <sup>2</sup>	0.47 a, D	0.56 a, B	>0.05
p	$7.94 \times 10^{-5}$	$1.12 \times 10^{-6}$	$4.45 \times 10^{-3}$	

<sup>1</sup>Numbers in lines followed by the same lower case letter do not differ significantly.

<sup>2</sup>Numbers in columns followed by the same capital letter do not differ significantly.

<sup>§</sup>OPW, outer periclinal wall.

levels in the periclinal walls increased significantly throughout development, whereas the other cellular components did not show substantial variation (Table 1).

Vesicles often fused with reticulate ingrowths and released their highly electron-dense contents (Figure 1F). TEM-EDS analysis revealed a fusing vesicle containing 9.10% Mn immediately adjacent to an electron-dense region in the reticulate ingrowths containing 8.27% Mn, whereas ~500 nm further away the reticulate ingrowths contained only 7.62% Mn (Figure 1F). This suggests that a substantial portion of lignin or its precursors must be transported through the vesicles into the reticulate ingrowths.

#### CLSM ANALYSIS OF ACRIFLAVINE-STAINED SAMPLES

The fluorescence of acriflavine was only detected in the 505–550 nm band, not above 615 nm, which suggests that it specifically detected lignin (Donaldson et al., 2001). Sections of maize kernels stained with acriflavine revealed weak fluorescence in the MBETCs at 6 DAP, except for the region next to the outer periclinal wall (OPW) where the fluorescence was more intense, with similar staining in the future starchy cells (data not shown). These data suggested that there is only a low level of lignification in the endosperm cell walls at this stage. Later in development (9 DAP), the fluorescence levels increased in the transfer cells (Figure 1G) and starchy cells (Figure 1H). This represented the mid-phase of ingrowth development in the transfer cells (Monjardino et al., 2013), whereas starch and protein accumulation was about to begin in the starchy endosperm cells. At 25 DAP, high-intensity acriflavine labeling was observed in both the transfer cell walls and their ingrowths (Figure 1I). At this stage, the walls of the MBETCs showed more intense fluorescence than the adjacent ingrowths, suggesting a greater degree of lignification. The starchy cell walls were also more intensely fluorescent at this stage (Figure 1J), suggesting that lignification increased throughout development. These data supported the TEM-EDS results. Lignification could be detected from early

developmental stages using both techniques. At 9 DAP, the walls and ingrowths of the transfer cells were more intensely stained than the starchy cell walls, but by 25 DAP the MBETC and starchy cell walls stained with similar intensity suggesting they contained equivalent amounts of lignin.

#### TEM ANALYSIS OF H<sub>2</sub>O<sub>2</sub>-TREATED SAMPLES

Ultrathin sections of differentiating transfer cells were treated with H<sub>2</sub>O<sub>2</sub> and analyzed by TEM, revealing that some vesicles lacked their electron-dense contents (Figures 2A,B). Because these samples were not stained prior to analysis, the observed electron density thus arose from their intrinsic characteristics, the osmium fixation and the treatment with H<sub>2</sub>O<sub>2</sub>. The visualization of untreated controls of the same samples showed that similar vesicles were electron dense (Figure 2C). This indicated that the loss of electron density was a direct consequence of the H<sub>2</sub>O<sub>2</sub> treatment, and strongly suggested the presence of polyphenolic compounds in the vesicles.

The lack of electron density was affected by the duration of H<sub>2</sub>O<sub>2</sub> treatment. After 15 min exposure, only part of the vesicles and a few scattered regions of the reticulate ingrowths and OPW lacked the electron density (Figure 2A). However, after 60 min exposure there was more extensive loss of electron density in the vesicles and partial or complete loss in the walls and ingrowths (Figure 2B). These data also supported the presence of polyphenolic compounds in the vesicles, walls and ingrowths of MBETCs.

#### TEM-EDS ANALYSIS OF H<sub>2</sub>O<sub>2</sub>-TREATED SAMPLES

The H<sub>2</sub>O<sub>2</sub> treatment prior to KMnO<sub>4</sub> staining caused drastic reductions of the Mn levels in the vesicles, ingrowths and walls of 6 and 12 DAP MBETCs (Table 2). The vesicles suffered the largest reduction in Mn levels, followed by the reticulate ingrowths, the walls and the flange ingrowths.

#### LIGNIN DETERMINATION BY ACETYL BROMIDE METHOD

The lignin levels in the wall extracts of transfer and starchy cells of 10 and 15 DAP kernels were relatively constant, ranging between 36.9 and 47.4  $\mu\text{g mg}^{-1}$  (Table 3). Although the extraction of the wall material involves steps that should remove the precursors of lignin, we aren't sure on whether they were totally removed, therefore they could have been extracted together with lignin by acetyl bromide. The small variability of lignin content between these tissues is similar to the TEM-EDS analysis, but the slight tendency of the lignin levels to decrease from 10 to 15 DAP is opposite to the TEM-EDS analysis. The pedicel and pericarp of 5 DAP kernels have a much higher lignin content, which is expected, because the vascular bundles had a positive phloroglucinol reaction, although the parenchyma cells had a negative reaction (data not shown). The *Populus nigra* wood sample had a lignin concentration of 199.2  $\mu\text{g mg}^{-1}$ , which is similar to previously published data using the same extraction and detection methods (Foster et al., 2010).

#### ANALYSIS OF CELL GROWTH AND FLANGE INGROWTH ANGLE

The transfer cells expanded until 120–140 GDD (9–10 DAP; Figure 3A) whereas the starchy cells were still expanding at 520

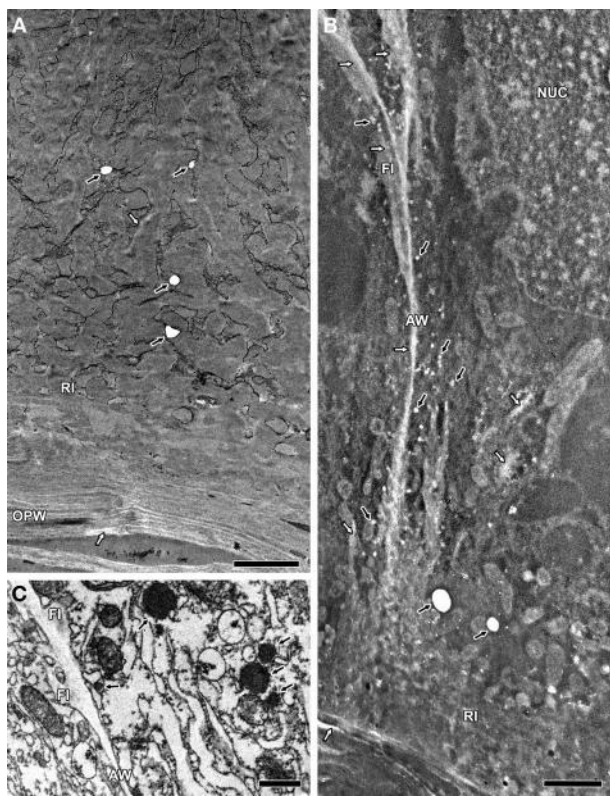


**FIGURE 2 |** TEM images of ultrathin MBETC sections at 10 DAP, after  $\text{H}_2\text{O}_2$  treatment without contrast (A and B) and control sections at 6 DAP without treatment and contrast (C). (A) After a 15-min  $\text{H}_2\text{O}_2$

treatment, some vesicles lacked electron density (black arrows), whereas reticulate ingrowths and the OPW show regions with less electron density (white arrows). (B) After a 60-min  $\text{H}_2\text{O}_2$  treatment, many vesicles lost their electron density (black arrows), whereas reticulate and flange ingrowths, the OPW and anticinal walls reveal large regions with less electron density (white arrows). (C) Control sections with electron-dense vesicles (black arrows), whereas the walls and flange ingrowths have a weak electron density. AW, anticinal wall; Fl, flange ingrowth; NUC, nucleus; OPW, outer pericinal wall; RI, reticulate ingrowth. Scale bars: (A,B) = 2  $\mu\text{m}$ , (C) = 1  $\mu\text{m}$ .

GDD (35 DAP; **Figure 3B**). The transfer cells reached their maximum growth rate at 96 GDD (6 DAP; **Figure 3A**), when the amount of lignin was relatively low in all structures except the reticulate ingrowths and vesicles (**Table 1**). The starchy cells also showed their highest growth rates prior to 100 GDD, but the subsequent reduction in growth rate was not as dramatic as observed for the transfer cells (**Figure 3B**). Indeed, lignification coincided with starchy cell growth throughout development, which clearly shows that lignification does not inhibit the growth of these cells. The starchy cells continued expanding intensively at 35 DAP, probably reflecting the active accumulation of assimilates at this stage.

The flange ingrowth angles varied dramatically throughout development (**Figure 3C**). At 6 DAP, most of the flange ingrowths had angles of less than 15° relative to the nearest anticinal wall, whereas later there was a greater proportion of angles between 15 and 30°. Furthermore, the proportion of angles between 30 and

**Table 2 |** The average percentage reduction of Mn deposition after  $\text{H}_2\text{O}_2$  treatment prior to  $\text{KMnO}_4$  staining in MBETC at 6 and 12 DAP, determined by TEM-EDS.

	6 DAP	12 DAP
Reticulate ingrowths	58.56	54.22
Vesicles adjacent to ingrowths	77.66	60.24
Flange ingrowths	48.77	43.98
Walls	47.96	48.15

**Table 3 |** Average lignin content ( $\pm$ standard error) in the dry matter of wall material ( $\mu\text{g mg}^{-1}$ ) extracted by the acetyl bromide method (Fukushima and Hatfield, 2001; Foster et al., 2010).

	Lignin content
<i>Populus nigra</i> wood	199.2
Pericarp and pedicel 5 DAP	80.5 $\pm$ 13.2
Transfer cells 10 DAP	46.4 $\pm$ 14.8
Starchy cells 10 DAP	47.9 $\pm$ 9.7
Transfer cells 15 DAP	38.0 $\pm$ 10.0
Starchy cells 15 DAP	36.9 $\pm$ 12.4

45° increased as the MBETCs developed. The proportion of flange ingrowths angles greater than 45° remained at <10% throughout development, which confirmed previous observations that such ingrowths tend to be oriented longitudinally and obliquely, rather than transversely to the longer axis of the cell (Monjardino et al., 2013).

## DISCUSSION

Our analysis revealed that transfer cells have extensive inward wall projections that contrast with the much thinner walls of the starchy cells (**Figure 1**). The inward growth of cell wall regions must overcome the outward pressure of the living cell cytoplasm, and it is not unreasonable to suggest that this process might require reinforcement, e.g., by the ubiquitous structural molecule lignin.

The TEM-EDS technique allowed the accurate quantification of elemental Mn deposited in the cell walls and their ingrowths. Our data were based on the trusted and reliable Clifft Lorimer thin ratio section quantification method, which revealed that Mn was deposited on the walls of the transfer cells and starchy cells (**Table 1**, **Figures 1A–F**). Because TEM-EDS elemental analysis offers a high degree of confidence, it was possible to conclude that Mn atoms were deposited in the walls and ingrowths in amounts that could not be attributed to background counts observed in the control sections (**Table 1**). Considering previous reports that  $\text{KMnO}_4$  does not react with cellulose, hemicelluloses or pectin (Kutscha and Gray, 1972) and that short exposure times prevent non-specific staining (Coleman et al., 2004), it would be reasonable to conclude that the  $\text{KMnO}_4$  reacted with lignin, leading to the deposition of Mn atoms. However, it cannot be ruled out the reaction of  $\text{KMnO}_4$  with other wall constituents, namely precursors of lignin like the ferulic and p-coumaric acids, which have been demonstrated to exist in relatively high content in the cell walls of *Poaceae* plants, as compared to lignin (Harris

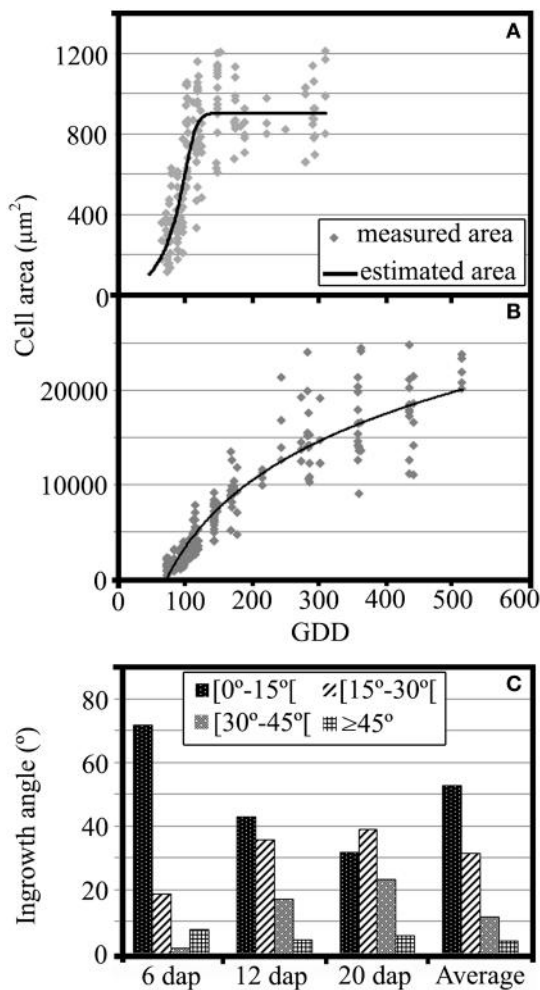


**FIGURE 3 | (A)** Growth analysis of MBETCs, showing cell areas ( $\mu\text{m}^2$ ) of developing kernels (4–20 DAP, equivalent to 62.0–300.2 GDD) and adjusted growth curve (cell area =  $903.04/(1 + \exp(15.81 - 0.15 \times \text{GDD})^{(1/4.37)})$ ,  $R^2 = 67.15\%$ ). **(B)** Growth analysis of starchy cells, showing cell areas ( $\mu\text{m}^2$ ) of developing kernels (5–35 DAP equivalent to 73.5–522.0 GDD) and adjusted growth curve (cell area =  $-43582.6 + 10195.3 \times \ln(\text{GDD})$ ,  $R^2 = 92.3\%$ ). **(C)** Flange ingrowth angles (in relation to the nearest anticlinal wall) of developing MBETCs (6, 12, and 20 DAP, and an average of the three sampling dates).

and Hartley, 1976). It is also possible that  $\text{KMnO}_4$  may react with some amino acids (Bland et al., 1971) and acidic groups (Hoffmann and Parameswaran, 1976) like galacturonic and glucuronic acids. Therefore, we consider that the  $\text{KMnO}_4$  staining and TEM–EDS analysis must have provided a proportional indication of the lignin content, but not the exclusive proof of its existence.

$\text{H}_2\text{O}_2$  treatment provided an indirect approach to confirm the presence of lignin: short-exposure experiments (15 min; Figure 2A) resulted in the loss of electron-dense material from vesicles compared with untreated control samples (Figure 2C), whereas longer exposure (60 min) also caused the loss of

electron-dense material from ingrowths and walls (Figure 2B). These results suggest that vesicles may contain the highest concentrations of polyphenolic compounds in the MBETCs but also that ingrowths and walls must have lower but still biologically-relevant concentrations of such constituents. The presence of vesicles that support ingrowth formation has been reported previously (Davis et al., 1990; our unpublished data). The vesicles are numerous (Figure 2B) and they contribute to ingrowth formation (Figure 1F), thus reinforcing the thesis of exocytosis supporting lignin deposition in the ingrowths.

We also tested the effects of  $\text{H}_2\text{O}_2$  treatment prior to  $\text{KMnO}_4$  staining and quantified it by TEM–EDS in the MBETCs (Table 2). The reduction of Mn deposition was the highest in the vesicles at 6 and 12 DAP, thus suggesting to contain the highest lignin and/or its precursors' content. The reticulate ingrowths had the second highest reduction of Mn deposition due to  $\text{H}_2\text{O}_2$  treatment, which is also in accordance with the TEM–EDS data (Table 1). The flange ingrowths and walls had the lowest reduction of Mn deposition, but it still was above 40%, which reinforces the concept of them also being lignified, although at lower levels than the reticulate ingrowths.

The acriflavine staining experiment confirmed the presence of lignin in the transfer cell walls and ingrowths, as well as in the walls of the starchy cells (Figures 1G–J). The intensity of the staining mirrored the TEM–EDS data, thus reinforcing our conclusions. It should be highlighted the tendency of the inner edges of the reticulate ingrowths to fluoresce more intensively than the rest of these ingrowths.

The determination of lignin content by the acetyl bromide method (Fukushima and Hatfield, 2001; Foster et al., 2010) was essential to confirm the presence of lignin and its precursors in the walls of the transfer and starchy cells of maize endosperm (Table 3), regardless of the negative phloroglucinol reaction. However, this methodology does not enable us to distinguish the ingrowths from the adjacent walls. The slight tendency of reduction of the lignin and its precursors content from 10 to 15 DAP (Table 3) is not fully in accordance to the TEM–EDS data (Table 1) and that could be due to: (a) non-specific determination of other wall and ingrowth components by TEM–EDS that would partially mask the lignin determination; (b) the extraction of wall material prior to the acetyl bromide analysis not being 100% efficient and still remnants of starch and other cell components of 15 DAP kernels causing an unforeseeable dilution of lignin. This analysis clearly makes the case that lignin exists in the transfer and starchy cell walls throughout kernel development.

Consistently higher levels of Mn were deposited in reticulate ingrowths compared to flange ingrowths, suggesting that larger amounts of lignin may be required to stabilize the former structures. Reticulate ingrowths contain less-compacted cellulose microfibrils that tend to be arranged in non-parallel arrays (Offler et al., 2003; McCurdy et al., 2008; Monjardino et al., 2013), whereas the cellulose microfibrils in flange ingrowths are arranged in tight parallel arrays. Therefore, it seems plausible that higher lignin levels may be required to stabilize the reticulate ingrowths because of their unique ultrastructure. The stronger fluorescence of acriflavine in the inner edges of

the reticulate ingrowths makes stronger the assumption of lignin to be determinant to stabilize the looser ingrowth structures. To our knowledge this trait has not been documented before and it makes a strong case for the relevance of lignin to ingrowth formation.

The presence of high Mn levels in vesicles adjacent to the reticulate ingrowths (**Figures 1B,F, Table 1**) and the most drastic reduction of Mn deposition after H<sub>2</sub>O<sub>2</sub> treatment (**Table 2**) support the exocytosis of lignin or its precursors in vesicles derived from the Golgi body (reviewed by Donaldson, 2001). In the transfer cells, the flux of vesicles apparently from the Golgi body is intense throughout development (Davis et al., 1990; Monjardino et al., 2013) and this offers a significant mechanism to transport lignin into the ingrowths and adjacent cell walls, although other mechanisms cannot be ruled out (Liu, 2012; Wang et al., 2013). These results point to the need of using other methods to assess the transportation role of Golgi vesicles before definite conclusions could be drawn.

Basic fuchsin in combination with fluorescence or light microscopy has also been used successfully as a staining method for lignified cell walls (Fuchs, 1963; Dharmawardhana et al., 1992; Kraus et al., 1998; Caño-Delgado et al., 2000; Möller et al., 2005; Soyano et al., 2008; Wagner et al., 2009). In a previous study, we showed that basic fuchsin reacts with ingrowths and adjacent walls (Machado, 2004). However, other reports indicated that basic fuchsin has affinity for the suberized and cutinized walls of plants cells and other structures devoid of lignin, such as chloroplasts, and starch granules in maize endosperm (Kraus et al., 1998; Machado, 2004; Pereira et al., 2008). Therefore, basic fuchsin staining cannot be considered unequivocal proof for the presence of lignin, but it reinforces the data reported in this study.

Taken together, these data support the general lignification of endosperm cell walls, with particular emphasis on the transfer cells despite previous contradictory reports (Gunning and Pate, 1974; Gaymann and Lörcher, 1990; Heide-Jørgensen and Kuijt, 1994; Vaughn et al., 2007). These discrepancies probably reflect the higher sensitivity of our staining methods compared to the periodic-Schiff reaction plus alcian blue or toluidine stains used by Gunning and Pate (1974), and the phloroglucinol stain used by Vaughn et al. (2007). We also tested phloroglucinol, and found as expected that this method did not detect any lignin in maize endosperm, only in the vascular tissue of the maize kernel (data not shown). Several authors have demonstrated that phloroglucinol is not sensitive enough for early lignification studies (Kutsch and McOrmond, 1972; Müsel et al., 1997).

The lack of significant differences in lignin content between ingrowths and adjacent walls after 6 DAP reinforces their similarity in composition (Vaughn et al., 2007). However, there seems to exist differences in lignin distribution at least in the reticulate ingrowths throughout development and differences in composition in the ingrowths and adjacent walls cannot be ruled out; this phenomenon must be addressed in future experiments.

Lignin is mainly associated with cell wall rigidity and strength, but it is also present in low amounts in the growing primary cell walls of several species (Joseleau and Ruel, 1997; Müsel et al., 1997; Christiernin et al., 2005; Gritsch and Murphy,

2005). We detected lignin in maize MBETCs at 6 DAP, an early developmental stage characterized by a high growth rate, allowing the cells to increase by up to 4-fold in area until 12 DAP (**Table 1, Figure 3A**). The ingrowths also form and develop extensively during this period (**Figures 1, 2**; Monjardino et al., 2013). The flange ingrowths may restrict cell expansion, because they are predominantly obliquely oriented in relation to the long axis of the cell, and are often as long as the cells themselves (Talbot et al., 2002; Monjardino et al., 2013). They also appear to be attached to the adjacent wall along most of their length and, as we demonstrate in this study, they are also lignified. Furthermore, the oblique orientation of the flange ingrowths does not facilitate cell expansion along the long axis, although this may not necessarily act as an impediment because the ingrowths may behave like the folding bellows of an accordion, expanding obliquely to their orientation. In addition, the increasing angle between flange ingrowths and the nearest anticlinal walls during development (**Figure 3C**) opposes the stretching effect of the predominant orientation of cell growth. Therefore, other factors may facilitate ingrowth reorientation in the MBETCs: (i) new ingrowths may be formed with greater angles; (ii) the distortion effect on the transfer cells caused by the growing embryo could promote unequal variations in ingrowth and anticlinal wall orientations; (iii) assimilate flow may contribute to distortions in the orientation of the ingrowths; and (iv) the connections between the ingrowths and walls may become weaker as the cell expands and develops, therefore enabling them to change their orientation.

The starchy cells also contain lignin throughout development (**Tables 1, 3**), despite the cells grew even more significantly than the transfer cells (**Figure 3B**). These cells accumulate large amounts of starch and protein, and at later developmental stages they lose most of their water content. Therefore, the walls of the starchy cells must be strong and flexible enough to endure such challenging conditions, and lignin is likely to be an important constituent that provides such abilities.

Our results suggest that the role of lignin in the structure of the cell wall should be reconsidered. Müsel et al. (1997) proposed that, in the process of cell wall growth, lignin may act to counterbalance independent wall-loosening processes (mediated by growth-promoting agents), thus allowing the cell wall to expand without losing rigidity. Our results support this hypothesis for maize transfer and starchy endosperm cells. The role of lignin in ingrowth formation must also be to stabilize its structure, as that seems particularly to be the case in the inner loose ends of the reticulate ingrowths.

## ACKNOWLEDGMENTS

This research was supported in part by the Instituto de Biotecnologia e Bioengenharia—Centro de Biotecnologia dos Açores, by Grant BIIC M3.1.6/F/038/2009 from Direcção Regional de Ciência e Tecnologia, and by Grant SFRH/BD/8122/2002 from Fundação para a Ciência e Tecnologia. The authors thank Carlos Sá (CEMUP—Universidade do Porto) for EDS analysis counseling and critical data interpretation, Sandra Barreto for data analysis, Sandra Barreto, Frederico Silva, Ana Carolina Tavares and António José Fernandes for technical support, and Richard M. Twyman for editing the article.

## REFERENCES

- Bland, D. E., Foster, R. C., and Logan, A. F. (1971). The mechanism of permananate and osmium tetroxide fixation and the distribution of the lignin in the cell wall of *Pinus radiata*. *Holzforschung* 25, 137–143.
- Boerjan, W., Ralph, J., and Baucher, M. (2003). Lignin biosynthesis. *Annu. Rev. Plant Biol.* 54, 519–546. doi: 10.1146/annurev.arplant.54.031902.134938
- Caño-Delgado, A. I., Metzlaff, K., and Bevan, M. W. (2000). The el1 mutation reveals a link between cell expansion and secondary cell wall formation in *Arabidopsis thaliana*. *Development* 127, 3395–3405.
- Cho, C. H., Lee, K. H., Kim, J. S., and Kim, Y. S. (2008). Micromorphological characteristics of bamboo (*Phyllostachys pubescens*) fibers degraded by a brown rot fungus (*Gloeophyllum trabeum*). *J. Wood Sci.* 54, 261–265. doi: 10.1007/s10086-007-0937-1
- Christiernin, M., Ohlsson, A. B., Berglund, T., and Henriksson, G. (2005). Lignin isolated from primary walls of hybrid aspen cell cultures indicates significant differences in lignin structure between primary and secondary cell wall. *Plant Physiol. Biochem.* 43, 777–785. doi: 10.1016/j.plaphy.2005.07.007
- Coleman, C. M., Prather, B. L., Valente, M. J., Dute, R. R., and Miller, M. E. (2004). Torus lignification in hardwoods. *IAWA J.* 25, 435–447. doi: 10.1163/22941932-90000376
- Davis, R. W., Smith, J. D., and Cobb, B. G. (1990). A light and electron microscope investigation of the transfer cell region of maize caryopses. *Can. J. Bot.* 68, 471–479. doi: 10.1139/b90-063
- Dharmawardhana, D. P., Ellis, B. E., and Carlson, J. E. (1992). Characterization of vascular lignification in *Arabidopsis thaliana*. *Can. J. Bot.* 70, 2238–2244. doi: 10.1139/b92-277
- Dixon, R. A., Chen, F., Guo, D., and Parvathi, K. (2001). The biosynthesis of monolignols: a “metabolic grid,” or independent pathways to guaiacyl and syringyl units? *Phytochemistry* 57, 1069–1084. doi: 10.1016/S0031-9422(01)00092-9
- Donaldson, L. A. (1992). Lignin distribution during latewood formation in *Pinus radiata* D. Don. *IAWA J.* 13, 381–387.
- Donaldson, L. A. (2001). Lignification and lignin topochemistry—an ultrastructural view. *Phytochemistry* 57, 859–873. doi: 10.1016/S0031-9422(01)00049-8
- Donaldson, L. A., and Bond, J. (2005). *Fluorescence Microscopy of Wood*. Rotorua: CD-ROM.
- Donaldson, L., Hague, J., and Snell, R. (2001). Lignin distribution in coppice poplar, linseed and wheat straw. *Holzforschung* 55, 379–385. doi: 10.1515/HF.2001.063
- Donaldson, L., Radotić, K., Kalauzi, A., Djikanović, D., and Jeremić, M. (2010). Quantification of compression wood severity in tracheids of *Pinus radiata* D. Don using confocal fluorescence imaging and spectral deconvolution. *J. Struct. Biol.* 169, 106–115. doi: 10.1016/j.jsb.2009.09.006
- Foster, C. E., Martin, T. M., and Pauly, M. (2010). Comprehensive compositional of plant cell walls (lignocellulosic biomass). Part I: lignin. *J. Vis. Exp.* 37:e1745. doi: 10.3791/1745
- Fuchs, C. H. (1963). Fuchsin staining with NaOH clearing for lignified elements of whole plants or plant organs. *Biotech. Histochem.* 38, 141–144. doi: 10.3109/10520296309067156
- Fukushima, R. S., and Hatfield, R. D. (2001). Extraction and isolation of lignin for utilization as a standard to determine lignin concentration using the acetyl bromide spectrophotometric method. *J. Agric. Food Chem.* 49, 3133–3139. doi: 10.1021/jf010449r
- Gaymann, W., and Lörcher, H. (1990). Transfer cells and lipid droplets of some *Valerianaceae*. *PI Syst. Evol.* 170, 37–51. doi: 10.1007/BF00937848
- Gilmore, E. C., and Rogers, J. S. (1958). Heat units as a method of measuring maturity in corn. *Agron. J.* 50, 611–615. doi: 10.2134/agronj1958.00021962005000100014x
- Gritsch, C. S., and Murphy, R. J. (2005). Ultrastructure of fibre and parenchyma cell walls during early stages of culm development in *Dendrocalamus asper*. *Ann. Bot.* 95, 619–629. doi: 10.1093/aob/mci068
- Grünwal, C., Ruel, K., Kim, Y. S., and Schmitt, U. (2002). On the cytochemistry of cell wall formation in poplar trees. *Plant Biol.* 4, 13–21. doi: 10.1055/s-2002-20431
- Gunning, B. E. S., and Pate, J. S. (1974). “Transfer cells,” in *Dynamic Aspects of Plant Ultrastructure*, ed A. W. Robards (London: McGraw-Hill), 441–479.
- Harris, P. J., and Hartley, R. D. (1976). Detection of bound ferulic acid in cell walls of the Gramineae by ultraviolet fluorescence microscopy. *Nature* 259, 508–510. doi: 10.1038/259508a0
- Hatfield, R. D., and Fukushima, R. S. (2005). Can lignin be accurately measured? *Crop Sci.* 45, 832–839. doi: 10.2135/cropsci2004.0238
- Heide-Jørgensen, H. S., and Kuijt, J. (1994). Epidermal derivatives as xylem elements and transfer cells: a study of the host-parasite interface in two species of Triphysaria (Scrophulariaceae). *Protoplasma* 174, 173–183. doi: 10.1007/BF01379049
- Hejri, S., and Saboora, A. (2009). Removal of phenolic compounds from synthetic wastewaters by enzymatic treatments. *JSUT* 35, 13–19.
- Hepler, P., Fosket, D., and Newcomb, E. (1970). Lignification during secondary wall formation in Coleus: an electron microscopic study. *Am. J. Bot.* 57, 85–96. doi: 10.2307/2440382
- Hoffmann, P., and Parameswaran, N. (1976). On the ultrastructural localization of hemicelluloses within delignified tracheids of spruce. *Holzforschung* 30, 62–70. doi: 10.1515/hfsg.1976.30.2.62
- Joseleau, J.-P., and Ruel, K. (1997). Study of lignification by noninvasive techniques in growing maize internodes. *Plant Physiol.* 114, 1123–1133. doi: 10.1104/pp.114.3.1123
- Kraus, J. E., de Sousa, H. C., Rezende, M. H., Castro, N. M., Vecchi, C., and Luque, R. (1998). Astra blue and basic fuchsin double staining of plant materials. *Biotech. Histochem.* 73, 235–243.
- Kutsch, N. P., and Gray, J. R. (1972). The suitability of certain stains for studying lignification in Balsam Fir, *Abies balsamea* (L.) Mill. *Tech. Bull. Life Sci. Agric. Exp. Stn.* 53, 1–50.
- Kutsch, N. P., and McOrmond, R. R. (1972). The suitability of using fluorescence microscopy for studying lignification in balsam fir. *Tech. Bull. Life Sci. Agric. Exp. Stn.* 62, 1–15.
- Lawn, A. M. (1960). The use of potassium permanganate as an electron-dense stain for sections of tissue embedded in epoxy resin. *J. Biophys. Biochem. Cytol.* 7, 197–198. doi: 10.1083/jcb.7.1.197
- Lee, K. H., Singh, A. P., and Kim, Y. S. (2007). Cellular characteristics of a traumatic frost ring in the secondary xylem of *Pinus radiata*. *Trees* 21, 403–410. doi: 10.1007/s00468-007-0131-5
- Lewis, N. G., and Yamamoto, E. (1990). Lignin: occurrence, biogenesis and biodegradation. *Annu. Rev. Plant Physiol. Plant Mol. Biol.* 41, 455–496. doi: 10.1146/annurev.arplant.41.1.455
- Liu, C. J. (2012). Deciphering the enigma of lignification: precursor transport, oxidation, and the topochemistry of lignin assembly. *Mol. Plant* 5, 304–317. doi: 10.1093/mp/ssr121
- Ma, J. F., Yang, G. H., Mao, J. Z., and Xu, F. (2011). Characterization of anatomy, ultrastructure and lignin microdistribution in *Forsythia suspense*. *Ind. Crop. Prod.* 33, 358–363. doi: 10.1016/j.indcrop.2010.11.009
- Machado, J. (2004). *Caracterização do Desenvolvimento de Grãos de Milho (Zea mays L.) nos Estadios Iniciais de Desenvolvimento. Relatório de Estágio de Licenciatura em Ciências Agrárias*. Açores: Universidade dos Açores.
- McCurdy, D. W., Patrick, J. W., and Offler, C. E. (2008). Wall ingrowth formation in transfer cells: novel examples of localized wall deposition in plant cells. *Curr. Opin. Plant Biol.* 11, 653–661. doi: 10.1016/j.pbi.2008.08.005
- Migneault, I., Dartiguenave, C., Bertrand, M. J., and Waldron, K. C. (2004). Glutaraldehyde: behavior in aqueous solution, reaction with proteins, and application to enzyme crosslinking. *Biotechniques* 37, 790–802.
- Möller, R., Koch, G., Nanayakkara, B., and Schmitt, U. (2005). Lignification in cell cultures of *Pinus radiata*: activities of enzymes and lignin topochemistry. *Tree Physiol.* 26, 201–210. doi: 10.1093/treephys/26.2.201
- Monjardino, P., Machado, J., Gil, F. S., Fernandes, R., and Salema, R. (2007). Structural and ultrastructural characterization of maize coenocyte and endosperm cellularization. *Can. J. Bot.* 85, 216–223. doi: 10.1139/B06-156
- Monjardino, P., Rocha, S., Tavares, A. C., Fernandes, R., Sampaio, P., Salema, R., et al. (2013). Development of flange and reticulate wall ingrowths in maize (*Zea mays L.*) endosperm transfer cells. *Protoplasma* 250, 495–503. doi: 10.1007/s00709-012-0432-4
- Monjardino, P., Smith, A. G., and Jones, R. J. (2005). Heat stress effects on protein accumulation of maize endosperm. *Crop Sci.* 45, 1203–1210. doi: 10.2135/cropsci2003.0122
- Müsel, G., Schindler, T., Bergfeld, R., Ruel, K., Jacquet, G., Lapierre, C., et al. (1997). Structure and distribution of lignin in primary and secondary cell walls of maize coleoptiles analyzed by chemical and immunological probes. *Planta* 20, 146–159. doi: 10.1007/BF01007699

- Nadji, H., Diouf, P. N., Benaboura, A., Bedard, Y., Riedl, B., and Stevanovic, T. (2009). Comparative study of lignins isolated from Alfa grass (*Stipa tenacissima* L.). *Bioresour. Technol.* 100, 3585–3592. doi: 10.1016/j.biortech.2009.01.074
- Nakagawa, K., Yoshinaga, A., and Takabe, K. (2012). Anatomy and lignin distribution in reaction phloem fibres of several Japanese hardwoods. *Ann. Bot.* 110, 897–904. doi: 10.1093/aob/mcs144
- O'Brien, T. P. (1970). Further observations on hydrolysis of the cell wall in the xylem. *Protoplasma* 69, 1–14. doi: 10.1007/BF01276648
- Offler, C. E., McCurdy, D. W., Patrick, J. W., and Talbot, M. J. (2003). Transfer cells: cells specialized for a special purpose. *Annu. Rev. Plant Biol.* 54, 431–454. doi: 10.1146/annurev.arplant.54.031902.134812
- Pereira, R. C., Davide, L. C., Pedrozo, C. A., Carneiro, N. P., Souza, I. R. P., and Paiva, E. (2008). Relationship between structural and biochemical characteristics and texture of corn grains. *Genet. Mol. Res.* 7, 498–505. doi: 10.4238/vol7-2gmr446
- Prioul, J. L., Méchin, V., Lessard, P., Trevenot, C., Grimmer, M., Chateau-Joubert, S., et al. (2008). A joint transcriptomic, proteomic and metabolic analysis of maize endosperm development and starch filling. *Plant Biotechnol. J.* 6, 855–869. doi: 10.1111/j.1467-7652.2008.00368x
- Ride, J. P. (1975). Lignification in wounded wheat leaves in response to fungi and its possible role in resistance. *Physiol. Plant Pathol.* 5, 125–134. doi: 10.1016/0048-4059(75)90016-8
- Soyano, T., Thitamadee, S., Machida, Y., and Chua, N. H. (2008). Asymmetric leaves2-like19/lateral organ boundaries domain30 and asl20/lbd18 regulate tracheary element differentiation in *Arabidopsis*. *Plant Cell* 20, 3359–3373. doi: 10.1105/tpc.108.061796
- Stein, B. D., Klomparens, K. L., and Hammerschmidt, R. (1992). Comparison of bromine and permanganate as ultrastructural stains for lignin in plants infected by the fungus *Colletotrichum lagenarium*. *Microsc. Res. Tech.* 23, 201–206. doi: 10.1002/jemt.1070230302
- Svitelska, G. V., Gallios, G. P., and Zouboulis, A. I. (2004). Sonochemical decomposition of natural polyphenolic compound (condensed tannin). *Chemosphere* 56, 981–987. doi: 10.1016/j.chemosphere.2004.05.022
- Talbot, M. J., Offler, C. E., and McCurdy, D. W. (2002). Transfer cell architecture: a contribution towards understanding localized wall deposition. *Protoplasma* 219, 197–209. doi: 10.1007/s007090200021
- Tao, S., Shahrokh, K., Hua, Z., and Shaoling, Z. (2009). Anatomy, ultrastructure and lignin distribution of stone cells in two *Pyrus species*. *Plant Sci.* 176, 413–419. doi: 10.1016/j.plantsci.2008.12.011
- Vaughn, K. C., Talbot, M. J., Offler, C. E., and McCurdy, D. W. (2007). Wall ingrowths in epidermal transfer cells of *Vicia faba* cotyledons are modified primary walls marked by localized accumulations of arabinogalactan proteins. *Plant Cell Physiol.* 48, 159–168. doi: 10.1093/pcp/pcl047
- Wagner, A., Donaldson, L., Kim, H., Phillips, L., Flint, H., Steward, D., et al. (2009). Suppression of 4-coumarate-coa ligase in the coniferous gymnosperm *Pinus radiata*. *Plant Physiol.* 149, 370–383. doi: 10.1104/pp.108.125765
- Wang, Y., Chantreau, M., Sibout, R., and Hawkins, S. (2013). Plant cell wall lignification and monolignol metabolism. *Front. Plant Sci.* 4:220. doi: 10.3389/fpls.2013.00220
- Wi, S. G., Singh, A. P., Lee, K. H., and Kim, Y. S. (2005). The pattern of distribution of pectin, peroxidase and lignin in the middle lamella of secondary xylem fibres in alfalfa (*Medicago sativa*). *Ann. Bot.* 95, 863–868. doi: 10.1093/aob/mci092
- Xiang, Q., and Lee, Y. Y. (2000). Oxidative cracking of precipitated hardwood lignin by hydrogen peroxide. *Appl. Biochem. Biotechnol.* 84–86, 153–162. doi: 10.1385/ABAB:84-86:1-9:153
- Xu, F., Zhong, X. C., Sun, R. C., and Lu, Q. (2006). Anatomy, ultrastructure and lignin distribution in cell wall of *Caragana Korshinskii*. *Ind. Crop. Prod.* 24, 186–193. doi: 10.1016/j.indcrop.2006.04.002
- Xu, L., Zhu, L., Tu, L., Liu, L., Yuan, D., Jin, L., et al. (2011). Lignin metabolism has a central role in the resistance of cotton to the wilt fungus *Verticillium dahliae* as revealed by RNA-Seq-dependent transcriptional analysis and histochemistry. *J. Exp. Bot.* 62, 5607–5621. doi: 10.1093/jxb/err245
- Yao, R. S., Sun, M., Wang, C. L., and Deng, S. S. (2006). Degradation of phenolic compounds with hydrogen peroxide catalyzed by enzyme from *Serratia marcescens* AB 90027. *Water Res.* 40, 3091–3098. doi: 10.1016/j.watres.2006.06.009
- Young, T. E., and Gallie, D. R. (2000). Programmed cell death during endosperm development. *Plant Mol. Biol.* 44, 283–301. doi: 10.1023/A:1026588408152
- Zhang, K., Bhuiya, M. W., Pazo, J. R., Miao, Y., Kim, H., Ralph, J., et al. (2012). An engineered monolignol 4-o-methyltransferase depresses lignin biosynthesis and confers novel metabolic capability in *Arabidopsis*. *Plant Cell* 24, 3135–3152. doi: 10.1105/tpc.112.101287

**Conflict of Interest Statement:** The authors declare that the research was conducted in the absence of any commercial or financial relationships that could be construed as a potential conflict of interest.

*Received: 26 November 2013; accepted: 02 March 2014; published online: 20 March 2014.*

*Citation: Rocha S, Monjardino P, Mendonça D, da Câmara Machado A, Fernandes R, Sampaio P and Salema R (2014) Lignification of developing maize (*Zea mays L.*) endosperm transfer cells and starchy endosperm cells. *Front. Plant Sci.* 5:102. doi: 10.3389/fpls.2014.00102*

*This article was submitted to Plant Physiology, a section of the journal Frontiers in Plant Science.*

*Copyright © 2014 Rocha, Monjardino, Mendonça, da Câmara Machado, Fernandes, Sampaio and Salema. This is an open-access article distributed under the terms of the Creative Commons Attribution License (CC BY). The use, distribution or reproduction in other forums is permitted, provided the original author(s) or licensor are credited and that the original publication in this journal is cited, in accordance with accepted academic practice. No use, distribution or reproduction is permitted which does not comply with these terms.*



# On the track of transfer cell formation by specialized plant-parasitic nematodes

**Natalia Rodiuc<sup>1</sup>, Paulo Vieira<sup>2</sup>, Mohamed Youssef Banora<sup>3</sup> and Janice de Almeida Engler<sup>1,4 \*</sup>**

<sup>1</sup> Laboratório de Interação Molecular Planta-Praga, Embrapa Recursos Genéticos e Biotecnologia, PqEB, Brasília, Brasil

<sup>2</sup> NemaLab – Instituto de Ciências Agrárias e Ambientais Mediterrânicas, Universidade de Évora, Évora, Portugal

<sup>3</sup> Department of Plant Pathology, Faculty of Agriculture, Ain Shams University, Cairo, Egypt

<sup>4</sup> Institut National de la Recherche Agronomique, Plant, Health and Environment, Plant-Nematodes Interaction Team, UMR 1355 ISA/Centre National de la Recherche Scientifique, UMR 7254 ISA/Université de Nice-Sophia Antipolis, UMR ISA, Sophia-Antipolis, France

**Edited by:**

David McCurdy, The University of Newcastle, Australia

**Reviewed by:**

Woei-Jiun Guo, National Cheng Kung University, Taiwan

Rachel Burton, University of Adelaide, Australia

**\*Correspondence:**

Janice de Almeida Engler, Institut National de la Recherche Agronomique, Plant, Health and Environment, Plant-Nematodes Interaction Team, UMR 1355 ISA/Centre National de la Recherche Scientifique, UMR 7254 ISA/Université de Nice-Sophia Antipolis, UMR ISA, 400, Route des Chappes BP 167, Sophia-Antipolis, Cote D'Azur, France  
e-mail: janice.almeida-engler@sophia.inra.fr

Transfer cells are ubiquitous plant cells that play an important role in plant development as well as in responses to biotic and abiotic stresses. They are highly specialized and differentiated cells playing a central role in the acquisition, distribution and exchange of nutrients. Their unique structural traits are characterized by augmented ingrowths of invaginated secondary wall material, unsheathed by an amplified area of plasma membrane enriched in a suite of solute transporters. Similar morphological features can be perceived in vascular root feeding cells induced by sedentary plant-parasitic nematodes, such as root-knot and cyst nematodes, in a wide range of plant hosts. Despite their close phylogenetic relationship, these obligatory biotrophic plant pathogens engage different approaches when reprogramming root cells into giant cells or syncytia, respectively. Both nematode feeding-cells types will serve as the main source of nutrients until the end of the nematode life cycle. In both cases, these nematodes are able to remarkably maneuver and reprogram plant host cells. In this review we will discuss the structure, function and formation of these specialized multinucleate cells that act as nutrient transfer cells accumulating and synthesizing components needed for survival and successful offspring of plant-parasitic nematodes. Plant cells with transfer-like functions are also a renowned subject of interest involving still poorly understood molecular and cellular transport processes.

**Keywords:** **nematode feeding sites, transfer cells, wall ingrowths, galls, syncytia, root-knot nematodes, cyst nematodes**

## INTRODUCTION

The plant cell wall consists of a dynamic extracellular complex that responds to external and internal cellular signals, and forms a bridge between the plasma membrane and the cytoskeleton (Humphrey et al., 2007). The cell wall is formed of a network of polysaccharides and proteins and is multifunctional in plants: it maintains and determines the cell shape (Szymanski, 2009; Singh and Montgomery, 2011), resists internal turgor pressure (Haswell et al., 2008), controls cell and plant growth (Wolf et al., 2012), contributes to plant morphology (Hamant et al., 2010), regulates diffusion through the apoplast and is involved in perception and signaling during plant development and defense mechanisms (Hamann, 2012; Nühse, 2012; Underwood, 2012). Plant cell walls are composed of primary and secondary walls. The primary cell wall is laid down during cytokinesis and keeps expanding until cells acquire their final shape. The composition and heterogeneity of cell walls rely on developmental programs, in addition to environmental conditions (Burton et al., 2010). Secondary cell walls are thicker, and are deposited at the inner side of the primary cell wall mainly in highly specialized tissues and cell types such as xylem vessels and fiber cells. While most cells deposit a uniformly thickened secondary wall, some cells, e.g., tracheary elements (Hogetsu, 1991) and transfer cells (TCs; Gunning and Pate, 1974), build up an intricate secondary wall at restricted regions.

TCs are highly specialized cells that are found in algae and fungi, and in all *taxa* of the plant kingdom, suggesting that every plant has the genomic ability to develop TCs under a particular array of environmental status and/or developmental signals (Gunning and Pate, 1974; Offler et al., 2003; Andriunas et al., 2013). TCs are situated at regions of functional nutrient transport (Gunning and Pate, 1969, 1974) with the multifaceted wall ingrowth/plasma membrane complex often oriented to the track of solute flow. They facilitate apo/symplastic exchange of solutes and their cytoplasm is typically dense and organelle rich, with numerous mitochondria and organelles of the endomembrane secretory system situated nearby the extended wall ingrowths (Gunning et al., 1968; Davis et al., 1990). Vacuoles in TCs may be small or not present.

Generally, TCs develop from a range of differentiated cell types by a process that involves de-differentiation followed by re-differentiation named *trans*-differentiation (Andriunas et al., 2013). Examples are xylem or phloem parenchyma cells, pericycle and epidermal cells. Since TCs arise from differentiated plant cells, these are named according to the initial cell type, e.g., companion-cell TCs (Gunning et al., 1968; Wimmers and Turgeon, 1991; Haritatos et al., 2000), nucellar projection TCs (Wang et al., 1994), and so on. The *trans*-differentiation process occurs either during the normal developmental course of a particular plant tissue or takes place in response to an abiotic or biotic stress. The

ensuing TC has a distinctive wall harboring intricately invaginated ingrowths unsheathed by a plasma membrane enriched in nutrient transporter proteins (Offler et al., 2003). Ingrowths on walls in TCs generally present the reticulate or flange architecture or a combination of both (Talbot et al., 2002). TCs may well develop at both sides of the tissue interface or only at one side and ingrowths may be asymmetrically distributed.

Although little is known about the molecular signals that induce TC differentiation, some genes expressed associated with TCs have been described (Hueros et al., 1995, 1999; Gómez et al., 2002; Gutiérrez-Marcos et al., 2004; Muñiz et al., 2006). Among these the Myb-related protein-1 (*MRP-1*) was the first TC-specific transcriptional activator identified in plants (Gómez et al., 2002) and was shown to be a key regulator of TCs differentiation process in maize endosperm (Gómez et al., 2009). In addition, *MRP-1* regulates the expression of several TC-specific genes, like *BETL-1* and *BETL-2* (Gómez et al., 2002), *Meg-1* (for *Maternally Expressed Gene 1*; Gutiérrez-Marcos et al., 2004), and *TCRR-1* (for transfer cell response regulator 1; Muñiz et al., 2006), through its interaction with the corresponding promoters (Barrero et al., 2006) and of *BETL-9* and *BETL-10* promoters (Gómez et al., 2009).

Transfer cells can also develop associated with biotic symbionts (nitrogen-fixing bacteria and mycorrhiza) and plant pathogens (e.g., nematodes, leafhoppers, fungus; Pate and Gunning, 1972; Offler et al., 2003). TC establishment is also linked to interactions connected with a reciprocally beneficial trade of nutrients between host and symbiont. Examples are *Frankia* hyphae on *Alnus rubra* root hair infection directing the development of nitrogen-fixing root nodules (Berry et al., 1986), or root epidermal cells in association with mycorrhizas (Allaway et al., 1985) and *Rhizobium* nodules on pea roots (Gunning et al., 1968). Examples of TC induction in response to pathogen strike comprise injury of leafhopper on companion cells of *Medicago sativa* (alfalfa) internodes (Ecale-Zhou and Backus, 1999) and disease caused on *Duchesnea indica* leaf cells by rust fungus (Mims et al., 2001).

Infection of plant roots by plant-parasitic nematodes also lead to the development of root swellings containing specialized host-derived feeding structures, with which nematodes acquire nutrients. The most studied specialized feeding sites are induced by root-knot (RKN, *Meloidogyne* spp.) and cyst (CN, *Globodera* spp., *Heterodera* spp.) nematodes, designated giant cells and syncytia, respectively (Jones and Northcote, 1972a,b). However, other minor economic species belonging to other taxa, such as *Rotylenchulus* spp., *Nacobbus* spp., and *Xiphinema* spp., are also able to induce specialized feeding sites in the host roots. In the case of RKN and CN, both feeding-cell types have the function to feed the pathogen (Jones and Northcote, 1972a,b; Schemes in Figures 1A,B). Products secreted by nematodes through their stylet induce the differentiation of root cells into feeding structures and the content of this secretion remains largely unidentified (Mitchum et al., 2013).

The molecular and cellular processes involved in solute transport in plant tissues via TCs is yet poorly understood, even though vital for the survival of plants and particular biotrophic plant pathogens. This review will focus on data available on cells with transfer-like function induced by biotrophic sedentary

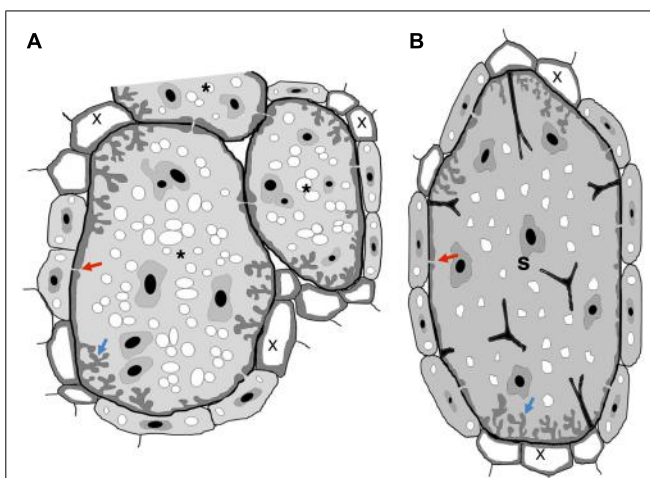


**FIGURE 1 | Schematic view of nematode feeding transfer-cells induced by plant-parasitic nematodes.** (A) Giant cells induced by RKN show cell wall thickenings with invaginations (blue arrow) often at the proximity of xylem vessels. Plasmodesmata (red arrow) also connect giant cells with phloem cells to facilitate solute transfer and may connect NCs. (B) Syncytium induced by a CN show cell wall thickenings with invaginations (blue arrow) often at the proximity of xylem vessels. Plasmodesmata (red arrow) also connect a syncytium with phloem cells to facilitate solute transfer and may connect NCs. Wall stubs are the result of cell dissolution of several root cells that fused to the syncytium itself. Asterisk, giant cell; X, xylem; S, syncytium.

plant-parasitic nematodes, such as RKN and CN nematodes. Cytological similarities between TCs suggest that at least part of the nematode feeding site developmental pathway might involve common routes regulating TC morphology and function.

## NEMATODE INDUCED TRANSFER CELLS: CELLULAR REARRANGEMENTS AND FUNCTION

Nematodes are devastating plant pathogens that trigger yield losses in numerous crop plants. A great part of the damage is caused by sedentary nematodes, which induce specialized feeding sites in plant roots, from which nutrients are withdrawn. Amongst these pathogens, CN (family Hoplolaimidae) and RKN nematodes (family Meloidogynidae) are considered the major economically important plant parasitic species (de Almeida Engler et al., 2005). Feeding sites induced by CN and RKN are regarded as resilient metabolic sinks (Grundler and Hofmann, 2011; Bartlem et al., 2014). Even though both feeding systems share common structural and functional features, their ontogeny differs considerably.

Root-knot nematodes induce galls composed of giant cells surrounded by neighboring cells (NCs), giving the root a shape of a knot (Figures 2A,B; de Almeida Engler et al., 1999, 2010). Giant cells are generated through sequential mitoses without cytokinesis (Huang and Maggenti, 1969; de Almeida Engler et al., 2004) and cycles of DNA replication (Jones and Payne, 1978; Wiggers et al., 1990; de Almeida Engler et al., 1999, 2012), leading to nuclear and cellular hypertrophy.

Cyst nematodes induce syncytia, formed by an initial feeding cell followed by fusion of hundreds of NCs causing root distension (Figures 2C,D; de Almeida Engler et al., 1999, 2010; Sobczak et al.,

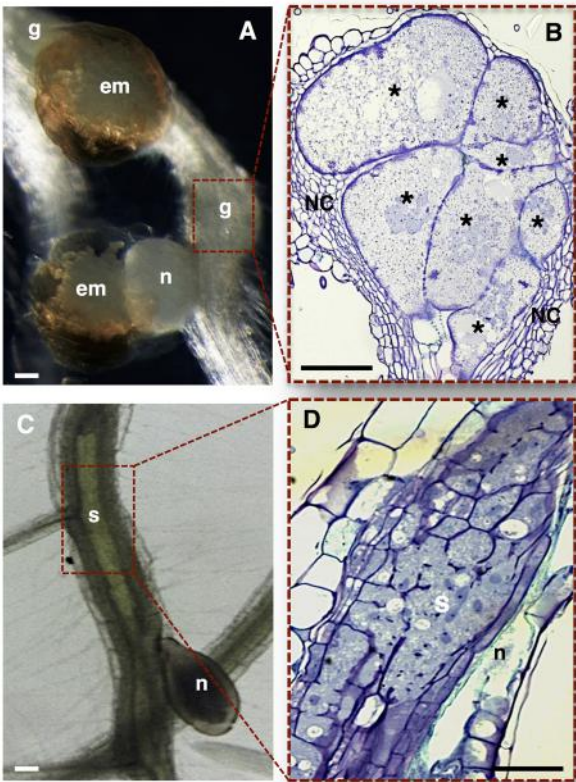


**FIGURE 2 | Nematode feeding sites induced by specialized sedentary biotrophic plant-parasitic nematodes. (A,B)** *Arabidopsis thaliana* roots infected with the RKN *Meloidogyne incognita*. **(A)** A typical gall induced in the plant host containing a mature female nematode, and associated gelatinous matrix filled with nematode eggs. **(B)** Longitudinal gall section containing seven multinucleated giant cells with unevenly thickened cell walls, surrounded by asymmetrically divided NCs. **(C,D)** *Arabidopsis thaliana* roots infected with the CN *Heterodera schachtii*. **(C)** A typical syncytium induced in plant host roots associated with a female CN. **(D)** Detailed longitudinal section of a syncytium resulting from the cell wall dissolution of several root cells. em, egg masses; g, gall; n, nematode; NC, neighboring cells; Asterisk, giant cells; S, syncytium. Bars = 50  $\mu$ m.

2011). The multinucleated state in a syncytium is most probably attained by cell wall dissolution of NCs (Endo, 1978) rather than by mitotic activity. Increase in cytoplasmic density and nuclear volume (de Almeida Engler et al., 1999, 2012) and cell wall modifications (Jones and Goto, 2011; Sobczak and Golinowski, 2011) have been observed for both syncytia and giant cells. Both feeding sites lead to root swellings disturbing water and nutrient transport thereby affecting plant growth.

Different arguments have been attributed to the choice of nematodes to induce feeding cells at the vascular parenchyma. The position of the initial syncytial cell ensures close contact of the feeding site at the proximity of the xylem and phloem necessary to provide nutrients to the developing gall (Bartlem et al., 2014) or syncytium. As well, the selected cells of the vascular tissue may be more amenable to the nematode-induced changes. Vascular parenchymal cells are not entirely differentiated and may thus be arrested at a particular cell cycle phase, allowing the switch to

other cell types like the nematode feeding site (de Almeida Engler et al., 2011). Roles of cortical or endodermal cells outside the vascular cylinder tissue have not yet been ascribed to syncytia induced by the CN, *Heterodera schachtii*, nor to galls induced by the RKN, *Meloidogyne incognita*, in *Arabidopsis thaliana* roots.

In the past years there has been extensive data reporting on the anatomy of the sophisticated nematode feeding sites induced by CN and RKN, comprising light, scanning and transmission electron microscopy (e.g., Bird, 1961; Jones and Dropkin, 1976; Wergin and Orion, 1981; Hussey and Mims, 1991; Berg et al., 2008; Sobczak and Golinowski, 2008). Both nematode feeding sites share common features, such as the increase of metabolic activity and cytoplasmic density, the replacement of a large central vacuole by several smaller ones, the large nuclei number of increased size, and the proliferation of organelles including Golgi stacks, mitochondria, plastids, ribosomes, and endoplasmic reticulum (Figure 3; Vieira et al., 2013 and Figure 4; Berg et al., 2008; Sobczak et al., 2011). Concomitant with the structural modifications in a gall or a syncytium, cell walls thicken and finger-like protuberances (ingrowths or cell wall labyrinths) form (Schemes in Figures 1, 3 and 4; Berg et al., 2008; Sobczak et al., 2011; Vieira et al., 2013) with the function to increase the membrane surface area for solute uptake (e.g., Golinowski et al., 1996; Hussey and Grundler, 1998). The cell wall degradation is also observed in syncytia (Scheme in Figures 1B and 2D; de Almeida Engler et al., 1999 and Figures 4A,B; Sobczak et al., 2011). Extensive changes of cell wall architecture in diverse types of TCs encountered in plants may comprise cell wall ingrowths and partial cell wall degradation (Offler et al., 2003) as occurring in syncytia. Increased giant cell wall ingrowths accompanied by intense surrounding vascularization will certainly contribute to the access to nutrient supply by the feeding nematode (Bartlem et al., 2014). Similar intense vascularization around syncytia will certainly enhance nutrient supply to the developing nematode.

Modifications of plant cell walls within nematode feeding cells appear to be coordinated by significant changes in host gene expression, as highlighted by a range of methods (e.g., Gheysen and Fenoll, 2002; Jammes et al., 2005; Hammes et al., 2005; Ithal et al., 2007a,b; Gheysen and Mitchum, 2009; Barcala et al., 2010; Damiani et al., 2012). Examples are plant cell wall and metabolism genes, shown to be differentially expressed in nematode feeding sites compared to uninfected root tissue. Although the origin of thickened cell walls, and elaborate cell wall labyrinths of combined reticulate or flange architecture are still not well understood, the elaborate structural design of nematode feeding cell walls reflects the hyperactivity of the cell wall synthesis machinery of the host plant. Similarly to walls of plant TCs (Offler et al., 2003), feeding cells are mainly composed of polysaccharides such as cellulose, hemicelluloses and pectin (Dropkin and Nelson, 1960; Littrell, 1966).

The large repertoire of host genes encoding plant cell wall modifying enzymes distinctively regulated in giant cells include for example; an extensin (*EXT*, Niebel et al., 1993), the expansin gene family (several members of  $\alpha$ - and  $\beta$ -expansins; Bar-Or et al., 2005; Jammes et al., 2005; Gal et al., 2006), a pectin acetyl esterase (putative pectin acetyl esterase, *PAE* homologue; Vercauteren et al.,

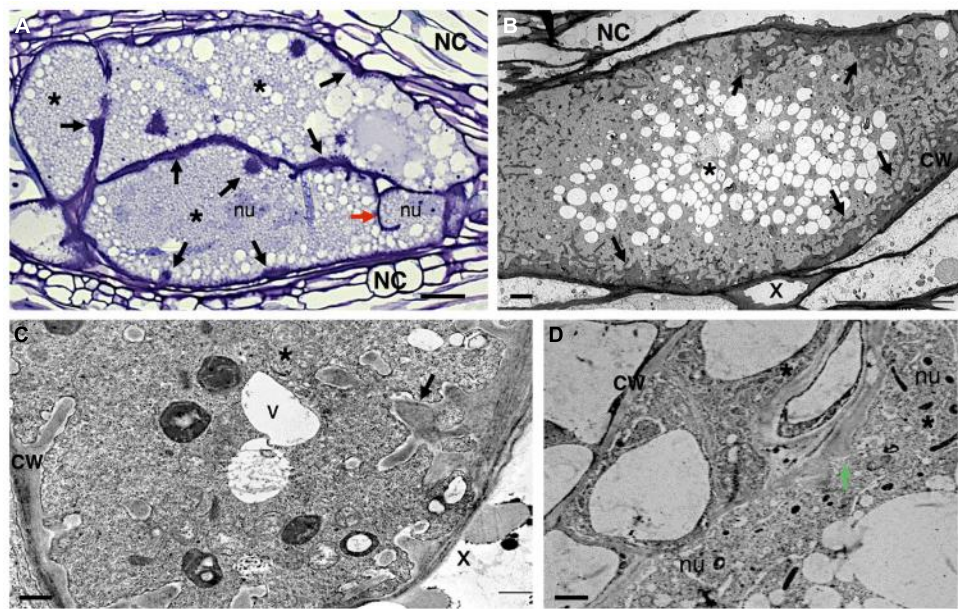


**FIGURE 3 | Anatomy of *Meloidogyne incognita*-induced giant cells in *Arabidopsis thaliana* roots. (A)** Light microscopy image of sectioned giant cells embedded in a gall and stained with toluidine blue. Cell wall thickenings (black arrows), and a cell wall stub (red arrow) indicating arrest of cytokinesis. **(B–D)** Ultra-structure of giant cell sections showing cell wall ingrowths (black arrows) along regions predominantly flanking

the vascular tissue. Note the xylem elements with thickened cell walls and dense cytoplasm containing numerous organelles including asymmetrically shaped nuclei and small vacuoles. **(D)** Detailed giant cells showing a PD (green arrow). Asterisk, giant cell; NC, neighboring cells; x, xylem; CW, cell wall; V, vacuole; nu, nucleus. Bars = **(A)** 25  $\mu$ m and **(B–D)** 5  $\mu$ m.

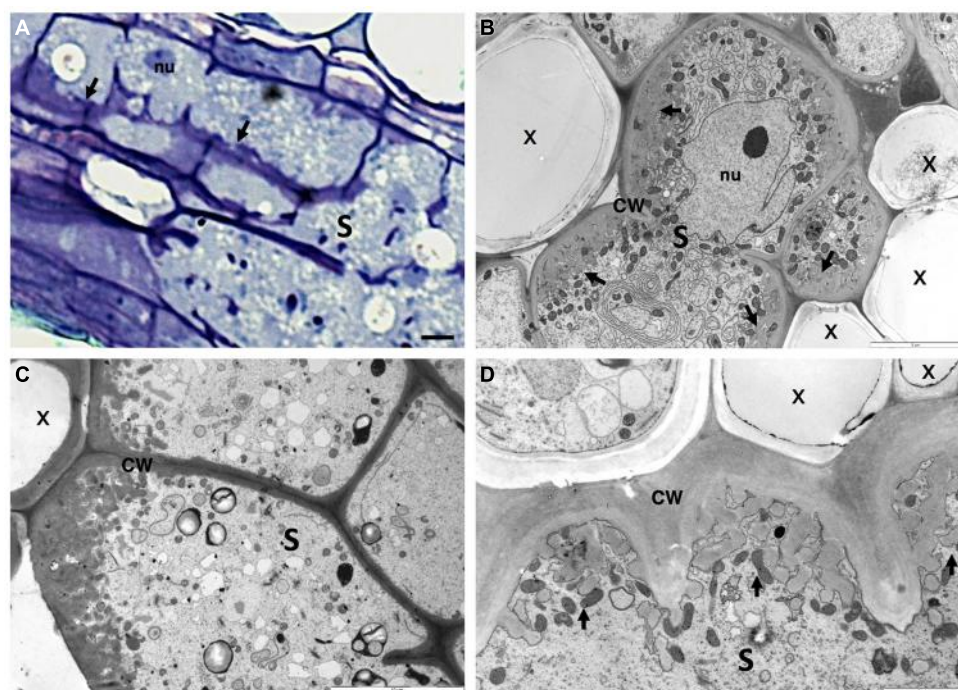


**FIGURE 4 | Anatomy of *Heterodera schachtii* induced-syncytium in *Arabidopsis thaliana* root cells. (A)** Light microscopy of a maturing syncytium section stained with toluidine blue, presenting cell wall thickenings (black arrows). **(B–D)** Ultra-structure of syncytia sections showing cell wall

ingrowths along regions mainly flanking the vascular tissue. Note the xylem elements with thickened cell walls and the dense cytoplasm containing numerous organelles including asymmetrically shaped nuclei and small vacuoles. S, syncytium; x, xylem; CW, cell wall; nu, nucleus. Bars = **(A)** 25  $\mu$ m.

2002), pectate lyases (*PEL*; Jammes et al., 2005) and endoglucanases (*endo- $\beta$ -1,4-glucanases*; Goellner et al., 2001; Sukno et al., 2006).

Similar cell wall related genes are up-regulated in syncytia, such as expansins ( $\alpha$ - and  $\beta$ -expansins; Golecki et al., 2002; Wieczorek et al., 2006; Fudali et al., 2008; Griesser and Grundler, 2008), endoglucanases (*endo- $\beta$ -1,4-glucanases*; Goellner et al., 2001; Wieczorek et al., 2008), *EXT*, and extension-like (*EXTL*) genes (Ithal et al., 2007a,b); polygalacturonases (*PG*; Mahalingam et al., 1999) and pectin acetylases (*PE*; Vercauteren et al., 2002; Ithal et al., 2007a,b). This data is suggestive of both unique and apparently common mechanisms orchestrated by these nematodes to provoke adaptations of the plant cell wall to facilitate feeding cell expansion and function.

Apart from cell wall changes pathogens may also locally interfere with signaling pathways changing the concentration of sugars such as sucrose (Hofmann et al., 2007) or plant hormones (e.g., Goverse and Bird, 2011; Rodiuc et al., 2012) in a coordinated manner that may directly or indirectly influence the function of feeding cells to act as TCs. Nematode secretions are likely to contain the proteins or peptides that can affect plant gene expression (Davis et al., 2008). In addition, for successful parasitism, nematodes can make use of plant genes as observed for the plant cell cycle or cytoskeleton machinery (de Almeida Engler et al., 1999, 2004, 2012; de Almeida Engler and Favory, 2011). Thus, nematodes may manipulate genes involved in cell wall rearrangements inducing the *trans*-differentiation of parenchyma vascular cells into giant or syncytial TCs.

### CELL WALL MODIFICATIONS AND CELLULAR COMMUNICATION IN ROOT-KNOT NEMATODE-INDUCED GIANT CELLS

As mentioned above, RKN species induce root galls containing giant-feeding cells in a large variety of plant hosts. In giant cells induced by RKN, wall thickening is observed as patches expanding, merging, branching and often of uneven cell wall material deposition at early stages of giant cell development suggesting an existing mechanism responsible for depositing irregular cell wall material (Figure 3; de Almeida Engler et al., 2004; Mordechai and Oka, 2006; Berg et al., 2008). Patches of wall thickenings are distributed in giant cells mainly in the proximity of the proliferating phloem and xylem elements, involved in the transfer of water and solutes, and may include NCs (Jones and Northcote, 1972a; Hoth et al., 2008). Throughout giant cell maturation these cell wall patches expand and cover large areas, generating regions with profuse reticulate TC wall labyrinths (Scheme in Figures 1A and 3; Berg et al., 2008; Vieira et al., 2013). It is fascinating to observe that cell wall ingrowths proliferate as RKN develop, then degenerate as nematodes reach maturity and complete their life cycle. Cell wall composition of young giant cells is similar to syncytia. Thus, these progressive cell wall changes suggest that the molecular dialog between nematodes and plant hosts is continuous, and might hold a key role in maintenance of the physiological status of giant cells (Jones and Northcote, 1972a).

Giant cells also present cell wall fragments, or stubs, thought initially to originate from cell wall breakdown as was observed in syncytia (Jones and Dropkin, 1975; Figure 3A; Vieira et al., 2013).

Subsequently, it has been demonstrated that cell wall stubs are the product of the abortion of phragmoplast expansion and cell wall formation (Jones and Payne, 1978; de Almeida Engler et al., 2004).

A significant demand for nutrients from feeding cells is created by nematodes. This is manifested by the development of TC wall labyrinths of wall ingrowths, an idea long sustained as a hallmark of giant cells (Jones and Northcote, 1972a,b; Jones and Gunning, 1976). These wall ingrowths notably increase the surface area of the plasma membrane, assisting the transport of nutrients into or out of the feeding cell, i.e., like symplast–apoplast exchange occurring in plant TCs (Gunning and Pate, 1969; Gunning et al., 1974; Offler et al., 2003). Furthermore, TC wall labyrinths can be observed on the cell walls of neighboring giant cells, indicating that nutrient transport in the apoplast, pooled from outlying cells, can be an important source of giant-cell nutrients. As shown by Berg et al. (2008), walls lying between giant cells are thickened and labyrinth-rich, suggesting that nutrients might also flow between these feeding cells (Jones and Northcote, 1972b; Jones and Gunning, 1976). As well, solutes that are phloem-derived are imported into the giant cells either via plasmodesmata (PD) (symplastically; Figure 3D; Vieira et al., 2013 and Figures 5B–E'; Hofmann et al., 2010; Vieira et al., 2012) or by means of active transport (apoplasmically).

Hofmann et al. (2010) gave insights into the role of PD frequency and distribution and callose deposition along cell walls of giant-feeding cells. This survey employed the double localization of callose and green fluorescent protein (GFP) in root sections. Initially, giant cells were reported to be symplastically isolated from NCs (Jones and Dropkin, 1976; Wolf et al., 1991; Hoth et al., 2008). Further studies using *Arabidopsis* transgenic plants containing a viral movement protein (MP) of the *Potato leaf roll polerovirus* fused to GFP (MP17PLRV-GFP; Hofius et al., 2001) as a PD marker (Figure 5A; Roberts and Oparka, 2003; Hofmann et al., 2010), reported that giant cells are connected by PD (Hofmann et al., 2010). No callose deposition has been detected in galls except in a number of NCs (Hofmann et al., 2010). Most viral MP attach to branched PD that are essentially secondary PD formed in existing cell walls. Primary PD are often not branched and appear during cell wall formation after cell division.

Plasmodesmata are unique membrane channels in plant cell walls that provide cytoplasmic continuity, cell-to-cell transport, and an intercellular exchange network (Crawford and Zambryski, 2000). The status of PD may change from closed to opened, allowing the flow of small or larger metabolites only when pertinent for plant tissue development (Kim and Zambryski, 2005). Inward compression of the plasma membrane can also play a role in reducing the size exclusion limit of the PD, or eventually cutting off solute passage (Wolf et al., 1991). As well, passage of most molecules is controlled by the size exclusion limit and therefore macromolecules such as proteins and RNA rely on specific trafficking processes. Passage through PD has to be tightly regulated due to its importance in signaling for information and solute exchange during plant cell development. In plant–nematode interactions, callose has been detected around the nematode stylet inserted into plant cells of *Criconemella xenoplax* (Hussey et al., 1992) and

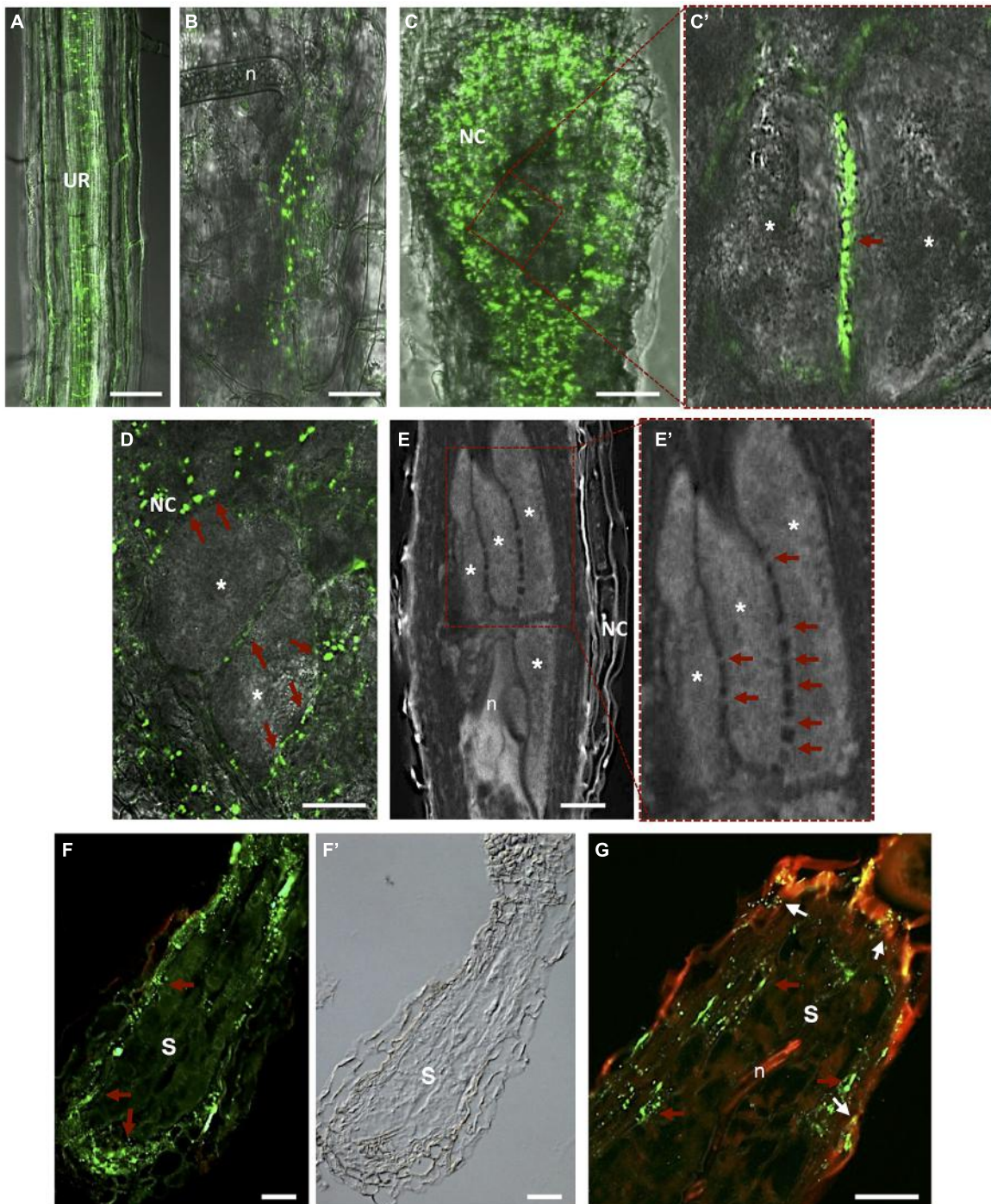


**FIGURE 5 |** Plasmodesmata localization in *Meloidogyne incognita*-induced galls and *Heterodera schachtii*-synctium in *Arabidopsis thaliana* roots. (A) In vivo localization of MP17<sup>PLRV</sup>-GFP (plasmodesmata localization marked by green fluorescence). In an uninfected root; (B) in a gall at early stage after nematode infection; and (C) in a mature gall. (C') Detail of two adjacent giant cells containing numerous PD (red arrow). (D) In vivo MP17<sup>PLRV</sup>-GFP localization between two giant cells and connecting NCs. Observations of Figures A–D were made on non- and infected material of *Arabidopsis* transgenic lines (35S:MP17<sup>PLRV</sup>-GFP). Non-infected roots, and galls were dissected from roots, embedded in 5% agar and fresh slices were observed using an

inverted confocal microscope. (E) Cleared whole-mount gall showing the complex network of PD between giant cells. (E') Detail of giant cells containing numerous PD (red arrows). (F,G) PD (red arrows point to green fluorescence of PD) in a section of a syncytium flanked by NCs, and (F') a differential interference contrast image is presented to show syncytium tissue morphology. (G) Double localization of PD (red arrows point to green fluorescence of PD) and callose (white arrows to yellow dots). Green dots hint at open PD whereas yellow dots suggest that solute transport can be blocked by callose in syncytia. UR, uninfected root; n, nematode; NC, neighboring cells; Asterisk, giant cell; S, syncytium. Bars = 50  $\mu$ m.

*H. schachtii* (Sobczak et al., 1999) and along PD of syncytia (Jones and Payne, 1977; Grundler et al., 1998). Deposition of callose ( $\beta$ -1,3-glucan) in the cell wall contiguous to PD, at both ends of the channel, may control the passage of water and solutes and can be transient or reversible. Numerous PD can be found in the cell walls of giant cells induced by RKN in *Arabidopsis*, suggesting massive symplastic solute transfer (Figure 5D; Hofmann et al., 2010). PD were detected not only in walls between giant cells but also in walls of NCs, including the proliferating vascular tissue (Figures 5B–E'; Hofmann et al., 2010; Vieira et al., 2012). Immunocytochemical analysis verified that these PD were not functionally impaired due to potential callose deposition, contrary to what is observed for syncytia. This suggests that the stress that RKN might cause to vascular parenchyma root cells dedifferentiated into feeding cells is not enough to induce callose deposition. The occurrence of cell wall ingrowths and PD at the feeding site induced by RKN thus imply that these cellular adaptations are responsible for bulk solute transport across the plasma membrane and via symplastic transport. In addition, solute transport may be aided by specialized membrane transport proteins that regulate the flow of nutrients into and out of giant cells. Giant cell morphology indicates that areas occupied by cell wall ingrowths have a lower frequency of PD (Huang and Maggenti, 1969; Jones, 1981) and thus regions with less wall ingrowths contain a higher density of PD.

## CELL WALL MODIFICATIONS AND CELLULAR COMMUNICATION IN A CYST NEMATODE-INDUCED SYNCYTUM

The initial syncytial cell induced by CN originates from a procambial cell for *Heterodera* spp. or a cortical parenchyma or endodermis cell for *Globodera* spp. (Golinowski et al., 1996; Sobczak et al., 2005). The first visible changes in this initial syncytial cell include alterations to the plant cell wall configuration and cell wall dissolution (Figures 2D and 4B; Golinowski et al., 1996; de Almeida Engler et al., 1999; Sobczak et al., 2011). The syncytium expands along the host root, NCs divide and fuse, and some cells differentiate into new xylem tissue (vessels) and phloem cells (sieve elements; Berg et al., 2008; Hoth et al., 2008). Although nematodes produce a range of cell wall degrading enzymes in their esophageal gland cells, which are secreted through the stylet (Mitchum et al., 2013), their specific involvement in the cell wall degradation within the syncytium is still unclear. The activity of plant cell wall degrading enzymes (Goellner et al., 2001) in syncytia suggest that degradation of cell walls in syncytium is mainly accomplished by plant enzymes, while nematode-specific enzymes assume greater importance for cell wall degradation and loosening during the migration of nematodes through the host root. Degradation of cell walls in syncytia accompanies the cell wall synthesis needed to produce cell wall ingrowths (Jones and Northcote, 1972a; Sobczak et al., 1997) close to the xylem and for the thickening of the outer cell wall of the syncytium (Golinowski et al., 1996).

In syncytia, finger-like cell wall ingrowths are elongated (Scheme in Figures 1B and 4; Sobczak et al., 2011), branch and form sophisticated reticulate labyrinths that expand apically, causing the basal parts of ingrowths to fuse, developing into extensive

cell wall thickenings. Deposition of wall ingrowths is only obvious around 5 to 7 days after CN infection once feeding cell development is well advanced (Golinowski et al., 1996). This indicates that wall ingrowth development may be a secondary response, unrelated to nematode feeding cell development (Jones and Northcote, 1972a), and might be caused by the augmented flow of solutes to the feeding nematode. While cell walls flanked by the syncytial elements are locally broken down, incorporating NCs into the syncytium (Golinowski et al., 1996; Grundler et al., 1998), the outer cell walls seem to be extended and thickened to resist augmented turgor pressure created inside the syncytium (Golinowski et al., 1996; Wieczorek et al., 2006). During nematode development, cell wall ingrowths fuse and form distinct depositions along the cell wall of the CN-induced syncytium. Thus, the formation and deposition of new ingrowths are continuously fashioned during nematode maturation (Golinowski et al., 1996; Sobczak et al., 2011), resulting in an increase of surface area of the plasma membrane at the interface predominantly between syncytium and xylem elements and phloem cells, facilitating water and nutrient transport into the syncytium.

Cell wall ingrowths occurring in syncytia, typical for TCs, involve myo-inositol oxygenases (MIOX; Kanter et al., 2005), which are strongly expressed in syncytia (Szakasits et al., 2009). MIOX genes are involved in the production of UDP- glucuronic acid, a precursor of sugars used for cell wall biosynthesis, and potentially involved in ascorbate synthesis (Lorenz et al., 2004). Thus, studies covering different aspects of cell wall rearrangements in a CN induced-syncytium reveal adjustments in cell wall morphology, thickness and possibly composition, presumably essential to maintain a functional feeding site. Likewise, the presence of cell wall ingrowths with transfer-like function most likely plays an important role in nutrient translocation to allow nematode development and reproduction.

Openings caused by cell fusion in the forming syncytium may also develop from PD that are widened and subsequently enlarged by gradual dissolution of cell walls (Jones and Northcote, 1972a; Wyss et al., 1984; Grundler et al., 1998). During the maturation of a syncytium wall in contact with vascular cells, invaginations develop at regions in close contact with the secondary xylem and phloem elements (Figure 4C; Golinowski et al., 1996; Sobczak et al., 2011). Nematode feeding is highly depending on transfer of solutes from neighboring phloem and xylem elements. The cell wall of a young syncytium thickens uniformly except for walls in contact with sieve tubes, which remain thin until the moment neighboring sieve tube cell wall start thickening (Grundler et al., 1998). Thus, an established syncytium is surrounded by thickened walls where NCs continue to be incorporated by progressive and local cell wall dissolution (Figures 4A,B; Sobczak et al., 2011). New cell wall openings can also be created between NC walls with no involvement of PD. After dissolution of the cell wall and middle lamella the plasmalemma fuses and the protoplast of the NC is incorporated into the syncytium. Often remnants of cell walls are present within an expanding syncytia (Figures 2D and 4; de Almeida Engler et al., 1999; Sobczak et al., 2011). Only a few PD are detected in young syncytia (Figures 5F,F'; Hofmann et al., 2010) and a temporal callose deposition implies impaired symplastic exchange (Figure 5G; Grundler et al., 1998; Hofmann

et al., 2007, 2010). Co-localization of MP17<sup>PLRV</sup>-GFP and callose confirmed the isolation of syncytia during the first days of feeding site development (**Figure 5G**; Hofmann et al., 2010). In the meantime, the outer syncytial wall becomes thickened and newly deposited cell wall material obstructs existing PD. This will lead to the symplastic isolation of young syncytia, thus nutrients are transported from phloem apoplastically via transmembrane carriers (Juergensen et al., 2003; Hofmann and Grundler, 2006). During syncytium development (4–7 days after inoculation-DAI) an increased frequency of PD is observed with less callose deposition, confirming previous fluorochrome transport studies (Hofmann and Grundler, 2006; Hofmann et al., 2007). At later developmental stages (>10 DAI), microscopy studies, in addition to microinjection assays, confirmed that syncytia are symplastically connected to new host phloem assembled as sieve elements and companion cells as illustrated by the presence of PD (Hoth et al., 2005, 2008; Hofmann et al., 2007, 2010). This symplastic transport is essential for transfer of nutrients into the syncytia and for nematode development.

It is a widespread event that plant tissues can switch between symplastic isolation to connectivity during development and functional analysis can validate this status. This has been shown for *Arabidopsis* embryos (Kim and Zambryski, 2005), or during cotton fiber elongation characterized by a period of symplastic isolation followed by increased expression of plasma membrane transporters and decreased callose PD gating (Ruan et al., 2001, 2004). Yet when mature syncytia are not symplastically isolated sucrose transporters are still required for additional sugar retrieval.

Functional analysis of the T-DNA line with an insertion in the exon of the  $\beta$ -1,3-glucanase (*AtBG\_ppap*; Levy et al., 2007) showed a reduced size of syncytia and the increased ratio of male nematodes after CN infection, suggesting stress conditions (Hofmann et al., 2010). The  $\beta$ -1,3-glucanase enzyme degrades callose deposited along PD. Decreased syncytial size most likely affected nutrient availability and nematode development, also affecting sexual differentiation (Betka et al., 1991). A second mutant line with a T-DNA insertion in the putative callose synthase gene *GLUCAN SYNTHASE-LIKE5* (*AtGSL5*), although showing a strong reduction in wound callose and papillary callose formation after mechanical wounding and infection with *Sphaerotheca fusca* (Jacobs et al., 2003), had no negative effect on nematode development (Hofmann et al., 2010). In fact, reduced callose deposition might facilitate PD-dependent cellular fusion during syncytium expansion, increasing its volume, thus enhancing nutrient availability for nematode growth (Hofmann et al., 2010).

Thus, the presence and functionality of PD in nematode-induced TCs may affect their structure, development, maintenance and morphogenesis through their impact on solute exchange. Unrestricted PD paths will assist intracellular communication facilitating solute import needed for the prompt nematode development and efficient reproduction.

## PLASMA MEMBRANE AND TRANSPORT FUNCTION OF NEMATODE FEEDING SITES

The main functions of TCs are nutrient and water transport. Both galls and syncytia are terminal sink tissues that require direct access to the plant vascular tissue (Jones, 1981; Grundler and

Hofmann, 2011). For nematodes, a food source coming from their feeding-TCs is essential for their development and reproduction. The presence in TCs of the typical “wall-membrane apparatus” provides evidence of an efficient mechanism facilitating transmembrane transport of solutes. Cell wall ingrowths are surrounded by the plasmalemma, amplifying significantly the symplast–apoplast interface (Pate and Gunning, 1972; Golikowski et al., 1996; Offler et al., 2003). The plasmalemma is tightly linked to cell wall protrusions and microtubules localized along wall ingrowths (Berg et al., 2008). Therefore, the large wall-membrane surface encountered in nematode feeding sites will facilitate great volumes of solute transfer. Sedentary nematodes need large amount of solutes containing nutrients and water to develop and reproduce in a short time. Thus, the presence of wall ingrowths increases short-distance solute transport between the apoplast (cell wall compartment) and symplast (cytoplasmic compartment) in plant cells. TCs are not the only cells particularly adapted for fast transport. As well, impressive solute fluxes can occur via PD symplastically linked as observed in nematode feeding sites (Hoth et al., 2008; Hofmann et al., 2010). Changes in cell size, as seen for giant cells, can also increase plasma membrane area as for cell wall ingrowths (Jones, 1981). As well, in species where TCs are absent, cells bordering the interface can become specialized for a transport function. Therefore, cells neighboring nematode feeding sites might be engaged to perform an analogous function. The occurrence of invaginations in giant cell walls and the large feeding-cell surface surrounded by NCs with transfer function would indubitably increase the efficiency of these feeding cells to import and translocate solutes to the feeding nematode. Increased plasma membrane surfaces in giant cells also requires increased proton pump and molecule carriers used for the translocation of nutrients to giant cells to nourish the nematode. As a consequence, genes encoding constitutive enzymes and structural proteins may be altered in their expression in order to support the increased cellular metabolic activity related to nematode feeding (Bleve-Zacheo and Melillo, 1997). Giant cells seem to employ a proton-coupled transport system located between the plasma membrane at wall ingrowths and xylem vessels (Dorhout et al., 1992; Grundler and Böckenhoff, 1997). Amino acid and sugar transport into plant cells is commonly assumed to be mediated by a proton force (Rheinhold and Kaplan, 1984) and there is evidence for a chemiosmotic model of proton-amino acid symport (Bush, 1993; DeWitt and Sussman, 1995). Sucrose/proton symport has also been observed in protoplasts derived from epidermal TCs of developing broad-bean cotyledons (McDonald et al., 1996).

Plasma membranes of TCs display large membrane potential dissimilarities (ranging from -150 to -200 mV at sites of solute influx; Jones et al., 1975; Robards and Stark, 1988; Bonnemain et al., 1991). These values are similar to other cell types implicated in solute influx like root hairs (Miedema et al., 2001). Membrane potential variation results from the activity of H<sup>+</sup>-ATPases, and most of these membrane proteins have been identified in plasma membranes of different TC types (Bouche-Pillon et al., 1994; McDonald et al., 1996; Harrington et al., 1997; Tegeder et al., 1999; Bagnall et al., 2000). The H<sup>+</sup>-ATPase gene has been found to be upregulated upon nematode infection in tomato roots (Bird

and Wilson, 1994). So far, two members of the  $\text{Ca}^{2+}$ -ATPase (ACA) family were verified to be upregulated in young nematode feeding sites (Hammes et al., 2005), implying a high energy demand (McClure, 1977; Gheysen and Fenoll, 2002). AtACA4 was localized to small vacuolar structures (Geisler et al., 2000) and is abundant at early stages of nematode feeding site development. Contrastingly, AtACA8 was located at the plasma membrane (Bonza et al., 2000) and its expression is higher in nematode feeding sites compared to uninfected root tissues, suggestive of playing a role during gall development. Thus, AtACA4, AtACA8, and AtCAX3 (Hirschi, 2001) a member of the  $\text{Ca}^{2+}$ :cation antiporter family, were proposed to modulate  $\text{Ca}^{2+}$ -mediated signaling events in plant cells (Sanders et al., 1999; Manohar et al., 2011), and most likely in nematode-induced feeding cells. Data generated by these studies suggests that  $\text{Ca}^{2+}$  influx and signaling are involved in nematode-induced giant-TC development (Hammes et al., 2005).

As mentioned herein, nematode feeding sites have been described as sink tissues supplied with phloem-derived solutes such as sugars. Sucrose has been described as the main transported sugar in the phloem of *Arabidopsis* from source to sink tissues (Haritatos et al., 2000; Kühn, 2003) and phloem is loaded both apoplasmically and symplastically. Sucrose is also the major source of carbohydrate into nematode feeding sites and metabolic analyses revealed considerably augmented sucrose levels in nematode-induced syncytia and giant cells (Hofmann et al., 2007; Baldacci-Cresp et al., 2012). Similarly, Hofmann et al. (2008) proposed that syncytia as induced plant structures make use of starch as an intermediate carbohydrate storage to compensate for the fluctuating sugar levels taking place during nematode feeding and development.

Phloem-specific sucrose transporters seem also to be involved in solute transport in nematode feeding sites. AtSUC2 is thought to recover sucrose into the phloem (Truernit and Sauer, 1995; Weise et al., 2000) whilst AtSUC4 seems to be in charge of phloem loading and unloading (Weise et al., 2000). In addition, sucrose transporters play a role in the development of sink tissues in various plant organs (Gottwald et al., 2000; Kühn, 2003). In young syncytia symplastic pathways are not functional and sucrose transporters like AtSUC2 and AtSUC4 seem critical for importing sucrose into syncytia (Juergensen et al., 2003; Hoth et al., 2008). Hofmann et al. (2007) reported that AtSUC4 silencing affected nematode development, suggesting its role during early syncytium development when no functional PD were present. Thus, it is believed that transporters are responsible for sucrose supply in young syncytia whereas at a later stage, connection to the phloem is established via PD although transporters seem also required for sucrose retrieval (Hofmann et al., 2007). The need to use different stratagems for solute retrieval from syncytia is understandable, given that a mature feeding site expands along the host root and must supply the nematode with enough solutes to grow and reproduce. In giant cells, sucrose is a major osmolyte and AtSUC1 induction is most likely involved in sucrose transport (Hammes et al., 2005).

Recently, Cabello et al. (2013) investigated the role of sucrose cleaving enzymes like sucrose synthases (SUS) and invertases (INV) during the CN, *H. schachtii* and RKN, *Meloidogyne javanica*

development, using single and multiple INV and SUS mutants. Both genes were shown to be transcriptionally regulated in nematode feeding sites (Szakasits et al., 2009; Barcala et al., 2010). Elevated sugar pools in multiple INV and SUS mutant lines promoted nematode development suggesting that these sugars have important nutritional value for the nematodes that may cleave sucrose with their own INVs (Grundler et al., 1991; Cabello et al., 2013). Syncytia and the plant shoot apex within these mutants exhibited changed sugar levels and enzyme activity suggestive of changes in the source-sink movement (Trouverie et al., 2003; Cabello et al., 2013). For the RKN, *Meloidogyne javanica*, development within INV and SUS mutants presented similar effects as observed for CN (Cabello et al., 2013). Hofmann et al. (2009) investigated, by Affymetrix gene chip, the expression of all genes annotated as sugar transporters in syncytia compared to non-infected roots using the *Arabidopsis* Membrane Protein Library. Expression of three significantly up-regulated (*STP12*, *MEX1*, and *GTP2*) and three down-regulated (*SFP1*, *STP7*, and *STP4*) genes in syncytia were validated by quantitative RT-PCR. While *STP4*, *STP7*, and *STP12* belong to the STP sugar transport protein family, *MEX1* and *GTP2* are plastidial transporter genes, and *SFP1* is a senescence-related monosaccharide transporter. A T-DNA insertion line of the most up-regulated gene (*STP12*) showed that insufficient sugar in feeding sites resulted in increased male ratios since females need higher sugar concentration in order to grow and reproduce (Hofmann et al., 2009). In addition, fluorescent-labeled glucose and membrane potential recordings performed following the application of several sugars deciphered sugar transporter activity across the plasma membrane of syncytia (Hofmann et al., 2009). Analyses of soluble sugar pools demonstrated a typical composition for syncytia. Besides sucrose, previously reported by Hofmann et al. (2007), glucose, galactose, raffinose, fructose, and trehalose were detected. Thus, sugar transporters are expressed and active in syncytia, indicative of their role in inter- and intracellular transport processes.

Besides sugars, amino acids are important as nutrient supply for nematode growth and development. Amino acids are the main form of transported organics, which is reduced nitrogen in the majority of plant species. Upon RKN infection noteworthy changes in the expression of genes involved in amino acid transport have been detected (Hammes et al., 2005, 2006; Marella et al., 2013). More peptide transporters than amino acid transporters were induced by CN (Puthoff et al., 2003). Most of the investigated amino acid transporters were expressed in galls suggesting a role for these transporters in the amino acid transport ability of infected roots (Fischer et al., 1995; Okumoto et al., 2002). Amino acid transporters of the amino acid permease (AAP) family were reported to be induced in syncytia (Szakasits et al., 2009; Hofmann et al., 2009). Also, amino acid transporters, like *AAP3* and *AAP6* were demonstrated to play a role during *Arabidopsis*-RKN interaction. RKN infection on *AtAAP3* and *AtAAP6* knock-out plants was significantly reduced in comparison with wild-type (Marella et al., 2013). Two putative auxin transporter genes of the AAAP (amino acid auxin permeases) superfamily, *AtAUX1* and *AtAUX4/LAX3*, were shown to be expressed in syncytia (Hammes et al., 2005). Beside of auxin that is essential for syncytia development (Viglierchio and Yu, 1968; Goverse et al., 2000), other

phytohormones such as cytokinin, ethylene, CLAVATA elements, CEP (C-terminally encoded peptide), and PSK (phytosulfokines) are also associated with the RKN or CN feeding cell formation (e.g., Goverse and Bird, 2011; Rodiuc et al., 2012). As well, the amino acid transporter, AtCAT6 is induced in giant cells similarly to other amino acid sink plant tissues, however, it is not essential for the establishment of RKN feeding sites (Hammes et al., 2006). This might be due to redundancy in transporter expression or compensatory expression of other transporters in *AtCAT6* knockout plants. In addition, nutrient loading into giant cells depends not only on the apoplastic step but also occurs symplastically via PD.

Water import into feeding sites seems to involve genes responsible for water transport (Grundler and Hofmann, 2011). Considering that the plasma membrane has a restricted ability for water transport and diffusion, this process can be assisted by aquaporins forming water pores along the plasmalemma (Johansson et al., 2000). Aquaporins in plants are observed within the plasma membrane and in the tonoplast (vacuolar membrane; Maurel et al., 1993; Kammerloher et al., 1994). Plasma membrane aquaporins and homologs are named PIPs (plasma membrane intrinsic proteins) and tonoplast aquaporins and homologs are called tonoplast intrinsic proteins (TIPs). Elevated expression of the aquaporins *TobRB7*, *AtPIP2.6* *AtPIP2.5* has been observed by microarray of *Meloidogyne incognita*-infected roots (Opperman et al., 1994; Hammes et al., 2005). Localization of *AtPIP2.5* in galls suggests that this gene might be a functional ortholog of a giant-cell-specific aquaporin *TobRB7* of tobacco (Opperman et al., 1994; Puthoff et al., 2003). *AtPIP2.5* was also induced upon infection with the beet CN, *H. schachtii* (Puthoff et al., 2003). Upregulation of both types of aquaporins (PIP and TIPs) in galls has been proposed to be associated with a volume increase of giant cells (Barcala et al., 2010). The developing nematode is continually ingesting the giant cell contents in order to rapidly grow and reproduce.

## CONCLUSIONS AND PERSPECTIVES

Plant parasitic nematodes are reliant on water and nutrient resources from their host plants. Feeding strategies applied by plant-parasitic nematodes will determine how efficient the supply of solutes will be. These strategies greatly depend on sophisticated cell wall modifications of the feeding site in order to transform vascular parenchymatic cells into TCs. These cellular adaptations are of key relevance in order that sedentary endoparasitic nematodes capture enough water and nutrient supply for their development and reproduction.

Nematode-induced syncytia or giant cells constitute a multinucleate model of TCs, and it is generally believed that wall protuberances arise as a result of nematode demand for nutrients. Although some information on solute supply has been mostly reported for syncytia induced by *H. schachtii* in *Arabidopsis*, many questions remain open. Currently it is not yet comprehensible what signals are employed to cause the establishment of these sink structures (galls and syncytia) and the transport occurring within these solute transfer sites involving the feeding cell and numerous phloem and xylem elements along this sink. It remains ambiguous as to what switches ordinary plant cells into transfer-feeding

cells that supply nematodes with solutes for their development and reproduction. These plant cellular morphological changes might be caused directly or indirectly by secreted products or feeding activity employed by the nematode during parasitism. What triggers and regulates the switch from apoplastic to symplastic solute supply and the gating of PD is yet to be discovered. Further functional genetic approaches as well as microscopic studies will help to elucidate genes involved in this process in order to comprehend how nematode induced TCs operate.

## ACKNOWLEDGMENTS

We thank Mirek Sobczak and Shahid Siddique for EM images of syncytia and Sophie Pagnotta for generating EM images of giant cells. We thank Julia Hofmann for supplying different references for the manuscript. NR was supported with grant of the National Council for Science and Technology (CNPq) and JAE had a 1 year foreign visiting professor grant from the Brazilian Federal Agency for Support and Evaluation of Graduate Education (CAPES) and work was supported by the CAPES/COFECUB program.

## REFERENCES

- Allaway, W. G., Carpenter, J. L., and Ashford, A. E. (1985). Amplification of inter-symbiont surface by root epidermal transfer cells in the *Pisonia myorrhiza*. *Protoplasma* 128, 227–231. doi: 10.1007/BF01276346
- Andriunas, F. A., Zhang, H.-M., Xia, X., Patrick, J. W., and Offler, C. E. (2013). Intersection of transfer cells with phloem biology—broad evolutionary trends, function, and induction. *Front. Plant Sci.* 4:221. doi: 10.3389/fpls.2013.00221
- Bagnall, N., Wang, X.-D., Scofield, G. N., Furbank, R. T., Offler, C. E., and Patrick, J. W. (2000). Sucrose transport-related genes are expressed in both maternal and filial tissues of developing wheat grains. *Aust. J. Plant Physiol.* 27, 1009–1020. doi: 10.1071/PP00012
- Baldacci-Cresp, F., Chang, C., Maucourt, M., Deborde, C., Hopkins, J., Lecomte, P., et al. (2012). (Homo)glutathione deficiency impairs root-knot nematode development in *Medicago truncatula*. *PLoS Pathog.* 8:e1002471. doi: 10.1371/journal.ppat.1002471
- Barcala, M., Garcia, A., Cabrera, J., Casson, S., Lindsey, K., Faverry, B., et al. (2010). Early transcriptomic events in microdissected *Arabidopsis* nematode-induced giant cells. *Plant J.* 61, 698–712. doi: 10.1111/j.1365-313X.2009.04098.x
- Bar-Or, C., Kapulnik, Y., and Kolta, H. (2005). A broad characterization of the transcriptional profile of the compatible tomato response to the plant parasitic root knot nematode *Meloidogyne javanica*. *Eur. J. Plant Pathol.* 111, 181–192. doi: 10.1007/s10658-004-2134-z
- Barrera, C., Muñiz, L. M., Gómez, E., Hueros, G., and Royo, J. (2006). Molecular dissection of the interaction between the transcriptional activator ZmMRP-1 and the promoter of BETL-1. *Plant Mol. Biol.* 62, 655–668. doi: 10.1007/s11103-006-9047-5
- Bartlem, D. G., Jones, M. G. K., and Hammes, U. Z. (2014). Vascularization and nutrient delivery at root-knot nematode feeding sites in host roots. *J. Exp. Bot.* 65, 1789–1798. doi: 10.1093/jxb/ert415
- Berg, R. H., Fester, T., and Taylor, C. G. (2008). “Development of the root-knot nematode feeding cell,” in *Plant Cell Monographs, Cell Biology of Plant Nematode Parasitism*, eds R. H. Berg and C. G. Taylor (Berlin Heidelberg: Springer), 115–152.
- Berry, A. M., McIntyre, L., and McCully, M. E. (1986). Fine structure of root hair infection leading to nodulation in the Frankia-Alnus symbiosis. *Can. J. Bot.* 64, 292–305. doi: 10.1139/l86-043
- Betka, M., Gründler, F. M. W., and Wyss, U. (1991). Influence of changes in the nurse cell system (syncytium) on sex determination and development of the cyst nematode *Heterodera schachtii*: single amino acids. *Phytopathology* 81, 75–79. doi: 10.1094/Phyto-81-75
- Bird, A. E. (1961). The ultrastructure and histochemistry of a nematode-induced giant-cell. *J. Biophys. Biochem. Cytol.* 11, 701–715. doi: 10.1083/jcb.11.3.701
- Bird, D. M., and Wilson, M. A. (1994). DNA sequence and expression analysis of root-knot nematode-elicited giant cell transcripts. *Mol. Plant Microbe Interact.* 7, 419–424. doi: 10.1094/MPMI-7-0419

- Bleve-Zacheo, T., and Melillo, M. (1997). "The biology of giant cells," in *Cellular and Molecular Aspects of Plant-Nematode Interaction*, eds C. Fenoll, F. M. W. Grundler, and S. A. OHL (Dordrecht: Kluwer Academic Publishers), 65–79.
- Bonnemain, J. L., Borquin, S., Renault, S., Offler, C., and Fisher, D. G. (1991). "Transfer cells: structure and physiology," in *Recent Advances in Phloem Transport and Assimilate Compartmentation*, Ouest Edn, eds J. L. Bonnemain, S. Delrot, W. L. Lucas, and L. Dainty (Nantes: Presses Académiques), 74–83.
- Bonza, M. C., Morandini, P., Luoni, L., Geisler, M., Palmgren, M. G., and De Michelis, M. I. (2000). At-ACA8 encodes a plasma membrane-localized calcium-ATPase of *Arabidopsis* with a calmodulin-binding domain at the N terminus. *Plant Physiol.* 123, 1495–1506. doi: 10.1104/pp.123.4.1495
- Bouche-Pillon, S., Fleurat-Lessard, P., Serrano, R., and Bonnemain, J. L. (1994). Asymmetric distribution of the plasma-membrane HC-ATPase in embryos of *Vicia faba* L. with special reference to transfer cells. *Planta* 193, 392–397. doi: 10.1007/BF00201818
- Burton, R. A., Gidley, M. J., and Fincher, G. B. (2010). Heterogeneity in the chemistry, structure and function of plant cell walls. *Nat. Chem. Biol.* 6, 724–732. doi: 10.1038/nchembio.439
- Bush, D. R. (1993). Proton-coupled sugar and amino acid transporters in plants. *Annu. Rev. Plant Physiol.* 44, 513–542. doi: 10.1146/annurev.pp.44.060193.002501
- Cabello, S., Lorenz, C., Crespo, S., Cabrera, J., Ludwig, R., Escobar, C., et al. (2013). Altered sucrose synthase and invertase expression affects the local and systemic sugar metabolism of nematode infected *Arabidopsis thaliana* plants. *J. Exp. Biol.* 65, 201–212. doi: 10.1093/jxb/ert359
- Crawford, K. M., and Zambryski, P. C. (2000). Subcellular localization determines the availability of non-target proteins to plasmodesmal transport. *Curr. Biol.* 10, 1032–1040. doi: 10.1016/S0960-9822(00)00657-6
- Damiani, I., Baldacci-Crespi, F., Hopkins, J., Andrio, E., Balzergue, S., Lecomte, P., et al. (2012). Plant genes involved in harbouring symbiotic rhizobia or pathogenic nematode. *New Phytol.* 194, 511–522. doi: 10.1111/j.1469-8137.2011.04046.x
- Davis, E. L., Hussey, R. S., and Baum, T. J. (2008). "Parasitism genes: what they reveal about parasitism," in *Plant Cell Monographs, Cell Biology of Plant Nematode Parasitism*, eds R. H. Berg and C. G. Taylor (Berlin Heidelberg: Springer), 15–44.
- Davis, R. W., Smith, J. D., and Cobb, B. G. (1990). A light and electron microscope investigation of the transfer cell region of maize caryopses. *Can. J. Bot.* 68, 471–479. doi: 10.1139/b90-063
- de Almeida Engler, J., De Vleesschauwer, V., Burssens, S., Celenza, J. L. J., Inzé, D., Van Montagu, M., et al. (1999). Molecular markers and cell cycle inhibitors show the importance of cell cycle progression in nematode-induced galls and syncytia. *Plant Cell* 11, 793–808. doi: 10.1105/tpc.11.5.793
- de Almeida Engler, J., Engler, G., and Gheysen, G. (2011). "Unravelling the plant cell cycle in nematode induced feeding sites," in *Genomics and Molecular Genetics of Plant-Nematode Interactions*, eds J. Jones, G. Gheysen, and C. Fenoll (Dordrecht: Springer Science+Business Media), 349–368.
- de Almeida Engler, J., and Favory, B. (2011). "The plant cytoskeleton remodelling in nematode induced feeding sites," in *Genomics and Molecular Genetics of Plant-Nematode Interactions*, eds J. Jones, G. Gheysen, and C. Fenoll (Dordrecht: Springer Science+Business Media), 369–393.
- de Almeida Engler, J., Favory, B., Engler, G., and Abad, P. (2005). Loss of susceptibility as an alternative for nematode resistance. *Curr. Opin. Biotech.* 16, 112–117. doi: 10.1016/j.copbio.2005.01.009
- de Almeida Engler, J., Kyndt, T., Vieira, P., Van Cappelle, E., Bouldolf, V., Sanchez, V., et al. (2012). CCS52 and DEL1 genes are key components of the endocycle in nematode induced feeding sites. *Plant J.* 72, 185–198. doi: 10.1111/j.1365-313X.2012.05054.x
- de Almeida Engler, J., Rodiuc, N., Smertenko, A., and Abad, P. (2010). Plant actin cytoskeleton re-modelling by plant parasitic nematodes. *Plant Signal. Behav.* 5, 213–217. doi: 10.4161/psb.5.3.10741
- de Almeida Engler, J., Van Poucke, K., Karimi, M., De Groodt, R., Gheysen, G., and Engler, G. (2004). Dynamic cytoskeleton rearrangements in giant cells and syncytia of nematode-infected roots. *Plant J.* 38, 12–26. doi: 10.1111/j.1365-313X.2004.02019.x
- DeWitt, N. D., and Sussman, M. R. (1995). Immunocytochemical localization of an epitope-tagged plasma membrane proton pump in phloem companion cells. *Plant Cell* 7, 2053–2067. doi: 10.1105/tpc.7.12.2053
- Dorhout, R., Kolloffel, C., and Gommers, F. J. (1992). Alteration of distribution of regions with high net proton extrusion in tomato roots infected with *Meloidogyne incognita*. *Physiol. Mol. Plant Pathol.* 40, 153–162. doi: 10.1016/0885-5765(92)90056-2
- Dropkin, V. H., and Nelson, P. E. (1960). The histopathology of root-knot nematode infections in soybeans. *Phytopathology* 50, 442–447.
- Ecale-Zhou, C. L., and Backus, E. A. (1999). Phloem injury and repair following potato leafhopper feeding on alfalfa stems. *Can. J. Bot.* 77, 537–547.
- Endo, B. Y. (1978). Feeding plug formation in soybean roots infected with the soybean cyst nematode. *Phytopathology* 68, 1022–1031. doi: 10.1094/Phyto-68-1022
- Fischer, W. N., Kwart, M., Hummel, S., and Frommer, W. B. (1995). Substrate specificity and expression profile of amino acid transporters (AAPs) in *Arabidopsis*. *J. Biol. Chem.* 270, 16315–16320. doi: 10.1074/jbc.270.27.16315
- Fudali, S., Janakowski, S., Sobczak, M., Griesser, M., Grundler, F. M., and Golinowski, W. (2008). Two tomato  $\alpha$ -expansins show distinct spatial and temporal expression patterns during development of nematode induced syncytia. *Plant Physiol.* 132, 370–383. doi: 10.1111/j.1399-3054.2007.01017.x
- Gal, T. Z., Aussenber, E. R., Burdman, S., Kapulnik, Y., and Kolai, H. (2006). Expression of a plant expansin is involved in the establishment of root-knot nematode parasitism in tomato. *Planta* 224, 155–162. doi: 10.1007/s00425-005-0204-x
- Geisler, M., Frangne, N., Gomes, E., Martinoia, E., and Palmgren, M. G. (2000). The ACA4 gene of *Arabidopsis* encodes a vacuolar membrane calcium pump that improves salt tolerance in yeast. *Plant Physiol.* 124, 1814–1827. doi: 10.1104/pp.124.4.1814
- Gheysen, G., and Fenoll, C. (2002). Gene expression in nematode feeding sites. *Annu. Rev. Phytopathol.* 40, 191–219. doi: 10.1146/annurev.phyto.40.121201.093719
- Gheysen, G., and Mitchum, M. G. (2009). "Molecular insights in the susceptible plant response to nematode infection," in *Plant Cell Monographs, Cell Biology of Plant Nematode Parasitism*, eds R. H. Berg and C. G. Taylor (Berlin Heidelberg: Springer), 45–81.
- Goellner, M., Wang, X., and Davis, E. L. (2001). Endo- $\beta$ -1,4-glucanase expression in compatible plant-nematode interactions. *Plant Cell* 13, 2241–2255. doi: 10.1105/tpc.010219
- Golecki, B., Fudali, S., Wieczorek, K., and Grundler, F. M. W. (2002). Identification and localisation of tomato expansin gene expression in nematode-induced syncytia. *Nematology* 4, 219.
- Golinowski, W., Grundler, F. M. W., and Sobczak, M. (1996). Changes in the structure of *Arabidopsis thaliana* during female development of the plant-parasitic nematode *Heterodera schachtii*. *Protoplasma* 194, 103–116. doi: 10.1007/BF01273172
- Gómez, E., Royo, J., Guo, Y., Thompson, R., and Hueros, G. (2002). Establishment of cereal endosperm expression domains: identification and properties of a maize transfer cell-specific transcription factor, ZmMRP-1. *Plant Cell* 14, 598–610. doi: 10.1105/tpc.010365
- Gómez, E., Royo, J., Muñiz, L. M., Sellam, O., Paul, W., Gerentes, D., et al. (2009). Maize transcription factor Myb-related protein-1 is a key regulator of the differentiation of transfer cells. *Plant Cell* 21, 2022–2035. doi: 10.1105/tpc.108.065409
- Goverse, A., and Bird, D. (2011). "The role of the plant hormones in nematode feeding cell formation," in *Genomics and Molecular Genetics of Plant-Nematode Interactions*, eds J. Jones, G. Gheysen, and C. Fenoll (Dordrecht: Springer Science+Business Media), 325–347.
- Goverse, A., Overmars, H., Engelbertink, J., Schots, A., Bakker, J., and Helder, J. (2000). Both induction and morphogenesis of cyst nematode feeding cells are mediated by auxin. *Mol. Plant Microbe Interact.* 13, 1121–1129. doi: 10.1094/MPMI.2000.13.10.1121
- Gottwald, J. R., Krysan, P. J., Young, J. C., Evert, R. F., and Sussman, M. R. (2000). Genetic evidence for the in planta role of phloem-specific plasma membrane sucrose transporters. *Proc. Natl. Acad. Sci. U.S.A.* 97, 13979–13984. doi: 10.1073/pnas.250473797
- Griesser, M., and Grundler, F. M. W. (2008). Quantification of tomato expansins in nematode feeding sites of cyst and root-knot nematodes. *J. Plant Dis. Prot.* 115, 263–272.
- Grundler, F. M. W., Betka, M., and Wyss, U. (1991). Influence of changes in the nurse cell system (syncytium) on sex determination and development of the

- cyst nematode *Heterodera schachtii*: total amounts of proteins and amino acids. *Phytopathology* 81, 70–74. doi: 10.1094/Phyto-81-70
- Grundler, F. M. W., and Böckenhoff, A. (1997). “Physiology of nematode feeding and feeding sites,” in *Cellular and Molecular Aspects of Plant-Nematode Interactions*, eds C. Fenoll, F. M. W. Grundler, and S. A. Ohl (Dordrecht: Kluwer Academic Publishers), 107–119. doi: 10.1007/978-94-011-5596-0\_9
- Grundler, F. M. W., and Hofmann, J. (2011). “Water and nutrient transport in nematode feeding sites,” in *Genomics and Molecular Genetics of Plant Nematode Interactions*, eds J. Jones, G. Gheysen, and C. Fenoll (Berlin Heidelberg: Springer), 423–439. doi: 10.1007/978-94-007-0434-3\_20
- Grundler, F. M. W., Sobczak, M., and Golinowski, W. (1998). Formation of cell wall openings in root cells of *Arabidopsis thaliana* following infection by the plant-parasitic nematode *Heterodera schachtii*. *Eur. J. Plant Pathol.* 104, 545–551. doi: 10.1023/A:1008692022279
- Gunning, B. E. S., and Pate, J. S. (1969). “Transfer cells” plant cells with wall ingrowths, specialized in relation to short distance transport of solutes—their occurrence, structure, and development. *Protoplasma* 68, 107–133. doi: 10.1007/BF01247900
- Gunning, B. E. S., and Pate, J. S. (1974). “Transfer cells,” in *Dynamic Aspects of Plant Ultrastructure*, ed. A. W. Robards (London: McGraw-Hill), 441–479.
- Gunning, B. E. S., Pate, J. S., and Briarty, L. G. (1968). Specialized “transfer cells” in minor veins of leaves and their possible significance in phloem translocation. *J. Cell Biol.* 37, 7–12. doi: 10.1083/jcb.37.3.C7
- Gunning, B. E. S., Pate, J. S., Minchin, F. R., and Marks, I. (1974). Quantitative aspects of transfer cell structure in relation to vein loading in leaves and solute transport in legume nodules. *Symp. Soc. Exp. Biol.* 28, 87–126.
- Gutiérrez-Marcos, J. F., Costa, L. M., Biderre-Petit, C., Khbaya, B., O’Sullivan, D. M., Wormald, M., et al. (2004). Maternally expressed gene1 is a novel maize endosperm transfer cell-specific gene with a maternal parent-of-origin pattern of expression. *Plant Cell* 16, 1288–1301. doi: 10.1105/tpc.019778
- Hamann, T. (2012). Plant cell wall integrity maintenance as an essential component of biotic stress response mechanisms. *Front. Plant Sci.* 3:77. doi: 10.3389/fpls.2012.00077
- Hamant, O., Traas, J., and Bouadaoud, A. (2010). Regulation of shape and patterning in plant development. *Curr. Opin. Genet. Dev.* 20, 454–459. doi: 10.1016/j.gde.2010.04.009
- Hammes, U. Z., Nielsen, E., Honaas, L. A., Taylor, C. G., and Schachtman, D. (2006). AtCAT6, a sink-tissue-localized transporter for essential amino acids in *Arabidopsis*. *Plant J.* 48, 414–426. doi: 10.1111/j.1365-313X.2006.02880.x
- Hammes, U. Z., Schachtman, D. P., Berg, R. H., Nielsen, E., Koch, W., McIntyre, L. M., et al. (2005). Nematode-induced changes of transporter gene expression in *Arabidopsis* roots. *Mol. Plant Microbe Interact.* 18, 1247–1257. doi: 10.1094/MPMI-18-1247
- Haritatos, E., Medville, R., and Turgeon, R. (2000). Minor vein structure and sugar transport in *Arabidopsis thaliana*. *Planta* 211, 105–111. doi: 10.1007/s004250000268
- Harrington, G. N., Franceschi, V. R., Offler, C. E., Patrick, J. W., Tegeder, M., Frommer, W. B., et al. (1997). Cell specific expression of three genes involved in plasma membrane sucrose transport in developing *Vicia faba* seed. *Protoplasma* 197, 160–173. doi: 10.1007/BF01288025
- Haswell, E. S., Peyronnet, R., Barbier-Brygoo, H., Meyerowitz, E. M., and Frachisse, J. M. (2008). Two MscS homologs provide mechanosensitive channel activities in the *Arabidopsis* root. *Curr. Biol.* 18, 730–734. doi: 10.1016/j.cub.2008.04.039
- Hirschi, K. (2001). Vacuolar H<sup>+</sup>/Ca<sup>2+</sup> transport: who’s directing the traffic? *Trends Plant Sci.* 6, 100–104. doi: 10.1016/S1360-1385(00)01863-X
- Hofius, D., Herbers, K., Melzer, M., Omid, A., Tacke, E., Wolf, S., et al. (2001). Evidence for expression level-dependent modulation of carbohydrate status and viral resistance by the Potato leafroll virus movement protein in transgenic tobacco plants. *Plant J.* 28, 529–543. doi: 10.1046/j.1365-313X.2001.01179.x
- Hofmann, J., and Grundler, F. M. W. (2006). Females and males of root parasitic cyst nematodes induce different symplasmic connections between their syncytial feeding cells and the phloem in *Arabidopsis thaliana*. *Plant Physiol. Biochem.* 44, 430–433. doi: 10.1016/j.plaphy.2006.06.006
- Hofmann, J., Banora, M. Y., De Almeida-Engler, J., and Grundler, F. M. W. (2010). The role of callose deposition along plasmodesmata in nematode feeding sites. *Mol. Plant Microbe Interact.* 23, 549–557. doi: 10.1094/MPMI-23-5-0549
- Hofmann, J., Hess, P. H., Szakasits, D., Blochl, A., Wieczorek, K., Daxböck-Horvath, S., et al. (2009). Diversity and activity of sugar transporters in nematode-induced root syncytia. *J. Exp. Bot.* 60, 3085–3095. doi: 10.1093/jxb/erp138
- Hofmann, J., Szakasits, D., Blochl, A., Sobczak, M., Daxböck-Horvath, S., Golinowski, W., et al. (2008). Starch serves as carbohydrate storage in nematode-induced syncytia. *Plant Physiol.* 146, 228–235. doi: 10.1104/pp.107.107367
- Hofmann, J., Wieczorek, K., Blochl, A., and Grundler, F. M. W. (2007). Sucrose supply to nematode-induced syncytia depends on the apoplasmic and symplasmic pathways. *J. Exp. Bot.* 58, 1591–1601. doi: 10.1093/jxb/erl285
- Hogetsu, T. (1991). Mechanism for formation of the secondary wall thickening in tracheary elements: microtubules and microfibrils of tracheary elements of *Pisum sativum* L. and *Commelinaceae* L. and the effects of amiprofoshomethyl. *Planta* 185, 190–200. doi: 10.1007/BF00194060
- Hoth, S., Schneidereit, A., Lauterbach, C., Scholz-Starke, J., and Sauer, N. (2005). Nematode infection triggers the de novo formation of unloading phloem that allows macromolecular trafficking of green fluorescent protein into syncytia. *Plant Physiol.* 138, 383–392. doi: 10.1104/pp.104.058800
- Hoth, S., Stadler, R., Sauer, N., and Hammes, U. Z. (2008). Differential vascularization of nematode-induced feeding sites. *Proc. Natl. Acad. Sci. U.S.A.* 105, 12617–12622. doi: 10.1073/pnas.0803835105
- Huang, J. S., and Maggenti, A. R. (1969). Mitotic aberrations and nuclear changes of developing giant cells in *Vicia faba* caused by root knot nematode, *Meloidogyne javanica*. *Phytopathology* 59, 447–455.
- Hueros, G., Royo, J., Maitz, M., Salamini, F., and Thompson, R. D. (1999). Evidence for factors regulating transfer cell-specific expression in maize endosperm. *Plant Mol. Biol.* 41, 403–414. doi: 10.1023/A:1006331707605
- Hueros, G., Varotto, S., Salamini, F., and Thompson, R. D. (1995). Molecular characterization of BET1, a gene expressed in the endosperm transfer cells of maize. *Plant Cell* 7, 747–757. doi: 10.1105/tpc.7.6.747
- Humphrey, T. V., Bonetta, D. T., and Goring, D. R. (2007). Sentinels at the wall: cell wall receptors and sensors. *New Phytol.* 176, 7–21. doi: 10.1111/j.1469-8137.2007.02192.x
- Hussey, R. S., and Grundler, F. M. W. (1998). “Nematode parasitism of plants,” in *The Physiology and Biochemistry of Free-Living and Plant-Parasitic Nematodes*, eds R. N. Perry and D. J. Wright (New York, NY: CABI International), 213–243.
- Hussey, R. S., and Mims, C. W. (1991). Ultrastructure of feeding tubes formed in giant-cells induced in plants by the root-knot nematode *Meloidogyne incognita*. *Protoplasma* 162, 99–107. doi: 10.1007/BF02562553
- Hussey, R. S., Mims, C. W., and Westcott, S. W. (1992). Immunocytochemical localization of callose in root cortical cells parasitized by the ring nematode *Criconemella xenoplax*. *Protoplasma* 171, 1–6. doi: 10.1007/BF01379274
- Ithal, N., Recknor, J., Nettleston, D., Hearne, L., Maier, T., Baum, T. J., et al. (2007a). Parallel genome-wide expression profiling of host and pathogen during soybean cyst nematode infection of soybean. *Mol. Plant Microbe Interact.* 20, 293–305. doi: 10.1094/MPMI-20-3-0293
- Ithal, N., Recknor, J., Nettleston, D., Maier, T., Baum, T. J., and Mitchum, M. G. (2007b). Developmental transcript profiling of cyst nematode feeding cells in soybean roots. *Mol. Plant Microbe Interact.* 20, 510–525. doi: 10.1094/MPMI-20-5-0510
- Jacobs, A. K., Lipka, V., Burton, R. A., Panstruga, R., Strizhov, N., Schulze-Lefert, P., et al. (2003). An *Arabidopsis* callose synthase, GSL5, is required for wound and papillary callose formation. *Plant Cell* 15, 2503–2513. doi: 10.1105/tpc.016009
- Jammes, F., Lecomte, P., de Almeida-Engler, J., Bitton, F., Martin-Magniette, M.-L., Renou, J. P., et al. (2005). Genome-wide expression profiling of the host response to root-knot nematode infection in *Arabidopsis*. *Plant J.* 44, 447–458. doi: 10.1111/j.1365-313X.2005.02532.x
- Johansson, I., Karlsson, M., Johanson, U., Larsson, C., and Kjellbom, P. (2000). The role of aquaporins in cellular and whole plant water balance. *Biochim. Biophys. Acta* 1465, 324–342. doi: 10.1016/S0005-2736(00)00147-4
- Jones, M. G. K. (1981). Host cell responses to endoparasitic nematode attack: structure and function of giant cells and syncytia. *Ann. Appl. Biol.* 97, 353–372. doi: 10.1111/j.1744-7348.1981.tb05122.x
- Jones, M. G. K., and Dropkin, V. H. (1975). Cellular alterations induced in soybean roots by three endoparasitic nematodes. *Physiol. Plant Pathol.* 5, 119–124. doi: 10.1016/0048-4059(75)90015-6
- Jones, M. G., and Dropkin, V. H. (1976). Scanning electron microscopy in nematode-induced giant transfer cells. *Cytobios* 15, 149–161.

- Jones, M. G. K., and Goto, D. B. (2011). "Root-knot nematodes and giant cells," in *Genomics and Molecular Genetics of Plant-Nematode Interactions*, eds J. Jones, G. Gheysen, and C. Fenoll (Dordrecht: Springer Science+Business Media), 83–100.
- Jones, M. G. K., and Gunning, B. E. S. (1976). Transfer cells and nematode induced giant cells in *Helianthemum*. *Protoplasma* 87, 273–279. doi: 10.1007/BF01623973
- Jones, M. G. K., and Northcote, D. H. (1972a). Nematode-induced syncytium – a multinucleate transfer cell. *J. Cell Sci.* 10, 789–809.
- Jones, M. G. K., and Northcote, D. H. (1972b). Multinucleate transfer cells induced in coleus roots by the root-knot nematode, *Meloidogyne arenaria*. *Protoplasma* 75, 381–395. doi: 10.1007/BF01282117
- Jones, M. G. K., Novacky, A., and Dropkin, V. H. (1975). Transmembrane potentials of parenchyma cells and nematode-induced transfer cells. *Protoplasma* 85, 15–37. doi: 10.1007/BF01567756
- Jones, M. G. K., and Payne, H. L. (1977). The structure of syncytia induced by the phytoparasitic nematode *Nacobbus aberrans* in tomato roots, and the possible role of plasmodesmata in their nutrition. *J. Cell Sci.* 23, 299–313.
- Jones, M. G. K., and Payne, H. L. (1978). Early stages of nematode-induced giant-cell formation in roots of impatiens balsamina. *J. Nematol.* 10, 70–84.
- Juergensen, K., Scholz-Starke, J., Sauer, N., Hess, P., van Bel, A. J. E., and Grundler, F. M. W. (2003). The companion cell-specific *Arabidopsis* disaccharide carrier AtSUC2 is expressed in nematode-induced syncytia. *Plant Physiol.* 131, 1–9. doi: 10.1104/pp.008037
- Kammerloher, W., Fischer, U., Piechottka, G. P., and Schaffner, A. R. (1994). Water channels in the plant plasma membrane cloned by immunoselection from a mammalian expression system. *Plant J.* 6, 187–199. doi: 10.1046/j.1365-313X.1994.6020187.x
- Kanter, U., Usadel, B., Guerineau, F., Li, Y., Pauly, M., and Tenhaken, R. (2005). The inositol oxygenase gene family of *Arabidopsis* is involved in the biosynthesis of nucleotide sugar precursors for cell-wall matrix polysaccharides. *Planta* 221, 243–254. doi: 10.1007/s00425-004-1441-0
- Kim, I., and Zambryski, P. C. (2005). Cell-to-cell communication via plasmodesmata during *Arabidopsis* embryogenesis. *Curr. Opin. Plant Biol.* 8, 1–7. doi: 10.1016/j.pbi.2005.09.013
- Kühn, C. (2003). A comparison of the sucrose transporter systems of different plant species. *Plant Biol.* 5, 215–232. doi: 10.1055/s-2003-40798
- Levy, A., Erlanger, M., Rosenthal, M., and Epel, B. L. (2007). A plasmodesmata-associated b-1,3-glucanase in *Arabidopsis*. *Plant J.* 49, 669–682. doi: 10.1111/j.1365-313X.2006.02986.x
- Littrell, R. H. (1966). Cellular responses of *Hibiscus esculentum* to *Meloidogyne incognita*. *Phytopathology* 56, 540–544.
- Lorenz, A., Chevone, B. I., Mendes, P., and Nessler, C. L. (2004). Myo-inositol oxygenase offers a possible entry point into plant ascorbate biosynthesis. *Plant Physiol.* 134, 1200–1205. doi: 10.1104/pp.103.033936
- Mahalingam, R., Wang, G., and Knap, K. H. (1999). Polygalacturonase and polygalacturonase-inhibitor protein: gene and transcription in glycine max-heterodera glycines interaction. *Mol. Plant Microbe Interact.* 12, 490–498. doi: 10.1094/MPMI.1999.12.6.490
- Manohar, M., Shigaki, T., and Hirschi, K. D. (2011). Plant cation/H<sup>+</sup> exchangers (CAxS): biological functions and genetic manipulations. *Plant Biol.* 13, 561–569. doi: 10.1111/j.1438-8677.2011.00466.x
- Marella, H. H., Nielsen, E., Schachtman, D. P., and Taylor, C. G. (2013). The amino acid permeases APP3 and AAP6 are involved in root-knot nematode parasitism of *Arabidopsis*. *Mol. Plant Microbe Interact.* 26, 44–54. doi: 10.1094/MPMI-05-1213-FI
- Maurel, C., Reizer, J., Schroeder, J. I., and Chrispeels, M. J. (1993). The vacuolar membrane protein Q-TIP creates water specific channels in *Xenopus* oocytes. *EMBO J.* 12, 2241–2247.
- McClure, M. A. (1977). *Meloidogyne incognita*: a metabolic sink. *J. Nematol.* 9, 88–90.
- McDonald, R., Fieuw, S., and Patrick, J. W. (1996). Sugar uptake by the dermal transfer cells of the developing cotyledons of *Vicia faba* L.: mechanism of energy coupling. *Planta* 198, 502–509. doi: 10.1007/BF00262635
- Miedema, H., Bothwell, J. H. F., Brownlee, C., and Davies, J. M. (2001). Calcium uptake by plant cells-channels and pumps acting in concert. *Trends Plant Sci.* 6, 514–519. doi: 10.1016/S1360-1385(01)02124-0
- Mims, C. W., Rodriguez-Loether, C., and Richardson, E. A. (2001). Ultrastructure of the host-parasite interaction in leaves of *Duchesnea indica* infected by the rust fungus *Frommeela mexicana* var. *indicae* as revealed by high pressure freezing. *Can. J. Bot.* 79, 49–57. doi: 10.1139/b00-139
- Mitchum, M. G., Hussey, R. S., Baum, T. J., Wang, X., Elling, A. A., Wubben, M., et al. (2013). Nematode effector proteins: an emerging paradigm of parasitism. *New Phytol.* 199, 879–894. doi: 10.1111/nph.12323
- Mordechai, M. M., and Oka, Y. (2006). Histological studies of giant cells formed by the root-knot nematode *Meloidogyne artiellia* as compared with *M. hapla* and *M. javanica* in cabbage, turnip and barley. *Phytoparasitica* 34, 502–509. doi: 10.1007/BF02981206
- Muñiz, L. M., Royo, J., Gómez, E., Barrero, C., Bergareche, D., and Hueros, G. (2006). The maize transfer cell-specific type-A response regulator ZmTCRR-1 appears to be involved in intercellular signalling. *Plant J.* 48, 17–27. doi: 10.1111/j.1365-313X.2006.02848.x
- Niebel, A., de Almeida Engler, J., Tire, C., Engler, G., Van Montagu, M., and Gheysen, G. (1993). Induction patterns of an extension gene in tobacco upon nematode infection. *Plant Cell* 5, 1697–1710.
- Nühse, T. (2012). Cell wall integrity signaling and innate immunity in plants. *Front. Plant Sci.* 3:280. doi: 10.3389/fpls.2012.00280
- Offler, C. E., McCurdy, D. W., Patrick, J. W., and Talbot, M. J. (2003). Transfer cells: cells specialized for a special purpose. *Annu. Rev. Plant Biol.* 54, 431–454. doi: 10.1146/annurev.arplant.54.031902.134812
- Okumoto, S., Schmidt, R., Tegeder, M., Fischer, W. N., Rentsch, D., Frommer, W. B., et al. (2002). High affinity amino acid transporters specifically expressed in xylem parenchyma and developing seeds of *Arabidopsis*. *J. Biol. Chem.* 277, 45338–45346. doi: 10.1074/jbc.M207730200
- Opperman, C. H., Taylor, C. G., and Conkling, M. A. (1994). Root-knot nematode-directed expression of a plant root-specific gene. *Science* 263, 221–223. doi: 10.1126/science.263.5144.221
- Pate, J. S., and Gunning, B. E. S. (1972). Transfer cells. *Annu. Rev. Plant Physiol.* 23, 173–196. doi: 10.1146/annurev.pp.23.060172.001133
- Puthoff, D. P., Nettleton, D., Rodermel, S. R., and Baum T. J. (2003). *Arabidopsis* gene expression changes during cyst nematode parasitism revealed by statistical analyses of microarray expression profiles. *Plant J.* 33, 911–921. doi: 10.1046/j.1365-313X.2003.01677.x
- Rheinhold, L., and Kaplan, A. (1984). Membrane transport of sugar and amino acids. *Annu. Rev. Plant Physiol.* 35, 45–83. doi: 10.1146/annurev.pp.35.060184.000401
- Robards, A. W., and Stark, M. (1988). Nectar secretion in Abutilon: a new model. *Protoplasma* 142, 79–91. doi: 10.1007/BF01290866
- Roberts, A. G., and Oparka, K. J. (2003). Plasmodesmata and the control of symplastic transport. *Plant Cell Environ.* 26, 103–124. doi: 10.1046/j.1365-3040.2003.00950.x
- Rodiuc, N., Marco, Y., Favory, B., and Keller, H. (2012). Plant resistant to pathogens and methods for production thereof. EP 2601296.
- Ruan, Y.-L., Llewellyn, D. J., and Furbank, R. T. (2001). The control of single-celled cotton fiber elongation by developmentally reversible gating of plasmodesmata and coordinated expression of sucrose and K<sup>+</sup> transporters and expansin. *Plant Cell* 13, 47–60.
- Ruan, Y.-L., Xu, S.-M., White, R., and Furbank, R. T. (2004). Genotypic and developmental evidence for the role of plasmodesmatal regulation in cotton fiber elongation mediated by callose turnover. *Plant Physiol.* 136, 4104–4113. doi: 10.1104/pp.104.051540
- Sanders, D., Brownlee, C., and Harper, J. F. (1999). Communicating with calcium. *Plant Cell* 11, 691–706.
- Singh, S. P., and Montgomery, B. L. (2011). Determining cell shape: adaptive regulation of cyanobacterial cellular differentiation and morphology. *Trends Microbiol.* 19, 278–285. doi: 10.1016/j.tim.2011.03.001
- Sobczak, M., Avrova, A., Jupowicz, J., Phillips, M. S., Ernst, K., and Kumar, A. (2005). Characterization of susceptibility and resistance responses to potato cyst nematode (*Globodera* spp.) infection of tomato lines in the absence and presence of the broad-spectrum nematode resistance Hero gene. *Mol. Plant Microbe Interact.* 18, 158–168. doi: 10.1094/MPMI-18-0158
- Sobczak, M., Fudali, S., and Wieczorek, K. (2011). "Cell wall modifications induced by nematodes," in *Genomics and Molecular Genetics of Plant-Nematode Interactions*, eds J. T. Jones, C. Fenoll, and G. Gheysen (Dordrecht: Springer Science+Business Media), 395–421.

- Sobczak, M., and Golinowski, W. (2008). "Structure of cyst nematode feeding sites," in *Plant Cell Monographs, Cell Biology of Plant Nematode Parasitism*, eds R. H. Berg and C. G. Taylor (Berlin Heidelberg: Springer), 153–187.
- Sobczak, M., and Golinowski, W. (2011). "Cyst nematodes and syncytia," in *Genomics and Molecular Genetics of Plant-Nematode Interactions*, eds J. Jones, C. Fenoll, and G. Gheysen (Dordrecht: Springer Science+Business Media B.V.), 61–82. doi: 10.1007/978-94-007-0434-3\_4
- Sobczak, M., Golinowski, W., and Grundler, F. M. W. (1997). Changes in the structure of *Arabidopsis thaliana* roots induced during development of males of the plant parasitic nematode *Heterodera schachtii*. *Eur. J. Plant Pathol.* 103, 113–124. doi: 10.1023/A:1008609409465
- Sobczak, M., Golinowski, W., and Grundler, F. M. W. (1999). Ultrastructure of feeding plugs and feeding tubes formed by *Heterodera schachtii*. *Nematology* 1, 363–374. doi: 10.1163/156854199508351
- Sukno, S., Shimerling, O., McGuiston, J., Tsabary, G., Shani, Z., Shoseyov, O., et al. (2006). Expression and regulation of the *Arabidopsis thaliana* cell Endo-1,4- $\beta$ -glucanase gene during compatible plant-nematode interactions. *J. Nematol.* 38, 354–361.
- Szakasits, D., Heinen, P., Wieczorek, K., Hofmann, J., Wagner, F., Kreil, D., et al. (2009). The transcriptome of syncytia induced by the cyst nematode *Heterodera schachtii* in *Arabidopsis* roots. *Plant J.* 57, 771–784. doi: 10.1111/j.1365-313X.2008.03727.x
- Szymanski, D. B. (2009). Plant cells taking shape: new insights into cytoplasmic control. *Curr. Opin. Plant Biol.* 12, 735–744. doi: 10.1016/j.pbi.2009.10.005
- Talbot, M. J., Offler, C. E., and McCurdy, D. W. (2002). Transfer cell wall architecture: a contribution towards understanding localized wall deposition. *Protoplasma* 219, 197–209. doi: 10.1007/s007090200021
- Tegeder, M., Wang, X.-D., Frommer, W. B., Offler, C. E., and Patrick, J. W. (1999). Sucrose transport into developing seeds of *Pisum sativum* L. *Plant J.* 18, 151–161. doi: 10.1046/j.1365-313X.1999.00439.x
- Trouverie, J., Thevenot, C., Rocher, J., Sotta, B., and Prioul, J. (2003). The role of abscisic acid in the response of a specific vacuolar invertase to water stress in the adult maize leaf. *J. Exp. Bot.* 54, 2177–2186. doi: 10.1093/jxb/erg234
- Truernit, E., and Sauer, N. (1995). The promotor of the *Arabidopsis thaliana* SUC2 sucrose-H<sup>+</sup> symporter gene directs expression of b-glucuronidase to the phloem: evidence of phloem loading and unloading by SUC2. *Planta* 196, 564–570. doi: 10.1007/BF00203657
- Underwood, W. (2012). The plant cell wall: a dynamic barrier against pathogen invasion. *Front. Plant Sci.* 3:85. doi: 10.3389/fpls.2012.00085
- Vercauteren, I., De Almeida Engler, J., De Groot, R., and Gheysen, G. (2002). An *Arabidopsis thaliana* pectin acetyl esterase gene is upregulated in nematode feeding sites induced by root-knot and cyst nematodes. *Mol. Plant Microbe Interact.* 15, 404–407. doi: 10.1094/MPMI.2002.15.4.404
- Vieira, P., Engler, G., and de Almeida Engler, J. (2012). Whole-mount confocal imaging of nuclei in giant feeding-cells induced by root-knot nematodes in *Arabidopsis*. *New Phytol.* 195, 488–496. doi: 10.1111/j.1469-8137.2012.04175.x
- Vieira, P., Escudero, C., Rodiuc, N., Boruc, J., Russinova, E., Glab, N., et al. (2013). Ectopic expression of Kip-related proteins restrains root-knot nematode-feeding site expansion. *New Phytol.* 199, 505–509. doi: 10.1111/nph.12255
- Viglierchio, D. R., and Yu, P. K. (1968). Plant growth substances and plant parasitic nematodes. II. Host influence on auxin content. *Exp. Parasitol.* 23, 88–95. doi: 10.1016/0014-4894(68)90046-5
- Wang, H.-L., Offler, C. E., and Patrick, J. W. (1994). Nucellar projection transfer cells in the developing wheat grain. *Protoplasma* 182, 39–52. doi: 10.1007/BF01403687
- Weise, A., Barker, L., Kühn, C., Lalonde, S., Buschmann, H., Frommer, W. B., et al. (2000). A new subfamily of sucrose transporters, SUT4, with low affinity/high capacity localized in enucleate sieve elements of plants. *Plant Cell* 12, 1345–1355.
- Wergin, W. P., and Orion, D. (1981). Scanning electron microscope study of the root-knot nematode (*Meloidogyne incognita*) on tomato root. *J. Nematol.* 13, 358–367.
- Wieczorek, K., Golecki, B., Gerdes, L., Heinen, P., Szakasits, D., Durachko, D. M., et al. (2006). Expansins are involved in the formation of nematode-induced syncytia in roots of *Arabidopsis thaliana*. *Plant J.* 48, 98–112. doi: 10.1111/j.1365-313X.2006.02856.x
- Wieczorek, K., Hofmann, J., Blöchl, A., Szakasits, D., Bohlmann, H., and Grundler, F. M. W. (2008). *Arabidopsis* endo-1,4-beta-glucanases are involved in the formation of root syncytia induced by *Heterodera schachtii*. *Plant J.* 53, 336–351. doi: 10.1111/j.1365-313X.2007.03340.x
- Wiggers, R. J., Starr, J. L., and Price, H. J. (1990). DNA content variation in chromosome number in plant cells affected by *Meloidogyne incognita* and *M. arenaria*. *Phytopathology* 80, 1391–1395. doi: 10.1094/Phyto-80-1391
- Wimmers, L. E., and Turgeon, R. (1991). Transfer cells and solute uptake in minor veins of *Pisum sativum* leaves. *Planta* 186, 2–12. doi: 10.1007/BF00201491
- Wolf, S., Deom, C. M., Beachy, R., and Lucas, W. J. (1991). Plasmodesmatal function is probed using transgenic tobacco plants that express a virus movement protein. *Plant Cell* 3, 593–604.
- Wolf, S., Hematy, K., and Hofte, H. (2012). Growth control and cell wall signaling in plants. *Annu. Rev. Plant Biol.* 63, 381–407. doi: 10.1146/annurev-arplant-042811-105449
- Wyss, U., Stender, C., and Lehmann, H. (1984). Ultrastructure of feeding sites of the cyst nematode *Heterodera schachtii* Schmidt in roots of susceptible and resistant *Raphanus sativus* L. var. *oleiformis* Pers. cultivars. *Physiol. Plant Pathol.* 25, 21–37. doi: 10.1016/0048-4059(84)90015-8

**Conflict of Interest Statement:** The authors declare that the research was conducted in the absence of any commercial or financial relationships that could be construed as a potential conflict of interest.

**Received:** 29 November 2013; **accepted:** 07 April 2014; **published online:** 05 May 2014. **Citation:** Rodiuc N, Vieira P, Banora MY and de Almeida Engler J (2014) On the track of transfer cell formation by specialized plant-parasitic nematodes. *Front. Plant Sci.* 5:160. doi: 10.3389/fpls.2014.00160

This article was submitted to Plant Physiology, a section of the journal *Frontiers in Plant Science*.

Copyright © 2014 Rodiuc, Vieira, Banora and de Almeida Engler. This is an open-access article distributed under the terms of the Creative Commons Attribution License (CC BY). The use, distribution or reproduction in other forums is permitted, provided the original author(s) or licensor are credited and that the original publication in this journal is cited, in accordance with accepted academic practice. No use, distribution or reproduction is permitted which does not comply with these terms.



# Transcriptomic signatures of transfer cells in early developing nematode feeding cells of *Arabidopsis* focused on auxin and ethylene signaling

Javier Cabrera, Marta Barcala, Carmen Fenoll and Carolina Escobar\*

Laboratory of Plant Physiology, Department of Environmental Sciences, Facultad de Ciencias Ambientales y Bioquímica, Universidad de Castilla-La Mancha, Toledo, Spain

**Edited by:**

Gregorio Hueros, Universidad de Alcalá, Spain

**Reviewed by:**

Uener Kolukisaoglu, University of Tuebingen, Germany  
Vasileios Fotopoulos, Cyprus University of Technology, Cyprus

**\*Correspondence:**

Carolina Escobar, Laboratory of Plant Physiology, Department of Environmental Sciences, Facultad de Ciencias Ambientales y Bioquímica, Universidad de Castilla-La Mancha, Avenida de Carlos III s/n, 45071 Toledo, Spain  
e-mail: carolina.escobar@uclm.es

Phyto-endoparasitic nematodes induce specialized feeding cells (NFCs) in their hosts, termed syncytia and giant cells (GCs) for cyst and root-knot nematodes (RKNs), respectively. They differ in their ontogeny and global transcriptional signatures, but both develop cell wall ingrowths (CIs) to facilitate high rates of apoplastic/symplastic solute exchange showing transfer cell (TC) characteristics. Regulatory signals for TC differentiation are not still well-known. The two-component signaling system (2CS) and reactive oxygen species are proposed as inducers of TC identity, while, 2CSs-related genes are not major contributors to differential gene expression in early developing NFCs. Transcriptomic and functional studies have assigned a major role to auxin and ethylene as regulatory signals on early developing TCs. Genes encoding proteins with similar functions expressed in both early developing NFCs and typical TCs are putatively involved in upstream or downstream responses mediated by auxin and ethylene. Yet, no function directly associated to the TCs identity of NFCs, such as the formation of CIs is described for most of them. Thus, we reviewed similarities between transcriptional changes observed during the early stages of NFCs formation and those described during differentiation of TCs to hypothesize about putative signals leading to TC-like differentiation of NFCs with particular emphasis on auxin and ethylene.

**Keywords:** plant-nematode interaction, giant cells, early transcriptomic signatures, syncytia, auxin, ethylene, transfer cells, cell wall ingrowths

## INTRODUCTION

Phyto-endoparasitic nematodes interact with their hosts in a subtle manner. They induce cells from the vascular cylinder to differentiate into specialized feeding cells (NFCs), syncytia, and giant cells (GCs), the nourishing cells for cyst and root-knot nematodes (RKNs), respectively (Jones and Goto, 2011; Sobczak and Golinowski, 2011). Although these two cell types clearly differ in their ontogeny, both develop cell wall ingrowths (CIs) believed to facilitate high rates of apoplastic/symplastic solute exchange typical of transfer cells (TCs; Jones and Dropkin, 1976; Siddique et al., 2012). In GCs the amplification of the plasma membrane surface area could be up to 20 fold (reviewed in Jones and Goto, 2011). CIs are less abundant in male-induced syncytia, suggesting a control probably associated with lower nutrient demand as the development of males inside the plant ends at the J3 stage (reviewed in Sobczak and Golinowski, 2009). Young syncytia are symplastically isolated, although this is lost at later stages (10–15 days post-infection, dpi; Hofmann et al., 2007) and symplastic isolation of GCs is under discussion (Hoth et al., 2008; Hofmann et al., 2010). Thus, amplification of plasma membrane area might be crucial for efficient apoplastic exchange at certain NFC developing stages. Polarized deposition of a thickened wall would need cell signals leading to this specialized differentiation. Those putative signals are still uncertain. Yet, some of the genes described to change their expression during TC differentiation participate in

downstream cascades for gene expression driven by ethylene and auxin in epidermal cells of *Vicia faba* (Dibley et al., 2009) or in barley endosperm (Thiel et al., 2008, 2012a). In addition, genes involved in the biosynthesis of hormones such as auxin, ethylene, jasmonic acid, brassinosteroids, gibberellins, and abscisic acid in maize basal endosperm (Xiong et al., 2011) are also differentially expressed in TCs.

Global transcriptomic changes of laser micro-dissected GCs at early developing stages (3 dpi; Barcala et al., 2010) and of micro-aspirated young syncytia (5 dpi; Szakasits et al., 2009) in *Arabidopsis* indicated that only 529 genes out of 1161 in GCs and 7225 in syncytia (representing 45.5 and 7.3% of the differentially expressed genes in each transcriptome, respectively) are shared. This indicates that transcriptomic similarities are not high between both nematode-induced cell types. However, key changes in the expression of genes related to several hormones such as auxin, ethylene, jasmonic acid, or abscisic acid are shared between both NFCs (Cabrera et al., 2013).

Only some data on TC regulatory signals in NFCs have been described, i.e., *ZmMRP-1* codes for a primary sensor of the putative signals for TCs and the activity of this TC-specific promoter *ZmMRP-1* (Gomez et al., 2002) was monitored in *Arabidopsis* transgenic plants; GUS activity was detected in the feeding sites induced by *Meloidogyne javanica*. Those are swollen parts of the roots (galls) where GCs are embedded surrounded

by heterogeneous tissues. Although gall microscopy sections were not examined, the confined GUS activity observed suggests that the promoter is probably active in GCs (Barrero et al., 2009). Further research will elucidate whether this TC-specific molecular signature is also present in syncytia formed by cyst nematodes. In order to unveil some clues on putative signals leading to TC-like differentiation of NFCs, we review similarities between transcriptional changes observed during the early stages of NFCs formation and those described during differentiation of TCs. Global gene expression studies comparing syncytia and GCs to TCs signatures could be a starting point to find some answers.

## AUXIN AND ETHYLENE AS PUTATIVE SIGNALS INITIATING TC-LIKE MORPHOLOGY OF NFCs

During the last few years, several transcriptomic studies on early developing TCs have assigned a major role to hormone regulation on the processes leading to the differentiation of these cell types. Auxin (Dibley et al., 2009) and ethylene (Thiel et al., 2008, 2012a,b; Dibley et al., 2009; Zhou et al., 2010; Xiong et al., 2011) raised as the two major phytohormones implicated in the differentiation of TCs from different plants and tissues. In adaxial epidermal cells of cultured *V. faba* cotyledons trans-differentiating to TCs, auxin and ethylene *cis*-responsive elements were over-represented in the promoters of induced genes. There is a clear functional demonstration that both hormones regulate CI formation in *V. faba* epidermis, based mainly in pharmacological experiments, indicating their participation in the signaling events leading to TCs differentiation (Dibley et al., 2009; Zhou et al., 2010). Moreover, an increase in auxin and ethylene levels boosts TC formation in tomato roots (Schikora and Schmidt, 2002). Accordingly, a clear over-representation of auxin-regulated genes among the 310 up-regulated genes in *Arabidopsis* 3 dpi GCs, relative to the total number of hormone responsive genes described in Nemhauser et al. (2006), was observed (Cabrera et al., 2013). Among those upstream genes regulated by auxin are genes in the *AUX/IAA* group, as *IAA8* (Table 1). Genes in this category were also induced in the transcriptome of *V. faba* developing TCs, such as *GH1* (Dibley et al., 2009). The development of *Heterodera shachttii*, a syncytia-forming nematode, was impaired in the *axr2* mutant, that also corresponds to the IAA group member *IAA7* (Goverse et al., 2000), and *IAA26* is induced in the transcriptome of 5 dpi microaspirated syncytia (Table 1; Szakasits et al., 2009). AUX/IAA proteins function by interacting with auxin responsive factors (ARFs) that were also induced in GCs, like *MONOPTEROS* (*MP*; *ARF5*) or *ARF19* (Table 1). In syncytia, *ARF4* and *ARF6* are up-regulated, but not co-regulated with GCs. *ARF4* has been defined to be preferentially expressed in the phloem companion cells of *Arabidopsis* (Table 1; Brady et al., 2007), the TCs found in loading and unloading areas of vascular tissues. Therefore, ARFs are induced in both NFCs triggered by cyst and RKNs at early infection stages, although different family members are involved in each NFC type. Strikingly, 20% of the genes defined by Brady et al. (2007) as preferentially expressed in the companion cells of *Arabidopsis* are also up-regulated in syncytia (44 out of 222 genes; Cabrera et al., 2013).

Other genes in the TCs induced in the epidermis of *V. faba* include those that could alter auxin transport through PINs

relocalization or enhanced biosynthesis, as nitrilases (Dibley et al., 2009), proposed to alter the pattern of auxin redistribution to drive CI formation. Redistribution of PINs and reduction of nematode reproduction in *PIN*-related mutants such as *pin2*, *pin3*, *pin4*, *pin7*, and several double mutants, together with pharmacological treatments with inhibitors of auxin transport, demonstrated that cyst nematodes are able to hijack the auxin distribution network (Grunewald et al., 2009). Similarly, the nematode effectors Hg19C07 and Hs19C07 of *H. glycines* and *H. schachtii* directly interact with the auxin influx transporter LAX3 and infectivity in *aux1/lax3* double mutants was severely affected (Lee et al., 2011). Interpretations pointed as a process to facilitate the infection and establishment of nematodes during early stages of the plant-nematode interaction. However, the ability of CIs formation that lead to the TCs nature of NFCs, have not been ever studied in those mutants. Thus, further research with loss of function mutants will be needed to characterize auxin signaling pathways involved in TC character of syncytia and GCs.

Other downstream auxin responsive genes up-regulated in GCs are *WES1* and *GH3* (Table 1). In syncytia, there is also the *GH3*-like, *DFL1* that regulates lateral root formation through the auxin signaling pathway (Table 1; Nakazawa et al., 2001). The synthetic promoter *DR5*, derived from the *GH3* promoter, has been extensively used to check early increases in local auxin also in NFCs (Karczmarek et al., 2004). It is interesting to point that *DR5::GUS* expression is located in the GCs and vascular surrounding tissues (Cabrera et al., unpublished results). This suggests that auxin concentration is very high at early infection stages in GCs as compared to the rest of the gall tissues. There are several hypotheses to explain this local increase in auxin levels, i.e., the presence of auxins in the nematode secretions (De Meutter et al., 2005), or the manipulation of auxin homeostasis through the interaction of nematode effectors as chorismate mutase with the plant biochemical machinery (Jones et al., 2003). Interestingly, local production of isoflavonoids could also result in a local auxin increase as they inhibit polar auxin transport. Promoters of genes encoding chalcone synthases involved in the first step of flavonoid biosynthesis are induced in galls of clover (Grunewald et al., 2009), and genes in the category of flavonoid metabolism were induced in syncytia (Cabrera et al., 2013). However, several *Arabidopsis* mutants impaired in isoflavonoid biosynthesis were not affected in either syncytia or GCs formation (Jones et al., 2007; Wasson et al., 2009). These studies indicate that it is unlikely that flavonoids mediate changes in auxin transport needed for nematode feeding site organogenesis, although galls of *Medicago truncatula* flavonoid-deficient roots were shorter (Wasson et al., 2009). These findings suggest that the local flavonoid increase encountered in galls (Hutangura et al., 1999; Wasson et al., 2009) might have an alternative role not directly related to the process of infection and establishment. Perhaps flavonoids are related to CI formation needed for the acquisition of TCs characteristics, as suggested by Dibley et al. (2009) in TCs from epidermal cells of *V. faba*. This is another open question that deserves further investigation.

During differentiation of TCs in the endosperm of barley (Thiel et al., 2012a) or trans-differentiation of epidermal cells in

**Table 1 | Genes induced in the 3 dpi GCs and 5 dpi syncytia transcriptomes (Szakasits et al., 2009; Barcala et al., 2010), that are also described to be regulated by auxin and/or ethylene in Nemhauser et al. (2006) and in Mapman (Thimm et al., 2004).**

Syncytia 5 dpi			
<b>CELL</b>			
AT1G10740	IAA	1.0	Unknown protein
AT3G10530	IAA	2.3	Transducin family protein/WD-40 repeat family protein
<b>CELL WALL</b>			
AT1G53840	IAA	2.1	PME1: encodes a pectin methylesterase
AT2G39700	IAA	4.2	EXPA4: putative expansin. Naming convention from the Expansin Working Group
AT4G25810	IAA	5.1	XTR6: xyloglucan endotransglycosylase-related protein (XTR6)
AT5G06860	IAA	3.4	PGIP1: Encodes a polygalacturonase-inhibiting protein involved in defense response
AT5G57560	IAA	4.4	TCH4: Encodes a cell wall-modifying enzyme
AT5G66460	IAA	3.1	MAN7: (1-4)-beta-mannan endohydrolase
<b>DEVELOPMENT</b>			
AT5G57390	ACC	1.1	AIL5: Encodes a member of the AP2 family of transcriptional regulators
AT1G01470	IAA	2.0	LEA14: Encodes late-embryogenesis abundant protein
<b>HORMONE METABOLISM</b>			
AT1G48420	ACC	1.4	D-CDES: Encodes an enzyme that decomposes D-cysteine into pyruvate, H2S, and NH3
AT2G42680	ACC	1.1	MBF1A: One of three genes in <i>A. thaliana</i> encoding multiprotein-bridging factor 1
AT3G16050	ACC	2.0	PDX1.2: Encodes a protein with pyridoxal phosphate synthase activity
AT3G58680	ACC	1.6	MBF1B: One of three genes in <i>A. thaliana</i> encoding multiprotein-bridging factor 1
AT4G26200	ACC	1.2	ACS7: Member of a family of proteins in Arabidopsis that encode ACC synthase
AT4G34410	ACC	1.5	RRTF1: encodes a member of the ERF (ethylene response factor) subfamily B-3
AT5G20550	ACC	1.7	Oxidoreductase, 2OG-Fe(II) oxygenase family protein
AT5G43440	ACC	1.3	Encodes a protein whose sequence is similar to ACC oxidase
AT5G43450	ACC, IAA	1.2	Encodes a protein whose sequence is similar to ACC oxidase
AT1G17350	IAA	3.3	Auxin-induced-related/indole-3-acetic acid induced-related
AT1G50580	IAA	1.5	Glycosyltransferase family protein
AT1G56150	IAA	3.1	Auxin-responsive family protein
AT1G60690	IAA	0.9	Aldo/keto reductase family protein
AT2G02560	IAA	1.4	CAND1: <i>Arabidopsis thaliana</i> homolog of human CAND1
AT3G25290	IAA	1.6	Auxin-responsive family protein
AT3G25780	IAA	1.2	AOC3: Encodes allene oxide cyclase
AT3G30300	IAA	1.2	FUNCTIONS IN: molecular_function unknown; INVOLVED IN: biological_process unknown
AT3G63440	IAA	3.2	CKX6: encodes a protein whose sequence is similar to cytokinin oxidase/dehydrogenase
AT4G12410	IAA	2.8	Auxin-responsive family protein
AT4G12980	IAA	0.7	Auxin-responsive protein
AT4G27450	IAA	1.1	Unknown protein
AT4G34760	IAA	1.5	Auxin-responsive family protein
AT5G20810	IAA	0.4	Auxin-responsive protein
AT5G54510	IAA	2.7	DFL1: Encodes an IAA-amido synthase that conjugates Ala, Asp, Phe, and Trp to auxin
AT5G55540	IAA	0.8	TRN1: Encodes a large plant-specific protein of unknown function
AT5G64600	IAA	2.3	Unknown protein
<b>METAL HANDLING</b>			
AT2G37330	IAA	1.3	ALS3: Encodes an ABC transporter-like protein
<b>MISCELLANEA</b>			
AT2G29440	ACC	1.7	GSTU6: Encodes glutathione transferase belonging to the tau class of GSTs
AT3G11210	ACC, IAA	1.2	GDSL-motif lipase/hydrolase family protein
AT1G30760	IAA	6.2	FAD-binding domain-containing protein
AT2G30140	IAA	2.8	UGT87A2: UDP-glucuronosyl/UDP-glucosyl transferase family protein
AT3G11210	IAA	1.2	GDSL-motif lipase/hydrolase family protein

(Continued)

**Table 1 | Continued**

Syncytia 5 dpi			
AT3G62720	IAA	1.3	XT1: Encodes a protein with xylosyltransferase activity
AT5G19440	IAA	2.3	Similar to <i>Eucalyptus gunnii</i> alcohol dehydrogenase
<b>N-METABOLISM</b>			
AT3G49640	IAA	1.5	FAD binding/catalytic/tRNA dihydrouridine synthase
<b>NOT ASSIGNED</b>			
AT3G02490	ACC	1.2	Pentatricopeptide (PPR) repeat-containing protein
AT4G33560	ACC	3.6	Unknown protein
AT5G49410	ACC	0.5	Unknown protein
AT5G02550	ACC, IAA	1.1	Unknown protein
AT1G03820	IAA	3.0	Unknown protein
AT1G08430	IAA	4.1	ALMT1: Encodes a AI-activated malate efflux transporter
AT1G18850	IAA	1.6	Unknown protein
AT1G28400	IAA	3.0	Unknown protein
AT1G32190	IAA	0.7	INVOLVED IN: N-terminal protein myristylation; LOCATED IN: plasma membrane
AT1G32920	IAA	1.6	Unknown protein
AT1G55500	IAA	1.1	ECT4
AT2G34260	IAA	2.3	WDR55: transducin family protein/WD-40 repeat family protein
AT2G39725	IAA	2.5	Complex 1 family protein/LVR family protein
AT3G16310	IAA	2.4	Mitotic phosphoprotein N' end (MPPN) family protein
AT4G20170	IAA	1.5	GALS3
AT5G52910	IAA	0.6	ATIM: homolog of Drosophila timeless
AT5G64780	IAA	1.1	FUNCTIONS IN: molecular_function unknown; INVOLVED IN: biological_process unknown
AT5G66440	IAA	1.6	Unknown protein
<b>TRANSPORT</b>			
AT1G77380	ACC	2.7	AAP3: Amino acid permease which transports basic amino acids
AT2G39350	ACC, IAA	1.9	ABCG1: ABC transporter family protein
AT2G23150	IAA	3.2	NRAMP3: Encodes a member of the Nramp2 metal transporter family
<b>PROTEIN</b>			
AT1G26270	ACC	2.6	Phosphatidylinositol 3- and 4-kinase family protein
AT5G65450	ACC	1.1	UBP17: Encodes a ubiquitin-specific protease
AT5G63650	ACC, IAA	2.0	SNRK2.5: encodes a member of SNF1-related protein kinases
AT3G04230	IAA	1.8	40S ribosomal protein S16
AT3G17090	IAA	1.1	Protein phosphatase 2C family protein
AT3G60640	IAA	2.0	ATG8G: microtubule binding
AT4G22380	IAA	1.7	Ribosomal protein L7Ae/L30e/S12e/Gadd45 family protein
<b>REDOX</b>			
AT2G16060	ACC	1.3	HB1: Encodes a class 1 non-symbiotic hemoglobin
AT4G14965	IAA	1.0	MAPR4: heme binding
<b>RNA</b>			
AT1G21910	ACC	1.0	DREB26: member of the DREB subfamily A-5 of ERF/AP2 transcription factor family
AT1G71450	ACC	0.6	Member of the DREB subfamily A-4 of ERF/AP2 transcription factor family
AT1G77200	ACC	0.7	Member of the DREB subfamily A-4 of ERF/AP2 transcription factor family
AT3G16770	ACC	1.8	EBP: member of the ERF subfamily B-2 of the ERF/AP2 transcription factor family
AT5G43170	ACC	0.8	ZF3: Encodes zinc finger protein
AT5G67180	ACC	0.8	TOE3: AP2 domain-containing transcription factor, putative
AT2G34140	ACC, IAA	0.7	Dof-type zinc finger domain-containing protein
AT1G16530	IAA	1.1	ASL9: Symbols: LBD3, ASL9  ASL9 (ASYMMETRIC LEAVES 2 LIKE 9)
AT1G27730	IAA	1.2	STZ: Related to Cys2/His2-type zinc-finger proteins

(Continued)

**Table 1 | Continued**

Syncytia 5 dpi			
AT1G30330	IAA	0.9	ARF6: Mediates auxin response via expression of auxin-regulated genes
AT2G33860	IAA	1.3	ARF3 (ETT) encodes a protein with homology to DNA-binding proteins which bind to AuxREs
AT2G47260	IAA	1.9	WRKY23: Encodes a member of WRKY Transcription Factor
AT3G11580	IAA	1.6	DNA-binding protein, putative
AT3G16500	IAA	1.8	IAA26 (PAP1) phytochrome-associated protein 1
AT3G23250	IAA	1.8	MYB15: Member of the R2R3 factor gene family
AT4G02220	IAA	1.2	Programmed cell death 2 C-terminal domain-containing protein
AT4G21550	IAA	1.4	VAL3: Symbols: VAL3  VAL3 (VP1/ABI3-LIKE 3); transcription factor
AT5G60450	IAA	0.8	ARF4: member of the ARF family of transcription factors which mediate auxin responses
<b>SECONDARY METAB.</b>			
AT5G01210	ACC, IAA	2.1	Transferase family protein
<b>SIGNALING</b>			
AT1G35140	IAA	2.8	PHI-1
AT1G76650	IAA	1.3	CML38: calcium-binding EF hand family protein
AT2G25790	IAA	1.3	Leucine-rich repeat transmembrane protein kinase
AT2G30060	IAA	0.9	Ran-binding protein 1b
AT4G08950	IAA	3.8	EXO: EXORDIUM
AT4G28490	IAA	1.9	HAE: member of Receptor kinase-like protein family
AT5G05160	IAA	1.1	RUL1: leucine-rich repeat transmembrane protein kinase
AT5G12940	IAA	1.1	Leucine-rich repeat family protein
AT5G37770	IAA	2.0	TCH2: Encodes a protein with 40% similarity to calmodulin
<b>STRESS</b>			
AT2G42530	ACC	1.8	COR15B: COLD REGULATED 15B
AT5G64900	IAA	1.4	PROPEP1: Encodes a putative 92-aa protein that is the precursor of AtPep1
Giant cells 3 dpi			
<b>CELL WALL</b>			
AT4G25810	IAA	1.1	XTR6: xyloglucan endotransglycosylase-related protein
<b>HORMONE METABOLISM</b>			
AT3G23150	ACC	2.1	ETR2: Involved in ethylene perception in Arabidopsis
AT4G20880	ACC	2.4	Ethylene-responsive nuclear protein/ethylene-regulated nuclear protein
AT2G23170	IAA	1.0	GH3.3: IAA-amido synthase that conjugates Asp and other amino acids to auxin <i>in vitro</i>
AT3G50660	IAA	1.0	DWF4: hydroxylase whose reaction is a rate-limiting step in brassinosteroid biosynthetic pathway
AT4G27260	IAA	0.8	WES1: IAA-amido synthase that conjugates Asp and other amino acids to auxin <i>in vitro</i>
AT4G39400	IAA	1.4	BRI1: plasma membrane localized leucine-rich repeat receptor kinase
AT5G25190	IAA, ACC	3.2	ESE3: encodes a member of the ERF (ethylene response factor) subfamily B-6 of ERF/AP2 family
<b>LIPID METABOLISM</b>			
AT4G12110	IAA	1.9	SMO1-1: Encodes a member of the SMO1 family of sterol 4alpha-methyl oxidases
<b>METAL HANDLING</b>			
AT3G24450	IAA	1.8	Copper-binding family protein
<b>NOT ASSIGNED</b>			
AT4G33560	ACC	2.3	Unknown protein
AT2G39370	IAA	2.9	MAKR4: unknown protein
<b>POLYAMINE METABOLISM</b>			
AT5G19530	IAA	1.8	ACL5: Encodes a spermine synthase
<b>PROTEIN</b>			
AT3G61160	IAA	1.8	Shaggy-related protein kinase beta/ASK-beta (ASK2)
AT3G27580	IAA, ACC	2.5	ATPK7: a member of a subfamily of Ser/Thr PKs

(Continued)

**Table 1 | Continued**

Giant cells 3 dpi			
<b>REDOX</b>			
AT2G16060	ACC	2.4	HB1: Encodes a class 1 non-symbiotic hemoglobin
<b>RNA</b>			
AT1G19220	IAA	1.6	ARF19: auxin response factor
AT1G19850	IAA	4.1	MP: Encodes a transcription factor (IAA24)
AT2G22670	IAA	1.2	IAA8: IAA8 (IAA8) gene is auxin inducible
AT3G02550	IAA	2.5	LBD41: LOB DOMAIN-CONTAINING PROTEIN 41
AT4G17460	IAA	4.3	HAT1: Encodes homeobox protein HAT1
AT4G36540	IAA	1.0	BEE2: BR Enhanced Expression 2
AT5G47370	IAA	2.7	HAT2: homeobox-leucine zipper genes induced by auxin
AT5G65310	IAA	1.1	HB5: class I HDZip (homeodomain-leucine zipper) protein
<b>SIGNALING</b>			
AT1G21980	IAA	1.4	PIP5K1: Type I phosphatidylinositol-4-phosphate 5-kinase
AT1G68400	IAA	1.8	Leucine-rich repeat transmembrane protein kinase
AT2G25790	IAA	1.1	Leucine-rich repeat transmembrane protein kinase

Third column shows the Log2 value for each gene in syncytia or GCs.

*V. faba* (Dibley et al., 2009), ethylene is proposed to participate in a signaling pathway initiating TCs morphology. Similarly to the auxin responsive genes induced in the NFC transcriptomes, some genes involved in ethylene perception, transduction, and responses are also up-regulated in GCs (Table 1; *ETR2*, *ESE3*). Ethylene responsive genes were over-represented among the 310 up-regulated genes in GCs, relative to the total number of hormone responsive genes in Nemhauser et al. (2006), Cabrera et al. (2013). *ETR2* induction coincides with the presence of other ethylene receptors (as *ETR1*) in developing TCs from barley and rice endosperm (Thiel et al., 2012b). The ethylene precursor 1-aminocyclopropane-1-carboxylic acid (ACC) directly enhanced TC formation in root epidermal cells of tomato (Schikora and Schmidt, 2002) and adaxial epidermal cells of *V. faba* cotyledons (Dibley et al., 2009). Consistently, a pool of genes encoding proteins related with ethylene synthesis like two ACC oxidases (Table 1), are induced in the transcriptome of microaspirated syncytia. Functional analysis of the *Arabidopsis* ethylene over-producing mutants *eto2* and *eto3* resulted in hyper-susceptibility to cyst nematodes (Govorse et al., 2000; Wubben et al., 2001). Interestingly, ethylene overproduction in *eto2* mutants stimulated the formation of CIs or protuberances in syncytia along the vascular tissue, at late infection stages (Govorse et al., 2000), providing a direct evidence for a putative role of ethylene in the stimulation of syncytia TCs characteristics. Accordingly, functional analysis of *Arabidopsis* mutants compromised in several steps of the signaling cascade leading to activation of ethylene responsive genes, as those altered in ethylene-insensitive mutants (*etr1-1*, *ein2-1*, *ein3-1*, *eir1-1*, and *axr2*), were less susceptible to *H. schachtii* (Wubben et al., 2001). Hence, several ACC synthase coding genes were induced at early infection stages, increasing and reaching a maximum at 20 dpi in soybean infected with *H. glycines* (Tucker et al., 2010). Strikingly, ethylene production upon nematode infection has been long known in tomato infected with RKNs (*M. Javanica*), with a peak at medium infection stages (4–16 dpi; Glazer et al., 1983), similar to several dicotyledonous

species (Glazer et al., 1985). However, not much is known on the behavior of ethylene-related mutants infected with RKNs. Experiments on *Lotus japonica* expressing *ETR-1* were not conclusive of its putative role on RKN infection (Lohar and Bird, 2003). Undoubtedly, analysis are still lacking on the morphologic characteristics of developed syncytia in loss of function mutants of genes related to ethylene transduction pathways that could confirm their role on the induction of syncytia TCs characteristics, such us the presence of CI. Regarding RKNs, virtually no data on the TCs features of GCs in ethylene mutants are still available.

## TWO-COMPONENT SIGNALING SYSTEMS AND REACTIVE OXYGEN SPECIES AS INDUCERS OF TC IDENTITY IN NFCs

Recently, Thiel et al. (2012b) suggested a role for a two-component signaling system (2CS) in cellularization and differentiation of barley endosperm TCs, possibly coupled to hormonal regulation by abscisic acid and ethylene. In plants, 2CSs require a hybrid histidine kinase (HK; located in the plasma membrane) with both histidine kinase and receiver domains, a histidine-containing phosphotransfer protein (HPt), and a response regulator that mediates downstream signaling through phosphorylation. In *Arabidopsis*, proteins with significant sequence similarities to all elements of the 2CSs have been identified (reviewed in Schaller et al., 2008). We have searched for genes encoding those components in the early GCs and syncytia transcriptomes (Szakasits et al., 2009; Barcala et al., 2010; Table S1). In *Arabidopsis*, genes encoding 8 HK and 9 HK-like proteins (HKL) have been identified and 2 of them are up-regulated in GCs (*ETR2*) or syncytia (*PDK*). However, most HKS and HKLs are down-regulated in NFCs. *ETR2*, *HK2*, *HK3*, *ERS1*, and *PHYA* are down-regulated in syncytia and *HK1* and *CKII* in GCs (Cabrera et al., 2013; Table S1). Moreover, the two up-regulated genes in NFCs are HKLs that lack residues essential to histidine kinase activity. The *Arabidopsis* genome encodes five HPt proteins (*AHP1-5*) that act as signaling intermediates

between HKs and response regulators. From them, *AHP3* is up-regulated in syncytia while *AHP1* is down-regulated, and the rest of the genes are not differentially expressed in the transcriptome of micro-dissected GCs and syncytia (Barcala et al., 2010; Cabrera et al., 2013; Table S1). The last components of the system are the response regulators, with 33 genes identified in the Arabidopsis genome (23 response regulators and 10 pseudo-response regulators; Schaller et al., 2008), most of them down-regulated as well in NFCs (only *ARR7* and *RR14* are up-regulated in syncytia; Cabrera et al., 2013; Table S1). Thus, the transcriptomic evidence at early differentiation stages of syncytia and GCs suggests that genes involved in 2CSs do not contribute substantially to the differential gene expression observed in NFCs. Thus, 2CSs are not likely participating in the first signaling steps involved in the acquisition of TCs identify in NFCs.

Recently, it has been shown that H<sub>2</sub>O<sub>2</sub> functions downstream of ethylene to activate cell wall biosynthesis and direct polarized deposition of a uniform wall on which CIs formed in TCs of *V. faba* cotyledons (Andriunas et al., 2012). The presence of a H<sub>2</sub>O<sub>2</sub>-generating mechanism dependent upon NADPH oxidase (NOX) activity was suggested (Andriunas et al., 2012). From the 10 *RBOH* genes encoding the catalytic subunit of NOX in Arabidopsis (reviewed in Sagi and Fluhr, 2006), 7 are down-regulated in syncytia, and none of them are differentially expressed in GCs (Cabrera et al., 2013). Additionally, defense-related genes described as related to TCs development, as in endosperm TCs where the ethylene response is possibly coupled to activated defense mechanisms (Thiel et al., 2008), are not abundant in NFCs. On the contrary, a general repression of plant defenses is obvious from the transcriptomes of early developing syncytia in Arabidopsis, where more than 35 peroxidases were repressed (Szakasits et al., 2009). Similarly, in early developing GCs of Arabidopsis and tomato not only peroxidases, but many genes from the secondary metabolism related to plant defenses were also down-regulated at 3 dpi (Barcala et al., 2010; Portillo et al., 2013). All these data suggest that active oxygen species such as H<sub>2</sub>O<sub>2</sub> very unlikely function as early inducing signals for TCs identity of NFCs coupled to hormone signaling. However, it is important to point that we cannot discard the possibility of the activation of an oxidative burst in medium-late stages of NFCs development that might be participating in this process.

## FINAL REMARKS

It is interesting to point that many genes induced in early differentiating NFCs correspond to typical categories of downstream regulated genes that might participate in CIs formation, as those involved in vesicle trafficking, cell wall biogenesis, cell shape control and expansion, or nutrient transport, also induced in cells undergoing differentiation into TCs (Thiel et al., 2008, 2012a; Dibley et al., 2009; Xiong et al., 2011). Many other downstream genes are also induced in NFCs contributing to their development or maintenance (reviewed in Kyndt et al., 2013). Genes associated to changes in the cytoskeleton include those encoding tubulins, actins, microtubule-binding proteins, as the IAA-induced *ATG8G* (Table 1) or *AtFH6*, a formin encoding gene that regulates

polarized growth by controlling the assembly of actin cables in *Arabidopsis* GCs (Favery et al., 2004). However, no functions directly associated to the TCs characteristics of NFCs have been yet described for those genes in NFCs (Kyndt et al., 2013). Other genes possibly related to active nutrient uptake into syncytia and GCs are also up-regulated by either auxin (*NRAMP3*), ethylene (*AAP3*), or both (*ABCG1*; Table 1). However, functional studies of these genes in NFCs are very scarce (reviewed in Kyndt et al., 2013). In addition, genes encoding cell wall modifying enzymes as pectin methylesterases, expansins, xyloglucan endotransglycosylases (*EXP4*, *XTR6*, *PME1*, *XTR6*), all induced by auxin, were also induced in NFCs (Table 1). Interestingly, the most clarifying study of a functional implication in TCs characteristic of NFCs, as the CIs formation, comes from the analysis of UDP-glucose dehydrogenase (UGD) coding genes. UGDs act through oxidation of UDP-glucose producing several cell wall polysaccharides. *UGD2* and *UGD3* are necessary for the production of CIs in syncytia and loss of function in double mutants severely affected nematode development (Siddique et al., 2012).

In conclusion, although genes encoding proteins with similar functions are differentially expressed in differentiating NFCs and typical TCs, a clear knowledge of their implication, either upstream or downstream, in the signaling cascades leading to TCs characteristics of NFCs is still lacking. Further research will probably elucidate the contribution of signals such as hormones to those differentiation events in NFCs.

## ACKNOWLEDGMENTS

This work was supported by the Spanish Government (AGL2010-17388 to Carolina Escobar, CSD2007-057 to Carmen Fenoll) and the Castilla-La Mancha Government (PCI08-0074-0294 to Carmen Fenoll and Carolina Escobar). Javier Cabrera was supported by a fellowship from the Ministry of Education, Spain.

## SUPPLEMENTARY MATERIAL

The Supplementary Material for this article can be found online at: <http://www.frontiersin.org/journal/10.3389/fpls.2014.00107/abstract>

## REFERENCES

- Andriunas, F. A., Zhang, H.-M., Xia, X., Offler, C. E., McCurdy, D. W., and Patrick, J. W. (2012). Reactive oxygen species form part of a regulatory pathway initiating trans-differentiation of epidermal transfer cells in *Vicia faba* cotyledons. *J. Exp. Bot.* 63, 3617–3629. doi: 10.1093/jxb/ers029
- Barcala, M., Garcia, A., Cabrera, J., Casson, S., Lindsey, K., Favery, B., et al. (2010). Early transcriptomic events in microdissected *Arabidopsis* nematode-induced giant cells. *Plant J.* 61, 698–712. doi: 10.1111/j.1365-313X.2009.04098.x
- Barrera, C., Royo, J., Grijota-Martinez, C., Faye, C., Paul, W., Sanz, S., et al. (2009). The promoter of ZmMRP-1, a maize transfer cell-specific transcriptional activator, is induced at solute exchange surfaces and responds to transport demands. *Planta* 229, 235–247. doi: 10.1007/s00425-008-0823-0
- Brady, S. M., Orlando, D. A., Lee, J.-Y., Wang, J. Y., Koch, J., Dinneny, J. R., et al. (2007). A high-resolution root spatiotemporal map reveals dominant expression patterns. *Science* 318, 801–806. doi: 10.1126/science.1146265
- Cabrera, J., Bustos, R., Favery, B., Fenoll, C., and Escobar, C. (2013). NEMATIC: a simple and versatile tool for the *in silico* analysis of plant-nematode interactions. *Mol. Plant Pathol.* doi: 10.1111/mpp.12114. [Epub ahead of print].

- De Meutter, J., Tytgat, T., Prinsen, E., Gheysen, G., Van Onckelen, H., and Gheysen, G. (2005). Production of auxin and related compounds by the plant parasitic nematodes *Heterodera schachtii* and *Meloidogyne incognita*. *Commun. Agric. Appl. Biol. Sci.* 70, 51–60.
- Dibley, S. J., Zhou, Y., Andriunas, F. A., Talbot, M. J., Offler, C. E., Patrick, J. W., et al. (2009). Early gene expression programs accompanying trans-differentiation of epidermal cells of *Vicia faba* cotyledons into transfer cells. *New Phytol.* 182, 863–877. doi: 10.1111/j.1469-8137.2009.02822.x
- Favery, B., Chelysheva, L. A., Lebris, M., Jammes, F., Marmagne, A., De Almeida-Engler, J., et al. (2004). Arabidopsis formin AtFH6 is a plasma membrane-associated protein upregulated in giant cells induced by parasitic nematodes. *Plant Cell Online* 16, 2529–2540. doi: 10.1105/tpc.104.024372
- Glazer, L., Orion, D., and Apelbaum, S. (1983). Interrelationships between ethylene production, gall formation, and root-knot nematode development in tomato plants infected with *Meloidogyne javanica*. *J. Nematol.* 15, 539–544.
- Glazer, L., Orion, D., and Apelbaum, S. (1985). Ethylene production by *Meloidogyne* spp.-infected plants. *J. Nematol.* 17, 61–63.
- Gomez, E., Royo, J., Guo, Y., Thompson, R., and Hueros, G. (2002). Establishment of cereal endosperm expression domains: identification and properties of a maize transfer cell-specific transcription factor, ZmMRP-1. *Plant Cell* 14, 599–610. doi: 10.1105/tpc.010365
- Goverse, A., Overmars, H., Engelbertink, J., Schots, A., Bakker, J., and Helder, J. (2000). Both induction and morphogenesis of cyst nematode feeding cells are mediated by auxin. *Mol. Plant Microbe Interact.* 13, 1121–1129. doi: 10.1094/MPMI.2000.13.10.1121
- Grunewald, W., Van Noorden, G., Van Isterdael, G., Beeckman, T., Gheysen, G., and Mathesius, U. (2009). Manipulation of auxin transport in plant roots during Rhizobium symbiosis and nematode parasitism. *Plant Cell* 21, 2553–2562. doi: 10.1105/tpc.109.069617
- Hofmann, J., El Ashry Ael, N., Anwar, S., Erban, A., Kopka, J., and Grundler, F. (2010). Metabolic profiling reveals local and systemic responses of host plants to nematode parasitism. *Plant J.* 62, 1058–1071. doi: 10.1111/j.1365-313X.2010.04217.x
- Hofmann, J., Wieczorek, K., Blochl, A., and Grundler, F. M. (2007). Sucrose supply to nematode-induced syncytia depends on the apoplastic and symplastic pathways. *J. Exp. Bot.* 58, 1591–1601. doi: 10.1093/jxb/erl285
- Hoth, S., Stadler, R., Sauer, N., and Hammes, U. Z. (2008). Differential vascularization of nematode-induced feeding sites. *Proc. Natl. Acad. Sci. U.S.A.* 105, 12617–12622. doi: 10.1073/pnas.0803835105
- Hutangura, P., Mathesius, U., Jones, M. G. K., and Rolfe, B. G. (1999). Auxin induction is a trigger for root gall formation caused by root-knot nematodes in white clover and is associated with the activation of the flavonoid pathway. *Funct. Plant Biol.* 26, 221–231. doi: 10.1071/PP98157
- Jones, J. T., Furlanetto, C., Bakker, E., Banks, B., Blok, V., Chen, Q., et al. (2003). Characterization of a chorismate mutase from the potato cyst nematode *Globodera pallida*. *Mol. Plant Pathol.* 4, 43–50. doi: 10.1046/j.1364-3703.2003.00140.x
- Jones, J. T., Furlanetto, C., and Phillips, M. S. (2007). The role of flavonoids produced in response to cyst nematode infection of *Arabidopsis thaliana*. *Nematology* 9, 671–677. doi: 10.1163/156854107782024875
- Jones, M. G. K., and Dropkin, V. H. (1976). Scanning electron microscopy in nematode-induced giant transfer cells. *Cytobios* 15, 149–161.
- Jones, M. G. K., and Goto, D. B. (2011). “Root-knot nematodes and giant cells,” in *Genomics and Molecular Genetics of Plant–Nematode Interactions*, eds J. Jones, G. Gheysen, and C. Fenoll (Dordrecht: Springer), 83–102. doi: 10.1007/978-94-007-0434-3\_5
- Karczmarek, A., Overmars, H., Helder, J., and Goverse, A. (2004). Feeding cell development by cyst and root-knot nematodes involves a similar early, local and transient activation of a specific auxin-inducible promoter element. *Mol. Plant Pathol.* 5, 343–346. doi: 10.1111/j.1364-3703.2004.00230.x
- Kyndt, T., Vieira, P., Gheysen, G., and De Almeida-Engler, J. (2013). Nematode feeding sites: unique organs in plant roots. *Planta* 238, 807–818. doi: 10.1007/s00425-013-1923-z
- Lee, C., Chronis, D., Kenning, C., Peret, B., Hewezi, T., Davis, E. L., et al. (2011). The novel cyst nematode effector protein 19C07 interacts with the *Arabidopsis* auxin influx transporter LAX3 to control feeding site development. *Plant Physiol.* 155, 866–880. doi: 10.1104/pp.110.167197
- Lohar, D. P., and Bird, D. M. (2003). *Lotus japonicus*: a new model to study root-parasitic nematodes. *Plant Cell Physiol.* 44, 1176–1184. doi: 10.1093/pcp/pcg146
- Nakazawa, M., Yabe, N., Ichikawa, T., Yamamoto, Y. Y., Yoshizumi, T., Hasunuma, K., et al. (2001). DFL1, an auxin-responsive GH3 gene homologue, negatively regulates shoot cell elongation and lateral root formation, and positively regulates the light response of hypocotyl length. *Plant J.* 25, 213–221. doi: 10.1111/j.1365-313X.2001.00957.x
- Nemhauser, J. L., Hong, F., and Chory, J. (2006). Different plant hormones regulate similar processes through largely nonoverlapping transcriptional responses. *Cell* 126, 467–475. doi: 10.1016/j.cell.2006.05.050
- Portillo, M., Cabrera, J., Lindsey, K., Topping, J., Andres, M. F., Emiliozzi, M., et al. (2013). Distinct and conserved transcriptomic changes during nematode-induced giant cell development in tomato compared with *Arabidopsis*: a functional role for gene repression. *New Phytol.* 197, 1276–1290. doi: 10.1111/nph.12121
- Sagi, M., and Fluhr, R. (2006). Production of reactive oxygen species by plant NADPH oxidases. *Plant Physiol.* 141, 336–340. doi: 10.1104/pp.106.078089
- Schaller, G. E., Kieber, J. J., and Shiu, S.-H. (2008). Two-component signaling elements and histidyl-aspartyl phosphorelays. *Arabidopsis Book* 6:e0112. doi: 10.1199/tab.0112
- Schikora, A., and Schmidt, W. (2002). Formation of transfer cells and H(+)-ATPase expression in tomato roots under P and Fe deficiency. *Planta* 215, 304–311. doi: 10.1007/s00425-002-0738-0
- Siddique, S., Sobczak, M., Tenhaken, R., Grundler, F. M. W., and Bohlmann, H. (2012). Cell wall ingrowths in nematode induced syncytia require *UGD2* and *UGD3*. *PLoS ONE* 7:e41515. doi: 10.1371/journal.pone.0041515
- Sobczak, M., and Golinowski, W. (2009). “Structure of cyst nematode feeding sites,” in *Genomics and Molecular Genetics of Plant–Nematode Interactions*, eds J. Jones, G. Gheysen, and C. Fenoll (Dordrecht: Springer), 153–188.
- Sobczak, M., and Golinowski, W. (2011). “Cyst nematodes and syncytia,” in *Genomics and Molecular Genetics of Plant–Nematode Interactions*, eds J. Jones, G. Gheysen, and C. Fenoll (Dordrecht: Springer), 83–102.
- Szakasits, D., Heinen, P., Wieczorek, K., Hofmann, J., Wagner, F., Kreil, D. P., et al. (2009). The transcriptome of syncytia induced by the cyst nematode *Heterodera schachtii* in *Arabidopsis* roots. *Plant J.* 57, 771–784. doi: 10.1111/j.1365-313X.2008.03727.x
- Thiel, J., Hollmann, J., Rutten, T., Weber, H., Scholz, U., and Weschke, W. (2012b). 454 Transcriptome sequencing suggests a role for two-component signalling in cellularization and differentiation of barley endosperm transfer cells. *PLoS ONE* 7:e41867. doi: 10.1371/journal.pone.0041867
- Thiel, J., Riewe, D., Rutten, T., Melzer, M., Friedel, S., Bollenbeck, F., et al. (2012a). Differentiation of endosperm transfer cells of barley: a comprehensive analysis at the micro-scale. *Plant J.* 71, 639–655. doi: 10.1111/j.1365-313X.2012.05018.x
- Thiel, J., Weier, D., Sreenivasulu, N., Strickert, M., Weichert, N., Melzer, M., et al. (2008). Different hormonal regulation of cellular differentiation and function in nucellar projection and endosperm transfer cells: a microdissection-based transcriptome study of young barley grains. *Plant Physiol.* 148, 1436–1452. doi: 10.1104/pp.108.127001
- Thimm, O., Blasing, O., Gibon, Y., Nagel, A., Meyer, S., Kruger, P., et al. (2004). MAPMAN: a user-driven tool to display genomics data sets onto diagrams of metabolic pathways and other biological processes. *Plant J.* 37, 914–939. doi: 10.1111/j.1365-313X.2004.02016.x
- Tucker, M. L., Xue, P., and Yang, R. (2010). 1-Aminocyclopropane-1-carboxylic acid (ACC) concentration and ACC synthase expression in soybean roots, root tips, and soybean cyst nematode (*Heterodera glycines*)-infected roots. *J. Exp. Bot.* 61, 463–472. doi: 10.1093/jxb/erp317
- Wasson, A. P., Ramsay, K., Jones, M. G., and Mathesius, U. (2009). Differing requirements for flavonoids during the formation of lateral roots, nodules and root knot nematode galls in *Medicago truncatula*. *New Phytol.* 183, 167–179. doi: 10.1111/j.1469-8137.2009.02850.x
- Wubben, M. J. E., Su, H., Rodermel, S. R., and Baum, T. J. (2001). Susceptibility to the sugar beet cyst nematode is modulated by ethylene signal transduction in *Arabidopsis thaliana*. *Mol. Plant Microbe Interact.* 14, 1206–1212. doi: 10.1094/MPMI.2001.14.10.1206
- Xiong, Y., Li, Q.-B., Kang, B.-H., and Chourey, P. (2011). Discovery of genes expressed in basal endosperm transfer cells in maize using 454 transcriptome sequencing. *Plant Mol. Biol. Rep.* 29, 835–847. doi: 10.1007/s11105-011-0291-8

Zhou, Y., Andriunas, F., Offler, C. E., McCurdy, D. W., and Patrick, J. W. (2010). An epidermal-specific ethylene signal cascade regulates trans-differentiation of transfer cells in *Vicia faba* cotyledons. *New Phytol.* 185, 931–943. doi: 10.1111/j.1469-8137.2009.03136.x

**Conflict of Interest Statement:** The authors declare that the research was conducted in the absence of any commercial or financial relationships that could be construed as a potential conflict of interest.

Received: 15 January 2014; accepted: 06 March 2014; published online: 24 March 2014.

**Citation:** Cabrera J, Barcala M, Fenoll C and Escobar C (2014) Transcriptomic signatures of transfer cells in early developing nematode feeding cells of *Arabidopsis* focused on auxin and ethylene signaling. *Front. Plant Sci.* 5:107. doi: 10.3389/fpls.2014.00107  
This article was submitted to Plant Physiology, a section of the journal *Frontiers in Plant Science*.

Copyright © 2014 Cabrera, Barcala, Fenoll and Escobar. This is an open-access article distributed under the terms of the Creative Commons Attribution License (CC BY). The use, distribution or reproduction in other forums is permitted, provided the original author(s) or licensor are credited and that the original publication in this journal is cited, in accordance with accepted academic practice. No use, distribution or reproduction is permitted which does not comply with these terms.



# Role of callose synthases in transfer cell wall development in tocopherol deficient *Arabidopsis* mutants

Hiroshi Maeda<sup>1,2,3†</sup>, Wan Song<sup>1,4†</sup>, Tammy Sage<sup>5</sup> and Dean DellaPenna<sup>1\*</sup>

<sup>1</sup> Department of Biochemistry and Molecular Biology, Michigan State University, East Lansing, MI, USA

<sup>2</sup> Cell and Molecular Biology Program, Michigan State University, East Lansing, MI, USA

<sup>3</sup> Department of Botany, University of Wisconsin-Madison, Madison, WI, USA

<sup>4</sup> Genetics Program, Michigan State University, East Lansing, MI, USA

<sup>5</sup> Department of Ecology and Evolutionary Biology, University of Toronto, Toronto, ON, Canada

**Edited by:**

Gregorio Hueros, Universidad de Alcalá, Spain

**Reviewed by:**

Prem S. Chourey, United States

Department of Agriculture, USA

Paulo Monjardino, Universidade dos Açores, Portugal

Jae-yeon Kim, Gyeongsang National University, South Korea

**\*Correspondence:**

Dean DellaPenna, Department of Biochemistry and Molecular Biology, Michigan State University, 2235 Molecular Plant Science, East Lansing, MI 48824-1319, USA  
e-mail: dellapen@msu.edu

<sup>†</sup>These authors have contributed equally to this work.

Tocopherols (vitamin E) are lipid-soluble antioxidants produced by all plants and algae, and many cyanobacteria, yet their functions in these photosynthetic organisms are still not fully understood. We have previously reported that the *vitamin E deficient 2* (*vte2*) mutant of *Arabidopsis thaliana* is sensitive to low temperature (LT) due to impaired transfer cell wall (TCW) development and photoassimilate export associated with massive callose deposition in transfer cells of the phloem. To further understand the roles of tocopherols in LT induced TCW development we compared the global transcript profiles of *vte2* and wild-type leaves during LT treatment. Tocopherol deficiency had no significant impact on global gene expression in permissive conditions, but significantly affected expression of 77 genes after 48 h of LT treatment. In *vte2* relative to wild type, genes associated with solute transport were repressed, while those involved in various pathogen responses and cell wall modifications, including two members of callose synthase gene family, *GLUCAN SYNTHASE LIKE 4* (*GSL4*) and *GSL11*, were induced. However, introduction of *gsl4* or *gsl11* mutations individually into the *vte2* background did not suppress callose deposition or the overall LT-induced phenotypes of *vte2*. Intriguingly, introduction of a mutation disrupting *GSL5*, the major GSL responsible for pathogen-induced callose deposition, into *vte2* substantially reduced vascular callose deposition at LT, but again had no effect on the photoassimilate export phenotype of LT-treated *vte2*. These results suggest that *GSL5* plays a major role in TCW callose deposition in LT-treated *vte2* but that this *GSL5*-dependent callose deposition is not the primary cause of the impaired photoassimilate export phenotype.

**Keywords:** tocopherols, transfer cells, callose synthase, *Arabidopsis*, sugar export, antioxidants, phloem parenchyma cells

## INTRODUCTION

Tocopherols are essential nutrients in mammals and, together with tocotrienols, are collectively known as vitamin E (Evans and Bishop, 1922; Bramley et al., 2000; Schneider, 2005). As lipid-soluble antioxidants tocopherols quench singlet oxygen and scavenge lipid peroxy radicals and hence terminate the autocatalytic chain reaction of lipid peroxidation (Tappel, 1972; Fahrenholz et al., 1974; Burton and Ingold, 1981; Liebler and Burr, 1992; Kamal-Eldin and Appelqvist, 1996). Tocopherols are localized in biological membranes and associated with highly unsaturated fatty acids, and thus may also affect membrane properties, such as permeability and stability of membranes (Erin et al., 1984; Kagan, 1989; Stillwell et al., 1996; Wang and Quinn, 2000).

Tocopherols are synthesized only in photosynthetic organisms, including all plants and algae, and some cyanobacteria. However, tocopherol functions in these organisms remain poorly understood. The tocopherol-deficient *vte2* (*vitamin e 2*) mutant of *Arabidopsis thaliana* is defective in homogentisate phytol transferase (HPT), the first committed enzyme of the pathway, and lacks all tocopherols and pathway intermediates (Collakova and DellaPenna, 2001; Savidge et al., 2002;

Sattler et al., 2004; Mene-Saffrane et al., 2010). The *vte2* mutants exhibit reduced seed viability and defective seedling development associated with elevated lipid peroxidation (Sattler et al., 2004; Mene-Saffrane et al., 2010; DellaPenna and Mene-Saffrane, 2011), demonstrating that a primary role of tocopherols is to limit non-enzymatic lipid oxidation of polyunsaturated fatty acids (PUFAs), especially during seed desiccation and seedling germination. Transcript profiling studies further confirmed the importance of non-enzymatic lipid oxidation in triggering the oxidative and defense responses in germinating seeds of *vte2* (Sattler et al., 2006).

In contrast to the drastic *vte2* seedling phenotype, the *vte2* mutants that do survive early seedling development become virtually indistinguishable from wild type under permissive conditions and also under high light stress (Sattler et al., 2004; Maeda et al., 2006), suggesting that tocopherols are dispensable in mature plants even under highly photooxidative stress conditions. However, when tocopherol-deficient *Arabidopsis* plants are subjected to low temperature (LT) they developed a series of biochemical and physiological phenotypes (Maeda et al., 2006). As early as 6 h after LT treatment the *vte2* mutants exhibit an

impairment of photoassimilate export. This transport phenotype is accompanied by an unusual deposition of cell wall materials (i.e., callose) in the vasculature which likely creates a bottleneck for photoassimilate transport. Reduced photoassimilate export subsequently leads to carbohydrate and anthocyanin accumulation in source leaves, feedback inhibition of photosynthesis and ultimately growth inhibition of whole plants at LT (Maeda et al., 2006). This LT phenotype was independent of light level and was not associated with typical symptoms of photooxidative stress (i.e., photoinhibition, photobleaching, accumulation of zeaxanthin, or lipid peroxides) (Maeda et al., 2006).

The carbohydrate accumulation and callose deposition phenotypes of LT-treated *vte2* resemble the phenotypes of maize *sucrose export defective 1* (*sxd1*) and potato *SXD1*-RNAi lines, which are also tocopherol deficient and accumulate carbohydrates without LT treatment (Russin et al., 1996; Provencher et al., 2001; Sattler et al., 2003; Hofius et al., 2004). Thus, a role for tocopherols in phloem loading is conserved among different plants with the unique, LT-inducibility of *Arabidopsis vte2* mutant phenotype providing a useful tool to dissect the underlying mechanism. Detailed ultrastructure analysis of the vasculature of the *Arabidopsis vte2* mutant during a LT time course revealed that callose deposition occurred before significant accumulation of carbohydrate and is restricted to the transfer cell wall (TCW) of phloem parenchyma cells adjacent to the companion cell/sieve element complex (Maeda et al., 2006). While the TCW is usually characterized by invaginated wall ingrowth toward the cytoplasm (Haritatos et al., 2000; Talbot et al., 2002; McCurdy et al., 2008), the phloem parenchyma cells of LT-treated *vte2* developed abnormally thickened TCW with irregular shaped ingrowths and massive callose deposition (Maeda et al., 2006). These results demonstrated that TCW-specific callose deposition is tightly linked with the defective photoassimilate export phenotype and is not a secondary effect caused by carbohydrate accumulation. However, the molecular mechanism underlying the callose deposition remains to be determined as does whether impaired phloem loading is due to vascular callose deposition in TCWs in the tocopherol-deficient mutants.

Analysis of membrane lipid composition in wild-type *Arabidopsis* and the *vte2* mutant during LT treatment further revealed that tocopherol deficiency in plastids alters the PUFA composition of endoplasmic reticulum (ER) derived membrane lipids prior to LT treatment (Maeda et al., 2008). Subsequently, mutations in *FATTY ACID DESATURASE 2* (*FAD2*) and *TRIGALACTOSYLDIACYLGLYCEROL 1* (*TGD1*), encoding the ER-localized oleate desaturase and the ER-to-plastid lipid ATP-binding cassette (ABC) transporter, respectively, were identified as *suppressors of the vte2 LT-induced phenotypes* (*sve* loci) (Maeda et al., 2008; Song et al., 2010). These results provided biochemical and genetic evidence that alterations in extra-plastidic lipid metabolism are an upstream event in the initiation and development of the *vte2* LT-induced phenotypes (Maeda et al., 2008; Song et al., 2010). The unexpected role of plastid-localized tocopherols in ER lipid metabolism has led to the recent discovery of a novel mechanism allowing biochemical continuity between the ER and chloroplast membranes (Mehrshahi et al., 2013). However, further investigation is required to understand the molecular links

between tocopherol deficiency, lipid metabolism, and reduced photoassimilate export in LT-treated *vte2*.

In this study, microarray analysis of wild-type *Arabidopsis* and the *vte2* mutant was used to investigate the effects of tocopherol deficiency on global gene expression at both permissive and LT conditions. While multiple studies have investigated transcriptome responses to vitamin E deficiency in animals (Barella et al., 2004; Rota et al., 2004, 2005; Nell et al., 2007; Oommen et al., 2007), no global gene expression profile of the effect of tocopherols in photosynthetic tissues has hitherto been undertaken in plants. Although almost no changes were observed in genome wide transcription between wild type and *vte2* under permissive conditions, 77 genes were identified as being differentially expressed in *vte2* compared to wild type in response to LT-treatment. Attempts to genetically suppress transfer cell callose deposition by introducing mutations for two *GLUCAN SYNTHASE LIKE* (*GSL*) genes, whose expression was strongly induced in LT treated *vte2*, or a mutation in *GSL5*, previously shown to be the primary *GSL* responsible for callose deposition in response to pathogen ingress, demonstrated that *GSL5* is responsible for the majority of the LT-induced vasculature callose deposition in *vte2*. However, genetic elimination of this *GSL5*-dependent callose deposition showed that it is not the direct cause of the LT-induced photoassimilate export phenotype of *vte2*.

## MATERIALS AND METHODS

### PLANT MATERIALS AND GROWTH CONDITIONS

*Arabidopsis* plants were grown and treated at LT as described previously (Maeda et al., 2008). Briefly, seed were stratified for 4–7 days (4°C), planted in an equal mixture of vermiculite, perlite, and soil with 1 × Hoagland solution, and grown under permissive conditions: 12 h, 120 µmol photon m<sup>-2</sup> s<sup>-1</sup> light at 22°C/12 h darkness at 18°C and 70% relative humidity. Plants were watered every other day and with a half strength Hoagland solution once a week. For LT treatments, 4-week-old plants were transferred at the beginning of the light cycle to 12 h, 120 µmol photon m<sup>-2</sup> s<sup>-1</sup> light/12 h darkness at 7°C. For microarray analysis, the 9–11th oldest rosetta leaves from three independent plants were harvested together into a tube filled with liquid nitrogen 1 h into the light cycle after 48 and 120 h of LT-treatment or without LT-treatment (referred to as 0 h LT treatment).

### RNA EXTRACTION, LABELING, AND HYBRIDIZATION FOR MICROARRAY

Total RNA was extracted using the RNAqueous RNA extraction kit and the Plant RNA Isolation Aid (Ambion) according to the manufacturer's instructions. Labeling and hybridization of RNA were conducted using standard Affymetrix protocols by the Michigan State University DNA Microarray Facility. ATH1 *Arabidopsis* GeneChips (Affymetrix, Santa Clara, CA) were used for measuring changes in gene expression levels. Total RNA was converted into cDNA, which was in turn used to synthesize biotinylated cRNA. The cRNA was fragmented into smaller pieces and then was hybridized to the GeneChips. After hybridization, the chips were automatically washed and stained with streptavidin phycoerythrin using a fluidics station. The chips were scanned by the GeneArray scanner at 570 nm emission and 488 nm excitation.

## MICROARRAY DATA EVALUATION AND PREPROCESSING

Raw chip data were analyzed with R software (version 2.9, <http://www.r-project.org/>). Because of various problems associated with mismatch (MM) probes (Bolstad et al., 2003; Irizarry et al., 2003), only perfect match (PM) probe intensities were used. To assess data quality, the AffyRNAdeg and QCReport functions in the simpleaffy package were used to generate the RNA degradation (**Supplemental Figure S1**) and quality control (QC) plots (**Supplemental Figure S2**) for all 18 chips. The Boxplot tool included in the affy and simpleaffy packages were used to investigate the data distribution of the 18 chips (**Supplemental Figure S3**). RMA function as implemented in the affy package was used for background adjustment, normalization and summarization. A cluster dendrogram (**Figure 1**) was generated by applying hclust function using average linkage clustering of Euclidean distance based on the normalized expression values from 18 chips.

## STATISTICAL ANALYSES FOR DIFFERENTIALLY EXPRESSED GENES

Signal intensity data were analyzed with the use of a linear statistical model and an empirical Bayes method in the LIMMA package implemented in Bioconductor of R software (Smyth, 2005) to identify genes differentially expressed between genotypes at different time points of LT treatment. The *p*-values were adjusted for multiple testing with the Benjamini and Hochberg method to control the false discovery rate (Benjamini and Hochberg, 1995). Genes with adjusted *p*-values < 0.05 were considered significant. A heat map of the 77 significantly different genes in *vte2* at 48 h of LT treatment was generated using the average linkage clustering of Euclidean distance based on the normalized average expression values for each genotype and timepoint.

The 49 genes that were significantly induced in 48 h LT-treated *vte2* relative to wild-type (Col) plants (**Table 1**)

were also examined using the Meta-Analyzer feature of GENEVESTIGATOR (Zimmermann et al., 2004) to assess their responses to various conditions or treatments. The gene expression responses were calculated as ratios between a given treatment and its negative control with the resulting values reflecting up- or down-regulation of genes by a treatment. Twelve different stress conditions were chosen: Biotic stress treatments with *Botrytis cinerea* (6 treatment chips + 6 control chips), *Pseudomonas syringae* (3 + 3), and *Myzus persicae* (3 + 3). Chemical stress treatments were hydrogen peroxide ( $H_2O_2$ ) (3 + 2) and ozone (3 + 3). Hormone stress treatments were with abscisic acid (ABA, 2 + 2), ethylene (3 + 3), indole acidic acid (IAA, 3 + 3), and zeatin (3 + 3). Abiotic stress treatments were cold (3 + 3), drought (3 + 1), and heat (2 + 2). All experiments selected from GENEVESTIGATOR utilized mature leaves except for the hormone treatment data sets (ethylene, IAA, and zeatin) that were performed on seedlings. In addition, to compare the transcriptional responses to tocopherol deficiency in seedlings and mature plants (**Table 3**), microarray data for 0-day and 3-day-old seedlings of Col and *vte2* (three biological replicates for each treatment and genotype, see Sattler et al., 2006) were subjected to the same procedure of preprocessing and statistical analysis as described above for *vte2* plants under LT treatment.

## GENERATION OF MUTANT GENOTYPES

The following *gsl* mutant lines were obtained from the Arabidopsis Biological Resource Center at Ohio State University: SALK\_000507 for *GSL4* (with a T-DNA insert in exon 34 of At3g14570), *gsl5-1/prm4-1* for *GSL5* (with a non-sense mutation in exon 2 of At4g03550), and SALK\_019534 for *GSL11* (with a T-DNA insert in exon 15 of At3g59100). Homozygous mutant lines for *gsl5-1* were identified by PCR using CAPs genotyping primers (Nishimura et al., 2003). Homozygous mutants for *gsl4* and *gsl11* were identified by PCR using gene specific primers; 5' - TTGCCTGAGAGGATTAGCAAG - 3' (forward) and 5' - TTGAAGGATACAAGGACGTGG - 3' (reverse) for *gsl4* and 5' - TCACACCTTCATTCCCTGTTC - 3' (forward) and 5' - GTTCCTGTGTAAGGCCATG - 3' (reverse) for *gsl11*. The double homozygous mutant genotypes *vte2 gsl4*, *vte2 gsl5*, and *vte2 gsl11* were obtained by HPLC analysis for tocopherol deficiency (Collakova and DellaPenna, 2001) and the above mentioned PCR-based genotyping for *gsl* homozygosity. *vte2* homozygosity was also confirmed by a CAPs marker developed for the *vte2-1* point mutation (Maeda et al., 2006). Plants of Col, *vte2*, the single mutants of *gsl4*, *gsl5*, *gsl11*, and the three double mutants were grown for 4 weeks at permissive conditions and then transferred to LT conditions for the time periods, indicated in each figure legend for evaluation of different LT-induced phenotypes. Optimal time points were chosen based on our previous time-course analysis of the appearance of different LT-induced *vte2* phenotypes (Maeda et al., 2006, 2008).

## <sup>14</sup>C PHOTOASSIMILATE LABELING AND ANALYSIS OF SUGARS

Analyses for leaf glucose, fructose, and sucrose levels were performed as previously described (Maeda et al., 2006). <sup>14</sup>CO<sub>2</sub> labeling of photoassimilate and measurement of phloem

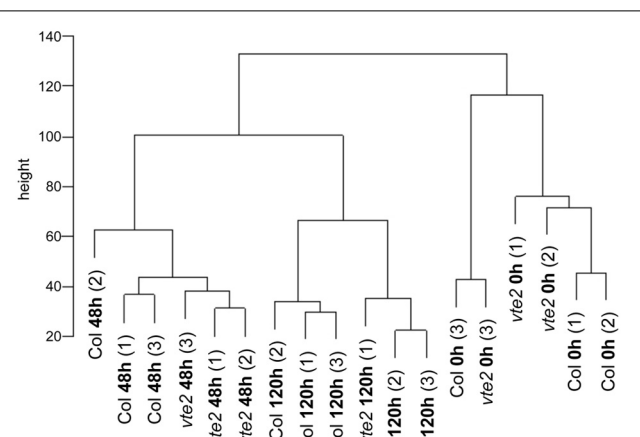


**FIGURE 1 | A cluster dendrogram of a correlation matrix for all-against-all chip comparisons.** The scale on the vertical bar "height" indicates Manhattan distance. The numbers (1) to (3) indicate three independent biological replications for treatments and genotypes. The samples cluster by different genotypes (Col and *vte2*) after LT treatment (48 and 120 h).

**Table 1 | The 49 genes significantly upregulated in *vte2* relative to Col at 48 h of LT treatment.**

AGI number	M <sup>a</sup>	adj-P-value <sup>b</sup>	B <sup>c</sup>	Annotated gene function <sup>d</sup>
At1g26450	2.62	0.00	11.64	Beta-1,3-glucanase-related
At4g23410	1.53	0.00	10.08	Senescence-associated family protein
At1g68290	2.39	0.00	7.97	Bifunctional nuclease, putative
At5g22860	1.38	0.00	7.04	Serine carboxypeptidase S28 family protein
At3g14570	1.85	0.00	6.88	Glycosyl transferase family 48 protein (glucan synthase like 4, GSL4)
At1g59500	1.58	0.00	6.79	Auxin-responsive GH3 family protein
At3g17690	1.80	0.00	6.74	Cyclic nucleotide-binding transporter 2/CNB2
At1g74590	1.50	0.00	6.31	Glutathione S-transferase, putative
At4g20320	1.08	0.00	5.80	CTP synthase, putative/UTP-ammonia ligase, putative
At3g22910	1.82	0.00	5.65	Ca-transporting ATPase, plasma membrane-type, putative (ACA13)
At5g13080	1.88	0.00	5.51	WRKY family transcription factor (WRKY75)
At5g47920	1.06	0.00	5.13	Expressed protein
At1g68620	2.08	0.00	4.95	Expressed protein
At1g65500	2.13	0.00	4.84	Expressed protein
At1g76640	2.52	0.00	4.54	Calmodulin-related protein, putative
At2g26020	2.01	0.00	4.40	Plant defensin-fusion protein, putative (PDF1.2b)
At1g74055	1.00	0.00	4.18	Expressed protein
At1g30370	1.60	0.01	3.80	Lipase class 3 family protein
At5g13880	1.45	0.01	3.60	Expressed protein
At3g49130	0.94	0.01	3.16	Hypothetical protein
At5g46590	1.31	0.01	3.09	No apical meristem (NAM) family protein
At3g21780	0.91	0.01	3.09	UDP-glucosyl transferase family protein
At1g17180	1.21	0.02	2.82	Glutathione S-transferase, putative
At1g65610	1.33	0.02	2.70	Endo-1,4-beta-glucanase, putative/cellulase, putative
At3g53600	0.70	0.02	2.39	Zinc finger (C2H2 type) family protein
At5g13170	1.01	0.02	2.37	Nodulin MtN3 family protein
At5g46350	1.02	0.02	2.34	WRKY family transcription factor (WRKY8)
At5g09470	0.93	0.02	2.26	Mitochondrial substrate carrier family protein
At4g35730	1.24	0.02	2.23	Expressed protein
At2g29090	1.07	0.03	2.15	Cytochrome P450 family protein
At2g30550	0.70	0.03	2.08	Lipase class 3 family protein
At4g38420	1.58	0.03	2.02	Multi-copper oxidase type I family protein
At4g27260	0.76	0.03	1.98	Auxin-responsive GH3 family protein
At3g59100	1.04	0.03	1.81	Glycosyl transferase family 48 protein (glucan synthase like 11, GSL11)
At4g19460	0.80	0.03	1.80	Glycosyl transferase family 1 protein
At3g09270	2.07	0.03	1.73	Glutathione S-transferase, putative
At5g22570	1.18	0.03	1.72	WRKY family transcription factor (WRKY38)
At1g32350	1.45	0.04	1.64	Alternative oxidase, putative
At5g17330	0.74	0.04	1.54	Glutamate decarboxylase 1 (GAD 1)
At4g28550	1.05	0.04	1.43	RabGAP/TBC domain-containing protein
At5g65600	1.27	0.04	1.38	Legume lectin family protein/protein kinase family protein
At4g36430	0.79	0.04	1.37	Peroxidase, putative
At5g04080	0.63	0.04	1.32	Expressed protein
At5g64905	1.78	0.04	1.25	Expressed protein
At5g66920	1.09	0.04	1.24	Multi-copper oxidase type I family protein
At5g63970	0.97	0.05	1.20	Copine-related
At2g23270	0.95	0.05	1.20	Expressed protein
At1g19250	0.86	0.05	1.10	Flavin-containing monooxygenase family protein
At5g67080	1.69	0.05	1.08	Protein kinase family protein

<sup>a</sup>M-value (M) is the value of the contrast and represents a log<sub>2</sub> fold change between 48 h-LT-treated *vte2* and Col.<sup>b</sup>adj-Pvalue is the p-value adjusted for multiple testing with Benjamini and Hochberg's method to control the false discovery rate.<sup>c</sup>B-statistic (B) is the log-odds that the gene is differentially expressed.<sup>d</sup>Annotation was obtained from the Gene Ontology of The Arabidopsis Information Resources.

exudation were also carried out as described (Maeda et al., 2006) except that 10 mM EDTA was used for exudation buffer and 0.05 mCi of NaH<sup>14</sup>CO<sub>3</sub> was used per labeling experiment. Phloem exudates were collected after 5 h of exudation.

### FLUORESCENCE AND TRANSMISSION ELECTRON MICROSCOPY

Leaves were prepared for aniline blue fluorescence microscopy and staining and visualization were performed as described (Maeda et al., 2006) except that the gain adjustment of the camera was set to 2.0 for images in **Figures 4B, 5A**. Leaves were prepared for transmission electron microscopy and immunolocalization of  $\beta$ -1,3-glucan as described (Maeda et al., 2006).

## RESULTS

### TOCOPHEROL DEFICIENCY HAS LITTLE IMPACT ON GLOBAL GENE EXPRESSION AT PERMISSIVE CONDITIONS

To identify changes in gene expression that might be specifically related to the absence of tocopherols, global transcript profiles were compared between *vte2* and Col plants grown under permissive conditions for 4 weeks, when they are physiologically and biochemically indistinguishable, and at two time points of LT treatment (48 and 120 h) selected based on our previous time-course study of the physiological and biochemical changes of *vte2* and Col during LT treatment (Maeda et al., 2006). After 48 h of LT, vascular callose deposition is strongly induced and photoassimilate export capacity is significantly lower in *vte2* compared to Col, though the visible whole plant phenotypes and soluble sugar accumulation between the two genotypes do not differ (Maeda et al., 2006). The 120 h LT timepoint represents a relatively late response time point when soluble sugars are significantly higher and callose deposition is even more extensive and wide spread in *vte2* (Maeda et al., 2006). Thus the 48 h time point should allow identification of early responses to tocopherol deficiency that are distinct from later, pleiotropic responses resulting from the strongly elevated sugar levels in *vte2* after 120 h of LT. The 0 h time point represents the absence of LT treatment (see Materials and Methods) and serves as a critical treatment control.

The *vte2* LT experiment comprised 18 chips in a factorial design. Three independent biological replicates were conducted for Col and *vte2* at each of the three time points, allowing rigorous statistical analysis of the data obtained. When the relationship of chips was examined by a cluster dendrogram, three clusters consistent with the three time points of LT treatment were apparent (**Figure 1**). The 48 and 120 h LT-treated samples were more closely related to each other than to the 0 h data, suggesting that the effect of LT treatment was greater than effects due to genotypic differences.

To investigate if tocopherol deficiency leads to any transcriptional changes before LT treatment, the linear models for microarray data (limma) analysis (Smyth, 2005) was performed to detect differently expressed genes between *vte2* and Col at 0 h (see Materials and Methods). With the exception of At2g18950, which encodes the mutated gene in the background (*VTE2/HPT*, Collakova and DellaPenna, 2003), no other statistically significant differences (at adjusted *p*-values of < 0.05) were observed. These data indicate that the lack of tocopherols *per se* has little impact

on global gene expression in mature *vte2* plants under permissive conditions.

### IDENTIFICATION OF DIFFERENTIALLY EXPRESSED GENES IN 48 h-LT-TREATED *vte2* AND Col

After 48 h at LT, 77 probe sets were found to be significantly different between *vte2* and Col: 49 genes were significantly induced (**Table 1**) and 28 were significantly repressed (**Table 2**) in *vte2* relative to Col. The expression patterns of these 77 genes across all time points are visualized in the gene tree in **Figure 2**. As discussed above, before LT treatment (0 h) expression levels of all genes are very similar between Col and *vte2* and changed differently between genotypes after LT treatment. Group I contains 43 genes whose expression is generally low at 0 h and induced in both Col and *vte2* after LT treatment, with induction in *vte2* being stronger and more persistent. Group II contains 17 genes whose expression is somewhat high at 0 h and then more strongly induced or repressed in *vte2* after LT treatment compared to Col. Group III (12 genes) and IV (5 genes) are expressed at moderately and very high levels at 0 h, respectively, and both repressed at LT more strongly and persistently in *vte2* than Col. Several genes in groups I, II, and III show opposite expression patterns in *vte2* and Col from 0 to 48 h of LT treatment (highlighted in red for induced or blue for repressed in *vte2* relative to Col, respectively) and are particularly interesting as they represent potential “marker genes” that are specifically impacted by tocopherol deficiency at LT.

Among the 49 induced genes at 48 h (**Table 1**), 6 are annotated as glycosyl transferases (At3g14570, At3g59100, At4g19460), UDP-glucosyl transferase (At3g21780), or glucanases (At1g26450, At1g65610). These genes are likely involved in aspects of cell wall modification, consistent with the major modifications to cell wall structure in phloem parenchyma cells of LT-treated *vte2* (Maeda et al., 2006, 2008). Notably, LT treatment induced significant, albeit low, expression of two putative callose synthase genes, *GSL4* (At3g14570) and *GSL11* (At3g59100) in *vte2* (**Table 1**). These genes are two members of the 12 member *GSL* callose synthase gene family in *Arabidopsis* and may contribute to the substantial callose deposition in transfer cells of LT-treated *vte2*. Other notable upregulated genes in LT-treated *vte2* are involved in stress and senescence responses, various signaling pathways, and transcriptional regulation, including WRKY (At5g13080, At5g46350, At5g22570), NAM (At5g46590), and zinc finger (C<sub>2</sub>H<sub>2</sub> type, At3g53600) transcription factors (**Table 1**).

The most significantly repressed gene in *vte2* at 48 h LT (**Table 2**) was *VTE2/HPT* (At2g18950, Collakova and DellaPenna, 2003), the locus mutated in the *vte2* background. Other downregulated genes of interest include a methionine sulfoxide reductase (At4g04830, EC 1.8.4.6), one member of a small gene family encoding enzymes that reduce oxidized methionine residues of proteins, and four genes encoding nodulin drug/metabolite transporters (**Table 2**). Nodulins are involved in nodulation of legume roots during symbiosis with *Rhizobia*, a process where extensive metabolite transport across peribacteroid membranes is required (Vandewiel et al., 1990; Hohnjec et al., 2009). Repression of these nodulins might be related to altered carbohydrate transport in LT-treated *vte2*.

**Table 2 | The 28 genes significantly downregulated in *vte2* relative to Col at 48 h of LT treatment.**

AGI number	M <sup>a</sup>	adj-P-value <sup>b</sup>	B <sup>c</sup>	Annotated gene function <sup>d</sup>
At2g18950	-2.36	0.00	7.93	HPT: tocopherol phytoltransferase
At5g14740	-0.77	0.00	6.32	Carbonate dehydratase 2 (CA2) (CA18)
At3g11930	-1.47	0.00	6.10	Universal stress protein (USP) family protein
At2g36830	-1.01	0.00	5.94	Major intrinsic family protein/MIP family protein
At1g04680	-0.74	0.00	5.41	Pectate lyase family protein
At1g76800	-1.43	0.00	5.36	Nodulin, putative
At4g08300	-2.98	0.00	4.58	Nodulin MtN21 family protein
At2g22330	-1.67	0.00	4.44	Cytochrome P450, putative
At3g10080	-0.72	0.01	3.86	Germin-like protein, putative
At5g44720	-1.05	0.02	2.89	Molybdenum cofactor sulfurase family protein
At5g23020	-3.81	0.02	2.88	2-isopropylmalate synthase 2 (IMS2)
At3g47470	-0.84	0.02	2.77	Chlorophyll A-B binding protein 4, chloroplast/LHCl type III CAB-4 (CAB4)
At1g51400	-0.88	0.02	2.61	Photosystem II 5 kD protein
At4g08290	-1.22	0.02	2.56	Nodulin MtN21 family protein
At1g21440	-1.17	0.03	2.18	Mutase family protein
At1g01620	-0.83	0.03	2.02	Plasma membrane intrinsic protein 1C (PIP1C)/aquaporin PIP1.3 (PIP1.3)/transmembrane protein B (TMPB)
At3g08940	-0.82	0.03	1.95	Chlorophyll A-B binding protein (LHCB4.2)
At5g24490	-1.22	0.03	1.91	30S ribosomal protein, putative
At4g04830	-1.57	0.04	1.58	Methionine sulfoxide reductase domain-containing protein
At2g37460	-1.93	0.04	1.54	Nodulin MtN21 family protein
At4g04040	-0.69	0.04	1.44	Pyrophosphate-fructose-6-phosphate 1-phosphotransferase beta sub-unit, putative
At1g31180	-0.85	0.04	1.41	3-isopropylmalate dehydrogenase, chloroplast, putative
At1g78370	-1.07	0.04	1.40	Glutathione S-transferase, putative
At5g02260	-1.23	0.04	1.38	Expansin, putative (EXP9)
At5g67070	-0.51	0.04	1.28	Rapid alkalinization factor (RALF) family protein
At1g13280	-0.94	0.04	1.26	Allene oxide cyclase family protein
At3g09580	-0.73	0.05	1.08	Amine oxidase family protein
At1g03600	-0.48	0.05	1.08	Photosystem II family protein

<sup>a</sup>M-value (M) is the value of the contrast and represents a log<sub>2</sub> fold change between 48 h-LT-treated *vte2* and Col.

<sup>b</sup>adj-Pvalue is the p-value adjusted for multiple testing with Benjamini and Hochberg's method to control the false discovery rate.

<sup>c</sup>B-statistic (B) is the log-odds that the gene is differentially expressed.

<sup>d</sup>Annotation was obtained from the Gene Ontology of The Arabidopsis Information Resources.

### THE 49 GENES INDUCED IN *vte2* ARE NOT UPREGULATED BY ABIOTIC STRESS *per se*

To investigate whether the 49 genes induced in LT-treated *vte2* are part of a general stress response their expression patterns under diverse abiotic and biotic stress conditions were examined using publically available Arabidopsis microarray data (**Figure 3**). Approximately half of the 49 genes induced in LT-treated *vte2* were also strongly and specifically upregulated by biotic treatments including the necrotrophic fungus *Botrytis cinerea* and pathogenic leaf bacterium *Pseudomonas syringae* but not the phloem-feeding aphid *Myzus persicae*. Interestingly, many of the genes that were upregulated by pathogen treatments were also induced by ozone treatment (**Figure 3**). These include most of the transcription factors (WRKY, NAM, and zinc finger family proteins) and some of the stress- and signaling-related genes (Glutathione S-transferases: At1g74590, At1g17180, At3g09270; auxin-responsive GH3 family proteins: At1g59500, At4g27260) induced in LT-treated *vte2*. In contrast, very few genes induced

in LT-treated *vte2* overlapped with genes responsive to abiotic stress conditions including heat, drought, and cold treatments or hormone treatments such as zeatin, IAA, ethylene, or ABA (**Figure 3**). These results suggest that the 49 genes with induced expression in LT-treated *vte2* are due to tocopherol deficiency rather than a general response to cold or other abiotic stresses.

A prior study showed that the transcriptome of germinating *vte2* seedlings (at permissive conditions) is substantially influenced by elevated non-enzymatic lipid peroxidation occurring in the mutant at this developmental stage (Sattler et al., 2006). To compare transcriptional responses of LT-treated *vte2* with those of 3-day-old *vte2* seedlings, our preprocessing and statistical analysis approach was applied to germinating Col and *vte2* seedling microarray datasets. Out of 744 genes identified as significantly different (adjusted *p* < 0.05) in 3-day-old *vte2* seedlings relative to 3-day-old Col, only 12 were in common with the 77 significant altered

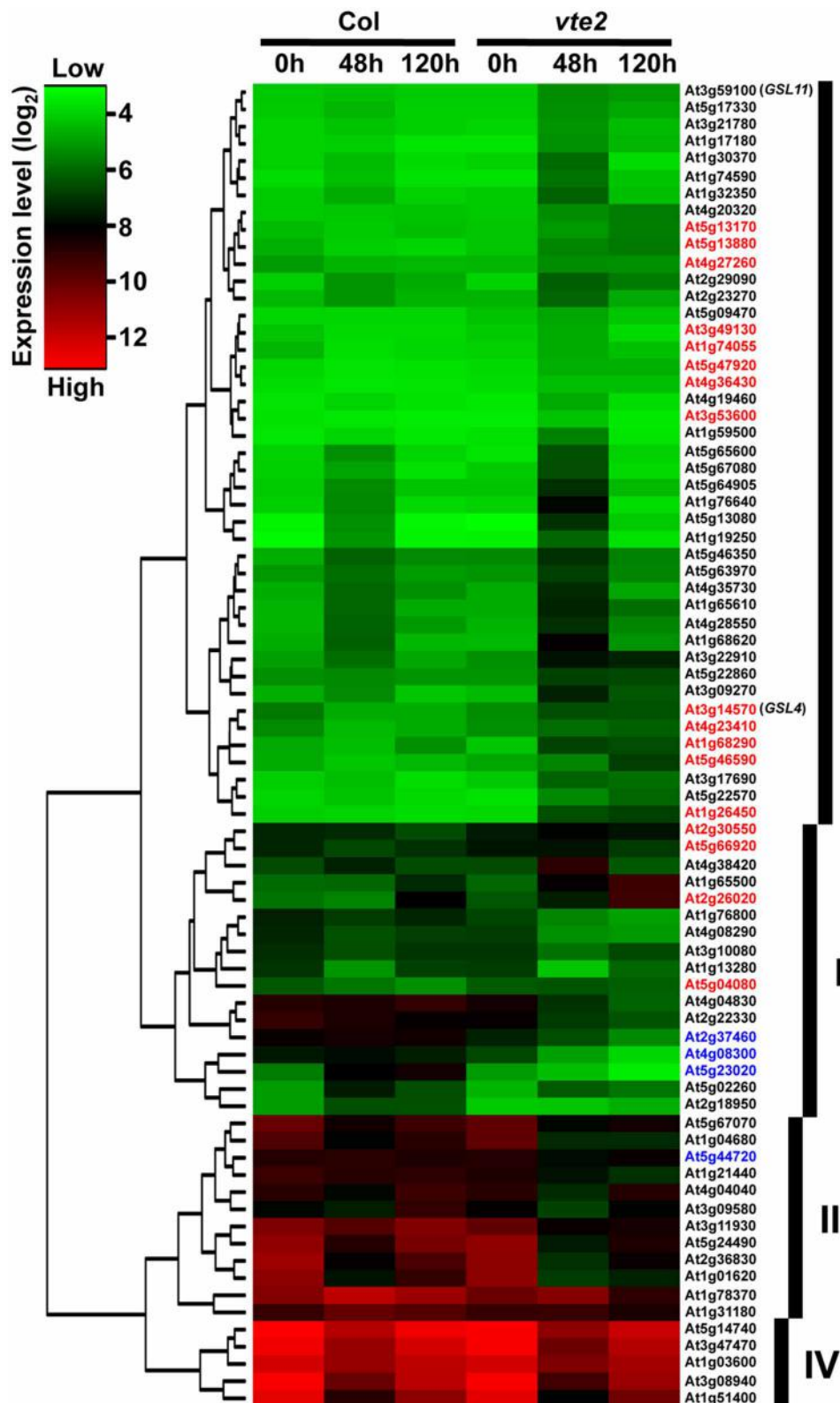
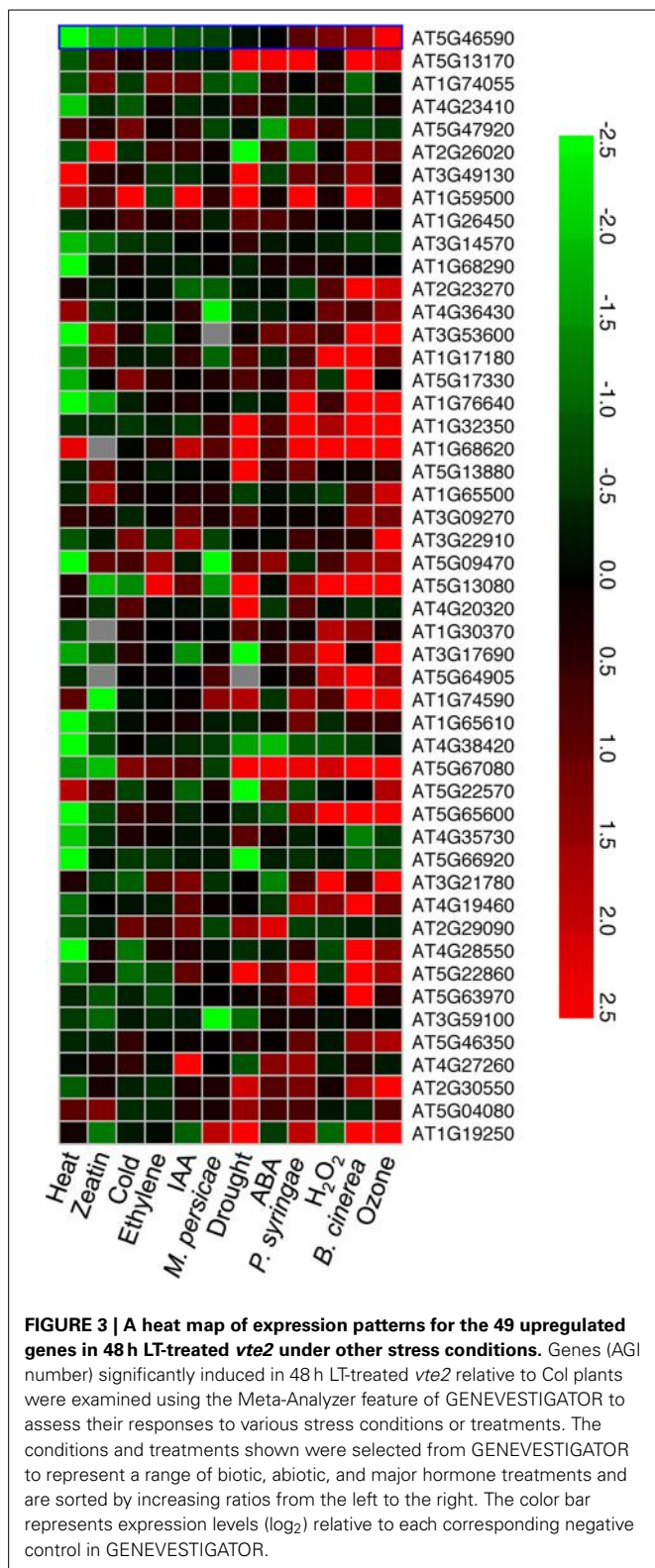


**FIGURE 2 | A gene tree of the 77 genes significantly altered in 48 h-LT-treated *vte2* relative to Col (adjusted *p*-value < 0.05).** The color bar represents expression levels (log<sub>2</sub>), with green to red being low to high expression. The groups (labeled as I, II, III, and IV) were based on general

expression patterns across Col and *vte2* at three time points of LT treatment. Genes showing opposite directions of expression from 0 to 48 h of LT treatment in Col and *vte2* are highlighted in red (induced in *vte2*) or blue (repressed in *vte2*). See text for additional details.



genes in 48 h-LT-treated *vte2* (Table 3). These results suggest that the majority of the transcriptional response of LT-treated *vte2* plants is largely distinct from that of *vte2* seedlings.

### *gsl4* AND *gsl11* HAVE LITTLE IMPACT ON LT-INDUCED *vte2* CALLOSE DEPOSITION

Vascular-specific callose deposition is a phenotype shared by tocopherol-deficient mutants in several plant species (Russin et al., 1996; Hofius et al., 2004; Maeda et al., 2006). It has been suggested that vascular-specific callose deposition may directly block photoassimilate translocation and lead to the subsequent carbohydrate accumulation and growth inhibition phenotypes in tocopherol-deficient plants (Russin et al., 1996; Hofius et al., 2004; Maeda et al., 2006). To test this hypothesis we attempted to genetically eliminate induced callose deposition in *vte2* by introducing mutations affecting specific callose synthase genes. Among the 12 GSL genes encoding putative callose synthases in the *Arabidopsis* genome (Richmond and Somerville, 2000; Hong et al., 2001), *GSL4* (*At3g14570*) and *GSL11* (*At3g59100*) were the only two family members whose expression was significantly altered in both 48 and 120 h LT-treated *vte2* relative to Col (adjusted  $p$ -value  $< 0.01$ ) (Table 1, Supplemental Figure S5). Homozygous mutants of *GSL4* and *GSL11* were therefore selected and introduced into the *vte2* background (see Materials and Methods) and the single *gsl* and *vte2* mutants and *gsl4 vte2* and *gsl11 vte2* double mutants were subjected to LT treatment to assess their phenotypes. Before LT treatment, the visible phenotypes of all the single and double mutants were similar to Col (Figure 4A). After prolonged LT treatment (28 days), which allows for full development of visible *vte2* LT phenotypes (Maeda et al., 2006), the *gsl4* and *gsl11* mutants appeared similar to Col while both of the double mutants were smaller, purple and similar to *vte2* (Figure 4A), indicating that neither the *gsl4* nor *gsl11* mutations have a substantial impact on the *vte2* LT phenotype. The levels of LT-induced vascular callose deposition (an early phenotype, as described in Maeda et al., 2006) detectable by aniline-blue fluorescence after 3 days LT treatment was also indistinguishable between the *vte2* single mutant and the *gsl4 vte2* or *gsl11 vte2* double mutants (Figure 4B). Thus, although *GSL4* and *GSL11* transcript levels are the only *GSL* family members induced higher in *vte2* than Col in response to LT treatment, loss of either gene activity does not have a major impact on callose deposition in LT-treated *vte2*.

### *gsl5* ATTENUATES THE MAJORITY OF CALLOSE DEPOSITION IN *vte2* WITHOUT SUPPRESSING THE PHOTOASSIMILATE EXPORT PHENOTYPE

Given that callose synthases are often post-transcriptionally regulated (Zavaliev et al., 2011), it is possible that enzymes responsible for the vascular-specific callose deposition of LT-treated *vte2* may be post-transcriptionally induced and not identified as differentially expressed between *vte2* and Col. *GSL5* is the best characterized of the 12 GSLs in *Arabidopsis* and has been shown to be required for callose formation in response to wounding and fungal pathogens (Jacobs et al., 2003; Nishimura et al., 2003). Although *GSL5* expression is modestly induced in response to LT-treatment and not differentially expressed in LT-treated *vte2* relative to wild type (Table 1, Supplemental Figure S5), it might still play a role in the vascular callose deposition of *vte2*. To test this possibility we introduced the *gsl5* mutation into the *vte2* background and examined its effect on LT-induced *vte2* phenotypes,

**Table 3 | The 12 genes that are common between the 77 significantly different genes in 48 h-LT-treated *vte2* plant and 744 significantly different genes in 3-d-old *vte2* seedling.**

AGI number	48 h-LT-treated <i>vte2</i> plant		3-day-old <i>vte2</i> seedling		Gene title <sup>c</sup>	GO molecular function <sup>c</sup>	GO cellular component <sup>c</sup>
	M <sup>a</sup>	adj-Pvalue <sup>b</sup>	M <sup>a</sup>	adj-Pvalue <sup>b</sup>			
At1g68290	2.39	0.00	2.01	0.00	Bifunctional nuclease, putative	Nucleic acid binding/endonuclease activity	Endomembrane system
At1g65500	2.13	0.00	4.33	0.00	Expressed protein	–	Endomembrane system
At1g74590	1.50	0.00	2.19	0.00	Glutathione S-transferase	Glutathione transferase activity	Cytoplasm
At5g46590	1.31	0.01	1.93	0.00	No apical meristem (NAM) family protein	Transcription factor activity/DNA binding	–
At1g17180	1.21	0.02	1.93	0.03	Glutathione S-transferase	Glutathione transferase activity	Cytoplasm
At5g46350	1.02	0.02	1.69	0.00	WRKY family transcription factor (WRKY8)	Transcription factor activity/DNA binding	Nucleus
At3g09270	2.07	0.03	1.29	0.02	Glutathione S-transferase	Glutathione transferase activity	Cytoplasm
At2g30550	0.07	0.03	1.02	0.05	Lipase class 3 family protein	Triacylglycerol lipase activity	Chloroplast
At4g36430	0.79	0.04	3.20	0.00	Peroxidase, putative	Peroxidase activity/calcium ion binding/oxidoreductase activity	Endomembrane system
At5g64905	1.78	0.04	1.10	0.01	Expressed protein	–	–
At1g76800	−1.43	0.00	−0.74	0.02	Nodulin, putative	–	–
At3g09580	−0.73	0.05	−0.90	0.02	Amine oxidase family protein	Oxidoreductase activity	Chloroplast

<sup>a</sup>M-value (M) is the value of the contrast and represents a log<sub>2</sub> fold change.<sup>b</sup>adj-Pvalue, the p-value adjusted for multiple testing with Benjamini and Hochberg's method to control the false discovery rate, were shown for 48 h-LT-treated *vte2* plant and 3-d-old *vte2* seedling, respectively.<sup>c</sup>Descriptions of gene function and cellular component were obtained from the Gene Ontology section of The Arabidopsis Information Resources.

Expression profiles of 0-day and 3-day-old seedling of Col and *vte2* were subjected to the same process of limma analysis for analysis of significant genes in 48 h-LT-treated *vte2* plants (see Materials and Methods). The list of 744 differentially expressed genes in 3-day-old *vte2* seedlings was compared with the list of 77 differentially expressed genes in 48 h-LT-treated *vte2* plants and overlapping 12 genes were listed.

including vascular callose deposition. Under permissive conditions, the *gsl5 vte2* double mutant had a visible phenotype similar to Col, *gsl5* and *vte2* (**Supplemental Figure S4**). When 4 week-old plants were subjected to 7 days of LT treatment (which induces a stronger callose deposition phenotype than 3 days of LT treatment), *vte2* exhibited the expected strong vascular-specific callose deposition, while no fluorescence signal was detectable in the vasculature of Col and *gsl5* (**Figure 5A**). Although the *gsl5 vte2* double mutant showed a substantial reduction in fluorescence intensity, weakly fluorescent spots were still present in the *gsl5 vte2* vasculature (**Figure 5A**). However, despite the strong reduction in callose deposition at LT, photoassimilate export capacity, elevated soluble sugar content, and the visible phenotype of *gsl5 vte2* were indistinguishable from that of *vte2* (**Figures 5B–D**).

To further address the role of the remaining GSL5-independent callose deposition in *gsl5 vte2*, transmission electron microscopy was used to examine the ultrastructure and

localization of callose in TCWs of Col, *gsl5*, *vte2*, and *gsl5 vte2*. The spatial organization and types of cells constituting the phloem and xylem of all genotypes were similar to prior reports (Haritatos et al., 2000; Maeda et al., 2006) and notable differences were observed only in the phloem parenchyma TCWs following 3 days of LT treatment. In all instances, cell wall differentiation ensued in phloem transfer cells of LT-treated plants. Both Col and *gsl5* developed uniform TCWs adjacent to the companion cell/sieve element complex (**Figures 6A,B,E,F**), whereas those in *vte2* and *gsl5 vte2* were not uniform and were abnormally thickened to varying degrees (**Figures 6C,D,G–I**). The extensive localized globular outgrowths of wall commonly found in transfer cells of *vte2* (Maeda et al., 2006) also developed in *gsl5 vte2* but were less frequent. Positive immunolocalization with monoclonal antibodies to callose ( $\beta$ -1,3-glucan) showed it was present in TCWs at the companion cell/sieve element boundary in *vte2* (Maeda et al., 2006), and also in *gsl5 vte2* (**Figures 6H,I**). Immunolabeling of



**FIGURE 4 | Whole plant and vascular callose phenotypes of *Col*, *vte2*, *gsl4*, *gsl4 vte2*, *gsl11*, and *gsl11 vte2*.** All genotypes were grown under permissive conditions for 4 weeks and then transferred to LT conditions for the specified periods previously shown to maximize each phenotype (Maeda et al., 2006). **(A)** Whole plant phenotype of the indicated

genotypes before (top) and after (bottom) 28 days of LT treatment. Bar = 2 cm. **(B)** Aniline-blue positive fluorescence in the lower portions of leaves after 3 days of LT treatment. Samples for callose staining were fixed in the middle of the light cycle. Representative images are shown ( $n = 3$ ). Bar = 1 mm.

callose was sometimes present but mostly rare to absent in all cell types of *Col* and *gsl5* (Figures 6E,F). These results indicate that although *GSL5* is responsible for the bulk of detectable callose deposition in LT treated *vte2* (Figure 5A), callose synthase(s) other than *GSL5* initiate the LT-induced callose deposition in transfer cells of *vte2* that may associate with the inhibition of photoassimilate export capacity in *vte2*.

## DISCUSSION

Genome wide transcriptional responses to tocopherol deficiency have been extensively studied in animals using  $\alpha$ -tocopherol transfer protein knock-out mice (*Ttpa*<sup>-/-</sup>) (Gohil et al., 2003; Vasu et al., 2007, 2009) or animals fed with tocopherol-deficient diets (Barella et al., 2004; Rota et al., 2004, 2005; Nell et al., 2007; Oommen et al., 2007). In addition to oxidative stress related transcripts (Gohil et al., 2003; Jervis and Robaire, 2004; Hyland et al., 2006), tocopherols were found to modulate the expression of genes involved in hormone metabolism and apoptosis in the brain (Rota et al., 2005), lipid metabolism, inflammation, and immune system in the heart (Vasu et al., 2007), cytoskeleton modulation in lungs (Oommen et al., 2007), synaptic vesicular trafficking in liver (Nell et al., 2007), and muscle contractility and protein degradation in muscle (Vasu et al., 2009). In contrast to the broad effects of tocopherol deficiency on the animal transcriptome, we found that the absence of tocopherols in *Arabidopsis* leads to

no significant changes in the global transcript profile of mature plants under permissive conditions. This finding extends a previous observation that *Arabidopsis* tocopherol-deficient mutants and wild type are virtually indistinguishable once they pass the oxidative stress bottlenecks of seed development and seedling germination (Maeda et al., 2006).

We previously showed that germinating seedlings of tocopherol-deficient *Arabidopsis vte2* mutants exhibit massive levels of non-enzymatic lipid peroxidation (Sattler et al., 2004) resulting in differential expression of more than 700 genes when compared to wild type (Sattler et al., 2006). In contrast to these drastic biochemical and transcriptional changes in *vte2* seedlings, lipid peroxidation was not detectable in mature *vte2* leaves subject to LT treatment (Maeda et al., 2006, 2008) with only 77 genes having significantly altered expression (Tables 1, 2). Just 12 of these 77 genes are in common with the > 700 altered genes in *vte2* seedlings, demonstrating that tocopherols play fundamentally distinct roles in seedlings and fully-expanded mature leaves. Moreover, of the 49 genes significantly upregulated in LT *vte2* (Table 1), very few were also induced in response to other abiotic stresses (see Results). Instead approximately half of the 49 induced genes in LT *vte2* were strongly and specifically upregulated by biotic and ozone treatments (Figure 3) with the latter significantly overlapping with transcriptional responses of plants to diseases (Eckeykaltenbach et al., 1994; Kangasjärvi

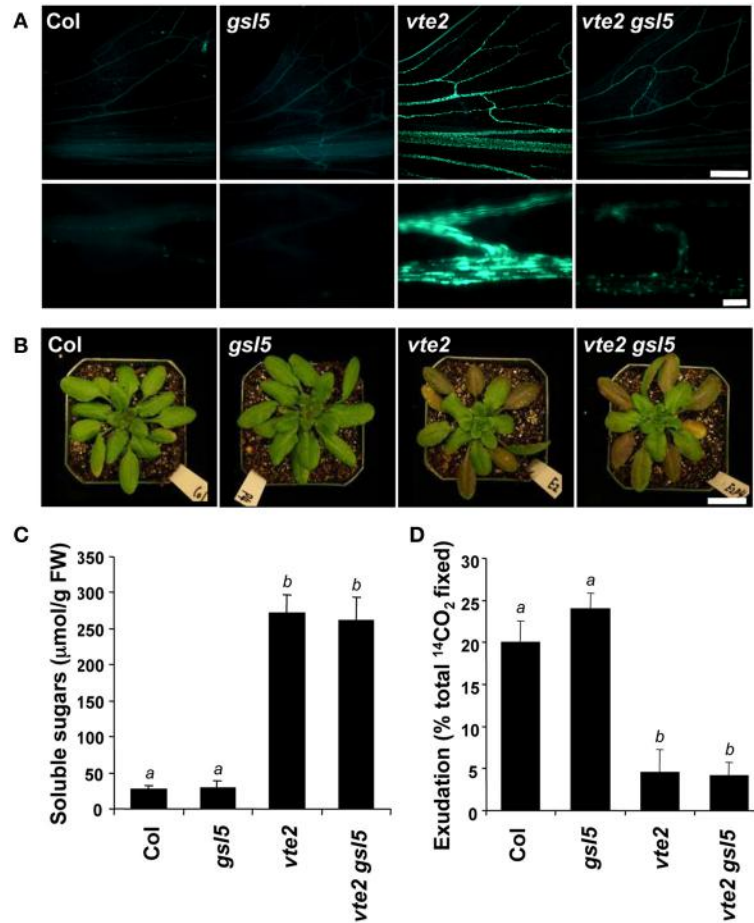


**FIGURE 5 | Characterization of the *gsl5 vte2* mutant at LT.** Col, *gsl5*, *vte2*, and *gsl5 vte2* were grown under permissive conditions for 4 weeks and transferred to LT conditions for the indicated times previously shown to maximize each phenotype (Maeda et al., 2006). **(A)** Aniline-blue positive fluorescence in the lower portions of leaves after 7 days of LT treatment. Samples for callose staining were fixed in the middle of the light cycle. Representative images are shown ( $n = 3$ ). The bottom panels are higher

magnification pictures of vasculature. Bars = 1 mm (top) and 100  $\mu$ m (bottom). **(B)** Whole plant phenotypes after 2 weeks of LT treatment. Bar = 2 cm. **(C)** Total soluble sugar content of mature leaves after 2 weeks of LT treatment. Data are means  $\pm$  SD ( $n = 5$ ). Non-significant groups are indicated by a and b ( $P < 0.05$ ). **(D)** <sup>14</sup>C-labeled photoassimilate export capacity of mature leaves after one additional week of LT treatment. Data are means  $\pm$  SD ( $n = 5$ ). Non-significant groups are indicated by a and b ( $P < 0.05$ ).

et al., 1994; Ludwikow et al., 2004). Thus, in contrast to the strong oxidative response of the *vte2* seedling transcriptome to germination, the transcriptome of mature *vte2* *Arabidopsis* leaves subjected to LT show a very limited oxidative stress response.

Prior studies have highlighted the involvement of tocopherols in extra-plastidic lipid metabolism under LT conditions (Maeda et al., 2006, 2008; Song et al., 2010). Based on these results, it might be expected that some genes related to lipid metabolism would be differentially expressed in *vte2* under LT. Surprisingly, however, only 2 of the 77 genes differentially expressed in LT-treated *vte2* are involved in lipid metabolism. Both are lipase class 3 family proteins and proposed to have triacylglycerol lipase activities, with one (At2g30550) localized in the chloroplast and the other (At1g30370) to mitochondria. The majority of fatty acid desaturase genes in *Arabidopsis*, with the exception of *FAD8* (Gibson et al., 1994), are not transcriptionally regulated in response to LT (Iba et al., 1993; Okuley et al., 1994;

Heppard et al., 1996) or alterations in the membrane fatty acid composition (Falcone et al., 1994). Thus, it seems that changes in extra-plastidic lipid metabolism in LT-treated *vte2* plants are not transcriptionally-regulated but rather are regulated at the post-transcriptional level.

As with biochemical analysis of LT treated plants, experimental materials for the current microarray analysis were of necessity taken from whole leaves (see Materials and Methods) and it is possible that *vte2* LT transcriptional “signatures” related to altered lipid metabolism or TCW synthesis are present but are restricted to such a small portion of specialized cell types (e.g., transfer cells) that their signals are diluted and difficult to identify in bulk leaf samples. Consistent with this idea, most of the genes identified as differentially expressed in LT-treated *vte2* have low expression levels and attempts to verify their expression by traditional RNA gel blot analysis often failed (data not shown). It is possible that differential transcriptional responses may only be present in transfer

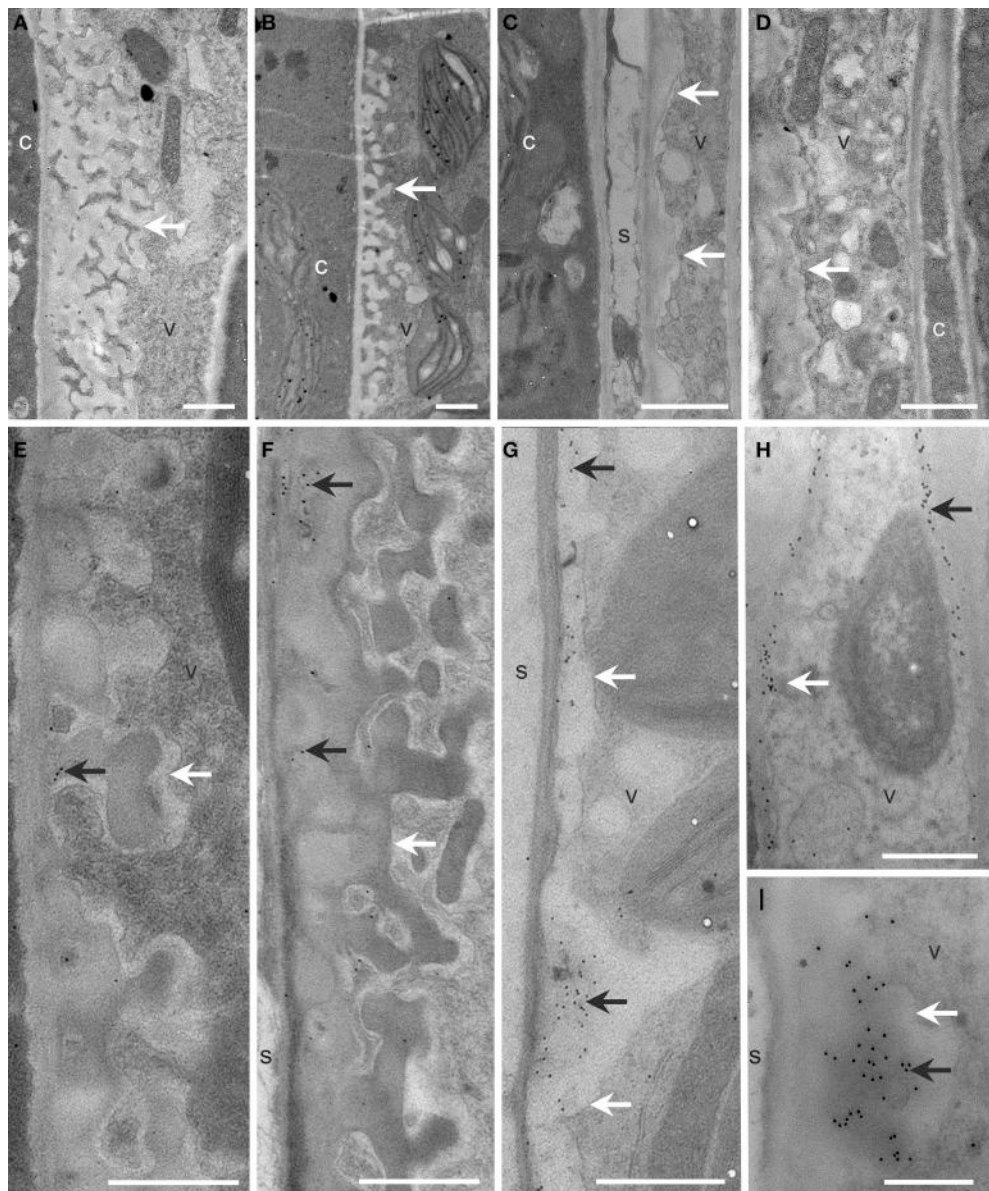


**FIGURE 6 | Cellular structure and immunodetection of callose after 3 days of LT treatment.** Col, *gs15*, *vte2*, and *gs15 vte2* were grown under permissive conditions for 4 weeks and transferred to LT conditions for 3 additional days. Col (**A,E**), *gs15* (**B,F**), *vte2* (**C,G**), and *gs15 vte2* (**D,H,I**). Black

arrows highlight wall ingrowths of phloem parenchyma transfer cells immunolabeled with anti- $\beta$ -1,3-glucan. White arrows mark transfer cell walls. c, companion cell; s, sieve element; v, vascular parenchyma transfer cell. Bars = 1  $\mu$ m (**A–H**), 0.5  $\mu$ m (**I**).

cells of *vte2*, where endomembrane biogenesis is strongly induced (Maeda et al., 2006) and the deposition of callose and abnormal cell wall ingrowths occur (Figure 6). Future experiments utilizing *in situ* hybridization or laser-microdissection of vascular parenchyma cells would be necessary to directly test whether more than the 77 genes identified in this study show such cell specific expression at LT and whether additional genes are regulated by tocopherols and also may contribute to the LT-induced phenotype of *vte2*.

The biochemical phenotype of 48 h-LT-treated *vte2* plants includes phloem transfer cell-specific callose deposition that

spreads from the petiole to the upper part of the mature leaves and potentially impacts the capacity of source to sink photoassimilate transportation (Maeda et al., 2006). Consistent with these phenotypes, the expression of several genes (e.g., glycosyl transferases, glucanases) that are potentially involved in cell wall polymer modification in transfer cells (Dibley et al., 2009) were significantly upregulated in *vte2* (Table 1). We also assessed the molecular nature of vasculature specific callose deposition observed in LT-treated *vte2* and its impact on the photoassimilate export phenotype. Based on our microarray analysis *GSL4* and *GSL11* were more strongly upregulated in LT-treated *vte2*

than in Col (**Supplemental Figure S5**) and therefore considered likely candidates for enzymes mediating the massive callose deposition observed in LT-treated *vte2*. However, introduction of *gsl4* and *gsl11* mutations into the *vte2* background did not visibly alter the callose deposition or overall phenotypes in LT-induced *gsl4 vte2* or *gsl11 vte2* double mutants (**Figure 4**). Somewhat surprisingly, though *GSL5* was not differentially expressed in LT-treated *vte2* and Col (**Supplemental Figure S5**), knocking out *GSL5* in the *vte2* background eliminated the majority, but not all, of callose deposition in LT-treated *vte2* (**Figures 5A** and **7**), indicating that the bulk of *vte2* callose deposition at LT is *GSL5*-dependent (**Figure 7**). Because *GSL5* is also responsible for callose deposition in response to wounding (Jacobs et al., 2003), tocopherol deficiency may improperly stimulate the wound response pathway in transfer cells and lead to post-transcriptional activation of the *GSL5* enzyme in transfer cells. However, Col and *vte2* showed similar levels of wound-induced callose deposition (data not shown). Taken together, these data suggest that tocopherols are required for post-transcriptional activation of *GSL5* in transfer cells by a mechanism that is likely independent of the wound-signaling pathway.

Unexpectedly, elimination of the majority of LT-inducible callose deposition by introduction of the *gsl5* mutation into the *vte2* background did not impact any of the other *vte2* LT phenotypes (**Figure 5**). The *vte2* mutant develops an abnormally thickened TCW structure with fewer to no reticulate wall ingrowths (**Figure 6**; Maeda et al., 2006, 2008). These structural anomalies are still retained in *vte2 gsl5* (**Figure 6**). Thus, although it can

be argued that the weaker, *GSL5*-independent fluorescent signals observed in the vasculature of *vte2 gsl5* may still impact photosynthate transport and development of the full suite of *vte2* LT phenotypes (**Figures 6A,C,E,G, 7**), these results indicate that the absolute level of callose deposition in transfer cells does not correlate with the photoassimilate export phenotype of *vte2*. This suggests that *GSL5*-dependent callose deposition is an event independent or downstream of the impaired photoassimilate export in LT-treated *vte2* (**Figure 7**). Future studies will focus on whether *GSL5*-independent callose deposition is involved in the impaired photoassimilate transportation phenotype by introducing additional *gsl* mutations into the *vte2 gsl5* background (e.g., by constructing *vte2 gsl5 gsl4 gsl11* quadruple mutant) to attempt elimination of all callose deposition in LT-treated *vte2*. Additional candidates to assess for this function include *GSL8* and *GSL12*, which contribute to the control of symplastic trafficking through plasmodesmata (Guseman et al., 2010; Vaten et al., 2011).

Previous and current studies have demonstrated that tocopherols are required for normal development of TCW ingrowths in *Arabidopsis* leaves in response to LT (**Figure 6**; Maeda et al., 2006, 2008). Although the precise underlying mechanism remains elusive, suppressor mutant analyses (Maeda et al., 2008; Song et al., 2010) and our recent transorganellar complementation study (Mehrshahi et al., 2013) suggest that deficiency in plastid-localized tocopherols directly impacts ER membrane lipid biogenesis. Although speculative at this point, these alterations in ER membrane lipid metabolism may in turn impact other endomembrane-related processes, such as the massive increase in vesicular trafficking required for deposition of cell wall material in transfer cells at LT (Talbot et al., 2002; McCurdy et al., 2008). Further investigation of the molecular links between altered ER lipid metabolism and the impairment of TCW development in LT-treated *vte2* (**Figure 7**) will illuminate the fundamental mechanisms underlying TCW development and function at LT.

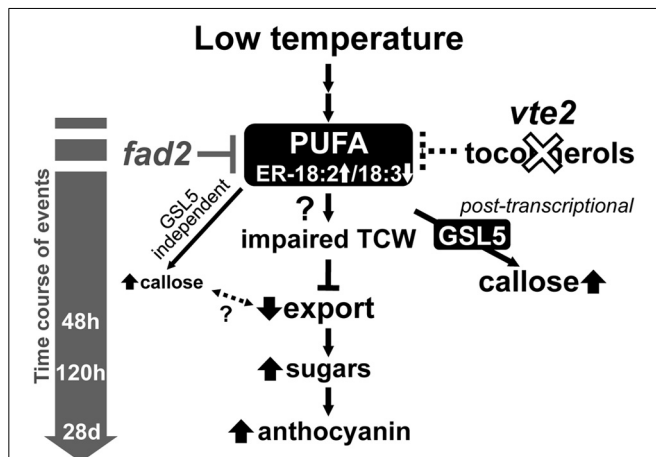


**FIGURE 7 | A proposed model of the timing of biochemical changes in LT-induced phenotypes of tocopherol-deficient mutants.** Tocopherol deficiency, e.g., by the *vte2* mutation, leads to constitutive alterations in the fatty acid composition of endoplasmic reticulum (ER) membrane lipids [i.e., reduced linolenic acid (18:3) and increased linoleic acid (18:2)]. These alterations are suppressed by the mutation of the *ER FATTY ACID DESATURASE 2* gene (*fad2*), which also suppresses all of the LT-induced *vte2* phenotypes (Maeda et al., 2008; Song et al., 2010). Subsequent vasculature-specific callose deposition is primarily mediated by the *GSL5* enzyme and tocopherol-deficiency affects its activity post-transcriptionally. Although low levels of *GSL5*-independent callose deposition still occurs, loss of the massive *GSL5*-dependent callose deposition in transfer cells does not affect the subsequent defect in photoassimilate export in LT-treated *vte2*.

## AUTHOR CONTRIBUTIONS

Hiroshi Maeda, Wan Song, and Dean DellaPenna designed research; Hiroshi Maeda, Wan Song, and Tammy Sage performed research; Hiroshi Maeda, Wan Song, Tammy Sage, and Dean DellaPenna analyzed data; Hiroshi Maeda, Wan Song, and Dean DellaPenna wrote the paper.

## ACKNOWLEDGMENTS

We are grateful to Maria Magallanes-Lundback for performing RNA extraction and labeling and the Research Technology Support Facility (RTSF) at Michigan State University for performing microarray analysis. We thank Kathy Sault for technical assistance with microscopy and other members of the DellaPenna lab for their critical advice and discussions. This work was supported by NSF grant MCB-023529 to Dean DellaPenna and a Connaught Award and NSERC of Canada Discovery Grant to Tammy Sage.

## SUPPLEMENTARY MATERIAL

The Supplementary Material for this article can be found online at: <http://www.frontiersin.org/journal/10.3389/fpls.2014.00046/abstract>

**Supplemental Figure S1 | RNA degradation plot for the 18 microarrays.****Supplemental Figure S2 | QC plot of 3': 5' ratios for control genes, percentage of present gene calls, and background levels of 18 microarrays.****Supplemental Figure S3 | Box plots of all perfect match (PM) intensities of non-normalized (upper) and quantile normalized (bottom) 18 array data set.****Supplemental Figure S4 | Whole plant phenotypes of the *gsf5 vte2* mutant grown under permissive conditions for 4 weeks.****Supplemental Figure S5 | Gene expression profiles for the 12 GSL family members in 4-week old Col and *vte2* treated at LT for 0, 48, and 120 h.****REFERENCES**

- Barella, L., Muller, P. Y., Schlachter, M., Hunziker, W., Stocklin, E., Spitzer, V., et al. (2004). Identification of hepatic molecular mechanisms of action of alpha-tocopherol using global gene expression profile analysis in rats. *Biochim. Biophys. Acta Mol. Basis Dis.* 1689, 66–74. doi: 10.1016/j.bbadic.2004.02.002
- Benjamini, Y., and Hochberg, Y. (1995). Controlling the false discovery rate - a practical and powerful approach to multiple testing. *J. R. Stat. Soc. B Methodol.* 57, 289–300.
- Bolstad, B. M., Irizarry, R. A., Astrand, M., and Speed, T. P. (2003). A comparison of normalization methods for high density oligonucleotide array data based on variance and bias. *Bioinformatics* 19, 185–193. doi: 10.1093/bioinformatics/19.2.185
- Bramley, P. M., Elmadfa, I., Kafatos, A., Kelly, F. J., Manios, Y., Roxborough, H. E., et al. (2000). Vitamin E. *J. Sci. Food Agric.* 80, 913–938. doi: 10.1002/(SICI)1097-0010(20000515)80:7<913::AID-JSFA600>3.0.CO;2-3
- Burton, G. W., and Ingold, K. U. (1981). Autoxidation of biological molecules. 1. The antioxidant activity of vitamin E and related chain-breaking phenolic antioxidants *in vitro*. *J. Am. Chem. Soc.* 103, 6472–6477. doi: 10.1021/ja0411a035
- Collakova, E., and DellaPenna, D. (2001). Isolation and functional analysis of homogentisate phytoltransferase from *Synechocystis* sp. PCC 6803 and *Arabidopsis*. *Plant Physiol.* 127, 1113–1124. doi: 10.1104/pp.010421
- Collakova, E., and DellaPenna, D. (2003). The role of homogentisate phytoltransferase and other tocopherol pathway enzymes in the regulation of tocopherol synthesis during abiotic stress. *Plant Physiol.* 133, 930–940. doi: 10.1104/pp.103.026138
- DellaPenna, D., and Mene-Saffrane, L. (2011). “Vitamin E,” in *Advances in Botanical Research*, eds F. Rebeille and R. Douces (Amsterdam: Elsevier Inc.), 179–227.
- Dibley, S. J., Zhou, Y. C., Andriunas, F. A., Talbot, M. J., Offler, C. E., Patrick, J. W., et al. (2009). Early gene expression programs accompanying trans-differentiation of epidermal cells of *Vicia faba* cotyledons into transfer cells. *New Phytol.* 182, 863–877. doi: 10.1111/j.1469-8137.2009.02822.x
- Eckeykaltenbach, H., Ernst, D., Heller, W., and Sandermann, H. (1994). Biochemical-plant responses to ozone. 4. Cross-induction of defensive pathways in parsley (*Petroselinum crispum* L.) plants. *Plant Physiol.* 104, 67–74. doi: 10.1104/pp.104.1.67
- Erin, A. N., Spirin, M. M., Tabidze, L. V., and Kagan, V. E. (1984). Formation of alpha-tocopherol complexes with fatty acids - a hypothetical mechanism of stabilization of biomembranes by vitamin E. *Biochim. Biophys. Acta* 774, 96–102. doi: 10.1016/0005-2736(84)90279-7
- Evans, H. M., and Bishop, K. S. (1922). On the existence of a hitherto unrecognized dietary factor essential for reproduction. *Science* 56, 650–651. doi: 10.1126/science.56.1458.650
- Fahrenholz, S. R., Doleiden, F. H., Trozzolo, A. M., and Lamola, A. A. (1974). Quenching of singlet oxygen by alpha-tocopherol. *Photochem. Photobiol.* 20, 505–509. doi: 10.1111/j.1751-1097.1974.tb06610.x
- Falcone, D. L., Gibson, S., Lemieux, B., and Somerville, C. (1994). Identification of a gene that complements an *Arabidopsis* mutant deficient in chloroplast omega-6 desaturase activity. *Plant Physiol.* 106, 1453–1459. doi: 10.1104/pp.106.4.1453
- Gibson, S., Arondel, V., Iba, K., and Somerville, C. (1994). Cloning of a temperature-regulated gene encoding a chloroplast omega-3 desaturase from *Arabidopsis thaliana*. *Plant Physiol.* 106, 1615–1621. doi: 10.1104/pp.106.4.1615
- Gohil, K., Schock, B. C., Chakraborty, A. A., Terasawa, Y., Raber, J., Farese, R. V., et al. (2003). Gene expression profile of oxidant stress and neurodegeneration in transgenic mice deficient in alpha-tocopherol transfer protein. *Free Radic. Biol. Med.* 35, 1343–1354. doi: 10.1016/S0891-5849(03)00509-4
- Guseman, J. M., Lee, J. S., Bogenschutz, N. L., Peterson, K. M., Virata, R. E., Xie, B., et al. (2010). Dysregulation of cell-to-cell connectivity and stomatal patterning by loss-of-function mutation in *Arabidopsis chorus* (glucan synthase-like 8). *Development* 137, 1731–1741. doi: 10.1242/dev.049197
- Haritatos, E., Medville, R., and Turgeon, R. (2000). Minor vein structure and sugar transport in *Arabidopsis thaliana*. *Planta* 211, 105–111. doi: 10.1007/s004250000268
- Heppard, E. P., Kinney, A. J., Stecca, K. L., and Miao, G. H. (1996). Developmental and growth temperature regulation of two different microsomal omega-6 desaturase genes in soybeans. *Plant Physiol.* 110, 311–319. doi: 10.1104/pp.110.1.311
- Hofius, D., Hajirezaei, M. R., Geiger, M., Tschiessch, H., Melzer, M., and Sonnewald, U. (2004). RNAi-mediated tocopherol deficiency impairs photoassimilate export in transgenic potato plants. *Plant Physiol.* 135, 1256–1268. doi: 10.1104/pp.104.043927
- Hohnjec, N., Lenz, F., Fehlberg, V., Vieweg, M. F., Baier, M. C., Hause, B., et al. (2009). The signal peptide of the *Medicago truncatula* modular nodulin MtNOD25 operates as an address label for the specific targeting of proteins to nitrogen-fixing symbiosomes. *Mol. Plant Microbe Interact.* 22, 63–72. doi: 10.1094/MPMI-22-1-0063
- Hong, Z., Delauney, A. J., and Verma, D. P. S. (2001). A cell plate specific callose synthase and its interaction with phragmoplastin. *Plant Cell* 13, 755–768. doi: 10.1105/tpc.13.4.755
- Hyland, S., Muller, D., Hayton, S., Stoecklin, E., and Barella, L. (2006). Cortical gene expression in the vitamin E-deficient rat: possible mechanisms for the electrophysiological abnormalities of visual and neural function. *Ann. Nutr. Metab.* 50, 433–441. doi: 10.1159/000094635
- Iba, K., Gibson, S., Nishiuchi, T., Fuse, T., Nishimura, M., Arondel, V., et al. (1993). A gene encoding a chloroplast omega-3 fatty acid desaturase complements alterations in fatty acid desaturation and chloroplast copy number of the *fad7* mutant of *Arabidopsis thaliana*. *J. Biol. Chem.* 268, 24099–24105.
- Irizarry, R. A., Bolstad, B. M., Collin, F., Cope, L. M., Hobbs, B., and Speed, T. P. (2003). Summaries of affymetrix GeneChip probe level data. *Nucleic Acids Res.* 31:e15. doi: 10.1093/nar/gng015
- Jacobs, A. K., Lipka, V., Burton, R. A., Panstruga, R., Strizhov, N., Schulze-Lefert, P., et al. (2003). An *Arabidopsis* callose synthase, GSL5, is required for wound and papillary callose formation. *Plant Cell* 15, 2503–2513. doi: 10.1105/tpc.016097
- Jervis, K. M., and Robaire, B. (2004). The effects of long-term vitamin E treatment on gene expression and oxidative stress damage in the aging brown Norway rat epididymis. *Biol. Reprod.* 71, 1088–1095. doi: 10.1095/biolreprod.104.028886
- Kagan, V. E. (1989). Tocopherol stabilizes membrane against phospholipase a, free fatty acids, and lysophospholipids. *Ann. N.Y. Acad. Sci.* 570, 121–135. doi: 10.1111/j.1749-6632.1989.tb14913.x
- Kamal-Eldin, A., and Appelqvist, L. A. (1996). The chemistry and antioxidant properties of tocopherols and tocotrienols. *Lipids* 31, 671–701. doi: 10.1007/BF02522884
- Kangasjarvi, J., Talvinen, J., Utriainen, M., and Katjalainen, R. (1994). Plant defence systems induced by ozone. *Plant Cell Environ.* 17, 783–794. doi: 10.1111/j.1365-3040.1994.tb00173.x
- Liebler, D. C., and Burr, J. A. (1992). Oxidation of vitamin E during iron-catalyzed lipid-peroxidation - evidence for electron-transfer reactions of the tocopheroxyl radical. *Biochemistry* 31, 8278–8284. doi: 10.1021/bi00150a022
- Ludwikow, A., Gallois, P., and Sadowski, J. (2004). Ozone-induced oxidative stress response in *Arabidopsis*: transcription profiling by microarray approach. *Cell. Mol. Biol. Lett.* 9, 829–842.
- Maeda, H., Sage, T. L., Isaac, G., Welti, R., and DellaPenna, D. (2008). Tocopherols modulate extraplastidic polyunsaturated fatty acid metabolism in *Arabidopsis* at low temperature. *Plant Cell* 20, 452–470. doi: 10.1105/tpc.107.054718
- Maeda, H., Song, W., Sage, T. L., and DellaPenna, D. (2006). Tocopherols play a crucial role in low-temperature adaptation and phloem loading in *Arabidopsis*. *Plant Cell* 18, 2710–2732. doi: 10.1105/tpc.105.039404
- McCurdy, D. W., Patrick, J. W., and Offler, C. (2008). Wall ingrowth formation in transfer cells: novel examples of localized wall deposition in plant cells. *Curr. Opin. Plant Biol.* 653–661. doi: 10.1016/j.pbi.2008.08.005

- Mehrshahi, P., Stefano, G., Andaloro, J. M., Brandizzi, F., Froehlich, J. E., and DellaPenna, D. (2013). Transorganellar complementation redefines the biochemical continuity of endoplasmic reticulum and chloroplasts. *Proc. Natl. Acad. Sci. U.S.A.* 110, 12126–12131. doi: 10.1073/pnas.1306331110
- Mene-Saffrane, L., Jones, A. D., and DellaPenna, D. (2010). Plastochromanol-8 and tocopherols are essential lipid-soluble antioxidants during seed desiccation and quiescence in *Arabidopsis*. *Proc. Natl. Acad. Sci. U.S.A.* 107, 17815–17820. doi: 10.1073/pnas.1006971107
- Nell, S., Bahtz, R., Bossecker, A., Kipp, A., Landes, N., Bumke-Vogt, C., et al. (2007). PCR-verified microarray analysis and functional *in vitro* studies indicate a role of alpha-tocopherol in vesicular transport. *Free Radic. Res.* 41, 930–942. doi: 10.1080/10715760701416988
- Nishimura, M. T., Stein, M., Hou, B. H., Vogel, J. P., Edwards, H., and Somerville, S. C. (2003). Loss of a callose synthase results in salicylic acid-dependent disease resistance. *Science* 301, 969–972. doi: 10.1126/science.1086716
- Okuley, J., Lightner, J., Feldmann, K., Yadav, N., Lark, E., and Browse, J. (1994). *Arabidopsis FAD2* gene encodes the enzyme that is essential for polyunsaturated lipid synthesis. *Plant Cell* 6, 147–158. doi: 10.1105/tpc.6.1.147
- Oommen, S., Vasu, V. T., Leonard, S. W., Traber, M. G., Cross, C. E., and Gohil, K. (2007). Genome wide responses of murine lungs to dietary alpha-tocopherol. *Free Radic. Res.* 41, 98–109. doi: 10.1080/10715760600935567
- Provencal, L. M., Miao, L., Sinha, N., and Lucas, W. J. (2001). Sucrose export defective1 encodes a novel protein implicated in chloroplast-to-nucleus signaling. *Plant Cell* 13, 1127–1141. doi: 10.1105/tpc.13.5.1127
- Richmond, T. A., and Somerville, C. R. (2000). The cellulose synthase superfamily. *Plant Physiol.* 124, 495–498. doi: 10.1104/pp.124.2.495
- Rota, C., Barella, L., Minihane, A. M., Stocklin, E., and Rimbach, G. (2004). Dietary alpha-tocopherol affects differential gene expression in rat testes. *IUBMB Life* 56, 277–280. doi: 10.1080/15216540410001724133
- Rota, C., Rimbach, G., Minihane, A. M., Stoecklin, E., and Barella, L. (2005). Dietary vitamin E modulates differential gene expression in the rat hippocampus: potential implications for its neuroprotective properties. *Nutr. Neurosci.* 8, 21–29. doi: 10.1080/10284150400027123
- Russin, W. A., Evert, R. F., Vanderveer, P. J., Sharkey, T. D., and Briggs, S. P. (1996). Modification of a specific class of plasmodesmata and loss of sucrose export ability in the sucrose export defective1 maize mutant. *Plant Cell* 8, 645–658. doi: 10.1105/tpc.8.4.645
- Sattler, S. E., Cahoon, E. B., Coughlan, S. J., and DellaPenna, D. (2003). Characterization of tocopherol cyclases from higher plants and cyanobacteria. Evolutionary implications for tocopherol synthesis and function. *Plant Physiol.* 132, 2184–2195. doi: 10.1104/pp.103.024257
- Sattler, S. E., Gilliland, L. U., Magallanes-Lundback, M., Pollard, M., and DellaPenna, D. (2004). Vitamin E is essential for seed longevity, and for preventing lipid peroxidation during germination. *Plant Cell* 16, 1419–1432. doi: 10.1105/tpc.021360
- Sattler, S. E., Mene-Saffrane, L., Farmer, E. E., Krischke, M., Mueller, M. J., and DellaPenna, D. (2006). Nonenzymatic lipid peroxidation reprograms gene expression and activates defense markers in *Arabidopsis* tocopherol-deficient mutants. *Plant Cell* 18, 3706–3720. doi: 10.1105/tpc.106.044065
- Savidge, B., Weiss, J. D., Wong, Y. H. H., Lassner, M. W., Mitsky, T. A., Shewmaker, C. K., et al. (2002). Isolation and characterization of homogentisate phytoltransferase genes from *Synechocystis* sp PCC 6803 and *Arabidopsis*. *Plant Physiol.* 129, 321–332. doi: 10.1104/pp.010747
- Schneider, C. (2005). Chemistry and biology of vitamin E. *Mol. Nutr. Food Res.* 49, 7–30. doi: 10.1002/mnfr.200400049
- Smyth, G. K. (2005). “Limma: linear models for microarray data,” in *Bioinformatics and Computational Biology Solutions Using R and Bioconductor*, eds V. C. R. Gentleman, S. Dudoit, R. Irizarry, and W. Huber (New York, NY: Springer), 397–420. doi: 10.1007/0-387-29362-0\_23
- Song, W., Maeda, H., and DellaPenna, D. (2010). Mutations of the ER to plastid lipid transporters TGD1, 2, 3 and 4 and the ER oleate desaturase FAD2 suppress the low temperature-induced phenotype of *Arabidopsis* tocopherol-deficient mutant vte2. *Plant J.* 62, 1004–1018. doi: 10.1111/j.1365-313X.2010.04212.x
- Stillwell, W., Dallman, T., Dumaual, A. C., Crump, F. T., and Jenski, L. J. (1996). Cholesterol versus alpha-tocopherol: effects on properties of bilayers made from heteroacid phosphatidylcholines. *Biochemistry* 35, 13353–13362. doi: 10.1021/bi961058m
- Talbot, M. J., Offler, C. E., and McCurdy, D. W. (2002). Transfer cell wall architecture: a contribution towards understanding localized wall deposition. *Protoplasma* 219, 197–209. doi: 10.1007/s007090200021
- Tappel, A. L. (1972). Vitamin E and free radical peroxidation of lipids. *Ann. N.Y. Acad. Sci.* 203, 12–28. doi: 10.1111/j.1749-6632.1972.tb27851.x
- Vandewiel, C., Norris, J. H., Bochenek, B., Dickstein, R., Bisseling, T., and Hirsch, A. M. (1990). Nodulin gene expression and Enod2 Localization in effective, nitrogen-fixing and ineffective, bacteria-free nodules of alfalfa. *Plant Cell* 2, 1009–1017. doi: 10.1105/tpc.2.10.1009
- Vasu, V. T., Hobson, B., Gohil, K., and Cross, C. E. (2007). Genome-wide screening of alpha-tocopherol sensitive genes in heart tissue from alpha-tocopherol transfer protein null mice (ATTP(-/-)). *FEBS Lett.* 581, 1572–1578. doi: 10.1016/j.febslet.2007.03.017
- Vasu, V. T., Ott, S., Hobson, B., Rashidi, V., Oommen, S., Cross, C. E., et al. (2009). Sarcolipin and ubiquitin carboxy-terminal hydrolase 1 mRNAs are over-expressed in skeletal muscles of alpha-tocopherol deficient mice. *Free Radic. Res.* 43, 106–116. doi: 10.1080/10715760802616676
- Vaten, A., Dettmer, J., Wu, S., Stierhof, Y. D., Miyashima, S., Yadav, S. R., et al. (2011). Callose biosynthesis regulates symplastic trafficking during root development. *Dev. Cell* 21, 1144–1155. doi: 10.1016/j.devcel.2011.10.006
- Wang, X. Y., and Quinn, P. J. (2000). The location and function of vitamin E in membranes (review). *Mol. Membr. Biol.* 17, 143–156. doi: 10.1080/09687680010000311
- Zavaliev, R., Ueki, S., Epel, B. L., and Citovsky, V. (2011). Biology of callose ( $\beta$ -1,3-glucan) turnover at plasmodesmata. *Protoplasma* 248, 117–130. doi: 10.1007/s00709-010-0247-0
- Zimmermann, P., Hirsch-Hoffmann, M., Hennig, L., and Gruisse, W. (2004). GENEVESTIGATOR. *Arabidopsis* microarray database and analysis toolbox. *Plant Physiol.* 136, 2621–2632. doi: 10.1104/pp.104.046367
- Conflict of Interest Statement:** The authors declare that the research was conducted in the absence of any commercial or financial relationships that could be construed as a potential conflict of interest.
- Received:** 02 December 2013; **accepted:** 29 January 2014; **published online:** 19 February 2014.
- Citation:** Maeda H, Song W, Sage T and DellaPenna D (2014) Role of callose synthases in transfer cell wall development in tocopherol deficient *Arabidopsis* mutants. *Front. Plant Sci.* 5:46. doi: 10.3389/fpls.2014.00046
- This article was submitted to Plant Physiology, a section of the journal *Frontiers in Plant Science*.
- Copyright © 2014 Maeda, Song, Sage and DellaPenna. This is an open-access article distributed under the terms of the Creative Commons Attribution License (CC BY). The use, distribution or reproduction in other forums is permitted, provided the original author(s) or licensor are credited and that the original publication in this journal is cited, in accordance with accepted academic practice. No use, distribution or reproduction is permitted which does not comply with these terms.



# Associations between the acclimation of phloem-cell wall ingrowths in minor veins and maximal photosynthesis rate

William W. Adams III<sup>1\*</sup>, Christopher M. Cohu<sup>1†</sup>, Véronique Amiard<sup>2</sup> and Barbara Demmig-Adams<sup>1</sup>

<sup>1</sup> Department of Ecology and Evolutionary Biology, University of Colorado, Boulder, CO, USA

<sup>2</sup> Genomics and Bioinformatics Unit, Agriaculture Nutritional Genomic Center, Temuco, Chile

**Edited by:**

David McCurdy, The University of Newcastle, Australia

**Reviewed by:**

Nabil I. Elsheery, Tanta University, Egypt

Hazem M. Kalaji, Warsaw University of Life Sciences, Poland

**\*Correspondence:**

William W. Adams III, Department of Ecology and Evolutionary Biology, University of Colorado, Boulder, CO 80309-0334, USA

e-mail: william.adams@colorado.edu

**†Present address:**

Christopher M. Cohu, Dow AgroSciences, Portland, OR, USA.

The companion cells (CCs) and/or phloem parenchyma cells (PCs) in foliar minor veins of some species exhibit invaginations that are amplified when plants develop in high light (HL) compared to low light (LL). Leaves of plants that develop under HL also exhibit greater maximal rates of photosynthesis compared to those that develop under LL, suggesting that the increased membrane area of CCs and PCs of HL-acclimated leaves may provide for greater levels of transport proteins facilitating enhanced sugar export. Furthermore, the degree of wall invagination in PCs (*Arabidopsis thaliana*) or CCs (pea) of fully expanded LL-acclimated leaves increased to the same level as that present in HL-acclimated leaves 7 days following transfer to HL, and maximal photosynthesis rates of transferred leaves of both species likewise increased to the same level as in HL-acclimated leaves. In contrast, transfer of *Senecio vulgaris* from LL to HL resulted in increased wall invagination in CCs, but not PCs, and such leaves furthermore exhibited only partial upregulation of photosynthetic capacity following LL to HL transfer. Moreover, a significant linear relationship existed between the level of cell wall ingrowths and maximal photosynthesis rates across all three species and growth light regimes. A positive linear relationship between these two parameters was also present for two ecotypes (Sweden, Italy) of the winter annual *A. thaliana* in response to growth at different temperatures, with significantly greater levels of PC wall ingrowths and higher rates of photosynthesis in leaves that developed at cooler versus warmer temperatures. Treatment of LL-acclimated plants with the stress hormone methyl jasmonate also resulted in increased levels of wall ingrowths in PCs of *A. thaliana* and *S. vulgaris* but not in CCs of pea and *S. vulgaris*. The possible role of PC wall ingrowths in sugar export versus as physical barriers to the movement of pathogens warrants further attention.

**Keywords:** biotic defense, companion cells, light acclimation, leaf vasculature, phloem, photosynthesis, temperature acclimation, transfer cells

## INTRODUCTION

Transfer cells, specialized for facilitating movement of molecules or ions into or out of cells as a result of enhanced cell-membrane area into which transport proteins are embedded, can be found at key junctures within and between plant tissues (Offler et al., 2003). The increased cell membrane area is achieved through invagination of the cell wall, leading to a labyrinth of wall and plasma membrane. In seeds of cotton, greater cell-wall ingrowths have been associated with a higher yield of fiber and seed biomass (Pugh et al., 2010), presumably due to greater fluxes of reduced carbon and nutrients from the mother plant to the developing seed. On the other hand, seed development was inhibited in a pea line with a mutation that blocked development of transfer cells between mother plant and seed (Borisjuk et al., 2002). There is thus clear evidence for a role of transfer cells in increasing the flux of nutrients into sinks resulting in enhanced sink development.

Transfer cells also occur in source tissues, e.g., in the phloem of minor leaf veins (Gunning et al., 1968; Offler et al., 2003). Such cells show enhanced levels of invagination in

response to various environmental conditions, including growth at higher levels of light (Henry and Steer, 1980; Wimmers and Turgeon, 1991) and, for the winter annual *Arabidopsis thaliana*, growth at lower temperatures (Edwards et al., 2010). Leaves of most plants grown in high compared to low light (Amiard et al., 2005), as well as those of winter annuals grown at low compared to warm temperature (Adams et al., 2013; Cohu et al., 2013b, 2014), exhibit higher rates of light- and CO<sub>2</sub>-saturated photosynthesis, and may therefore have a higher capacity for foliar sugar export. The extent to which transfer-cell enhancements in minor veins may enable increased levels of source activity has received little attention, although greater levels of sucrose export were associated with higher levels of wall ingrowth in pea (Wimmers and Turgeon, 1991). In addition, it was noted that pea leaves grown under high versus low light had both higher maximal rates of photosynthesis and higher levels of companion cell wall ingrowths (Amiard et al., 2005). Furthermore, several species exhibited greater levels of wall ingrowth in either phloem parenchyma or companion cells (or both cell types)

in leaves grown under high versus low light (Amiard et al., 2007).

In the present study, a comprehensive examination of associations between the extent of foliar minor-vein transfer-cell wall ingrowth and photosynthetic capacity was undertaken for leaves of three species grown under three different growth light regimes and for the leaves of two ecotypes of *A. thaliana* grown under three different temperature regimes. In addition, the impact of the stress hormone methyl jasmonate on foliar phloem-cell wall ingrowths is also reviewed, calling for a resolution (by future research) of the question of an involvement of phloem-parenchyma cell-wall ingrowth in either sugar export (as suggested by correlations between ingrowth level and maximal photosynthesis rate) and/or potential physical barriers to the passage of pathogens (as suggested by the responsiveness to methyl jasmonate).

## MATERIALS AND METHODS

### PLANTS, GROWTH CONDITIONS, AND EXPERIMENTAL TREATMENTS

Three species with transfer cells in their foliar minor veins (Pate and Gunning, 1969; Henry and Steer, 1980; Haritatos et al., 2000), *A. thaliana* (L.) Heynhold (ecotype Columbia, i.e., Col-0), *Pisum sativum* L. cv. Alaska (pea), and *Senecio vulgaris* L., were grown as described in Amiard et al. (2007) under either 100  $\mu\text{mol}$  photons  $\text{m}^{-2}\text{s}^{-1}$  (low light = LL) or 1000  $\mu\text{mol}$  photons  $\text{m}^{-2}\text{s}^{-1}$  (high light = HL) at 25°C during the day and 20°C during the

night. A third group of plants were grown under LL-conditions and then abruptly transferred to HL-conditions for a period of seven days. A fourth and fifth group of plants were grown under LL-conditions and sprayed daily with a solution of either 10  $\mu\text{M}$  methyl jasmonate (MeJA) in water and 0.05% Tween or only water and 0.05% Tween (control group for the MeJA-treated group) for 7 days. To evaluate the impact of growth temperature on transfer-cell wall ingrowths and photosynthesis, two ecotypes of *A. thaliana* (from Sweden and Italy; see Ågren and Schemske, 2012) were grown as described in Cohu et al. (2013a) under 400  $\mu\text{mol}$  photons  $\text{m}^{-2}\text{s}^{-1}$  with day/night leaf temperatures of approximately 14/12.5°C, 18/15°C, or 36/25°C. Only mature leaves that had expanded fully under the respective light and temperature growth conditions were characterized, with the exception that leaves transferred from LL to HL, or sprayed with a solution, had expanded fully prior to the 1-week treatment in each case.

### MINOR-VEIN TRANSFER CELL CHARACTERIZATION

Leaf tissue was fixed, sectioned, and stained, and electron micrographs of minor veins imaged, as described in Amiard et al. (2005). The percentage increase in cross-sectional cell membrane perimeter, relative to such cells possessing no cell wall ingrowths, was determined according to Wimmers and Turgeon (1991) as described in Amiard et al. (2005) using EEB Viewer software or

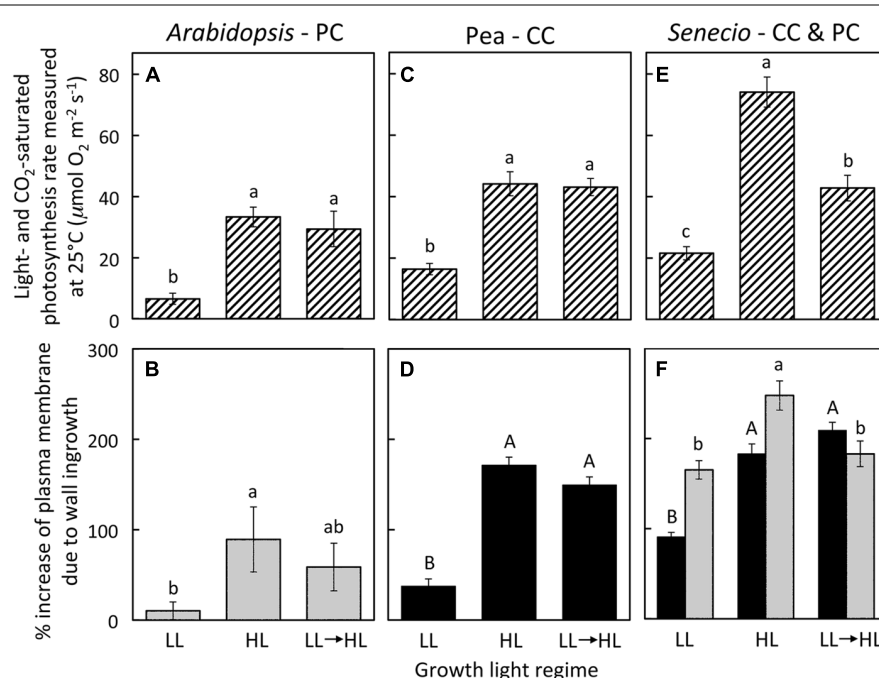


**FIGURE 1 | (A,C,E)** Foliar light- and  $\text{CO}_2$ -saturated rate of photosynthetic oxygen evolution ascertained at 25°C and **(B,D,F)** percent increase in plasma membrane length due to cell wall ingrowths estimated from cross-sections of phloem transfer cells (parenchyma = PC, companion = CC) relative to the hypothetical membrane area in the absence of wall ingrowths in foliar minor veins of *A. thaliana* **(A,B)**, pea **(C,D)**, and *S. vulgaris* **(E,F)** that developed in low light (LL), high light (HL), or LL and then transferred to HL for seven days. Light-gray columns indicate

PCs and black-filled columns indicate CCs. Significant differences between means ( $P < 0.05$ ) within each species are denoted by different lower-case letters, with the exception that upper-case letters are used to designate significant differences among the level of cell wall ingrowths for CCs, i.e., means sharing a common letter are not statistically different from each other. Photosynthetic capacities for pea from Amiard et al. (2005) and for *A. thaliana* and *S. vulgaris* grown in HL from Amiard et al. (2007).

Image-J (Rasband W. S., ImageJ, U.S. National Institute of Health, Bethesda, MD, USA, <http://imagej.nih.gov/ij/>, 1997–2012).

#### PHOTOSYNTHETIC CAPACITY (MAXIMAL RATE OF PHOTOSYNTHESIS)

The rate of light- and CO<sub>2</sub>-saturated photosynthetic oxygen evolution at 25°C in a water-saturated atmosphere was determined from leaf disks (Delieu and Walker, 1981) as described in Amiard et al. (2005). Saturating levels of CO<sub>2</sub> (5%) were provided to overcome all resistances (stomatal, cuticular, and mesophyll-related) to CO<sub>2</sub> diffusion to the chloroplasts. Saturating light of 1,475 or 2,425 μmol photons m<sup>-2</sup>s<sup>-1</sup> was used for leaves grown under 100 versus 400 and 1000 μmol photons m<sup>-2</sup> s<sup>-1</sup>, respectively.

#### STATISTICAL ANALYSES

For the Columbia ecotype of *A. thaliana* (Col-0), pea, and *S. vulgaris*, mean values of light- and CO<sub>2</sub>-saturated photosynthetic oxygen evolution (±standard deviation) were determined from three leaves from three different plants, and mean values for percent increase in plasma membrane length (±standard error) were determined from 26 to 87 cells from three to six leaves each. In the case of the Swedish and Italian ecotypes of *A. thaliana*, mean values of light- and CO<sub>2</sub>-saturated photosynthetic oxygen evolution (±standard deviation) were determined from three to four leaves from three to four different plants, and mean values for percent increase in plasma membrane length (±standard error) were determined from 27 to 48 cells from three to four leaves each. Comparison of means (ANOVA or *t*-test) and correlation coefficients and significance level of linear relationships (ANOVA) were determined using JMP software (SAS Institute, Cary, NC, USA).

#### RESULTS

Growth of *A. thaliana*, pea, and *S. vulgaris* under HL resulted in leaves with significantly higher photosynthetic capacities (maximal rates of photosynthesis; Figures 1A,C,D) and foliar minor veins with phloem transfer cells possessing a significantly higher level of cell-wall ingrowths (Figures 1B,D,F) compared to leaves from plants grown under LL. Photosynthetic capacity of fully expanded leaves of *A. thaliana* and pea was not statistically different from (i.e., was equivalent to) the high rates of HL-acclimated leaves one week following transfer of LL-acclimated plants to HL (Figures 1A,C), and the extent of transfer-cell wall invagination of minor vein phloem was also not statistically different between HL-acclimated leaves and those transferred from LL to HL (Figures 1B,D). On the other hand, fully expanded leaves of *S. vulgaris* plants transferred from LL to HL exhibited only partial upregulation of photosynthesis that was not only significantly higher than that of LL-acclimated leaves, but also significantly lower than that of HL-acclimated leaves (Figure 1E). The extent of minor-vein companion cell (CC) wall ingrowths of LL-to-HL transferred *S. vulgaris* leaves was significantly greater than that of LL-acclimated leaves and equivalent to that of HL-acclimated leaves (Figure 1F). On the other hand, minor-vein parenchyma cell (PC) wall ingrowths of LL-to-HL transferred *S. vulgaris* leaves were the same as that of LL-acclimated leaves and therefore significantly lower than that of HL-acclimated leaves (Figure 1F).

Plotting of the data from Figure 1 revealed a positive linear relationship between the level of minor-vein phloem transfer-cell wall ingrowth and photosynthetic capacity among all three species and all three growth-light conditions (Figure 2).

Development of leaves at low temperature (Figures 3B,D) resulted in enhanced levels of minor-vein phloem-PC wall ingrowths and photosynthetic capacities in both Italian (Figures 3A,B) and Swedish (Figures 3C,D) ecotypes of *A. thaliana* compared to development at warmer temperature (Figures 3A,C), such that both parameters were significantly higher in leaves of both ecotypes that developed at a leaf temperature of 14°C compared to leaves that developed at 36°C (Figure 4). Moreover, there were linear relationships between the level of such foliar minor-vein PC wall ingrowths and photosynthetic capacity of the leaves for each ecotype across three growth temperatures, with both metrics increasing significantly between growth at warm versus low temperature (Figure 5).

Treatment of LL-acclimated leaves with methyl jasmonate for one week resulted in a significantly greater level of cell wall ingrowths in the foliar minor vein phloem PCs of both *A. thaliana* (Figure 6A) and *S. vulgaris* (Figure 6C), but had no impact on the level of cell wall ingrowths in minor-vein phloem CCs of either pea (Figure 6B) or *S. vulgaris* (Figure 6C).

#### DISCUSSION

The regulatory factors modulating deposition of cellulose and lignin to form wall ingrowths are a subject of active research (e.g., Edwards et al., 2010; Arun Chinnappa et al., 2013). It has recently

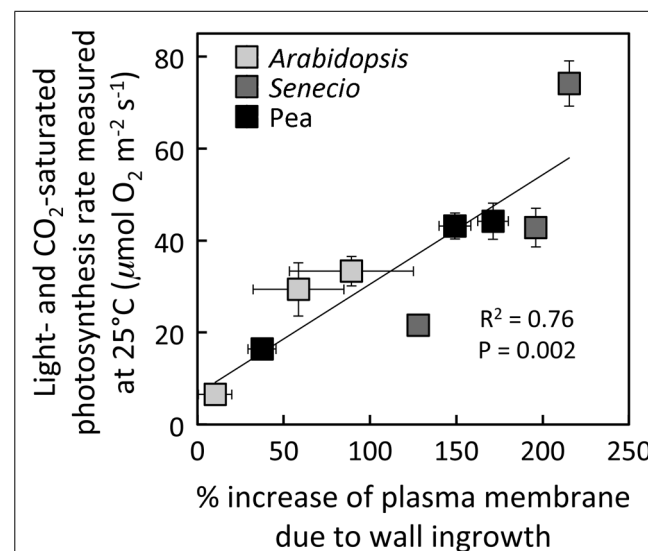


**FIGURE 2 |** Relationship between the percent increase of transfer-cell plasma membrane length in foliar minor veins and photosynthetic capacity from leaves of *A. thaliana* (light gray), pea (black), and *S. vulgaris* (dark gray) developed under LL or HL, or seven days after transfer of leaves developed under LL to HL. For *S. vulgaris*, the values for percent increase in transfer-cell plasma membrane length are averages of the mean values obtained from PCs and CCs. For additional information, see Figure 1.

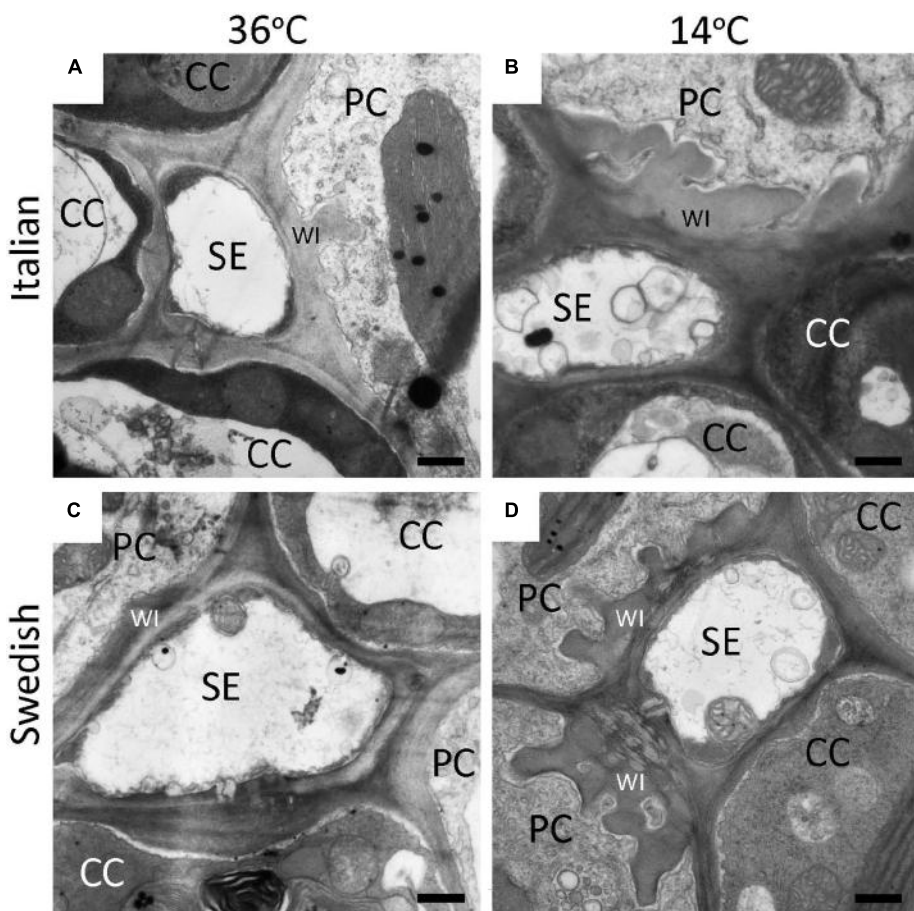


**FIGURE 3 |** Representative transmission electron-micrographic cross-sectional images of sieve elements (SE) surrounded by parenchyma (PC) and companion (CC) cells in foliar minor veins of Italian (A,B) or Swedish (C,D) ecotypes of *A. thaliana* that developed under  $400 \mu\text{mol photons m}^{-2}\text{s}^{-1}$  at a daytime leaf temperature of  $36^\circ\text{C}$  (A,C) or

$14^\circ\text{C}$  (B,D). Cell-wall ingrowths (WI) in the PCs are adjacent to the area abutting a neighboring SE, sometimes extend over the area of adjacent CCs (particularly apparent at lower temperature), and are more pronounced (greater level of invagination) in both ecotypes that developed at lower temperature. Black bar = 500 nm in length.

been demonstrated that reactive-oxygen species play a central role in stimulating such ingrowth formation (Andriunas et al., 2012), as we had postulated previously (Amiard et al., 2007). Any abiotic stress, such as the high growth light or low growth temperatures employed in this study, might be expected to generate higher levels of reactive oxygen species (Suzuki et al., 2012). Wounding through attack by pests or infection by pathogens also leads to elevated levels of reactive oxygen (Bell et al., 1995; Torres, 2010). Increased levels of reactive oxygen can, in turn, be expected to result in increased formation of oxylipin hormones (e.g., jasmonic acid and methyl jasmonate) through peroxidation of polyunsaturated fatty acids (Demmig-Adams et al., 2013). An increase in the synthesis of jasmonate hormones, that stimulate jasmonate responsive genes important to the defense of plants, is one of the major responses of plants to abiotic and biotic (e.g., pathogen and insect attack) stress (Avanci et al., 2010; Ballare, 2011; Kazan and Manners, 2011; Hu et al., 2013; Santino et al., 2013).

The synthesis of jasmonates has, moreover, been localized to the vasculature of plants (Hause et al., 2003; Stenzel et al., 2003;

Howe, 2004). This is perhaps not surprising, given that the PCs are typically the primary cells of the phloem subject to invasion by pathogenic viruses and fungi (Ding et al., 1995, 1998; Heller and Gierth, 2001; Zhou et al., 2002) as a means to gain access to sieve elements for distribution throughout the plant (Gilbertson and Lucas, 1996; Lucas and Wolf, 1999; Waigman et al., 2004; Scholthof, 2005; Vuorinen et al., 2011). The specific localization of PC-cell wall ingrowths to the region adjacent to sieve elements, coupled with the fact that PC wall ingrowth development was stimulated by MeJA, are both consistent with the hypothesis that such augmentation of cell wall material could serve as an increased physical barrier to the transmission of pathogens into the plant vascular system (for further discussion, see Amiard et al., 2007 and Demmig-Adams et al., 2013). Furthermore, the greater level of cell-wall ingrowth in the Italian compared to the Swedish *A. thaliana* ecotype when grown at higher temperature ( $36^\circ\text{C}$ ) may be related to the higher temperatures naturally experienced by the Italian ecotype (Ågren and Schemske, 2012) as well as the greater susceptibility to pathogenic infection that plants may

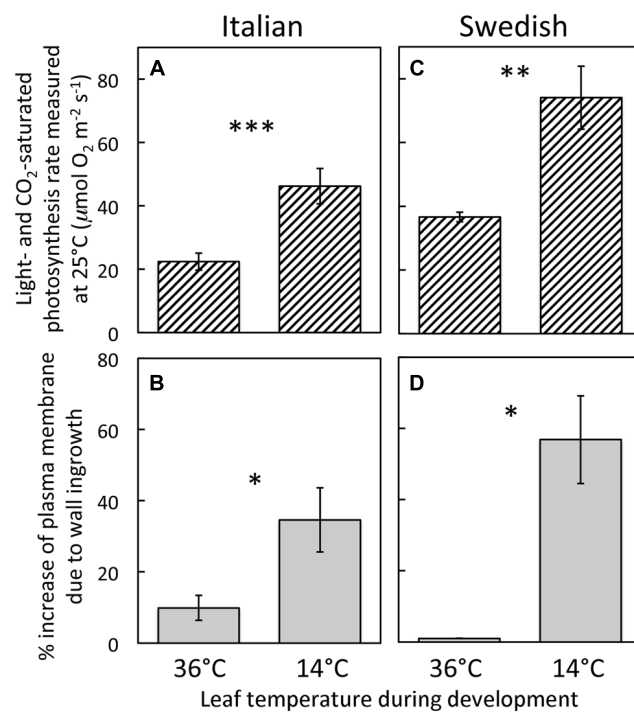


**FIGURE 4 | (A,C)** Foliar light- and  $\text{CO}_2$ -saturated rate of photosynthetic oxygen evolution ascertained at 25°C and **(B,D)** percent increase in plasma-membrane length due to cell-wall ingrowths estimated from cross-sections of phloem-parenchyma transfer cells relative to the hypothetical membrane area in the absence of wall ingrowths in foliar minor veins of Italian **(A,B)** and Swedish **(C,D)** ecotypes of

*A. thaliana* that developed under 400  $\mu\text{mol}$  photons  $\text{m}^{-2} \text{s}^{-1}$  at daytime leaf temperatures of 36 or 14°C. Significant differences between the means within each ecotype are denoted by asterisks (\* $P < 0.05$ , \*\* $P < 0.01$ , and \*\*\* $P < 0.001$ ). Photosynthetic capacities from leaves that developed at 14°C from Cohu et al. (2013b).

experience at elevated temperature (Celebi-Toprak et al., 2003; Qu et al., 2005).

While higher light and lower temperature both represent conditions of potentially greater levels of excess light and therefore the potential for higher levels of reactive oxygen formation, they also represent the opportunity for higher rates of photosynthesis. The greater energy content of a higher flux of photons can be beneficial for any species capable of upregulating photosynthesis in the absence of environmental and/or genetic constraints (Amiard et al., 2005), and winter annual species likewise respond to lower temperature with strong upregulation of photosynthesis (Cohu et al., 2013b, 2014). The significant correlation between the level of minor-vein phloem cell wall ingrowths and photosynthetic capacity in the leaves of multiple species/ecotypes grown under different conditions of light and temperature documented here would be consistent with a role of these transfer cells in supporting foliar export of the products of photosynthesis. The increase in plasma membrane resulting from such ingrowths may thus serve to facilitate greater levels of assimilate export through (1) an increased area for sugar efflux from PCs into the apoplast adjacent to the sieve elements and CCs or from the apoplast to the cytosol of the CC transfer cells, (2) increased levels of ATPases for actively transporting protons from the cytosol of the transfer cells to the apoplast, and (3) increased levels of  $\text{H}^+$ -sucrose symporters for moving sucrose from the apoplast into CC transfer cells as a critical

step in the active loading of the phloem (Pate and Gunning, 1972; Gunning and Pate, 1974; Kühn, 2003; Offler et al., 2003; Sondergaard et al., 2004; Amiard et al., 2007). Cell-wall ingrowths provide a scaffold on which to lay down a significantly higher plasma-membrane area in which greater numbers of membrane-spanning transport proteins can be embedded. It should be kept in mind, however, that the metric assessed in the present study, as a two-dimensional measure of cell membrane length from cross-sections of transfer cells, can only serve as a proxy for the actual magnified membrane area arising from the labyrinth of cell-wall ingrowths.

It has been firmly established that the level of demand for products of photosynthesis by distant sinks in the plant can influence the rate of photosynthesis in source leaves, e.g., higher levels of utilization of sugars through metabolism, growth, and/or storage by heterotrophic, non-photosynthetic tissues result in higher rates of photosynthesis (Paul and Foyer, 2001; Körner, 2013). However, recent evidence indicates that features influencing the flux of reduced carbohydrates between photosynthetic mesophyll cells of the leaf and the plant's sinks may also play a role in setting the upper ceiling for photosynthesis (Amiard et al., 2005; Adams et al., 2007, 2013; Cohu et al., 2013b, 2014; Muller et al., 2014; see also Ainsworth and Bush, 2011). Thus, despite the association between the degree of foliar minor-vein phloem cell-wall ingrowth and photosynthesis demonstrated in the present study, this relationship is only correlative in nature and should be considered as one

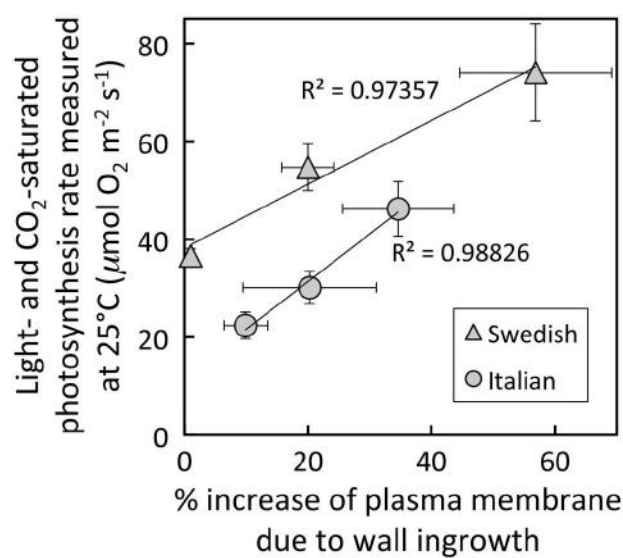


**FIGURE 5 | Relationship between the percent increase of parenchyma-cell plasma-membrane length in foliar minor veins and photosynthetic capacity from leaves of Italian (circles) or Swedish (triangles) ecotypes of *A. thaliana* that developed under  $400 \mu\text{mol photons m}^{-2} \text{s}^{-1}$  at a daytime leaf temperature of  $36^\circ\text{C}$  (lowest values),  $18^\circ\text{C}$  (intermediate values), or  $14^\circ\text{C}$  (highest values). The linear relationship among all six values (not shown) was significant at  $P < 0.05$ , whereas the linear relationships shown for each ecotype were not. Photosynthetic capacities from leaves that developed at  $14^\circ\text{C}$  from Cohu et al. (2013b).**

of a suite of features that may be co-regulated and contribute to facilitating a given maximal rate of photosynthesis. For instance, in the case of *A. thaliana* (three ecotypes grown under four different sets of environmental conditions), we recently showed (Cohu et al., 2013b) that photosynthetic capacity is significantly correlated with number and cross-sectional area of minor-vein phloem cells (sieve elements, as well as CCs + PCs). In fact, the higher rate of photosynthesis for a given level of foliar minor-vein PC wall ingrowth in the Swedish compared to the Italian ecotype of *A. thaliana* shown in the present study may be related to higher numbers and a greater cross-sectional area of minor vein phloem cells in leaves of the Swedish ecotype relative to the Italian ecotype (Cohu et al., 2013a,b). Furthermore, across multiple species that load foliar veins apoplastically, photosynthetic capacity was significantly correlated with the product of foliar vein density and the number of phloem cells (Adams et al., 2013; Cohu et al., 2014; Muller et al., 2014). In addition, symplastic loaders do not have minor-vein phloem transfer cells, nor are transfer cells even present in all apoplastic loaders. Thus the degree to which minor-vein transfer cell walls are invaginated is an attractive candidate for being a contributor to the maximal photosynthesis that a leaf can exhibit, but is only one factor among many including, e.g., the number of palisade cell layers, vein density, characteristics of the xylem supplying water to the leaves, and other features of the phloem (Amiard et al., 2005; Dumlaow et al., 2012; Cohu et al., 2013b; Cohu et al., 2014; Muller et al., 2014). The correlations between photosynthesis rate and phloem-cell wall invagination presented here clearly warrant further inquiry into a role of both CC and PC wall

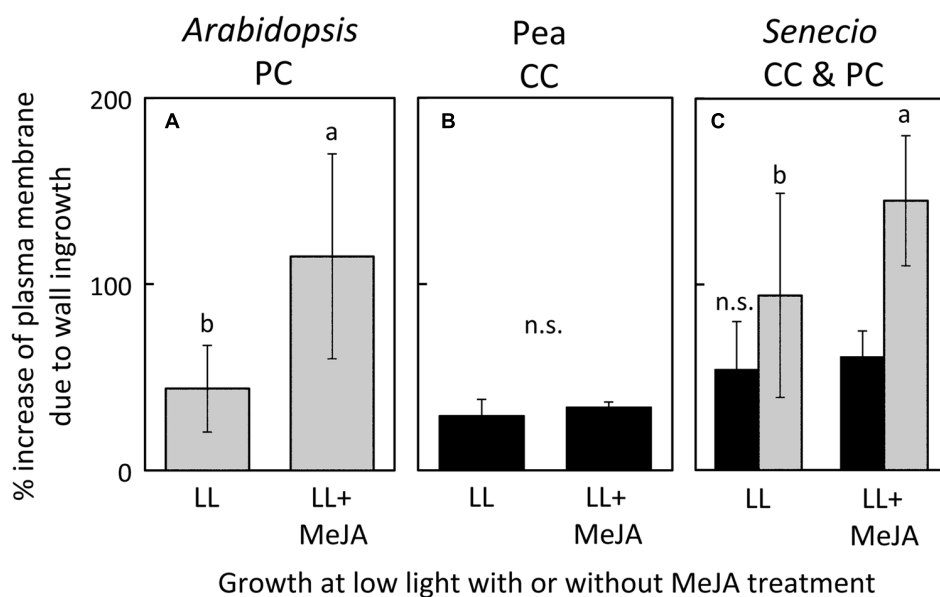


**FIGURE 6 | Percent increase in plasma-membrane length due to cell-wall ingrowths estimated from cross-sections of phloem transfer cells (parenchyma = PC, companion = CC) relative to the hypothetical membrane area in the absence of wall ingrowths in foliar minor veins of *A. thaliana* (A), pea (B), and *S. vulgaris* (C) that developed in low light and were sprayed with a 0.05% solution of Tween (LL) or a 0.05% solution of Tween with  $10 \mu\text{M}$**

methyl jasmonate (LL+MeJA) for seven days. Gray columns indicate PCs and black columns indicate CCs. Significant differences between the means ( $P < 0.05$ ) of *A. thaliana* (A) and *S. vulgaris* (C) are denoted by different lower case letters. Percent increase of plasma membrane length was not significantly different (n.s.) between control and MeJA-treated companion cells of either pea (B) or *S. vulgaris* (C). Data from Amiard et al. (2007).

invagination in sugar export. Especially for the case of PC wall invaginations, the contrasting possible roles in sugar export versus obstruction of pathogen spread should be elucidated.

## ACKNOWLEDGMENTS

Supported by the National Science Foundation (Award Numbers IBN-0235351 and DEB-1022236 to Barbara Demmig-Adams and William W. Adams) and the University of Colorado at Boulder. We thank our colleagues Profs. Douglas Schemske and Jon Ågren for providing seeds of the *Arabidopsis* ecotypes, Tyler Dowd for embedding and cutting of some tissue samples, and Dr. Onno Muller for some photosynthesis measurements.

## REFERENCES

- Adams, W. W. III., Cohu, C. M., Muller, O., and Demmig-Adams, B. (2013). Foliar phloem infrastructure in support of photosynthesis. *Front. Plant Sci.* 4:194. doi: 10.3389/fpls.2013.00194
- Adams, W. W. III., Watson, A. M., Mueh, K. E., Amiard, V., Turgeon, R., Ebbert, V., et al. (2007). Photosynthetic acclimation in the context of structural constraints to carbon export from leaves. *Photosynth. Res.* 94, 455–466. doi: 10.1007/s11120-006-9123-3
- Ågren, J., and Schemske, D. W. (2012). Reciprocal transplants demonstrate strong adaptive differentiation of the model organism *Arabidopsis thaliana* in its native range. *New Phytol.* 194, 1112–1122. doi: 10.1111/j.1469-8137.2012.04112.x
- Ainsworth, E. A., and Bush, D. R. (2011). Carbohydrate export from the leaf: a highly regulated process and target to enhance photosynthesis and productivity. *Plant Physiol.* 155, 64–69. doi: 10.1104/pp.110.167684
- Amiard, V., Demmig-Adams, B., Mueh, K. E., Turgeon, R., Combs, A. F., and Adams, W. W. III. (2007). Role of light and jasmonic acid signaling in regulating foliar phloem cell wall ingrowth development. *New Phytol.* 173, 722–731. doi: 10.1111/j.1469-8137.2006.01954.x
- Amiard, V., Mueh, K. E., Demmig-Adams, B., Ebbert, V., Turgeon, R., and Adams, W. W. III. (2005). Anatomical and photosynthetic acclimation to the light environment in species with differing mechanisms of phloem loading. *Proc. Natl. Acad. Sci. U.S.A.* 102, 12968–12973. doi: 10.1073/pnas.0503784102
- Andriunas, F. A., Zhang, H. M., Xia, X., Offler, C. E., McCurdy, D. W., and Patrick, J. W. (2012). Reactive oxygen species form part of a regulatory pathway initiating trans-differentiation of epidermal transfer cells in *Vicia faba* cotyledons. *J. Exp. Bot.* 63, 3617–3629. doi: 10.1093/jxb/ers029
- Arun Chinnappa, K. S., Nguyen, T. T. S., Hou, J., Wu, Y., and McCurdy, D. W. (2013). Phloem parenchyma transfer cells in *Arabidopsis* – an experimental system to identify transcriptional regulators of wall ingrowth formation. *Front. Plant Sci.* 4:102. doi: 10.3389/fpls.2013.00102
- Avanci, N. C., Luche, D. D., Goldman, G. H., and Goldman, M. H. S. (2010). Jasmonates are phytohormones with multiple functions, including plant defense and reproduction. *Gen. Mol. Res.* 9, 484–505. doi: 10.4238/vol9-1gm754
- Ballare, C. L. (2011). Jasmonate-induced defenses: a tale of intelligence, collaborators and rascals. *Trends Plant Sci.* 16, 249–257. doi: 10.1016/j.tplants.2010.12.001
- Bell, E., Creelman, R. A., and Mullet, J. E. (1995). A chloroplast lipoxygenase is required for wound-induced jasmonic acid accumulation in *Arabidopsis*. *Proc. Natl. Acad. Sci. U.S.A.* 92, 8675–8679.
- Borisjuk, L., Wang, T. L., Rolletschek, H., Wobus, U., and Weber, H. (2002). A pea seed mutant affected in the differentiation of the embryonic epidermis is impaired in embryo growth and seed maturation. *Development* 129, 1595–1607.
- Celebi-Toprak, F., Slack, S. A., and Russo, P. (2003). Potato resistance to cucumber mosaic virus is temperature sensitive and virus-strain specific. *Breed. Sci.* 53, 69–75. doi: 10.1270/jbsb.53.69
- Cohu, C. M., Muller, O., Demmig-Adams, B., and Adams, W. W. III. (2013a). Minor loading vein acclimation for three *Arabidopsis thaliana* ecotypes in response to growth under different temperature and light regimes. *Front. Plant Sci.* 4:240. doi: 10.3389/fpls.2013.00240
- Cohu, C. M., Muller, O., Stewart, J. J., Demmig-Adams, B., and Adams, W. W. III. (2013b). Association between minor loading vein architecture and light- and CO<sub>2</sub>-saturated photosynthetic oxygen evolution among *Arabidopsis thaliana* ecotypes from different latitudes. *Front. Plant Sci.* 4:264. doi: 10.3389/fpls.2013.00264
- Cohu, C. M., Muller, O., Adams, W. W. III., and Demmig-Adams, B. (2014). Leaf anatomical and photosynthetic acclimation to cool temperature and high light in two winter versus two summer annuals. *Physiol. Plant.* doi: 10.1111/ppl.12154 [Epub ahead of print].
- Delieu, T., and Walker, D. A. (1981). Polarographic measurement of photosynthetic oxygen evolution by leaf discs. *New Phytol.* 89, 165–178. doi: 10.1111/j.1469-8137.1981.tb07480.x
- Demmig-Adams, B., Cohu, C. M., Amiard, V., Zadelhoff, G., Veldink, G. A., Muller, O., et al. (2013). Emerging trade-offs – impact of photoprotectants (PsbS, xanthophylls, and vitamin E) on oxylipins as regulators of development and defense. *New Phytol.* 197, 720–729. doi: 10.1111/nph.12100
- Ding, X. S., Carter, S. A., Deom, C. M., and Nelson, R. S. (1998). Tobamovirus and potyvirus accumulation in minor veins of inoculated leaves from representatives of the Solanaceae and Fabaceae. *Plant Physiol.* 116, 125–136. doi: 10.1104/pp.116.1.125
- Ding, X. S., Shintaku, M. H., Arnold, S. A., and Nelson, R. S. (1995). Accumulation of mild and severe strains of tobacco mosaic virus in minor veins of tobacco. *Mol. Plant Microbe Interact.* 8, 32–40. doi: 10.1094/MPMI-8-0032
- Dumlao, M. R., Darehshouri, A., Cohu, C. M., Muller, O., Mathias, J., Adams, W. W. III., et al. (2012). Low temperature acclimation of photosynthetic capacity and leaf morphology in the context of phloem loading type. *Photosynth. Res.* 113, 181–189. doi: 10.1007/s11120-012-9762-5
- Edwards, J., Martin, A. P., Andriunas, F., Offler, C. E., Patrick, J. W., and McCurdy, D. W. (2010). GIGANTEA is a component of a regulatory pathway determining wall ingrowth deposition in phloem parenchyma transfer cells of *Arabidopsis thaliana*. *Plant J.* 63, 651–661. doi: 10.1111/j.1365-313X.2010.04269.x
- Gilbertson, R. I., and Lucas, W. J. (1996). How do viruses traffic on the ‘vascular highway’? *Trends Plant Sci.* 1, 260–268. doi: 10.1016/1360-1385(96)10029-7
- Gunning, B. E. S., and Pate, J. S. (1974). “Transfer cells,” in *Dynamic Aspects of Plant Ultrastructure*, ed. A. W. Robards (London: McGraw-Hill), 441–479.
- Gunning, B. E. S., Pate, J. S., and Briarty, L. G. (1968). Specialized “transfer cells” in minor veins of leaves and their possible significance in phloem translocation. *J. Cell Biol.* 37, 7–12. doi: 10.1083/jcb.37.3.C7
- Haritatos, E., Medville, R., and Turgeon, R. (2000). Minor vein structure and sugar transport in *Arabidopsis thaliana*. *Planta* 211, 105–111. doi: 10.1007/s004250000268
- Hause, B., Hause, G., Kutter, C., Miersch, O., and Wasternack, C. (2003). Enzymes of jasmonate biosynthesis occur in tomato sieve elements. *Plant Cell Physiol.* 44, 643–648. doi: 10.1093/pcp/pcg072
- Heller, A., and Gierth, K. (2001). Cytological observations of the infection process by *Phomopsis helianthi* (Munt.-Cvet) in leaves of sunflower. *J. Phytopathol.* 149, 347–357. doi: 10.1046/j.1439-0434.2001.00635.x
- Henry, Y., and Steer, M. W. (1980). A re-examination of the induction of phloem transfer cell development in pea leaves (*Pisum sativum*). *Plant Cell Environ.* 3, 377–380. doi: 10.1111/1365-3040.ep11581888
- Howe, G. A. (2004). Jasmonates as signals in the wound response. *J. Plant Growth Reg.* 23, 223–237. doi: 10.1007/s00344-004-0030-6
- Hu, P., Zhou, W., Cheng, Z. W., Fan, M., Wang, L., and Xie, D. X. (2013). JAV1 controls jasmonate-regulated plant defense. *Mol. Cell* 50, 504–515. doi: 10.1016/j.molcel.2013.04.027
- Kazan, K., and Manners, J. M. (2011). The interplay between light and jasmonate signalling during defence and development. *J. Exp. Bot.* 62, 4087–4100. doi: 10.1093/jxb/err142
- Körner, C. (2013). Growth controls photosynthesis – mostly. *Nova Acta Leopoldina NF* 114, 273–283.
- Kühn, C. (2003). A comparison of the sucrose transporter systems of different plant species. *Plant Biol.* 5, 215–232. doi: 10.1055/s-2003-40798
- Lucas, W. J., and Wolf, S. (1999). Connections between virus movement, macromolecular signaling and assimilate allocation. *Curr. Opin. Plant Biol.* 2, 192–197. doi: 10.1016/S1369-5266(99)80035-1
- Muller, O., Cohu, C. M., Stewart, J. J., Protheroe, J. A., Demmig-Adams, B., and Adams, W. W. III. (2014). Association between photosynthesis and contrasting features of minor veins in leaves of summer annuals loading phloem via symplastic versus apoplastic routes. *Physiol. Plant.* doi: 10.1111/ppl.12155 [Epub ahead of print].

- Offler, C. E., McCurdy, D. W., Patrick, J. W., and Talbot, M. J. (2003). Transfer cells: cells specialized for a special purpose. *Annu. Rev. Plant Biol.* 54, 431–454. doi: 10.1146/annurev.arplant.54.031902.134812
- Pate, J. S., and Gunning, B. E. S. (1969). Vascular transfer cells in angiosperm leaves. A taxonomic and morphological survey. *Protoplasma* 68, 135–156. doi: 10.1007/BF01247901
- Pate, J. S., and Gunning, B. E. S. (1972). Transfer cells. *Annu. Rev. Plant Physiol.* 23, 173–196. doi: 10.1146/annurev.pp.23.060172.001133
- Paul, M. J., and Foyer, C. H. (2001). Sink regulation of photosynthesis. *J. Exp. Bot.* 52, 1383–1400. doi: 10.1093/jexbot/52.360.1383
- Pugh, D. A., Offler, C. E., Talbot, M. J., and Ruan, Y. L. (2010). Evidence for the role of transfer cells in the evolutionary increase in seed and fiber biomass yield in cotton. *Mol. Plant* 3, 1075–1086. doi: 10.1093/mp/ssq054
- Qu, F., Ye, X. H., Hou, G. C., Sato, S., Clemente, T. E., and Morris, T. J. (2005). RDR6 has a broad but temperature-dependent antiviral defense role in *Nicotiana benthamiana*. *J. Virol.* 79, 15209–15217. doi: 10.1128/JVI.79.24.15209-15217.2005
- Santino, A., Taurino, M., DeDominico, S., Bonsegna, S., Poltronieri, P., Pastor, V., et al. (2013). Jasmonate signaling in plant development and defense response to multiple (a)biotic stresses. *Plant Cell Rep.* 32, 1085–1098. doi: 10.1007/s00299-013-1441-2
- Scholthof, H. B. (2005). Plant virus transport: motions of functional equivalence. *Trends Plant Sci.* 10, 376–382. doi: 10.1016/j.tplants.2005.07.002
- Søndergaard, T. E., Schulz, A., and Palmgren, M. G. (2004). Energization of transport processes in plants. Roles of the plasma membrane H<sup>+</sup>-ATPase. *Plant Physiol.* 136, 2475–2482. doi: 10.1104/pp.104.048231
- Stenzel, I., Hause, B., Maucher, H., Pitzschke, A., Miersch, O., Ziegler, J., et al. (2003). Allene oxide cyclase dependence of the wound response and vascular bundle-specific generation of jasmonates in tomato – amplification in wound signalling. *Plant J.* 33, 577–589. doi: 10.1046/j.1365-313X.2003.01647.x
- Suzuki, N., Koussevitsky, S., Mittler, R., and Miller, G. (2012). ROS and redox signaling in the response of plants to abiotic stress. *Plant Cell Environ.* 35, 259–270. doi: 10.1111/j.1365-3040.2011.02336.x
- Torres, M. A. (2010). ROS in biotic interactions. *Physiol. Plant.* 138, 414–429. doi: 10.1111/j.1399-3054.2009.01326.x
- Vuorinen, A. L., Kelloniemi, J., and Valkonen, J. P. T. (2011). Why do viruses need phloem for systemic invasion of plants? *Plant Sci.* 181, 355–363. doi: 10.1016/j.plantsci.2011.06.008
- Waigman, E., Ueki, S., Trutnyeva, K., and Citovsky, V. (2004). The ins and outs of nondestructive cell-to-cell systemic movement of plant viruses. *Crit. Rev. Plant Sci.* 23, 195–250. doi: 10.1080/07352680490452807
- Wimmers, J. W., and Turgeon, R. (1991). Transfer cells and solute uptake in minor veins of *Pisum sativum* leaves. *Planta* 186, 2–12. doi: 10.1007/BF00201491
- Zhou, C. L. E., El-Desouky, A., Sheta, H., Kelley, S., Polek, M., and Ullman, D. E. (2002). Citrus tristeza virus ultrastructure and associated cytopathology in *Citrus sinensis* and *Citrus aurantifolia*. *Can. J. Bot.* 80, 512–525. doi: 10.1139/b02-030

**Conflict of Interest Statement:** The authors declare that the research was conducted in the absence of any commercial or financial relationships that could be construed as a potential conflict of interest.

Received: 27 November 2013; accepted: 21 January 2014; published online: 06 February 2014.

Citation: Adams WW III, Cohu CM, Amiard V and Demmig-Adams B (2014) Associations between the acclimation of phloem-cell wall ingrowths in minor veins and maximal photosynthesis rate. *Front. Plant Sci.* 5:24. doi: 10.3389/fpls.2014.00024

This article was submitted to Plant Physiology, a section of the journal *Frontiers in Plant Science*.

Copyright © 2014 Adams III, Cohu, Amiard and Demmig-Adams. This is an open-access article distributed under the terms of the Creative Commons Attribution License (CC BY). The use, distribution or reproduction in other forums is permitted, provided the original author(s) or licensor are credited and that the original publication in this journal is cited, in accordance with accepted academic practice. No use, distribution or reproduction is permitted which does not comply with these terms.